UNIVERSIDAD DE CHILE
FACULTAD DE CIENCIAS FÍSICAS Y MATEMÁTICAS
DEPARTAMENTO DE INGENIERÍA MATEMÁTICA

THE INVERSE PROBLEM OF OBSTACLE DETECTION VIA OPTIMIZATION METHODS

TESIS PARA OPTAR AL GRADO DE DOCTOR EN CIENCIAS DE LA INGENIERÍA, MENCIÓN MODELACIÓN MATEMÁTICA
EN COTUTELA CON LA UNIVERSIDAD TOULOUSE III PAUL SABATIER

MATÍAS MAXIMILIANO GODOY CAMPBELL

PROFESOR GUÍA:
CARLOS CONCA ROSENDE

PROFESOR COGUÍA:
FABIEN CAUBET

MIEMBROS DE LA COMISIÓN:
GRÉGOIRE ALLAIRE
FRANCK BOYER
MARC DAMBRINE
AXEL OSSES ALVARADO

Este trabajo ha sido parcialmente financiado por CONICYT-Beca Doctorado Nacional 2012 y el programa ECOS-CONICYT proyecto C13E05

SANTIAGO DE CHILE
2016

RESUMEN
THE INVERSE PROBLEM OF OBSTACLE DETECTION VIA OPTIMIZATION METHODS

Esta tesis está dedicada al estudio del **problema inverso de detección de obstáculos/objetos** utilizando **métodos de optimización**. Este problema consiste en localizar un objeto desconocido ω dentro de un dominio acotado conocido Ω por medio de mediciones en el borde, más precisamente dadas por un dato de tipo Cauchy en una parte Γ_{obs} de $\partial\Omega$. Estudiamos los casos escalares y vectoriales para este problema, considerando las **ecuaciones de Laplace y de Stokes**. En ambos casos nos apoyamos en resultados de identificabilidad, los cuales aseguran la existencia de un único obstáculo/objeto asociado a la medición de borde considerada.

La estrategia utilizada en este trabajo se basa en reducir el problema inverso a la **minimización de un funcional de costo**: el **funcional de Kohn-Vogelius**. Esta estrategia es utilizada frecuentemente y permite el uso de métodos de optimización para las implementaciones numéricas. Sin embargo, en virtud de poder definir el funcional, este método requiere conocer una medida sobre toda la frontera exterior $\partial\Omega$.

Este último punto nos lleva a estudiar el **problema de completación de datos** que consiste en recuperar las condiciones de borde sobre una región inaccesible, *i.e.* sobre $\partial\Omega \setminus \Gamma_{obs}$, a partir del conocimiento de los datos de Cauchy sobre la región accesible Γ_{obs}. Este problema inverso es igualmente estudiado vía la minimización de un funcional de tipo Kohn-Vogelius. Dado que este problema está mal puesto, debemos regularizar el funcional por medio de una **regularización de Tikhonov**. Obtenemos numerosas propiedades teóricas, como propiedades de convergencia, en particular cuando los datos poseen ruido.

Teniendo en cuenta los resultados teóricos, **reconstruímos numéricamente los datos de borde** por medio de la implementación de un algoritmo de tipo gradiente para minimizar el funcional regularizado. Luego estudiamos el problema de detección de obstáculos cuando solo se poseen mediciones parciales. Consideramos las condiciones en el borde inaccesible y el objeto desconocido como variables del funcional y entonces, usando **herramientas de optimización geométrica**, en particular el **gradiente de forma del funcional de Kohn-Vogelius**, realizamos la **reconstrucción numérica del objeto desconocido**.

Finalmente, consideramos, en el caso vectorial bidimensional, un nuevo grado de libertad, al estudiar el caso en que el número de objetos es desconocido. Así, utilizamos la **optimización de forma topológica** con el fin de minimizar el funcional de Kohn-Vogelius. Obtenemos el **desarrollo asintótico topológico** de la solución de las ecuaciones de Stokes 2D y caracterizamos el **gradiente topológico** de este funcional. Determinamos entonces numéricamente el número de obstáculos como su posición. Además, proponemos un algoritmo que combina los métodos de optimización de forma topológica y geométrica, con el fin de determinar numéricamente el número de obstáculos, su posición y su forma.

Palabras Clave: Problema inverso geométrico, optimización de forma, problema de completación de datos, análisis de sensibilidad topológico, gradiente topológico, gradiente de forma, funcional de Kohn-Vogelius, ecuación de Laplace, ecuación de Stokes.

RÉSUMÉ
SUR LE PROBLÈME INVERSE DE DÉTECTION D'OBSTACLES PAR DES MÉTHODES D'OPTIMISATION

Cette thèse porte sur l'étude du **problème inverse de détection d'obstacle/objet** par des **méthodes d'optimisation**. Ce problème consiste à localiser un objet inconnu ω situé à l'intérieur d'un domaine borné connu Ω à l'aide de mesures de bord et plus précisément de données de Cauchy sur une partie Γ_{obs} de $\partial\Omega$. Nous étudions les cas scalaires et vectoriels pour ce problème en considérant les **équations de Laplace et de Stokes**. Dans tous les cas, nous nous appuyons sur une résultat d'identifiabilité qui assure qu'il existe un unique obstacle/objet qui correspond à la mesure de bord considérée.

La stratégie utilisée dans ce travail est de réduire le problème inverse à la **minimisation d'une fonctionnelle coût**: la **fonctionnelle de Kohn-Vogelius**. Cette approche est fréquemment utilisée et permet notamment d'utiliser des méthodes d'optimisation pour des implémentations numériques. Cependant, afin de bien définir la fonctionnelle, cette méthode nécessite de connaître une mesure sur tout le bord extérieur $\partial\Omega$.

Ce dernier point nous conduit à étudier le **problème de complétion de données** qui consiste à retrouver les conditions de bord sur une région inaccessible, *i.e.* sur $\partial\Omega\backslash\Gamma_{\text{obs}}$, à partir des données de Cauchy sur la région accessible Γ_{obs}. Ce problème inverse est également étudié en minimisant une fonctionnelle de type Kohn-Vogelius. La caractère mal posé de ce problème nous amène à régulariser la fonctionnelle via une **régularisation de Tikhonov**. Nous obtenons plusieurs propriétés théoriques comme des propriétés de convergence, en particulier lorsque les données sont bruitées.

En tenant compte de ces résultats théoriques, nous **reconstruisons numériquement les données de bord** en mettant en oeuvre un algorithme de gradient afin de minimiser la fonctionnelle régularisée. Nous étudions ensuite le problème de détection d'obstacle lorsque seule une mesure de bord partielle est disponible. Nous considérons alors les conditions de bord inaccessibles et l'objet inconnu comme les variables de la fonctionnelle et ainsi, en utilisant des **méthodes d'optimisation de forme géométrique**, en particulier le **gradient de forme de la fonctionnelle de Kohn-Vogelius**, nous obtenons la **reconstruction numérique de l'inclusion inconnue**.

Enfin, nous considérons, dans le cas vectoriel bi-dimensionnel, un nouveau degré de liberté en étudiant le cas où le nombre d'objets est inconnu. Ainsi, nous utilisons l'**optimisation de forme topologique** afin de minimiser la fonctionnelle de Kohn-Vogelius. Nous obtenons le **développement asymptotique topologique** de la solution des équations de Stokes 2D et caractérisons le **gradient topologique** de cette fonctionnelle. Nous déterminons alors numériquement le nombre d'obstacles ainsi que leur position. De plus, nous proposons un algorithme qui combine les méthodes d'optimisation de forme topologique et géométrique afin de déterminer numériquement le nombre d'obstacles, leur position ainsi que leur forme.

Mots clés: Problème inverse géométrique, optimisation de forme, problème de complétion de données, analyse de la sensibilité topologique, gradient topologique, gradient de forme, fonctionnelle de Kohn-Vogelius, équation de Laplace, équations de Stokes.

ABSTRACT
THE INVERSE PROBLEM OF OBSTACLE DETECTION VIA OPTIMIZATION METHODS

This PhD thesis is dedicated to the study of the **inverse problem of obstacle/object detection** using **optimization methods**. This problem consists in localizing an unknown object ω inside a known bounded domain Ω by means of boundary measurements and more precisely by a given Cauchy pair on a part Γ_{obs} of $\partial\Omega$. We cover the scalar and vector scenarios for this problem considering both **the Laplace and the Stokes equations**. For both cases, we rely on identifiability result which ensures that there is a unique obstacle/object which corresponds to the considered boundary measurements.

The strategy used in this work is to reduce the inverse problem into the **minimization of a cost-type functional**: the **Kohn-Vogelius functional**. This kind of approach is widely used and permits to use optimization tools for numerical implementations. However, in order to well-define the functional, this approach needs to assume the knowledge of a measurement on the whole exterior boundary $\partial\Omega$.

This last point leads us to first study the **data completion problem** which consists in recovering the boundary conditions on an inaccessible region, *i.e.* on $\partial\Omega\setminus\Gamma_{\text{obs}}$, from the Cauchy data on the accessible region Γ_{obs}. This inverse problem is also studied through the minimization of a Kohn-Vogelius type functional. The ill-posedness of this problem enforces us to regularize the functional via a **Tikhonov regularization**. We obtain several theoretical properties as convergence properties, in particular when data is corrupted by noise.

Based on these theoretical results, we **reconstruct numerically the boundary data** by implementing a gradient algorithm in order to minimize the regularized functional. Then we study the obstacle detection problem when only partial boundary measurements are available. We consider the inaccessible boundary conditions and the unknown object as the variables of the functional and then, using **geometrical shape optimization tools**, in particular the **shape gradient of the Kohn-Vogelius functional**, we perform the **numerical reconstruction of the unknown inclusion**.

Finally, we consider, into the two dimensional vector case, a new degree of freedom by studying the case when the number of objects is unknown. Hence, we use the **topological shape optimization** in order to minimize the Kohn-Vogelius functional. We obtain the **topological asymptotic expansion** of the solution of the 2D Stokes equations and characterize the **topological gradient** for this functional. Then we determine numerically the number and location of the obstacles. Additionally, we propose a blending algorithm which combines the topological and geometrical shape optimization methods in order to determine numerically the number, location and shape of the objects.

Keywords: Geometrical inverse problem, shape optimization, data completion problem, topological sensitivity analysis, topological gradient, shape gradient, Kohn-Vogelius functional, Laplace equation, Stokes equations.

A mis padres con cariño,
a Javiera con amor.

Agradecimientos

Agradezco en primer lugar a mis padres, Soledad y Víctor, por haberme dado las herramientas para llegar a este momento de mi vida. Esto no es más que el resultado de todas las oportunidades que me han brindado. Sigo esperando llegar tan lejos como ustedes en la vida. Gracias a mis hermanos, por su confianza y apoyo durante todos estos años y gracias a Antonia, que con su alegría nos cambió la vida.

Agradezco, con la misma fuerza que a mis padres, a Javiera, mi gran compañera en esta aventura. Gracias por tu amor (paciencia, comprensión, apoyo) incondicional e ilimitado, por haber dejado literalmente todo en pos de vivir una aventura que parecía tan incierta y que ha resultado, afortunadamente, una increíble historia que recordaremos por siempre. Gracias por vivir junto a mi este sueño, que como bien sabes recién está comenzando. Gracias también a tus padres por hacerme parte de su familia y por sobretodo por su apoyo en todo lo que ha sido esta aventura.

Agradezco a mis directores, Carlos Conca y Fabien Caubet, por su apoyo y soporte durante estos años. A Carlos, por su confianza y experiencia, por ser un guía en toda la dimensión de la palabra, por buscar siempre una forma de hacer más fácil mi trabajo y por sus consejos en el ámbito profesional y personal. A Fabien, por su hospitalidad, optimismo y motivación, por su paciencia cuando las cosas se vieron más difíciles, por su permanente disposición para ayudarme (y motivarme) a presentar nuestro trabajo en diversos lugares (o a solucionar cualquier problema, aunque fuese el más sencillo), ha sido una gran experiencia trabajar juntos.

Muchísimas gracias a mis *rapporteurs* Grégoire Allaire y Marc Bonnet, la titánica tarea de leer este trabajo en detalle ha sido realizada con la excelencia que los caracteriza y sus reportes han permitido mejorar sustancialmente el contenido de este trabajo. Es un honor que sus nombres estén asociados a esta tesis. Del mismo modo agradezco a los profesores Marc Dambrine, Axel Osses y Franck Boyer por haber aceptado ser parte del jurado.

Agradecimientos especiales para Jérémi Dardé, del Institut de Mathématiques de Toulouse, por su valioso aporte en la realización de la primera parte de este trabajo. Igualmente agradezco, nuevamente, a Marc Dambrine por su valiosa contribución en la segunda parte de este trabajo y su permanente interés durante el desarrollo de esta tésis.

Muchas gracias a mis grandes amigos durante esta aventura: Orly, Nico, Emilio, Víctor, Sebastián, Joce. Siempre es una alegría tenerlos cerca, ya sea aquí o allá. Y por supuesto que gracias a todos mis amigos de la vida, me encantaría agradecerles uno por uno pero *el margen de esta tesis es muy pequeño para contenerles.*

Agradezco a mis compañeros de doctorado, tanto en el DIM como en el IMT, por su simpatía y buena disposición. En particular agradezco a todos con quienes compartí oficina: Emilio, Viviana, Sebastián, Víctor, Marc y Guillaume.

No puedo terminar sin agradecer a todos los funcionarios del DIM y el CMM, en particular a Eterin, Silvia, Luis, Oscar y María Inés. Me han *salvado la vida* innumerables veces y no puedo si no agradecerles por ello. Del mismo modo agradezco a todo el personal del Institut de Mathématiques de Toulouse por ayudarme en todo lo necesario para tener una agradable y óptima estadía en un lugar donde *se vive* la matemática de una forma muy especial.

Finalmente agradezco a CONICYT por financiar esta tesis por medio de la Beca Doctorado Nacional 2012, al programa ECOS-CONICYT por financiar esta tesis por medio del proyecto C13E05 y la Embajada de Francia en Chile por financiar parte de mi cotutela en Toulouse por medio de la beca de Movilidad Doctoral 2015.

Contents

List of Tables

List of Figures

General Introduction

Inverse problems are an extensive, active and multidisciplinary research field which touches several main areas of research: mathematics, physics, biology, medicine, geophysics, etc. The term "Inverse Problem" appeared in the 1960's in geophysics, however many problems which can be classified into this area were studied long time before. After their 'classification' in the 1960's, they become an active research field in mid 1970's after the classical work of A.N. Tikhonov and V. Arsenin [83] and their definitive impulse became in 1980's and 1990's where the study of this kind of problems became a major object of interest of several other areas, for example: Medical Imaging, Biology, etc. This kind of problems have also several industrial applications, such as image processing, seismology, medical imaging, chemistry, fluid mechanics, etc. Inverse problems can be described, roughly speaking, as the problem of determine the causes of some phenomena from the knowledge of the effects of this phenomena.

Shape optimization is an active field of applied mathematics which consists basically in finding the shape which is optimal in the sense that it minimizes a certain cost-type functional while satisfying some given constraints. One of the first problems of this kind has been formulated by Newton in his famous *Principia Mathematica* in 1686, the problem consisted of determining, in dimension three, the shape of an axis-symmetric body, with assigned radius and height, which offers minimum resistance when it is moving in a fluid. After that and more recently in the beginning of the 1900's, Hadamard developed a method in order to formulate the differential of functions or functionals of the solution of some PDEs, with respect to boundary variations. This approach has been widely used and became a standard as the field was growing. The industrial applications and the interest on the subject made it very popular in the last 40 years, particularly from aeronautical industry and civil engineering. As the interest on the subject have been increased, the improvements and propositions of new methods became necessary, the boundary variation method resorts in the assumption of a fixed topology, so no topological changes are allowed. To overcome this difficulty, two other main methods were developed: the first one, the *level set method* was introduced in 1980's by Osher and Sethian (see [74]) as a numerical tool to study topological changes. Roughly speaking their method consists in studying the evolution of a function which represents the interface between two medias while this function is perturbed in the normal direction relative to the interface. The second method, the *topological gradient method* was introduced in

1990's by Schumacher (see [76]). In this method the basic idea is to study how a cost functional varies when a small obstacle is introduced in the domain of study.

In this thesis work we deal with the **inverse problem of obstacle detection**, this is: Given a reference domain Ω, where a function u is governed by some PDE (Laplace, Stokes), the aim is to determine the localization and shape of one or several obstacles, which will be denoted by ω^*, inside the reference domain from boundary measurements of the function u, this is, from the knowledge of u or some operator applied to u into the boundary $\partial\Omega$ or a relatively open part of it. Typically we want to recover ω^* from given Cauchy data on (a part of) the boundary $\partial\Omega$. In particular, we focus our study in methods of resolution which 'translate' the inverse problem into an optimization problem, more precisely a **shape optimization problem**, based on the minimization of a (shape) cost-type functional, where well-posed boundary value problems are considered. This strategy allows to implement and perform numerical simulations based on gradient algorithms, which at the same time acts as a feedback to us in order to explore techniques of resolution compatibles with this type of algorithms.

The obstacle inverse problem arises, for example, in mold filling during which small gas bubbles can be created and trapped inside the material (as it is mentioned in [17]). We can also mention the fact that the most common devices used to spot immersed bodies, such as submarines or banks of fish, are sonars, using acoustic waves: Active sonars emit acoustic waves (making themselves detectable), while passive sonars only listen (and can only detect targets that are noisy enough). To overcome those limitations, one want to design systems imitating the *lateral line systems* of fish, a sense organ they use to detect movement and vibration in the surrounding water (as emphasized in [41]).

One of our scenarios will be the case where, in a system governed by the Laplace equation, the boundary data is obtained only in an 'accessible' part of the boundary, however, as our strategy is based in considering well-posed boundary value problems related with an equivalent optimization problem, we have to 'complete' the available data in such a way that the solution is close to the 'real one', in order to apply an optimization method to determine the approximate location and shape of the unknown obstacle(s) ω^*. The problem of reconstructing data into the unaccessible part of the boundary from the data in the accessible part is known as the inverse problem of **data completion** (or **Cauchy problem**). This data completion problem will be studied through the minimization of a **Kohn-Vogelius functional**. We will study this problem in detail, theoretically and numerically in the case where no obstacle has to be found and then the results of this analysis will be used in a proposed method in which we perform the **numerical obstacle detection with partial boundary data**, where the obstacle shape is reconstructed by using a **geometrical shape optimization tool**: the **shape gradient**. This latter object measures the variation of the cost-type functional when a normal perturbation on the obstacle shape is applied.

The other scenario in consideration will be the case when, having Dirichlet data

over the full boundary $\partial\Omega$ and having Neumann data only on a part of the boundary, we intend to detect the number, location and shape of an unknown number of small obstacles inside the reference domain Ω when the system is governed by the stationary Stokes equations in the bi-dimensional case. The problem is still stated as the minimization of a **Kohn-Vogelius type shape functional** but, unlike the partial data case, as we consider the number of obstacles as an unknown, we are enforced to consider a different point of view, as the classical shape gradient method consider only a fixed topology. For this, with a **topological asymptotic analysis**, we compute the **topological gradient** for the cost functional, which measures the variation of the functional under topological perturbations of the reference domain, this is, when a small obstacle is introduced. From the numerical point of view we propose an algorithm which **combines the topological and geometrical shape optimization** in order to obtain our final aim: detect the number, location and shape of an unknown number of obstacles.

So, we can conclude that the main objective of this work is to develop methods in order to localize unknown obstacles inside a reference domain by means of (possibly partial) boundary measurements in several scenarios.

Let us introduce each considered problem in more detail.

The data completion problem and the inverse obstacle problem with partial boundary data.

As we said before, the data completion problem is stated as: given a partial differential operator in a domain Ω and overspecified data on an 'accessible' part of the boundary, we want to recover the value of the boundary data on the remaining part of the boundary. This problem is known in the literature as the data completion problem. We assume in this case that the differential operator involved is the Laplacian and the given overspecified data in the accessible part of the boundary are Dirichlet and Neumann boundary conditions.

This problem arises in several areas of study in the scientific, engineering or industrial contexts, as a concrete examples we have: medical and geophysical imaging, thermal or electrical inspection/prospection.

The data completion problem is known to be ill-posed, in the sense that the solution dependence (and therefore the 'missing data' dependence) on the given data is not continuous, the famous example of Hadamard [55] is an example of this behavior. This ill-posedness leads to difficulties for numerical resolution schemes, small errors on the retrieved data will lead to big errors on the obtained solutions. In order to deal with these difficulties a regularization technique is mandatory.

The data completion problem has been studied both in theoretical and numerical approaches by several authors. In the theoretical setting we recall the works

of Cimetière *et al.* [40] who consider a fixed point scheme for an appropriate operator, in the works of Ben Belgacem *et al.* [19, 13, 20] a complete development of both theoretical and numerical approaches is studied based on the study of the Steklov-Poincaré operator covering even the noisy data case, where a Lavrentiev regularization is considered. We also mention Bourgeois *et al.* works [24, 26] in which the approach is based on the quasi-reversibility (QR) method, a generalization to a wider family of systems is presented by Dardé [45]. On the numerical side we mention the work of Kozlov *et al.* [63] which propose the 'classical' KMF algorithm used widely for numerical simulations, several works consider modifications of the KMF algorithm in order to improve their speed of convergence, as an example we mention the work of Abouchabaka *et al.* [1]. In another approach, the work of Andrieux *et al.* [12] considers the minimization of an energy-like functional and presents an algorithm which is proved to be equivalent to the KMF algorithm formulation. The work of Aboulaich *et al.* [2] consider a control type method for the numerical resolution of the Cauchy problem for Stokes system and finally we mention the work of Han *et al.* [56] in which a regularization of an energy functional is considered for an annular domain.

In our case, we consider an energy-like functional approach, similar as in the work of Andrieux *et al.* [12]. We split the overdetermined system into two different systems: each one considers one of the boundary conditions on the 'accessible part' of the boundary, and we impose the 'other' boundary condition on the 'unaccessible part' of the boundary. More precisely, we consider a Kohn-Vogelius energy-like functional which measures the error between the solutions of our considered systems for each imposed conditions on the 'unaccessible part' of the boundary. We see that, when there exists a solution, this will be characterized as the minimum of our proposed functional, so our problem now is reduced to minimize the Kohn-Vogelius functional. In order to handle with the ill-posedness previously mentioned we consider a Tikhonov regularization of our problem.

We have obtained several results for our primary energy functional, as the existence of minimizers is not assured for any data we have defined a generalized concept of solution whose existence is assured, moreover if this defined object satisfies some conditions, the solution for the whole problem is assured. For the regularized functional we have also several results, the existence of minimizers is assured for any data thanks to the gained coercivity and in case of having compatible data we have a convergence result. When we consider noisy date we have proven that we can consider a strategy, using a slightly-modified Morozov discrepancy principle (following the work of Ben Belgacem *et al.* in [20]), for the choice of the regularization parameter in order to have convergence to the unpolluted solution. From the numerical point of view, using a gradient method via the differentiation of the regularized functional with respect to its variables, we are able to perform simulations which show us that the proposed method is effective in order to reconstruct the data into the inaccessible part of the boundary.

As an application of the obtained results, we proposed a method in order to solve the obstacle problem with partial boundary data for the Laplace operator.

We extend the previously proposed Kohn-Vogelius functional in order to add the obstacle as an additional variable of the functional, by means of an identifiability result we have an equivalent formulation between the detection of the obstacle (and the completion of the data) and the minimization of the extended functional. The use of a regularized extended functional is suggested in order to deal with the ill-posedness of the data completion part and the convergence results apply analogously to this extended functional. We implement an algorithm which uses the previous gradient algorithm for the unknown boundary data, and a shape gradient algorithm, based on the computation of the derivative of the regularized functional with respect to a normal variation of the boundary of the obstacle (this is, using the boundary variation method) in order to reconstruct the unknown obstacle only from partial boundary measurements.

The main novelty of the proposed methods resides lies in the formalization and rigorous analysis of a natural and 'easy-to-implement' strategy in order to solve the data completion problem. The division in two well-posed problems allows to implement an algorithm with any finite element library (such as FreeFEM++ [60] for example) and the consideration of a Kohn-Vogelius approach allows to implement optimization tools such as gradient methods. Moreover, we extend this method to solve another inverse problem of interest for which we show positive results.

The inverse obstacle problem using topological shape optimization in a 2D Stokes flow.

As we said before, in this part we work with the inverse problem of determining the number, the position and the shape of relatively small objects inside a two dimensional fluid. We assume that the fluid motion is governed by the steady-state Stokes equations. In order to reconstruct the obstacles, we assume that a Cauchy pair is given on a part of the surface of the fluid, that is a Dirichlet boundary condition and the measurement of the Cauchy forces. Hence, the identifiability result of Alvarez *et al.* [6, Theorem 1.2] implies that this problem could be seen as the minimization of a cost functional, which in our case will be a Kohn-Vogelius type cost functional.

The small size assumption on the objects leads us to perform asymptotic expansions on the involved functional. For this, we will use the notion of *topological gradient* which will determine a criterion in order to minimize the cost functional. The topological sensitivity analysis consists in studying the variation of a cost functional with respect to the modification of the topology of the domain, for example when we insert 'holes' (or objects) in the domain. It was introduced by Schumacher in [76] and Sokolowski *et al.* in [80] for the compliance minimization in linear elasticity.

Topological sensitive analysis related to Stokes equations have been studied in the past by several authors, especially relevant are the works of Guillaume *et al.* [54],

Maatoug [57], Amstutz [9] with steady-state Navier-Stokes equations and [10] with generalization for some non-linear systems and Sid Idris [77] which develops a detailed work in the two-dimensional case. In all of these works the focus is set to find topological asymptotic expansions for a general class of functionals where the system satisfies only Dirichlet boundary conditions.

Closer works to our problem have been presented in the past by Ben Abda *et al.* [17] and by Caubet *et al.* [36]. In the first reference they consider a Neumann boundary condition on the small objects obtaining general results in two and three dimensional cases, with a complete development of the theory only on the three dimensional case. In the work of Caubet *et al.*, they deal with the same problem as the one we consider here but only again on the three-dimensional case. In our two-dimensional case, due to the impossibility to have an asymptotic expansion of the solution of Stokes equations by means of an exterior problem (phenomena which is related to the Stokes paradox), we have to approximate it by means of a different problem. The deduction of this approximation is strongly influenced by the recent work of Bonnaillie-Noël *et al.* [21]. Indeed the same problem appears for the Laplace equation: it is based on the fact that the existence of a solution of the boundary value problem

$$\left\{\begin{array}{rcll} -\Delta V & = & 0 & \text{in } \mathbb{R}^2\backslash\overline{\omega} \\ V & = & u_0(z) & \text{on } \partial\omega \\ V & \to & 0 & \text{at infinity} \end{array}\right. \tag{1}$$

is not guaranteed except when $u_0(z) = 0$. The classical analysis of elliptic equation in unbounded domain is made in the functional setting of weighted Sobolev spaces. It is known that (1) has a unique solution in a space containing the constants, hence this solution is the constant $u_0(z)$ which prohibits the condition at infinity if $u_0(z) \neq 0$. Taking into account this, we can define the asymptotic expansion for the Stokes system which is a crucial part in order to obtain the desired expansion for the functional involved. It is important to remark that (for a given real number $u_0(z)$) several technical results which lead to the main result are different to the ones in the three-dimensional setting which involves additional difficulties to our problem.

From the obtained theoretical results, we present some numerical simulations in order to confirm and deepen our theoretical results by testing the influence of some parameters in our algorithm of reconstruction such as the shape and the size of the obstacles. We also propose an algorithm which joins the topological optimization procedure with the classical shape optimization method using the previous computation of the shape gradient for the Kohn-Vogelius functional made by Caubet *et al.* in [37]. This blending method allows not only to obtain the number and qualitative location of the objects, moreover it allows to approximate the shape of this ones. Nevertheless, we precise that the geometrical shape optimization step will fail if the previous topological step doesn't give the total number of objects.

To conclude, we also mention the recent developments on topological sensitivity based iterative schemes made by Carpio *et al.* in [31, 32, 33]. We also refer to some

works using the level set method by Lesselier *et al.* in [64, 46, 47]. Combinations of several shape optimization methods was also recently tested by several authors. Allaire *et al.* propose in [4] to couple the classical geometrical shape optimization through the level set method and the topological gradient in order to minimize the compliance. The same combination is made for another problem by He *et al.* in [59]. In [30], Burger *et al.* use also this combination for inverse problems. There, the topological gradient is incorporated as a source term in the transport Hamilton-Jacobi equation used in the level set method. Concerning the minimization of the compliance, Pantz *et al.* propose in [73] an algorithm using boundary variations, topological derivatives and homogenization methods (without a level set approach).

The main novelty in this second part, from the theoretical point of view is the comprehensive study of the topological asymptotic expansion of the solution of Stokes equations for the considered boundary conditions, the important technical and conceptual differences with the classical three (and superior) dimensional case gives to the explored one a specific weight and importance. From the numerical point of view, the implementation of an algorithm which combines the two considered shape optimization approaches is new for the obstacle problem, and the results appear to justify the potential of this technique.

We finish this introduction by presenting an overview of each chapter, presenting its main results:

PART I: The data completion problem and the inverse obstacle problem with partial boundary data

Chapter 1: Theoretical analysis of the data completion problem for Laplace operator.

In this chapter we consider the problem of reconstruct boundary data in an inaccessible part of the boundary from overdetermined boundary data in an accessible part of the boundary, this problem is known in the literature as the data completion problem or the Cauchy problem.

Consider a reference domain Ω governed by Laplace equation, whose boundary $\partial\Omega$ is composed by two relatively open, non empty parts: an accessible one Γ_{obs} where Dirichlet and Neumann measurements are given in a pair $(g_N, g_D) \in \mathrm{H}^{-1/2}(\Gamma_{obs}) \times \mathrm{H}^{1/2}(\Gamma_{obs})$ and an unaccessible one Γ_{i} where no measurements can be made, these parts satisfy $\overline{\Gamma_{obs}} \cup \overline{\Gamma_{\mathrm{i}}} = \partial\Omega$. The data completion problem consists in recovering data on the whole boundary, specifically on Γ_{i} from the over-determined data on

Γ_{obs}. Formally speaking: *Find* $u \in \mathrm{H}^1(\Omega, \Delta)$ *such that*

$$\begin{cases} -\Delta u &= 0 & \text{in } \Omega \\ u &= g_D & \text{on } \Gamma_{obs} \\ \partial_{\mathbf{n}} u &= g_N & \text{on } \Gamma_{obs}. \end{cases} \tag{2}$$

As (g_N, g_D) could be any data (obtained for example from experiments), such a u may not exist. Due to this, we will recall the concept of **compatible data**.

Definition 0.1 *A pair* $(g_N, g_D) \in \mathrm{H}^{-1/2}(\Gamma_{obs}) \times \mathrm{H}^{1/2}(\Gamma_{obs})$ *will be called* ***compatible*** *if there exists (a necessarily unique)* $u \in \mathrm{H}^1(\Omega, \Delta)$ *harmonic such that* $u|_{\Gamma_{obs}} = g_D$, $\partial_{\mathbf{n}} u|_{\Gamma_{obs}} = g_N$.

The following relevant result states that the compatible data is dense in the set of all possible data, which implies in particular the ill-posedness of the considered inverse problem:

Lemma 0.2 *(see [51]) For* $(g_N, g_D) \in \mathrm{H}^{-1/2}(\Gamma_{obs}) \times \mathrm{H}^{1/2}(\Gamma_{obs})$ *given data, we have:*

1. *For a fixed* $g_D \in \mathrm{H}^{1/2}(\Gamma_{obs})$, *the set of data* g_N *for which there exists a function* $u \in \mathrm{H}^1(\Omega, \Delta)$, *satisfying the Cauchy problem* (1.1) *is dense in* $\mathrm{H}^{-1/2}(\Gamma_{obs})$.
2. *For a fixed* $g_N \in \mathrm{H}^{-1/2}(\Gamma_{obs})$, *the set of data* g_D *for which there exists a function* $u \in \mathrm{H}^1(\Omega, \Delta)$, *satisfying the Cauchy problem* (1.1) *is dense in* $\mathrm{H}^{1/2}(\Gamma_{obs})$.

On the other hand this result is essential in the sense that it assures several properties of the functional that we will consider in the formulation of our problem as an optimization problem.

In order to introduce our strategy, we recall that a classical example from Hadamard (see Chapter 1) shows that this problem is ill-posed in the sense that the solution does not have a continuous dependence on the given data (g_N, g_D). Therefore, any small perturbation of the (experimental) data may lead to considerable errors in the obtained solutions. Our aim is then to develop a method which allows us to prevent 'wrong solutions'.

Let us define the Kohn-Vogelius functional which will depend on the *missing data* on Γ_{i}, following the idea proposed by Andrieux et al in [12].

To solve the problem (2), we will solve the following equivalent optimization problem:

$$(\varphi^*, \psi^*) \in \underset{(\varphi,\psi)\in \mathrm{H}^{-1/2}(\Gamma_{\mathrm{i}})\times \mathrm{H}^{1/2}(\Gamma_{\mathrm{i}})}{\operatorname{argmin}} \mathcal{K}(\varphi, \psi) \tag{3}$$

where $\mathcal{K}$ is the nonnegative Kohn-Vogelius cost functional defined by

$$\mathcal{K}(\varphi, \psi) := \frac{1}{2} \int_\Omega |\nabla u_\varphi^{g_D} - \nabla u_\psi^{g_N}|^2 \tag{4}$$

where $u_\varphi^{g_D} \in \mathrm{H}^1(\Omega)$ and $u_\psi^{g_N} \in \mathrm{H}^1(\Omega)$ are the respective solutions of the following problems

$$\left\{\begin{array}{rcll} -\Delta u_\varphi^{g_D} & = & 0 & \text{in } \Omega \\ u_\varphi^{g_D} & = & g_D & \text{on } \Gamma_{obs} \\ \partial_{\mathbf{n}} u_\varphi^{g_D} & = & \varphi & \text{on } \Gamma_{\mathrm{i}}, \end{array}\right. \quad \text{and} \quad \left\{\begin{array}{rcll} -\Delta u_\psi^{g_N} & = & 0 & \text{in } \Omega \\ \partial_{\mathbf{n}} u_\psi^{g_N} & = & g_N & \text{on } \Gamma_{obs} \\ u_\psi^{g_N} & = & \psi & \text{on } \Gamma_{\mathrm{i}}. \end{array}\right. \tag{5}$$

Notice that if the inverse problem (2) has a solution, then we have that $\mathcal{K}(\varphi,\psi) = 0$ if and only if $(\varphi,\psi) = (\varphi^*,\psi^*)$, and in this case we obtain: $u_{\varphi^*}^{g_D} = u$ and $u_{\psi^*}^{g_N} = u + C$, $C \in \mathbb{R}$ where u is the solution of the Cauchy problem in Ω. This justifies the proposed approach.

This strategy is similar to the one presented by Ben Belgacem *et al.* in [19]. However, their exposition is based in the solution of a variational problem, which induces the minimization of a similar Kohn-Vogelius system in which they consider only Dirichlet data in Γ_{i} as the unknown. This allows to work in the framework of Steklov-Poincaré operator. Our strategy of considering both Dirichlet and Neumann data in Γ_{i} as unknowns allows us to work in a 'natural way' with the optimization strategy throughout.

Our study begins proving some properties of the Kohn-Vogelius functional $\mathcal{K}$, in particular that:

$$\inf_{(\varphi,\psi)} \mathcal{K}(\varphi,\psi) = 0,$$

for any data (g_N, g_D), compatible or not, is a key point to the analysis. The numerical minimization of the Kohn-Vogelius functional may approach the value 0, even in the case when there is no solution to the data completion problem.

As $\mathcal{K}$ is not coercive, and from the previous property, we cannot assume that the functional reaches its minimum. From the exploration of the first order optimality condition we define, following Ben Belgacem idea in [19], a generalized notion of first order optimality condition:

Definition 0.3 *We say that a sequence $(\varphi_n,\psi_n) \subset \mathrm{H}^{-1/2}(\Gamma_{\mathrm{i}})\times\mathrm{H}^{1/2}(\Gamma_{\mathrm{i}})$ is a **pseudo-solution** of (3) if*

$$\lim_{n\to\infty} \sup_{(\widetilde{\varphi},\widetilde{\psi})\in \mathrm{H}^{-1/2}(\Gamma_{\mathrm{i}})\times\mathrm{H}^{1/2}(\Gamma_{\mathrm{i}})} \frac{|a((\varphi_n,\psi_n),(\widetilde{\varphi},\widetilde{\psi})) - \ell(\widetilde{\varphi},\widetilde{\psi})|}{\|(\widetilde{\varphi},\widetilde{\psi})\|_{\mathrm{H}^{-1/2}(\Gamma_{\mathrm{i}})\times\mathrm{H}^{1/2}(\Gamma_{\mathrm{i}})}} = 0, \tag{6}$$

where a and ℓ are a bilinear and linear forms associated with the first order optimality condition for a minimizer of the Kohn-Vogelius:

$$\begin{aligned} a\left((\varphi,\psi),(\widetilde{\varphi},\widetilde{\psi})\right) &= \int_\Omega \nabla(v_\varphi - v_\psi)\cdot\nabla(v_{\widetilde{\varphi}} - v_{\widetilde{\psi}}) \\ \ell(\varphi,\psi) &= \int_\Omega \left(\nabla u_0^{g_D}\cdot\nabla v_\psi + \nabla u_0^{g_N}\cdot\nabla v_\varphi\right), \end{aligned}$$

and where $v_\varphi := u_\varphi^0$, $v_\psi := u_\psi^0$ satisfies

$$\left\{\begin{array}{rcll} -\Delta v_\varphi &=& 0 & \text{in } \Omega \\ v_\varphi &=& 0 & \text{on } \Gamma_{obs} \\ \partial_{\mathbf{n}} v_\varphi &=& \varphi & \text{on } \Gamma_{\mathrm{i}} \end{array}\right. \quad \textit{and} \quad \left\{\begin{array}{rcll} -\Delta v_\psi &=& 0 & \text{in } \Omega \\ \partial_{\mathbf{n}} v_\psi &=& 0 & \text{on } \Gamma_{obs} \\ v_\psi &=& \psi & \text{on } \Gamma_{\mathrm{i}}. \end{array}\right. \tag{7}$$

Moreover, using the density Lemma 0.2, we can obtain an existence result of this new object, which defines a criterion for the existence of solution of the data completion problem:

Proposition 0.4 *For any $(g_N, g_D) \in \mathrm{H}^{-1/2}(\Gamma_{obs}) \times \mathrm{H}^{1/2}(\Gamma_{obs})$, there exists a pseudo-solution $(\varphi_n^*, \psi_n^*) \subset \mathrm{H}^{-1/2}(\Gamma_{\mathrm{i}}) \times \mathrm{H}^{1/2}(\Gamma_{\mathrm{i}})$ of (3). Moreover, any pseudo-solution satisfies the following alternative:*

1. *$\|(\varphi_n^*, \psi_n^*)\|_{\mathrm{H}^{-1/2}(\Gamma_{\mathrm{i}}) \times \mathrm{H}^{1/2}(\Gamma_{\mathrm{i}})}$ is bounded and then weakly converges, up to a subsequence, in $\mathrm{H}^{-1/2}(\Gamma_{\mathrm{i}}) \times \mathrm{H}^{1/2}(\Gamma_{\mathrm{i}})$ to $(\varphi^*, \psi^*) \in \mathrm{H}^{-1/2}(\Gamma_{\mathrm{i}}) \times \mathrm{H}^{1/2}(\Gamma_{\mathrm{i}})$ which minimizes $\mathcal{K}$. Therefore u_{φ^*} solves the Cauchy problem (2) and we have also the weak convergence $u_{\varphi_n^*} \rightharpoonup u_{\varphi^*}$ in $\mathrm{H}^1(\Omega)$;*
2. *$\|(\varphi_n^*, \psi_n^*)\|_{\mathrm{H}^{-1/2}(\Gamma_{\mathrm{i}}) \times \mathrm{H}^{1/2}(\Gamma_{\mathrm{i}})}$ diverges.*

In order to overcome the possible numerical problems due to the non-coercivity of the Kohn-Vogelius functional, and therefore the non-assured convergence to a minimizer, and to deal with the ill-posedness of the problem stated in [18, 55], we propose to consider a regularization of the Kohn-Vogelius functional. The most natural regularization to overcome the non-existence of minimizers is the well known Tikhonov regularization, which, by adding a small penalization term, adds coercivity to the minimization problem.

Then, we introduce the regularized Kohn-Vogelius functional $\mathcal{K}_\varepsilon : \mathrm{H}^{-1/2}(\Gamma_{\mathrm{i}}) \times \mathrm{H}^{1/2}(\Gamma_{\mathrm{i}}) \to \mathbb{R}$ given by, for $\varepsilon > 0$:

$$\mathcal{K}_\varepsilon(\varphi, \psi) := \mathcal{K}(\varphi, \psi) + \frac{\varepsilon}{2}\left(\|v_\varphi\|^2_{\mathrm{H}^1(\Omega)} + \|v_\psi\|^2_{\mathrm{H}^1(\Omega)}\right) =: \mathcal{K}(\varphi, \psi) + \frac{\varepsilon}{2}\|(v_\varphi, v_\psi)\|^2_{(\mathrm{H}^1(\Omega))^2}, \tag{8}$$

where $v_\varphi := u^0_\varphi$, $v_\psi := u^0_\psi$ satisfies (7).

We study this functional which is more 'well-behaved' than its non-regularized version, in particular we have the existence of minimizers for every $\varepsilon > 0$. Moreover, our main result for this functional is the following convergence theorem in the case that the data (g_N, g_D) is compatible:

Theorem 0.5 *Let us suppose that (g_D, g_N) is compatible data related to u_{ex} and let us denote by $u_{\varphi_\varepsilon^*}$ the function associated with φ_ε^* minimizer of $\mathcal{K}_\varepsilon$. Then*

$$\lim_{\varepsilon \to 0} \|u_{\varphi_\varepsilon^*} - u_{\mathrm{ex}}\|_{\mathrm{H}^1(\Omega)} = 0. \tag{9}$$

We also have a result which relates the sequence formed by minimizers of the regularized Kohn-Vogelius functional for each ε with the previously defined concept of

pseudo-solution, and moreover, defines an existence criterion to the data completion problem based into the behavior of the sequence of minimizers:

Theorem 0.6 *For each $\varepsilon > 0$, let $(\varphi_\varepsilon^*, \psi_\varepsilon^*) \in \mathrm{H}^{-1/2}(\Gamma_\mathrm{i}) \times \mathrm{H}^{1/2}(\Gamma_\mathrm{i})$ the minimizer of $\mathcal{K}_\varepsilon$. The sequence $(\varphi_\varepsilon^*, \psi_\varepsilon^*)_\varepsilon$ $(\varepsilon \to 0)$ defines a minimizing sequence of $\mathcal{K}$ and therefore a defines a pseudo-solution of (3). If $(\varphi_\varepsilon^*, \psi_\varepsilon^*)_\varepsilon$ is bounded, then this sequence converges in $\mathrm{H}^{-1/2}(\Gamma_\mathrm{i}) \times \mathrm{H}^{1/2}(\Gamma_\mathrm{i})$ to (φ^*, ψ^*) minimizer of $\mathcal{K}$.*

All the presented results consider that, in the case of existence of solution, the data (g_N, g_D) are perfect. This situation is far from the reality, as any real measurement will lead to some degree of error (white noise, instrumental limitations, etc.), due to this, we also have studied the case when the available data contains some level of noise $\delta > 0$, data which will be denoted (g_N^δ, g_D^δ) (which may be compatible or not) and will satisfy:

$$\|g_D - g_D^\delta\|_{\mathrm{H}^{1/2}(\Gamma_{obs})} + \|g_N - g_N^\delta\|_{\mathrm{H}^{-1/2}(\Gamma_{obs})} \leq \delta. \tag{10}$$

In this case, we should establish a relationship between the regularization parameter ε and the noise level δ in order to have convergence, this is known in the regularization of inverse problems literature (see for example [48]) as a 'parameter choice rule', and in this case, we have the following result:

Proposition 0.7 *Given (g_N, g_D) compatible data associated with exact solution (φ^*, ψ^*). Let us consider $\varepsilon = \varepsilon(\delta)$ such that*

$$\lim_{\delta \to 0} \varepsilon(\delta) = 0 \qquad \textit{and} \qquad \lim_{\delta \to 0} \frac{\delta}{\sqrt{\varepsilon}} = 0. \tag{11}$$

Then, we have:

$$\lim_{\delta \to 0} \|(\varphi_{\varepsilon,\delta}^*, \psi_{\varepsilon,\delta}^*) - (\varphi^*, \psi^*)\|_{\mathrm{H}^{-1/2}(\Gamma_\mathrm{i}) \times \mathrm{H}^{1/2}(\Gamma_\mathrm{i})} = 0,$$

where $(\varphi_{\varepsilon,\delta}^*, \psi_{\varepsilon,\delta}^*)$ are the minimizer of the regularized Kohn-Vogelius functional with noisy Cauchy data (g_N^δ, g_D^δ).

This type of result gives us a relationship which ε and δ must meet in order to have convergence in the noisy case (when the data available is compatible). However, in the practice they don't respond to any criteria in particular. So, as a final analysis in this chapter, we explore the possibility of defining a 'choice parameter rule'. In our case, this choice will relate the level of noise and the noisy solution of the regularized Kohn-Vogelius functional 'the approximate solution', to the regularization parameter following the so-called Morozov discrepancy principle.

This principle is based on choosing the biggest $\varepsilon = \varepsilon(\delta, (g_N^\delta, g_D^\delta))$, in order to have the highest possible regularity of the obtained solution, such that the Kohn-Vogelius functional with the polluted data is at the same order of the discrepancy measure, which is defined as the value (or discrepancy) when one evaluates the real

solution into the Kohn-Vogelius functional with polluted data. Due to monotonicity properties of the Kohn-Vogelius functional this parameter is uniquely defined, and moreover, we conclude this chapter by proving that this strategy defines an $\varepsilon(\delta)$ that satisfies the conditions of Proposition 0.7.

Chapter 2: Numerical resolution of the data completion problem.

In this chapter, we reconstruct numerically an harmonic function only from the knowledge of Dirichlet and Neumann data in an 'accessible' part of the boundary Γ_{obs}. By considering the theoretical approach given in the previous chapter we implement a gradient algorithm in order to minimize the regularized Kohn-Vogelius functional $\mathcal{K}_\varepsilon$, the obtained results asserts that if we choose a small regularization parameter the obtained solution will be close to the real solution, whenever it exists, due to the convergence to the real solution as the regularization parameter $\varepsilon \to 0$ and the monotone behavior of the Kohn-Vogelius functional with respect to ε.

In order to implement a gradient algorithm we begin by computing the partial derivatives of the regularized functional and, using adjoint problems, we find descent directions as the following proposition details:

Proposition 0.8 *For all* $(\varphi,\psi),(\widetilde{\varphi},\widetilde{\psi}) \in \mathrm{H}^{-1/2}(\Gamma_{\mathrm{i}})\times\mathrm{H}^{1/2}(\Gamma_{\mathrm{i}})$*, the partial derivatives of the functional* $\mathcal{K}_\varepsilon(\varphi,\psi)$ *are given by*

$$\frac{\partial \mathcal{K}_\varepsilon}{\partial \varphi}(\varphi,\psi)\,[\widetilde{\varphi}] = \int_{\Gamma_{\mathrm{i}}} \widetilde{\varphi}\cdot(u_\varphi + \varepsilon v_\varphi + w_D - \psi)$$

and

$$\frac{\partial \mathcal{K}_\varepsilon}{\partial \psi}(\varphi,\psi)\left[\widetilde{\psi}\right] = \langle(\partial_\nu u_\psi + \varepsilon\partial_\nu v_\psi + \partial_\nu w_N - \varphi),\widetilde{\psi}\rangle_{\Gamma_{\mathrm{i}}},$$

where, $w_N, w_D \in \mathrm{H}^1(\Omega)$ *are the respective solutions of the following adjoint problems:*

$$\left\{\begin{array}{rcll} -\Delta w_N &=& -\varepsilon v_\psi & \text{in } \Omega \\ \partial_{\mathbf{n}} w_N &=& \partial_{\mathbf{n}} u_\varphi - g_N & \text{on } \Gamma_{obs} \\ w_N &=& 0 & \text{on } \Gamma_{\mathrm{i}} \end{array}\right.$$

and

$$\left\{\begin{array}{rcll} -\Delta w_D &=& \varepsilon v_\varphi & \text{in } \Omega \\ w_D &=& u_\psi - g_D & \text{on } \Gamma_{obs} \\ \partial_{\mathbf{n}} w_D &=& 0 & \text{on } \Gamma_{\mathrm{i}}. \end{array}\right.$$

In particular, the directions $\left(\widetilde{\varphi},\widetilde{\psi}\right) \in \mathrm{H}^{-1/2}(\Gamma_{\mathrm{i}})\times\mathrm{H}^{1/2}(\Gamma_{\mathrm{i}})$ *given by:*

$$\widetilde{\varphi} = \psi - u_\varphi|_{\Gamma_{\mathrm{i}}} - \varepsilon v_\varphi|_{\Gamma_{\mathrm{i}}} - w_D|_{\Gamma_{\mathrm{i}}},$$

and

$$\widetilde{\psi} = -v_W|_{\Gamma_{\mathrm{i}}},$$

with $W = \varphi - \partial_\nu u_\psi|_{\Gamma_{\mathrm{i}}} - \varepsilon\partial_\nu v_\psi|_{\Gamma_{\mathrm{i}}} - \partial_\nu w_N|_{\Gamma_{\mathrm{i}}} \in \mathrm{H}^{-1/2}(\Gamma_{\mathrm{i}})$*, are descent directions.*

The obtained expression for the descent directions allow us to implement a gradient algorithm. The implementation of the algorithm is made using the finite element library 'FreeFEM++' [60].

We test the algorithm under two scenarios with their own interest. The first one is when the accessible and unaccessible part of the boundary have common points, this is, $\overline{\Gamma_{obs}} \cap \overline{\Gamma_{\mathrm{i}}} \neq \emptyset$. The regularity of the involved systems may become an issue (see [75]) and the obtained results follows this behavior as the obtained error is at least one order of magnitude higher than the more regular case. The second case is when the accessible and unaccessible part of the boundary do not have common points, this is, $\overline{\Gamma_{obs}} \cap \overline{\Gamma_{\mathrm{i}}} = \emptyset$. The classical regularity results from elliptic equations are applicable and the obtained results are in concordance with this.

We explore additionally the case when the accessible boundary data contains noise, the error between the real and obtained solution is higher in relation with the unpolluted case, as expected, however the obtained solution is close to the real one.

In the case when the boundaries have common points we propose a method in order to improve the convergence, the idea is to interpolate the value into the unaccessible part of the boundary based on the value given in the common points, simulations suggest that this improves the convergence, and in fact, they suggest that the convergence is influenced by the initial guess for unaccessible data (φ_0, ψ_0). When the boundaries do not have common points we consider $(\varphi_0, \psi_0) = (0, 0)$, the simulations suggests that the convergence to the real solution are not compromised by this choice.

We give in Figure 1 below an example of reconstruction with $\overline{\Gamma_{obs}} \cap \overline{\Gamma_{\mathrm{i}}} \neq \emptyset$.

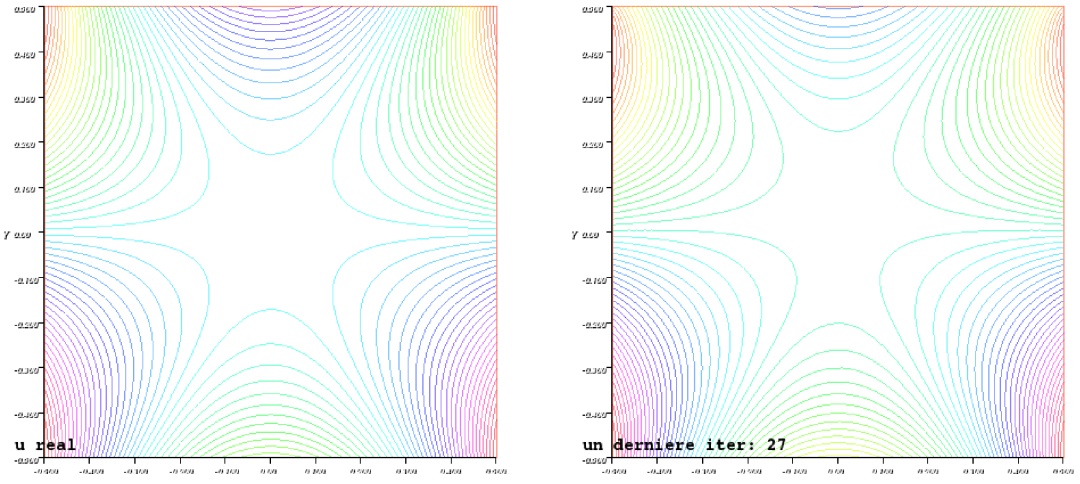

Figure 1: Example when $\overline{\Gamma_{obs}} \cap \overline{\Gamma_{\mathrm{i}}} \neq \emptyset$, real solution (left) and obtained solution (right).

Chapter 3: Obstacle detection with incomplete data via geometrical shape optimization.

In this chapter we consider the numerical reconstruction of an obstacle by means of partial boundary measurements from a harmonic function. We want to reconstruct an obstacle which is supposed to be static, by reconstruct we mean determine their position and shape. We will suppose that the obstacle ω is completely inside the reference domain Ω, governed by the Laplace equation, and we will obtain Dirichlet and Neumann data into the accessible part of the boundary Γ_{obs}, while no information is available into Γ_{i}, the unaccessible part of the boundary, these parts are such that $\overline{\Gamma_{obs}} \cup \overline{\Gamma_{\mathrm{i}}} = \partial\Omega$. We also assume the homogeneous Dirichlet boundary condition is imposed on the boundary $\partial\omega$ of the obstacle.

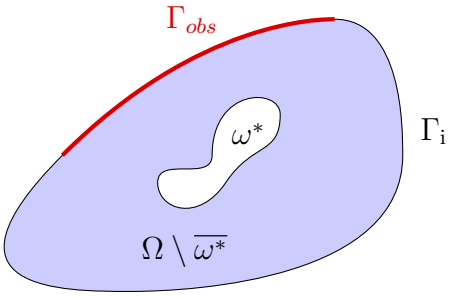

Figure 2: Illustration of the problem.

Assuming that the obstacle ω^* is regular enough, more precisely belongs to the following set of admissible domains

$$\mathcal{D} := \left\{ \omega \subset\subset \Omega \text{ of class } C^{1,1} \text{ such that } \Omega \setminus \overline{\omega} \text{ is connected} \right\},$$

and given a Cauchy pair $(g_N, g_D) \in \mathrm{H}^{-1/2}(\Gamma_{obs}) \times \mathrm{H}^{1/2}(\Gamma_{obs})$ such that $(g_N, g_D) \neq (0,0)$, we introduce the following inverse problem:

$$\begin{array}{c} \textit{Find a set } \omega^* \in \mathcal{D} \textit{ and a solution } u \in \mathrm{H}^1\left(\Omega \backslash \overline{\omega^*}\right) \cap C^0\left(\overline{\Omega \backslash \overline{\omega^*}}\right) \\ \textit{of the following overdetermined boundary value problem:} \\ \left\{ \begin{array}{rcll} -\Delta u & = & 0 & \text{in } \Omega \backslash \overline{\omega^*} \\ u & = & g_D & \text{on } \Gamma_{obs} \\ \partial_{\mathbf{n}} u & = & g_N & \text{on } \Gamma_{obs} \\ u & = & 0 & \text{on } \omega^*. \end{array} \right. \end{array}$$

Identifiability results (see [44, Proposition 4.4, page 87], for example) asserts that this problem has a unique solution, whose proof is based on a unique continuation argument. The important point here is to recall that we do not need any information on the unaccessible boundary Γ_{i}. However, if we would like to solve it by means of the minimization of a shape functional, we will need to consider well-posed PDE problems, which in particular need data over the whole boundary $\partial\Omega$. To overcome this difficulty we propose to extend the previously studied problem: the data completion problem. The basic idea resides in using an algorithm which in first place 'complete' the data in a way that the obtained solution is good enough

to use it for the obstacle reconstruction by means of minimizing the Kohn-Vogelius functional with geometrical shape optimization methods, which demands the solution of a well-posed problem, in this case, the completed one. To this end we extend the data completion problem by adding the unknown object ω as a parameter to the Kohn-Vogelius functional and its regularized version, with a prescribed Dirichlet homogeneous condition over $\partial\omega$. So, we will consider in this chapter the following optimization problem:

$$(\omega^*, \varphi^*, \psi^*) \in \underset{(\omega,\varphi,\psi)\in\mathcal{D}\times \mathrm{H}^{-1/2}(\Gamma_\mathrm{i})\times \mathrm{H}^{1/2}(\Gamma_\mathrm{i})}{\operatorname{argmin}} \mathcal{K}_\varepsilon(\omega, \varphi, \psi)$$

where $\mathcal{K}_\varepsilon$ is the nonnegative regularized Kohn-Vogelius cost functional defined by

$$\begin{aligned} \mathcal{K}_\varepsilon(\omega, \varphi, \psi) &:= \mathcal{K}(\omega, \varphi, \psi) + \frac{\varepsilon}{2}\|(v_\varphi, v_\psi)\|^2_{\mathrm{H}^1(\Omega\setminus\overline{\omega})} \\ &= \frac{1}{2}\int_{\Omega\setminus\overline{\omega}} |\nabla u_\varphi - \nabla u_\psi|^2 + \frac{\varepsilon}{2}\|(v_\varphi, v_\psi)\|^2_{\mathrm{H}^1(\Omega\setminus\overline{\omega})} \end{aligned}$$

where $u_\varphi \in \mathrm{H}^1(\Omega\setminus\overline{\omega})$ and $u_\psi \in \mathrm{H}^1(\Omega\setminus\overline{\omega})$ satisfies the extended problems:

$$\left\{\begin{array}{rcll} -\Delta u_\varphi(\omega) &=& 0 & \text{in } \Omega\setminus\overline{\omega} \\ u_\varphi(\omega) &=& g_D & \text{on } \Gamma_{obs} \\ \partial_\mathbf{n} u_\varphi(\omega) &=& \varphi & \text{on } \Gamma_\mathrm{i} \\ u_\varphi(\omega) &=& 0 & \text{on } \partial\omega \end{array}\right. \quad \text{and} \quad \left\{\begin{array}{rcll} -\Delta u_\psi(\omega) &=& 0 & \text{in } \Omega\setminus\overline{\omega} \\ \partial_\mathbf{n} u_\psi(\omega) &=& g_N & \text{on } \Gamma_{obs} \\ u_\psi(\omega) &=& \psi & \text{on } \Gamma_\mathrm{i} \\ u_\psi(\omega) &=& 0 & \text{on } \partial\omega, \end{array}\right.$$

An analogous extension with an homogeneous Dirichlet condition on $\partial\omega$, applies to the problems solved by $v_\varphi := u^0_\varphi, v_\psi := u^0_\psi$.

The utilization of the regularized functional is justified by the ill-posedness of the data completion problem, as we have remarked in Chapter 1. However, it is interesting to observe that the identifiability result ensures that $\mathcal{K}(\omega, \varphi, \psi) = 0$ if and only if $(\omega, \varphi, \psi) = (\omega^*, \varphi^*, \psi^*)$, where ω^* is the real obstacle, and (φ^*, ψ^*) correspond to the real Cauchy data in Γ_i for the harmonic function u for which the given data (g_N, g_D) is taken.

In order to reconstruct the obstacle ω^* we use a geometrical shape optimization method in order to minimize the regularized Kohn-Vogelius functional: we use the shape gradient of this functional. The shape gradient of a functional measures, roughly speaking, the variation of the functional whenever we perform a small regular perturbation of the boundary in the direction of exterior normal. In our case we have, for properly defined perturbation directions, the following result for the regularized Kohn-Vogelius functional:

Proposition 0.9 (First order shape derivative of the functional) *For* $\boldsymbol{V} \in \boldsymbol{U} := \left\{\theta \in \mathbf{W}^{2,\infty}(\mathbb{R}^\mathrm{d}) :\ \text{Supp } \theta \subset\subset \Omega\right\}$, *an admissible perturbation direction, the regular-*

ized Kohn-Vogelius cost functional $\mathcal{K}_\varepsilon$ is differentiable at ω in the direction $\boldsymbol{V}$ with

$$\begin{aligned}\mathrm{D}\mathcal{K}_\varepsilon(\Omega\backslash\overline{\omega})\cdot\boldsymbol{V} = &-\int_{\partial\omega}(\partial_{\mathbf{n}}\rho_N^u\cdot\partial_{\mathbf{n}}u_\varphi+\partial_{\mathbf{n}}\rho_N^v\cdot\partial_{\mathbf{n}}v_\varphi)(\boldsymbol{V}\cdot\mathbf{n})+\frac{1}{2}\int_{\partial\omega}|\nabla w|^2\,(\boldsymbol{V}\cdot\mathbf{n})\\ &-\int_{\partial\omega}(\partial_{\mathbf{n}}\rho_D^u\cdot\partial_{\mathbf{n}}u_\psi+\partial_{\mathbf{n}}\rho_D^v\cdot\partial_{\mathbf{n}}v_\psi)(\boldsymbol{V}\cdot\mathbf{n})\\ &+\frac{\varepsilon}{2}\int_{\partial\omega}(|\nabla v_\varphi|^2+|\nabla v_\psi|^2+|v_\varphi|^2+|v_\psi|^2)(\boldsymbol{V}\cdot\mathbf{n}),\end{aligned}$$

where $w := u_\varphi - u_\psi$ and where $\rho_D^u, \rho_N^u, \rho_D^v, \rho_N^v \in \mathrm{H}^1(\Omega\backslash\overline{\omega})$ are the respective solutions of the following adjoint states

$$\left\{\begin{array}{rcll}-\Delta\rho_N^u &=& 0 & \text{in } \Omega\backslash\overline{\omega}\\ \rho_N^u &=& g_D-u_\psi & \text{on } \Gamma_{obs}\\ \partial_{\mathbf{n}}\rho_N^u &=& 0 & \text{on } \Gamma_{\mathrm{i}}\\ \rho_N^u &=& 0 & \text{on } \partial\omega,\end{array}\right. \qquad \left\{\begin{array}{rcll}-\Delta\rho_N^v &=& -\varepsilon v_\varphi & \text{in } \Omega\backslash\overline{\omega}\\ \rho_N^v &=& 0 & \text{on } \Gamma_{obs}\\ \partial_{\mathbf{n}}\rho_N^v &=& 0 & \text{on } \Gamma_{\mathrm{i}}\\ \rho_N^v &=& 0 & \text{on } \partial\omega\end{array}\right.$$

and

$$\left\{\begin{array}{rcll}-\Delta\rho_D^u &=& 0 & \text{in } \Omega\backslash\overline{\omega}\\ \partial_{\mathbf{n}}\rho_D^u &=& 0 & \text{on } \Gamma_{obs}\\ \rho_D^u &=& \psi-u_\varphi & \text{on } \Gamma_{\mathrm{i}}\\ \rho_D^u &=& 0 & \text{on } \partial\omega,\end{array}\right. \qquad \left\{\begin{array}{rcll}-\Delta\rho_D^v &=& -\varepsilon v_\psi & \text{in } \Omega\backslash\overline{\omega}\\ \partial_{\mathbf{n}}\rho_D^v &=& 0 & \text{on } \Gamma_{obs}\\ \rho_D^v &=& \varepsilon\psi & \text{on } \Gamma_{\mathrm{i}}\\ \rho_D^v &=& 0 & \text{on } \partial\omega.\end{array}\right.$$

The utility of the adjoint problems introduced in the above result relies on obtaining an expression of the shape gradient of the regularized Kohn-Vogelius functional which depends explicitly on the perturbation direction $\boldsymbol{V}$, which permits the computation of this object from numerical point of view. It is important to remark that the existence of shape derivative is not trivial, however the arguments are standard with the same analysis as in [61].

In order to perform the numerical simulations, we consider an algorithm which in first place performs the completion of the given data supposing we have a potential obstacle ω and applying the same gradient algorithm as in Chapter 2, and then, performing the update of the obstacle ω by using a shape gradient algorithm. For this we follow the same strategy as in [3] or in [37], a regularization by parametrization of the obstacle boundary $\partial\omega$. Indeed, we need to regularize the functional with respect to the shape since, according to [3, Theorem 2], the shape gradient has not a uniform sensitivity with respect to the deformation direction. Hence, we restrict ourselves to star-shaped domains and use polar coordinates for parametrization: the boundary $\partial\omega$ of the object can be then parametrized by

$$\partial\omega = \left\{\begin{pmatrix}x_0\\ y_0\end{pmatrix} + r(\theta)\begin{pmatrix}\cos\theta\\ \sin\theta\end{pmatrix},\ \theta\in[0,2\pi)\right\},$$

where $x_0, y_0 \in \mathbb{R}$ and where r is a $C^{1,1}$ function, 2π-periodic and without double point. Taking into account the ill-posedness of the problem, we approximate the

polar radius r by its truncated Fourier series

$$r_N(\theta) := a_0^N + \sum_{k=1}^{N} a_k^N \cos(k\theta) + b_k^N \sin(k\theta),$$

for the numerical simulations. This regularization by projection permits to remove *high frequencies* generated by $\cos(k\theta)$ and $\sin(k\theta)$ for $k >> 1$, for which the functional is degenerated. Then, the unknown shape is entirely defined by the coefficients $(a_{\mathrm{i}}, b_{\mathrm{i}})$. Hence, for $k = 1, \ldots, N$, the corresponding deformation directions are respectively,

$$\boldsymbol{V}_1 := \boldsymbol{V}_{x_0} := \begin{pmatrix} 1 \\ 0 \end{pmatrix}, \quad \boldsymbol{V}_2 := \boldsymbol{V}_{y_0} := \begin{pmatrix} 0 \\ 1 \end{pmatrix}, \quad \boldsymbol{V}_3(\theta) := \boldsymbol{V}_{a_0}(\theta) := \begin{pmatrix} \cos\theta \\ \sin\theta \end{pmatrix},$$

$$\boldsymbol{V}_{2k+2}(\theta) := \boldsymbol{V}_{a_k}(\theta) := \cos(k\theta) \begin{pmatrix} \cos\theta \\ \sin\theta \end{pmatrix}, \quad \boldsymbol{V}_{2k+3}(\theta) := \boldsymbol{V}_{b_k}(\theta) := \sin(k\theta) \begin{pmatrix} \cos\theta \\ \sin\theta \end{pmatrix},$$

$\theta \in [0, 2\pi)$. The gradient is then computed component by component using its characterization, from the previous proposition:

$$\Big(\nabla \mathcal{K}_\varepsilon(\Omega \backslash \overline{\omega})\Big)_k = \mathrm{D}\mathcal{K}_\varepsilon(\Omega \backslash \overline{\omega}) \cdot \boldsymbol{V}_k, \qquad k = 1, \ldots, 2N + 3.$$

We have tested our algorithm in several scenarios, with different shapes to be reconstructed with unpolluted and polluted given data. We obtain interesting results in the reconstruction itself, however the data completion process seems to be of lower precision than the one without the unknown obstacle.

We present a 'difficult' example in Figure 3 below, on the left we have the real obstacle (a square) and on the right the obtained obstacle.

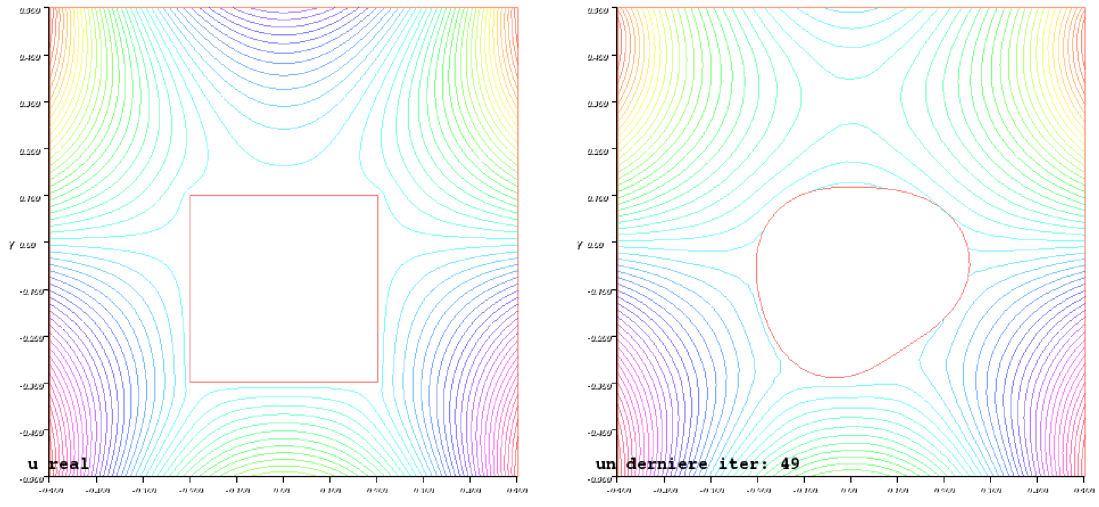

Figure 3: Detection of a square with incomplete boundary data: Positive results.

PART II: The inverse obstacle problem using topological shape optimization in a bidimensional Stokes flow.

Chapter 4: Small object detection using topological optimization.

In this chapter we change our point of view. Our aim now is, considering a region Ω containing a Newtonian and incompressible fluid with coefficient of kinematic viscosity $\nu > 0$ governed by the stationary 2D Stokes equations, reconstruct an unknown number of small obstacles which are considered with a no-slip boundary condition. Then, our aim is to determine the number, relative location and approximate shape of each obstacle.

We have two main differences with the previous considered work: We are considering now a vectorial case and we are adding a new degree of freedom: the number of obstacles, which implies that the topology of the problem can change during the numerical reconstruction.

The hypothesis of small objects allows us to perform the so-called topological sensitivity analysis (see [17]), in which we study the variation of a cost functional when we add an obstacle to the domain of study. The precise object which measure this variation is the so-called topological derivative introduced by Schumacher in 1995 (see [76]) and formalized by Sokolowski *et al.* in 1997 (see [80]). Posing the inverse problem as the minimization of a Kohn-Vogelius type functional, the topological sensitivity analysis will allow, based on the study of the topological derivative of the Kohn-Vogelius functional, determine the number and relative location of the obstacles inside the region Ω. In order to determine the shape of the obstacles we need an additional tool, for example the shape gradient used in the precedent chapter, however this additional feature will be considered in the numerical reconstruction in the final chapter of this thesis.

Let $\omega \subset \mathbb{R}^2$ a fixed bounded Lipschitz domain containing the origin, such that $\overline{\omega} \subset B(0,1)$. For $z \in \Omega$ and $0 < \varepsilon << 1$, we introduce:

$$\omega_{z,\varepsilon} := z + \varepsilon\omega.$$

The aim of is to detect some unknown objects included in Ω. We assume that a finite number m^* of obstacles $\omega_{z_j^*,\varepsilon_j^*} \subset \Omega,\ j \in \{1,\dots,m^*\}$ have to be detected. Moreover, we assume that they are well separated (that is: $\overline{\omega}_{z_{\mathrm{i}}^*,\varepsilon_{\mathrm{i}}^*} \cap \overline{\omega}_{z_j^*,\varepsilon_j^*} = \emptyset$ for all $1 \leq \mathrm{i}, j \leq m^*$ with $\mathrm{i} \neq j$) and have the geometry form

$$\omega_{z_k^*,\varepsilon_k^*} = z_k^* + \varepsilon_k^*\omega, \qquad 1 \leq k \leq m^*,$$

where ε_k^* is the diameter and the points $z_k^* \in \Omega$, $1 \leq k \leq m^*$, determine the location of the objects.

Let $\boldsymbol{f} \in \mathbf{H}^{1/2}(\partial\Omega)$ such that $\boldsymbol{f} \neq \mathbf{0}$ a measurement over the whole boundary

which satisfies the compatibility condition

$$\int_{\partial\Omega} \boldsymbol{f}\cdot\mathbf{n} = 0. \tag{12}$$

In order to determine the location of the objects, we also make a measurement $\boldsymbol{g}\in\mathbf{H}^{-1/2}(O)$ on a part O of the exterior boundary $\partial\Omega$ with $O\subset\partial\Omega,\ O\neq\partial\Omega$. Then, we denote $\omega_\varepsilon^* := \bigcup_{k=1}^{m^*}\omega_{z_k^*,\varepsilon_k^*}$ and consider the following overdetermined Stokes problem:

$$\left\{\begin{array}{rcll} -\nu\Delta\boldsymbol{u}+\nabla p &=& \mathbf{0} & \text{in } \Omega\backslash\overline{\omega_\varepsilon^*}\\ \operatorname{div}\boldsymbol{u} &=& 0 & \text{in } \Omega\backslash\overline{\omega_\varepsilon^*}\\ \boldsymbol{u} &=& \boldsymbol{f} & \text{on } \partial\Omega\\ \boldsymbol{u} &=& \mathbf{0} & \text{on } \partial\omega_\varepsilon^*\\ \sigma(\boldsymbol{u},p)\mathbf{n} &=& \boldsymbol{g} & \text{on } O\subset\partial\Omega. \end{array}\right. \tag{13}$$

Here $\boldsymbol{u}$ represents the velocity of the fluid and p the pressure and $\sigma(\boldsymbol{u},p)$ represents the stress tensor defined by

$$\sigma(\boldsymbol{u},p) := \nu\left(\nabla\boldsymbol{u}+{}^t\nabla\boldsymbol{u}\right)-p\mathrm{I}.$$

Thus we consider the following geometric inverse problem:

Find $\omega_\varepsilon^*\subset\subset\Omega$ *and a pair* $(\boldsymbol{u},p)$ *which satisfy the overdetermined problem* (13). (14)

To study this inverse problem, we consider two forward problems:

$$\left\{\begin{array}{l} \text{Find } (\boldsymbol{u}_D^\varepsilon,p_D^\varepsilon)\in\mathbf{H}^1(\Omega\backslash\overline{\omega_\varepsilon})\times\mathrm{L}^2_0(\Omega\backslash\overline{\omega_\varepsilon}) \text{ such that}\\ \quad\begin{array}{rcll} -\nu\Delta\boldsymbol{u}_D^\varepsilon+\nabla p_D^\varepsilon &=& \mathbf{0} & \text{in } \Omega\backslash\overline{\omega_\varepsilon}\\ \operatorname{div}\boldsymbol{u}_D^\varepsilon &=& 0 & \text{in } \Omega\backslash\overline{\omega_\varepsilon}\\ \boldsymbol{u}_D^\varepsilon &=& \boldsymbol{f} & \text{on } \partial\Omega\\ \boldsymbol{u}_D^\varepsilon &=& \mathbf{0} & \text{on } \partial\omega_\varepsilon \end{array}\end{array}\right. \tag{15}$$

and

$$\left\{\begin{array}{l} \text{Find } (\boldsymbol{u}_M^\varepsilon,p_M^\varepsilon)\in\mathbf{H}^1(\Omega\backslash\overline{\omega_\varepsilon})\times\mathrm{L}^2(\Omega\backslash\overline{\omega_\varepsilon}) \text{ such that}\\ \quad\begin{array}{rcll} -\nu\Delta\boldsymbol{u}_M^\varepsilon+\nabla p_M^\varepsilon &=& \mathbf{0} & \text{in } \Omega\backslash\overline{\omega_\varepsilon}\\ \operatorname{div}\boldsymbol{u}_M^\varepsilon &=& 0 & \text{in } \Omega\backslash\overline{\omega_\varepsilon}\\ \sigma(\boldsymbol{u}_M^\varepsilon,p_M^\varepsilon)\mathbf{n} &=& \boldsymbol{g} & \text{on } O\\ \boldsymbol{u}_M^\varepsilon &=& \boldsymbol{f} & \text{on } \partial\Omega\backslash\overline{O}\\ \boldsymbol{u}_M^\varepsilon &=& \mathbf{0} & \text{on } \partial\omega_\varepsilon, \end{array}\end{array}\right. \tag{16}$$

where $\omega_\varepsilon := \bigcup_{k=1}^{m}\omega_{z_k,\varepsilon_k}$ for a finite number m of objects located in $z_1,\ldots,z_m$. These two forward problems are classically well-defined.

Notice that, assuming that $\boldsymbol{f},\boldsymbol{g}$ are the real data (this is, obtained without error), if ω_ε coincides with the actual domain ω_ε^*, then $\boldsymbol{u}_D^\varepsilon=\boldsymbol{u}_M^\varepsilon$ in $\Omega\backslash\overline{\omega_\varepsilon}$. According to this observation, we propose a resolution of the inverse problem (14) of reconstructing ω_ε^* based on the minimization of the following Kohn-Vogelius functional

$$\mathcal{F}_\varepsilon^{KV}(\boldsymbol{u}_D^\varepsilon,\boldsymbol{u}_M^\varepsilon) := \frac{1}{2}\int_{\Omega\backslash\overline{\omega_\varepsilon}}\nu|\mathcal{D}(\boldsymbol{u}_D^\varepsilon)-\mathcal{D}(\boldsymbol{u}_M^\varepsilon)|^2,$$

where $\mathcal{D}(\cdot) = \nabla(\cdot) + {}^t\nabla(\cdot)$.

We then define

$$\mathcal{J}_{KV}(\Omega\backslash\overline{\omega_\varepsilon}) := \mathcal{F}_\varepsilon^{KV}(\boldsymbol{u}_D^\varepsilon, \boldsymbol{u}_M^\varepsilon).$$

As we said before the topological sensitivity analysis consists in the study of the variations of a design functional $\mathcal{J}$ with respect to the insertion of a small obstacle $\omega_{z,\varepsilon}$ at the point $z \in \Omega$. The aim is to obtain an asymptotic expansion of $\mathcal{J}$ of the form

$$\mathcal{J}(\Omega_{z,\varepsilon}) = \mathcal{J}(\Omega) + \xi(\varepsilon)\delta\mathcal{J}(z) + o(\xi(\varepsilon)) \qquad \forall z \in \Omega, \tag{17}$$

where $\varepsilon > 0$, ξ is a positive scalar function intended to tend to zero with ε and where

$$\Omega_{z,\varepsilon} := \Omega\backslash\overline{\omega_{z,\varepsilon}},$$

with $\omega_{z,\varepsilon} := z + \varepsilon\omega$. We summarize the notations concerning the domains in Figure 4.

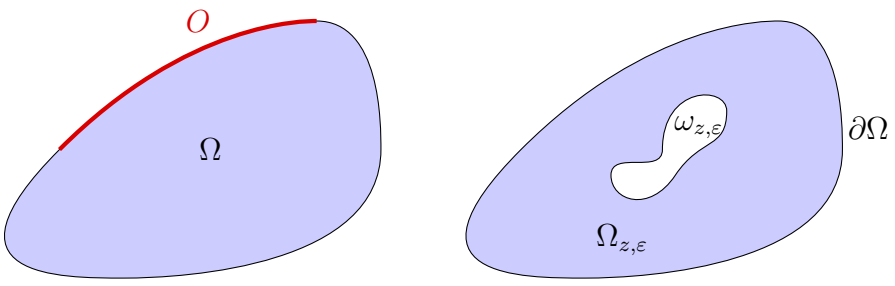

Figure 4: The initial domain and the same domain after inclusion of an object

In order to provide an asymptotic expansion of the Kohn-Vogelius functional $\mathcal{J}_{KV}$, we need first an asymptotic expansion of the solution of the Stokes problems (15) and (16).

Unlike the three-dimensional case, the two-dimensional problem cannot be approximated by an 'exterior problem', which in general in this case doesn't have a solution which vanishes at infinity. This kind of problem has been treated by Bonnaillie-Noël and Dambrine in [21] for the Laplace equation in the plane: we have followed this procedure in order to find a suitable approximation for the Stokes problem.

It is important to remark that the topological sensitivity analysis will be considered only for a single obstacle, this is not a problem in our aim to detect several obstacles because in the numerical algorithm we will apply the single obstacle result iteratively: first on Ω, then on $\Omega \setminus \overline{\omega_{z_1,\varepsilon_1}}$ and so on.

Proposition 0.10 *The respective solutions* $\boldsymbol{u}_D^\varepsilon \in \mathbf{H}^1(\Omega_{z,\varepsilon})$ *and* $\boldsymbol{u}_M^\varepsilon \in \mathbf{H}^1(\Omega_{z,\varepsilon})$ *of Problems* (15) *and* (16) *admit the following asymptotic expansion (with the subscript*

$\natural = D$ *and* $\natural = N$ *respectively):*

$$\boldsymbol{u}_\natural^\varepsilon(x) = \boldsymbol{u}_\natural^0(x) + \frac{1}{-\log\varepsilon}(\boldsymbol{C}_\natural(x) - \boldsymbol{U}_\natural(x)) + O_{\mathbf{H}^1(\Omega_{z,\varepsilon})}\left(\frac{1}{-\log\varepsilon}\right),$$

where $(\boldsymbol{U}_\natural, P_\natural) \in \mathbf{H}^1(\Omega) \times \mathrm{L}^2_0(\Omega)$ *solves the following Stokes problem defined in the whole domain* Ω

$$\left\{\begin{array}{rcll} -\nu\Delta\boldsymbol{U}_\natural + \nabla P_\natural &=& \mathbf{0} & \text{in } \Omega \\ \operatorname{div}\boldsymbol{U}_\natural &=& 0 & \text{in } \Omega \\ \boldsymbol{U}_\natural &=& \boldsymbol{C}_\natural & \text{on } \partial\Omega, \end{array}\right. \tag{18}$$

with

$$\boldsymbol{C}_\natural(x) := -4\pi\nu E(x-z)\boldsymbol{u}_\natural^0(z), \tag{19}$$

where E *is the fundamental solution of the Stokes equations in* $\mathbb{R}^2$ *given by*

$$E(x) = \frac{1}{4\pi\nu}\left(-\log\|x\|\mathrm{I} + \mathrm{e}_r{}^t\mathrm{e}_r\right), \qquad \boldsymbol{P}(x) = \frac{x}{2\pi\|x\|^2},$$

with $\mathrm{e}_r = \dfrac{x}{\|x\|}$*; that is* $-\nu\Delta E_j + \nabla\boldsymbol{P}_j = \delta\mathbf{e}_j$*, where* E_j *denotes the* j^{th} *column of* E*,* $(\mathbf{e}_j)_{j=1}^2$ *is the canonical basis of* $\mathbb{R}^2$ *and* δ *is the Dirac distribution. The notation* $O_{\mathbf{H}^1(\Omega_{z,\varepsilon})}\left(\frac{1}{-\log\varepsilon}\right)$ *means that there exist a constant* $c > 0$ *(independent of* ε*) and* $\varepsilon_1 > 0$ *such that for all* $0 < \varepsilon < \varepsilon_1$

$$\left\|\boldsymbol{u}_\natural^\varepsilon(x) - \boldsymbol{u}_\natural^0(x) - h_\varepsilon(\boldsymbol{C}_\natural(x) - \boldsymbol{U}_\natural(x))\right\|_{1,\Omega_{z,\varepsilon}} \leq \frac{c}{-\log\varepsilon}.$$

In order to perform the asymptotic expansion of the Kohn-Vogelius functional using the previous result, we need to rewrite the functional difference $\mathcal{J}_{KV}(\Omega_\varepsilon) - \mathcal{J}_{KV}(\Omega)$ to obtain a decoupled expression. This is, an expression in which each integral only depends on $\boldsymbol{u}_D^\varepsilon, \boldsymbol{u}_D^0$ or $\boldsymbol{u}_M^\varepsilon, \boldsymbol{u}_N^0$, without mixed terms. The following lemma shows the desired decomposition:

Lemma 0.11 *We have*

$$\mathcal{J}_{KV}(\Omega_\varepsilon) - \mathcal{J}_{KV}(\Omega) = A_D + A_M, \tag{20}$$

where

$$A_D := \frac{1}{2}\nu\int_{\Omega_\varepsilon}\mathcal{D}(\boldsymbol{u}_D^\varepsilon - \boldsymbol{u}_D^0) : \mathcal{D}(\boldsymbol{u}_D^\varepsilon - \boldsymbol{u}_D^0) + \nu\int_{\Omega_\varepsilon}\mathcal{D}(\boldsymbol{u}_D^\varepsilon - \boldsymbol{u}_D^0) : \mathcal{D}(\boldsymbol{u}_D^0) - \frac{1}{2}\nu\int_{\omega_\varepsilon}|\mathcal{D}(\boldsymbol{u}_D^0)|^2$$

and

$$A_M := \int_{\partial\omega_\varepsilon}\left[\sigma(\boldsymbol{u}_M^\varepsilon - \boldsymbol{u}_M^0, p_M^\varepsilon - p_M^0)\mathbf{n}\right]\cdot\boldsymbol{u}_M^0 - \frac{1}{2}\nu\int_{\omega_\varepsilon}|\mathcal{D}(\boldsymbol{u}_M^0)|^2.$$

Finally, using Proposition 0.10 in Lemma 0.11 we can obtain the desired result:

Theorem 0.12 *For $z \in \Omega$, the functional $\mathcal{J}_{KV}$ admits the following topological asymptotic expansion*

$$\mathcal{J}_{KV}(\Omega_{z,\varepsilon}) - \mathcal{J}_{KV}(\Omega) = \frac{4\pi\nu}{-\log\varepsilon}(|\boldsymbol{u}_D^0(z)|^2 - |\boldsymbol{u}_M^0(z)|^2) + o\left(\frac{1}{-\log\varepsilon}\right),$$

where $\boldsymbol{u}_D^0 \in \mathbf{H}^1(\Omega)$ and $\boldsymbol{u}_M^0 \in \mathbf{H}^1(\Omega)$ solve respectively Problems (15) and (16) with $\omega_\varepsilon = \emptyset$ and $o(f(\varepsilon))$ is the set of functions $g(\varepsilon)$ such that $\lim_{\varepsilon\to 0}\frac{g(\varepsilon)}{f(\varepsilon)} = 0$. Therefore, we have

$$\xi(\varepsilon) = \frac{1}{-\log\varepsilon} \quad \text{and} \quad \delta\mathcal{J}_{KV}(z) = 4\pi\nu(|\boldsymbol{u}_D^0(z)|^2 - |\boldsymbol{u}_M^0(z)|^2)$$

in the general asymptotic expansion (17).

It is interesting to notice that, unlike the 3-dimensional case, the obtained expression is valid for any possible admissible geometry of ω. Which is in concordance with the literature (see for example [9, 10, 53, 54]).

With the obtained results we have to remark that, using expression (17)

$$\mathcal{J}(\Omega_{z,\varepsilon}) - \mathcal{J}(\Omega) = \xi(\varepsilon)\delta\mathcal{J}(z) + o(\xi(\varepsilon)) \quad \forall z \in \Omega,$$

thus, the functional will decrease its value if we add an obstacle with shape ω_ε in $z \in \Omega$ such that $\delta\mathcal{J}(z) < 0$. Moreover, this means that the minimization of $\mathcal{J}$ will be equivalent to the inclusion of an obstacle centered in the point z where $\delta\mathcal{J}(z)$ is the most negative. In the final chapter we will implement an algorithm in which we use this criterion to perform the numerical resolution of the considered problem.

Chapter 5: Numerical detection of obstacles: Topological and mixed optimization method.

In this chapter we perform the numerical reconstruction of an unknown number of obstacles immersed in a stationary fluid governed by the incompressible 2D Stokes equations from boundary measurements. Using the Kohn-Vogelius functional and its topological derivative, obtained in the previous chapter and summarized into Theorem 0.12, we are capable to minimize the functional using a topological gradient algorithm, which allows to obtain the number and relative location of the desired obstacles.

We implement and explore the capabilities of the topological gradient algorithm using FreeFEM++ [60], the basic idea of the algorithm is, for a given domain, analyze the value of the topological derivative and insert an obstacle in the point $z \in \Omega$ where the topological gradient of the Kohn-Vogelius functional $\delta\mathcal{J}_{KV}(z)$ is the most negative, and iterates this procedure until the functional begins to increase. We naturally implement some thresholding conditions in order to avoid adding two potential obstacles too close (we increase the size of the actual one in that case)

and avoid adding a potential obstacle which may cross the boundary (we force the object to be a little more 'inside' the domain).

We test the algorithm under several situations:

1. **When the obstacles are far between them and close to the boundary:** The obtained results are positive, the algorithm is capable to determine the number and relative location of the obstacles.
2. **When the obstacles have other geometry than circles:** The obtained results are interesting, (small) squares are properly detected in number and relative location. A more challenging problem is considered with a 'donut' and a circle far from each-other, both are detected and the relative size of the 'donut' is properly estimated by the algorithm.
3. **When the obstacles are far from the boundary:** Similarly to the results obtained by Caubet *et al.* in [36], we have seen that, if the obstacle is far from the boundary, then the obtained results may be wrong, in relative location or even in the capability of detect the obstacle.
4. **When the size of the obstacles is 'big':** As one can expect, if the size of the obstacle becomes too big, the asymptotic expansion cannot be longer valid. Numerically the results are diverse: wrong number of obstacles is predicted, or wrong size of the obstacles is predicted.
5. **When we introduce noise to the boundary data:** We have tested our algorithm in the case when the boundary data is polluted by noise, simulations shown that a relative high amount of noise is allowed (25%) to obtain correct estimates of the number of obstacles and their relative location, in the best case proposed: small obstacles close to the boundary.

We present two examples in Figures 5 and 6 below.

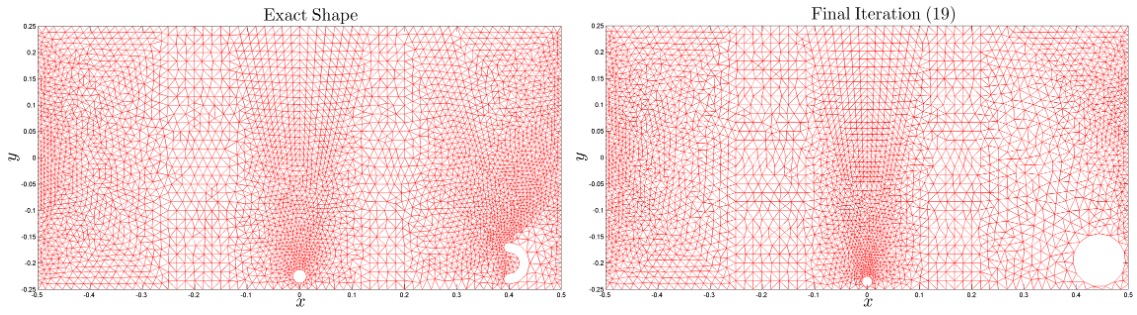

Figure 5: Detection of small circle and 'donut': Positive results.

Additionally, in order to improve the quality of the obtained results, we propose a new algorithm, which combines the capabilities of the topological gradient algorithm with the capabilities of an algorithm tested before: the shape gradient algorithm. The idea is to combine the capability of the topological gradient algorithm to determine the number and relative position of obstacles inside the domain of reference with the capability of the shape gradient algorithm to determine the relative shape of the obstacles, when the number of them is known.

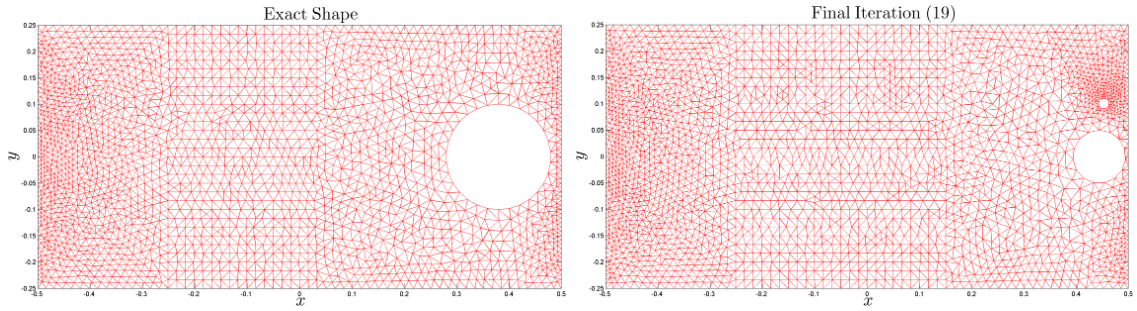

Figure 6: Bad Detection for a 'very big sized' object

Our mixed optimization method performs in first place a topological optimization, in order to fix the topology of the domain, this is, to fix the number of obstacles and their relative location, and then, we execute the shape gradient algorithm, which we can compute in this case, thanks to the following expression of the shape derivative of the Kohn-Vogelius functional (see [37, Proposition 2] for the existence proof and computation):

Proposition 0.13 (First order shape derivative of the functional) *For $\boldsymbol{V}$ an admissible deformation, the Kohn-Vogelius cost functional J_{KV} is differentiable at ω in the direction $\boldsymbol{V}$ with*

$$\mathrm{D}J_{KV}(\Omega\backslash\overline{\omega})\cdot\boldsymbol{V} = -\int_{\partial\omega}(\sigma(\boldsymbol{w},q)\,\mathbf{n})\cdot\partial_{\mathbf{n}}\boldsymbol{u_D}(\boldsymbol{V}\cdot\mathbf{n}) + \frac{1}{2}\nu\int_{\partial\omega}|\mathcal{D}(\boldsymbol{w})|^2\,(\boldsymbol{V}\cdot\mathbf{n}) \quad (21)$$

where $(\boldsymbol{w},q)$ is defined by

$$\boldsymbol{w} := \boldsymbol{u}_D - \boldsymbol{u}_M \qquad \text{and} \qquad q := p_D - p_M.$$

As in Chapter 3, due to the ill-posedness of the reconstruction of the boundary (in this particular case, see [37] for a detailed explanation), we have to take the same considerations on the boundary parametrization using truncated Fourier series.

The performed simulation (see Figure 7) shows an improvement in the shape of the obtained obstacle in comparison with the real obstacle and an improvement on the value of the Kohn-Vogelius functional, which justifies the extension of the topological gradient algorithm.

Publications

The studies in this manuscript have resulted in two articles: one is already published and one will be submitted shortly:

- *On the detection of several obstacles in 2D Stokes flow: topological sensitivity and combination with shape derivatives*, written with F. Caubet and C. Conca (see [35]).

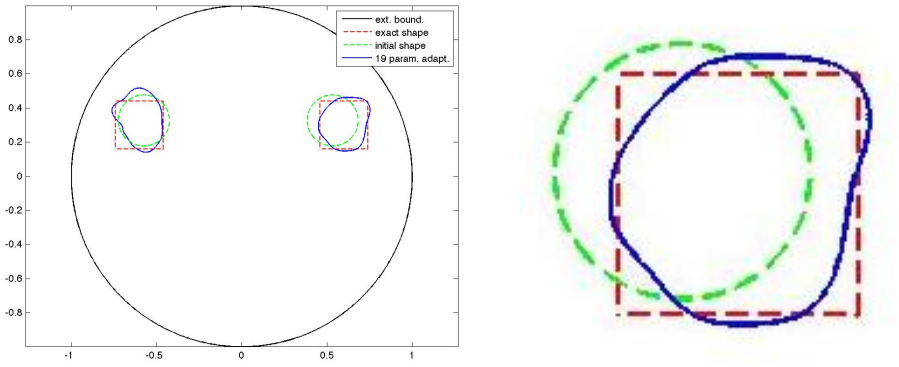

Figure 7: Detection with the combined approach (the initial shape is the one obtained after the "topological step") and zoom on the improvement with the geometrical step for the obstacle in the right.

- *A Kohn-Vogelius approach to study the data completion problem and the inverse obstacle problem with partial Cauchy data for Laplace's equation*, written with F. Caubet and J. Dardé. (to be submitted).

Notations

General Notations

d	:	Natural number, dimension of the space of work.
Ω	:	Open bounded connected subset of $\mathbb{R}^{\mathrm{d}}$ with Lipschitz boundary, set of reference.
$\partial\Omega$	:	Boundary of Ω.
$\mathbf{n}$	:	Exterior normal of $\partial\Omega$.
$\partial_{\mathbf{n}}$	:	Normal derivative.
$u, (\boldsymbol{u}, p)$	:	Solutions of the considered PDEs (Laplace: u, Stokes: $(\boldsymbol{u}, p)$) on $\Omega \setminus \overline{\omega}$ (Ω in Chapter 1 and 2).
${}^t\nabla\boldsymbol{u}$	:	Transpose matrix of $\nabla\boldsymbol{u}$.
L^p	:	Lebesgue spaces, $p \geq 1$ with norm $\|\cdot\|_{\mathrm{L}^p}$.
$\mathrm{W}^{m,p}$	:	Sobolev spaces, $m \in \mathbb{R}$, $p \geq 1$ with norm $\|\cdot\|_{m,p}$.
H^m	:=	$\mathrm{W}^{m,2}$, with norm $\|\cdot\|_m$ and seminorm $\|\cdot\|_m$.
$\mathbf{L}^p, \mathbf{H}^m, etc.$	:	Spaces of vector functions.
$\mathrm{L}^2_0(\Omega)$	:=	$\mathrm{L}^2(\Omega)/\mathbb{R}$, characterized by $p \in \mathrm{L}^2_0(\Omega) \Leftrightarrow p \in \mathrm{L}^2(\Omega) \wedge \int_\Omega p(x)\mathrm{d}x = 0$.
C	:	Positive (unless specified) constant.

Chapter 1

Γ_{obs}	:	Accessible part of the boundary $\Gamma_{obs} \subset \partial\Omega$.
Γ_{i}	:	Unaccessible part of the boundary $\Gamma_{\mathrm{i}} \subset \partial\Omega$.
(g_N, g_D)	:	Cauchy data in Γ_{obs}, $(g_N, g_D) \in \mathrm{H}^{-1/2}(\Gamma_{obs}) \times \mathrm{H}^{1/2}(\Gamma_{obs})$.
(g_D^n, g_N^n)	:	Sequence of Cauchy data in $\mathrm{H}^{-1/2}(\Gamma_{obs}) \times \mathrm{H}^{1/2}(\Gamma_{obs})$.
u_{ex}	:	Exact solution of the data completion problem.
(φ, ψ)	:	Cauchy data in Γ_{i}.
$(u_\varphi^{g_D}, u_\psi^{g_N})$	:	Solutions of mixed boundary problems.
(u_φ, u_ψ)	:=	$(u_\varphi^{g_D}, u_\psi^{g_N})$.
(v_φ, v_ψ)	:=	(u_φ^0, u_ψ^0).
$\mathcal{K}(\varphi, \psi)$	:	Kohn-Vogelius functional defined in $\mathrm{H}^{-1/2}(\Gamma_{\mathrm{i}}) \times \mathrm{H}^{1/2}(\Gamma_{\mathrm{i}})$.
(φ^*, ψ^*)	:	Minimizer of Kohn-Vogelius functional.
(φ_n, ψ_n)	:	Sequence of Cauchy data in $\mathrm{H}^{-1/2}(\Gamma_{\mathrm{i}}) \times \mathrm{H}^{1/2}(\Gamma_{\mathrm{i}})$.

$a((\varphi_1,\psi_1),(\varphi_2,\psi_2))$	:	Bilinear form associated with the optimality condition of $\mathcal{K}$.
$\ell^{g_D,g_N}((\varphi,\psi))$	:	Linear form associated with the optimality condition of $\mathcal{K}$.
$\ell((\varphi,\psi))$	:=	$\ell^{g_D,g_N}((\varphi,\psi))$.
$\ell_n((\varphi,\psi))$	:=	$\ell^{g_D^n,g_N^n}((\varphi,\psi))$.
γ_0	:	Trace operator.
ε	:	Regularization parameter.
$\mathcal{K}_\varepsilon(\varphi,\psi)$	:	Regularized Kohn-Vogelius functional.
$(\varphi_\varepsilon^*,\psi_\varepsilon^*)$	:	Minimizer of $\mathcal{K}_\varepsilon$.
$b((\varphi_1,\psi_1),(\varphi_2,\psi_2))$	:	Bilinear form associated with the regularizing term of $\mathcal{K}_\varepsilon$.
δ	:	Level of noise.
(g_N^δ,g_D^δ)	:	Cauchy data with noise of level δ.
$\mathcal{K}^\delta$	:	Kohn-Vogelius functional associated to the data (g_N^δ,g_D^δ).
$\mathcal{K}_\varepsilon^\delta$	:	Regularized Kohn-Vogelius functional associated with the data (g_N^δ,g_D^δ).
$(\varphi_{\varepsilon,\delta}^*,\psi_{\varepsilon,\delta}^*)$	:	Minimizers of $\mathcal{K}_\varepsilon^\delta$.
ℓ^δ	:=	$\ell^{g_D^\delta,g_N^\delta}$.
$\mathrm{d}\ell^\delta$	:=	$\ell^\delta-\ell$.
$(\mathrm{d}g_N,\mathrm{d}g_D)$	:=	$(g_N^\delta-g_N,g_D^\delta-g_D)$.
$\varepsilon(\delta)$	:	Regularization parameter with dependence on the noise level.
$\varepsilon(\delta,(\varphi_{\varepsilon,\delta}^*,\psi_{\varepsilon,\delta}^*))$	:	Regularization parameter with dependence on the noise level and the solution to that noise level.

Chapter 2

$\dfrac{\partial\mathcal{K}_\varepsilon}{\partial\varphi}$	:	Partial derivative of $\mathcal{K}_\varepsilon$ with respect to $\varphi\in\mathrm{H}^{-1/2}(\Gamma_\mathrm{i})$.
$\dfrac{\partial\mathcal{K}_\varepsilon}{\partial\psi}$	:	Partial derivative of $\mathcal{K}_\varepsilon$ with respect to $\psi\in\mathrm{H}^{1/2}(\Gamma_\mathrm{i})$.
(w_N,w_D)	:	Solutions of adjoint problems.
$\{p_1,p_2\}$	:	Common points between Γ_{obs} and Γ_i.
$(\widetilde{\varphi},\widetilde{\psi})$	:	Descent directions for gradient method to minimize $\mathcal{K}_\varepsilon$.
k_{max}	:	Maximum number of iterations.
tol	:	Tolerance parameter.
α_i	:	Step size parameter for descent directions, $\mathrm{i}=1,2,3$.
(φ_0,ψ_0)	:	Initial guess for the unknown data.
(φ_k,ψ_k)	:	Obtained guess for the unknown data at step k.
σ	:	Level of noise.
g^σ	:	Data with level of noise σ.

Chapter 3

$\mathcal{D}$	:	Set of admissible obstacles.
ω	:	Admissible obstacle (in $\mathcal{D}$).
ω^*	:	Real obstacle.
$C^0(\overline{\mathcal{O}})$	:	Set of continuous functions up to the boundary of $\mathcal{O}$.
(ω, φ, ψ)	:	Triplet of admissible obstacle, Neumann data and Dirichlet data over Γ_{i}.
$\mathcal{K}(\omega, \varphi, \psi)$	:	Kohn-Vogelius functional with shape dependance.
$\mathcal{K}_\varepsilon(\omega, \varphi, \psi)$	:	Regularized Kohn-Vogelius functional with shape dependance.
$\mathcal{K}(\omega)$	:=	$\mathcal{K}(\omega, \varphi, \psi)$.
$\mathcal{K}_\varepsilon(\omega)$	:=	$\mathcal{K}_\varepsilon(\omega, \varphi, \psi)$.
$(\omega^*, \varphi^*, \psi^*)$	:	Optimal triplet: Real obstacle, real Neumann and Dirichlet data. which is also a minimizer of $\mathcal{K}(\omega, \varphi, \psi)$.
$\boldsymbol{V}$	:	Set of admissible deformation directions.
$\boldsymbol{U}$	:	Deformation direction (in $\boldsymbol{V}$).
d_0	:	Positive real parameter.
Ω_{d_0}	:	A C^∞ domain compactly contained in Ω.
$D\mathcal{K}_\varepsilon(\omega) \cdot \boldsymbol{V}$	:	Shape gradient of $\mathcal{K}_\varepsilon$ in ω with deformation direction $\boldsymbol{V}$.
w	:=	$u_\varphi - u_\psi$.
ρ_N^u, ρ_D^u	:	Solutions of adjoint problems related to u_ψ, u_φ.
ρ_N^v, ρ_D^v	:	Solutions of adjoint problems related to v_ψ, v_φ.
u'_φ, u'_ψ	:	Shape (Eulerian) derivative of u_φ, u_ψ.
v'_φ, v'_ψ	:	Shape (Eulerian) derivative of v_φ, v_ψ.
w'	:=	$u'_\varphi - u'_\psi$.
$r(\theta)$	:	Polar radius of the parametrizacion of $\partial\omega$.
$r_N(\theta)$	:	Truncated Fourier series expansion of $r(\theta)$.
$a_{\mathrm{i}}^N, b_{\mathrm{i}}^N$	:	Fourier series coefficiens of $r_N(\theta)$.
ω_k	:	Obstacle shape after k iterations.
(φ_0, ψ_0)	:	Initial guess for the unknown data.
(φ_k, ψ_k)	:	Obtained guess for the unknown data at step k.
(u_D^k, u_N^k)	:=	$(u_{\varphi_k}, u_{\psi_k})$.
(v_D^k, v_N^k)	:=	$(v_{\varphi_k}, v_{\psi_k})$.
$D((x_0, y_0), r)$	:=	$\{(x, y) \in \mathbb{R}^2 : \ (x - x_0)^2 + (y - y_0)^2 \leq r^2\}$.
$\partial D((x_0, y_0), r)$	:=	$\{(x, y) \in \mathbb{R}^2 : \ (x - x_0)^2 + (y - y_0)^2 = r^2\}$.

Chapter 4

ν	:	Real positive number, kinematic viscocity.
ω	:	A bounded Lipschitz domain in $\mathbb{R}^2$ such that $0 \in \omega$, shape of reference.
ε	:	A small parameter, $0 < \varepsilon << 1$.
$\omega_{z,\varepsilon}$	:=	$z + \varepsilon\omega$, small obstacle with relative center $z \in \Omega$ and relative size ε.
m^*	:	Number of obstacles to be detected.
O	:	(Relatively) open subset of the boundary $\partial\Omega$.

$\omega^*_{z,\varepsilon}$	:	Real small obstacle with relative center $z \in \Omega$ and relative size ε.
ω^*_ε	:=	$\cup_{k=1}^{m^*} \omega^*_{z_k,\varepsilon_k}$, collection of real objects.
$\Omega_{z,\varepsilon}$	:=	$\Omega \setminus \overline{\omega_{z,\varepsilon}}$
$\sigma(\boldsymbol{u}, p)$	:	Cauchy stress tensor.
$\sigma(\boldsymbol{u}, p)\mathbf{n}$	:	Cauchy forces.
$\boldsymbol{f}$	:	Dirichlet data over $\partial\Omega$.
$\boldsymbol{g}$	:	Neumann data over $O \subset \partial\Omega$.
$\mathcal{D}(\cdot)$	:=	$(\nabla(\cdot) + {}^t\nabla(\cdot))$
$(\boldsymbol{u}^\varepsilon_D, p^\varepsilon_D)$	:	Solution of the Dirichlet problem in $\Omega_{z,\varepsilon}$.
$(\boldsymbol{u}^\varepsilon_M, p^\varepsilon_M)$	:	Solution of the mixed problem in $\Omega_{z,\varepsilon}$.
$(\boldsymbol{u}^0_D, p^0_D)$	:	Solution of the Dirichlet problem in Ω.
$(\boldsymbol{u}^0_M, p^0_M)$	:	Solution of the mixed problem in Ω.
$\mathcal{J}_{KV}(\Omega\setminus\overline{\omega_\varepsilon})$	:	The Kohn-Vogelius functional evaluated with an obstacle ω_ε.
$(E, \boldsymbol{P})$	:	Fundamental solution of the Stokes equation in $\mathbb{R}^2$
$\xi(\varepsilon)$	:	A positive scalar function intended to tend to zero with ε
$\delta\mathcal{J}_{KV}(z)$	:	Topological derivative of the Kohn-Vogelius functional in the point z.

Chapter 5

$\boldsymbol{f}$	:	Dirichlet data over $\partial\Omega$.
$\boldsymbol{g}$	:	Neumann data over $O \subset \partial\Omega$.
$\mathcal{J}_{KV}$	:	The Kohn-Vogelius functional.
ω_ε	:	Obstacle(s) inside the domain of reference Ω.
$\delta\mathcal{J}_{KV}$	:	The topological gradient of the Kohn-Vogelius functional.
$(\boldsymbol{u}^\varepsilon_D, p^\varepsilon_D)$	:	Solution of the Dirichlet problem in $\Omega_{z,\varepsilon}$.
$(\boldsymbol{u}^\varepsilon_M, p^\varepsilon_M)$	:	Solution of the mixed problem in $\Omega_{z,\varepsilon}$.
$(\boldsymbol{u}^0_D, p^0_D)$	:	Solution of the Dirichlet problem in Ω.
$(\boldsymbol{u}^0_M, p^0_M)$	:	Solution of the mixed problem in Ω.
$(\boldsymbol{u}_D, p_D)$	:=	$(\boldsymbol{u}^\varepsilon_D, p^\varepsilon_D)$.
$(\boldsymbol{u}_M, p_M)$	:=	$(\boldsymbol{u}^\varepsilon_M, p^\varepsilon_M)$.
P^*	:=	$\operatorname{argmin}_{P\in\Omega} \delta\mathcal{J}_{KV}(P)$.
$B(P, r)$	:=	$\{P' \in \Omega \text{ such that } \|P' - P\| < r\}$.
$\boldsymbol{g}^\sigma$	:	Vector field polluted with noise of amplitude $\sigma > 0$.

Part I

The data completion problem and the inverse obstacle problem with partial boundary data

Chapter 1

Theoretical analysis of the data completion problem for Laplace operator

In this chapter we present the data completion problem for the Laplace operator, this is, the problem of reconstructing boundary data in an inaccessible part of the boundary from overdetermined boundary data in an accessible part of the boundary. We deal with this problem by considering a Kohn-Vogelius strategy: We split the overdetermined problem in two subproblems, each one has one of the overdetermined boundary data, and, in order to have well-posed problems we impose boundary data into the inaccessible part of the boundary, then, we measure the error between these functions which will be zero only when we have chosen the exact boundary data into the unaccessible part of the boundary. Therefore, we restate the inverse problem as an optimization problem: the minimization of the cost-type functional, the Kohn-Vogelius functional. Additionally, due to the ill-posedness of the problem we propose a regularization of the minimization problem, considering a Tikhonov regularization of the functional, which transforms the initial minimization problem into another one which always has solution. We study convergence properties for this regularized functional in case when the given overdetermined data is perfect and in the case when the data is polluted by noise.

This chapter is divided in three sections. In the first one we present the problem, the corresponding notations and we present the inverse problem equivalently as the minimization of a cost-type functional: The Kohn-Vogelius functional. In the second section we explore the properties of the Kohn-Vogelius functional and present, in order to overcome the exponential ill-posedness of the problem (see [18]), the regularized Kohn-Vogelius functional, based in a Tikhonov regularization. We study this new functional, obtaining in particular the convergence of its minimizers to the minimizer of the original Kohn-Vogelius functional when the regularization parameter tends to zero. We also explore monotony properties of this functional, and some others related, viewed as a function of the regularization parameter. Finally,

in the last section, we explore the problem when the Cauchy data into the observable part of the boundary contains noise. We see that, in order to have convergence to the original solution (with respect to the unpolluted data), we have to establish some requirements between the noise level and the regularization parameter. We define an strategy to relate the level of noise and the regularization parameter and we prove that this strategy effectively provides convergence to the solution of the Cauchy problem when it exists.

Our main references to this work are [12, 13, 20, 18, 19], in [12] Andrieux et al. propose the strategy of solving the problem by the restatement as an optimization problem, however the analysis is purely numerical. In [19] Ben Belgacem et al. propose a similar strategy but focused in a variational formulation instead of an optimization one and focused in only reconstruct the Dirichlet data. We perform a complement between our main references, performing a theoretical analysis of the work of Andrieux et al. using several tools from the works of [13, 20, 19], and, the most interesting improvement is the development of an extension of the strategy of Andrieux et al., by considering even noisy cases and proposing strategies to deal with them.

1.1 The problem setting

Introduction of the general notations. For a bounded open set Ω of $\mathbb{R}^{\mathrm{d}}$ ($\mathrm{d} \in \mathbb{N}^*$) with a boundary $\partial\Omega$, we remark that the notation $\int_\Omega u$ means $\int_\Omega u(x)\mathrm{d}x$ which is the classical Lebesgue integral. Moreover, we use the notation $\int_{\partial\Omega} u$ to denote the boundary integral $\int_{\partial\Omega} u(x)\mathrm{d}s(x)$, where $\mathrm{d}s$ represents the surface Lebesgue measure on the boundary. The aim is to simplify the notations when there is no confusion. We also introduce the exterior unit normal $\mathbf{n}$ of the domain Ω and $\partial_{\mathbf{n}}u$ will denote the normal derivative of u.

For $s \geq 0$ we denote by $\mathrm{L}^2(\Omega)$, $\mathrm{L}^2(\partial\Omega)$, $\mathrm{H}^s(\Omega)$, $\mathrm{H}^s(\partial\Omega)$, $\mathrm{H}^s_0(\Omega)$, the usual Lebesgue and Sobolev spaces of scalar functions in Ω or on $\partial\Omega$. The classical scalar product, norm and semi-norm on $\mathrm{H}^s(\Omega)$ are respectively denoted by $(\cdot,\cdot)_{\mathrm{H}^s(\Omega)}$, $\|\cdot\|_{\mathrm{H}^s(\Omega)}$ and $|\cdot|_{\mathrm{H}^s(\Omega)}$. Moreover, we introduce the space $\mathrm{H}^1(\Omega,\Delta)$ given by

$$\mathrm{H}^1(\Omega,\Delta) := \left\{u \in \mathrm{H}^1(\Omega) : \Delta u \in \mathrm{L}^2(\Omega)\right\}.$$

This space endowed with the scalar product

$$(u,v)_{\mathrm{H}^1(\Omega,\Delta)} := (u,v)_{\mathrm{H}^1(\Omega)} + (\Delta u, \Delta v)_{\mathrm{L}^2(\Omega)}$$

is an Hilbert space. As a subspace of $\mathrm{H}^1(\Omega)$, we can define a trace for each $u \in \mathrm{H}^1(\Omega,\Delta)$. Additionally we can define a normal derivative on the boundary $\partial\Omega$ of Ω which defines a continuous application into $\mathrm{H}^{-1/2}(\partial\Omega)$ and we have an integration

by parts formula. These results can be found into appendix A.1. We can finally note that this space is an intermediate one between $\mathrm{H}^1(\Omega)$ and $\mathrm{H}^2(\Omega)$, *i.e.*

$$\mathrm{H}^2(\Omega) \subset \mathrm{H}^1(\Omega, \Delta) \subset \mathrm{H}^1(\Omega).$$

The data completion problem Let Ω be a bounded connected (at least) Lipschitz open set of $\mathbb{R}^{\mathrm{d}}$ (in applications we will consider $\mathrm{d} = 2$ or $\mathrm{d} = 3$) with boundary $\partial\Omega$ which has two components: the nonempty (relatively) open sets Γ_{obs} and Γ_{i}, such that $\overline{\Gamma_{obs}} \cup \overline{\Gamma_{\mathrm{i}}} = \partial\Omega$. We will say that Γ_{obs} is the observable part of $\partial\Omega$ where we will be able to obtain measurements on our system, the Cauchy datum (g_N, g_D), and Γ_{i} will be considered as the inaccessible part of the boundary $\partial\Omega$, where we cannot obtain any information of our system.

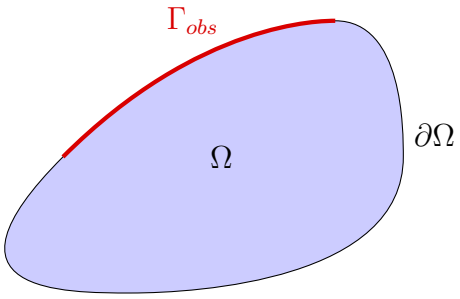

Figure 1.1: An example domain

The data completion problem consists of recovering data on the whole boundary, specifically on Γ_{i} from the over-determined data on Γ_{obs}, this is: *find* $u \in \mathrm{H}^1(\Omega, \Delta)$ *such that*

$$\begin{cases} -\Delta u &= 0 & \text{in } \Omega \\ u &= g_D & \text{on } \Gamma_{obs} \\ \partial_{\mathbf{n}} u &= g_N & \text{on } \Gamma_{obs}, \end{cases} \tag{1.1}$$

naturally, as (g_N, g_D) could be any data (obtained for example from experiments), such a u may not exist, so we need to specify if we are in the favorable case or not:

Definition 1.1 *A pair* $(g_N, g_D) \in \mathrm{H}^{-1/2}(\Gamma_{obs}) \times \mathrm{H}^{1/2}(\Gamma_{obs})$ *will be called* ***compatible*** *if there exists (a necessarily unique)* $u \in \mathrm{H}^1(\Omega, \Delta)$ *harmonic such that* $u|_{\Gamma_{obs}} = g_D$, $\partial_{\mathbf{n}} u|_{\Gamma_{obs}} = g_N$.

Remark The uniqueness result of such a solution is classical and is based on a unique continuation result, we refer to [44, Chapter 1] for a detailed proof.

The following relevant result states that, if a given pair (g_N, g_D) is not compatible, we may approximate it by a sequence of compatible data, which implies in particular the ill-posedness of the considered inverse problem:

Lemma 1.2 *For* $(g_N, g_D) \in \mathrm{H}^{-1/2}(\Gamma_{obs}) \times \mathrm{H}^{1/2}(\Gamma_{obs})$ *given data, we have:*

1. *For a fixed $g_D \in \mathrm{H}^{1/2}(\Gamma_{obs})$, the set of data g_N for which there exists a function $u \in \mathrm{H}^1(\Omega, \Delta)$, satisfying the Cauchy problem (1.1) is dense in $\mathrm{H}^{-1/2}(\Gamma_{obs})$.*
2. *For a fixed $g_N \in \mathrm{H}^{-1/2}(\Gamma_{obs})$, the set of data g_D for which there exists a function $u \in \mathrm{H}^1(\Omega, \Delta)$, satisfying the Cauchy problem (1.1) is dense in $\mathrm{H}^{1/2}(\Gamma_{obs})$.*

Proof. See Fursikov [51, Chapter 3] or Andrieux [12] □

Remark Let us explore the Cauchy problem: this problem is ill-posed in the sense of Hadamard, this is, if the data (g_N, g_D) is compatible, the associated solution $u \in \mathrm{H}^1(\Omega, \Delta)$ does not depend continuously of the compatible data, as the classical example of Hadamard [55] shows:

Let us consider $\Omega = (0, \pi) \times (0, \pi)$ and $\Gamma_{obs} = \{0\} \times (0, \pi)$ and for $n \in \mathbb{N}^*$ take $u_n(x, y) = \frac{1}{n^2} \sin(ny) \sinh(nx)$. It is immediate to see that u_n is harmonic in Ω for all $n \in \mathbb{N}^*$ and $\partial_{\mathbf{n}} u_n(x, y) = -\frac{1}{n} \sin(ny)$ on Γ_{obs}.

Now, we have:

$$\|\partial_{\mathbf{n}} u_n\|_{\mathrm{H}^{-1/2}(\Gamma_{obs})} \leq \|\partial_{\mathbf{n}} u_n\|_{\mathrm{L}^2(\Gamma_{obs})} = \left(\int_{\Gamma_{obs}} \frac{1}{n^2} \sin^2(ny) \mathrm{d}s(y) \right)^{1/2} = \frac{1}{n} \sqrt{\frac{\pi}{2}} \to_{n \to \infty} 0,$$

and

$$\|u_n\|_{\mathrm{L}^2(\Omega)} = \left(\int_{\Omega} \frac{1}{n^4} \sin^2(ny) \sinh^2(nx) \mathrm{d}x\mathrm{d}y \right)^{1/2} = \left(\frac{\pi}{2n^4} \cdot \left(\frac{\sinh(2\pi n)}{4n} - \frac{\pi}{2} \right) \right)^{1/2},$$

therefore:

$$\|u_n\|_{\mathrm{L}^2(\Omega)} \to \infty \text{ as } n \to \infty$$

Noticing that we have:

$$\|u_n\|_{\mathrm{H}^1(\Omega, \Delta)} \geq \|u_n\|_{\mathrm{L}^2(\Omega)},$$

We deduce that is impossible to have a continuous dependence, i.e. we cannot find a constant $c > 0$ such that:

$$\|u\|_{\mathrm{H}^1(\Omega, \Delta)} \leq c \left(\|u\|_{\mathrm{H}^{1/2}(\Gamma_{obs})} + \|\partial_{\mathbf{n}} u\|_{\mathrm{H}^{-1/2}(\Gamma_{obs})} \right).$$

Moreover, with this example we will be able to see that the operator $A : u \in \mathrm{H}^1(\Omega, \Delta) \to (u|_{\Gamma_{obs}}, \partial_{\mathbf{n}} u|_{\Gamma_{obs}}) \in \mathrm{H}^{1/2}(\Gamma_{obs}) \times \mathrm{H}^{-1/2}(\Gamma_{obs})$ is not surjective, which in particular proves that there exists data (g_N, g_D) which is not compatible.

Proposition 1.3 *The operator A is not surjective.*

Proof. By contradiction, let us suppose that A is surjective. The uniqueness of the problem (and the linearity) implies that A is bijective and continuous from $\mathrm{H}^1(\Omega)$ to $Y := \mathrm{H}^{1/2}(\Gamma_{obs}) \times \mathrm{H}^{-1/2}(\Gamma_{obs})$ which are Banach spaces. By open mapping theorem

(to be more specific, a classic corollary of it) we deduce the continuity of A^{-1}, which is equivalent to the existence of a constant $C > 0$ such that:

$$\|u\|_{\mathrm{H}^1(\Omega)} \leq C\|Au\|_Y,$$

which is a contradiction with the previously proven ill-posedness of the problem. □

The Kohn-Vogelius functional. In order to solve this problem our idea is to define a well-appropriated Kohn-Vogelius functional which will depend on the *missing data* in Γ_{i}, following the idea proposed by Andrieux *et al.* in [12].

Hence, in order to solve the initial inverse problem (1.1), we will focus on the following optimization problem:

$$(\varphi^*, \psi^*) \in \underset{(\varphi,\psi)\in \mathrm{H}^{-1/2}(\Gamma_{\mathrm{i}})\times \mathrm{H}^{1/2}(\Gamma_{\mathrm{i}})}{\operatorname{argmin}} \mathcal{K}(\varphi, \psi) \tag{1.2}$$

where $\mathcal{K}$ is the nonnegative Kohn-Vogelius cost functional defined by

$$\mathcal{K}(\varphi, \psi) = \frac{1}{2}\int_\Omega |\nabla u_\varphi^{g_D} - \nabla u_\psi^{g_N}|^2 \tag{1.3}$$

where $u_\varphi^{g_D} \in \mathrm{H}^1(\Omega)$ and $u_\psi^{g_N} \in \mathrm{H}^1(\Omega)$ are the respective solutions of the following problems

$$\left\{\begin{array}{rcll} -\Delta u_\varphi^{g_D} &=& 0 & \text{in } \Omega \\ u_\varphi^{g_D} &=& g_D & \text{on } \Gamma_{obs} \\ \partial_{\mathbf{n}} u_\varphi^{g_D} &=& \varphi & \text{on } \Gamma_{\mathrm{i}}, \end{array}\right. \quad \text{and} \quad \left\{\begin{array}{rcll} -\Delta u_\psi^{g_N} &=& 0 & \text{in } \Omega \\ \partial_{\mathbf{n}} u_\psi^{g_N} &=& g_N & \text{on } \Gamma_{obs} \\ u_\psi^{g_N} &=& \psi & \text{on } \Gamma_{\mathrm{i}}. \end{array}\right. \tag{1.4}$$

Indeed, if the inverse problem (1.1) has a solution, then we have that $\mathcal{K}(\varphi, \psi) = 0$ if and only if $(\varphi, \psi) = (\varphi^*, \psi^*)$ (and we can notice that, in this case, using Holmgren Theorem: $u_{\varphi^*}^{g_D} = u$ and $u_{\psi^*}^{g_N} = u + C,\ C \in \mathbb{R}$ where u is the solution of the Cauchy problem in Ω). Thus, from now, we focus on the optimization problem (1.2).

In the rest of the following chapters, we will note u_φ and u_ψ instead of $u_\varphi^{g_D}$ and $u_\psi^{g_N}$. We will only precise the dependence with respect to g_D and g_N when it is necessary. Moreover, we introduce the notations $v_\varphi := u_\varphi^0$ and $v_\psi := u_\psi^0$. Indeed, they will play an important role in the following. We precise that they satisfy respectively

$$\left\{\begin{array}{rcll} -\Delta v_\varphi &=& 0 & \text{in } \Omega \\ v_\varphi &=& 0 & \text{on } \Gamma_{obs} \\ \partial_{\mathbf{n}} v_\varphi &=& \varphi & \text{on } \Gamma_{\mathrm{i}} \end{array}\right. \quad \text{and} \quad \left\{\begin{array}{rcll} -\Delta v_\psi &=& 0 & \text{in } \Omega \\ \partial_{\mathbf{n}} v_\psi &=& 0 & \text{on } \Gamma_{obs} \\ v_\psi &=& \psi & \text{on } \Gamma_{\mathrm{i}}. \end{array}\right. \tag{1.5}$$

1.2 Theoretical results concerning the data completion problem

Let us consider a given Cauchy pair $(g_N, g_D) \in \mathrm{H}^{-1/2}(\Gamma_{obs}) \times \mathrm{H}^{1/2}(\Gamma_{obs})$ (it may be compatible or not). Hence, the previous Kohn-Vogelius functional (1.3) is defined,

for $(\varphi, \psi) \in \mathrm{H}^{-1/2}(\Gamma_\mathrm{i}) \times \mathrm{H}^{1/2}(\Gamma_\mathrm{i})$, using the previously defined notation as:

$$\mathcal{K}(\varphi, \psi) = \frac{1}{2} \int_\Omega |\nabla u_\varphi - \nabla u_\psi|^2 \tag{1.6}$$

and the previous problems (1.4) become

$$\left\{ \begin{array}{rcll} -\Delta u_\varphi & = & 0 & \text{in } \Omega \\ u_\varphi & = & g_D & \text{on } \Gamma_{obs} \\ \partial_\mathbf{n} u_\varphi & = & \varphi & \text{on } \Gamma_\mathrm{i} \end{array} \right. \quad \text{and} \quad \left\{ \begin{array}{rcll} -\Delta u_\psi & = & 0 & \text{in } \Omega \\ \partial_\mathbf{n} u_\psi & = & g_N & \text{on } \Gamma_{obs} \\ u_\psi & = & \psi & \text{on } \Gamma_\mathrm{i}. \end{array} \right. \tag{1.7}$$

Remark We can note that these two problems are natural. They permit to *split* the overdetermined objective system (1.1) into two systems where we impose boundary conditions on the unaccessible part of the boundary. These problems have the advantage of being well-posed, and as we will see, if we chose properly the imposed boundary conditions on the unaccessible part of the boundary we will be able to reconstruct the desired solution of our main problem (1.1).

Remark We can notice that (assuming enough regularity, if not we obtain a similar expression with duality products), after integration by parts, we get:

$$\mathcal{K}(\varphi, \psi) = \frac{1}{2} \int_{\Gamma_{obs}} (\partial_\nu u_\varphi - g_N)\,(g_D - u_\psi) + \frac{1}{2} \int_{\Gamma_\mathrm{i}} (\varphi - \partial_\nu u_\psi)\,(u_\varphi - \psi).$$

This expression shows that the cost functional $\mathcal{K}$ measures the error between u_φ and u_ψ as integrals only involving the boundary of the domain Ω.

1.2.1 Properties of $\mathcal{K}$

We first explore the properties of the Kohn-Vogelius functional $\mathcal{K} : \mathrm{H}^{-1/2}(\Gamma_\mathrm{i}) \times \mathrm{H}^{1/2}(\Gamma_\mathrm{i}) \to \mathbb{R}$ given by (1.6).

Proposition 1.4 *The functional $\mathcal{K}$ satisfies the following properties.*

1. *$\mathcal{K}$ is continuous, convex, positive, and its infimum is zero.*
2. *When $\mathcal{K}(\varphi, \psi)$ reaches its minimum with $(\varphi^*, \psi^*) = \operatorname{argmin}_{(\varphi,\psi)} \mathcal{K}(\varphi, \psi)$ we have: $u_{\varphi^*} = u_{\psi^*} + C = u_{\psi^*+C}$ where C is any constant in $\mathbb{R}$. Therefore $(\varphi^*, \psi^* + C)$ is also a minimizer of $\mathcal{K}$. Moreover, in this case, u_{φ^*} solves the Cauchy problem.*
3. *If we restrict $\mathcal{K}$ to the space $\mathrm{H}^{-1/2}(\Gamma_\mathrm{i}) \times \mathrm{H}^{1/2}(\Gamma_\mathrm{i})/\mathbb{R}$ then a minimizer of $\mathcal{K}$ is unique.*
4. *The first order optimality condition for $(\varphi^*, \psi^*) \in \mathrm{H}^{-1/2}(\Gamma_\mathrm{i}) \times \mathrm{H}^{1/2}(\Gamma_\mathrm{i})$ to be a minimizer is, for all $(\widetilde{\varphi}, \widetilde{\psi}) \in \mathrm{H}^{-1/2}(\Gamma_\mathrm{i}) \times \mathrm{H}^{1/2}(\Gamma_\mathrm{i})$,*

$$\int_\Omega \nabla(v_{\varphi^*} - v_{\psi^*}) \cdot \nabla(v_{\widetilde{\varphi}} - v_{\widetilde{\psi}}) = \int_\Omega \left(\nabla u_0^{g_D} \cdot \nabla v_{\widetilde{\psi}} + \nabla u_0^{g_N} \cdot \nabla v_{\widetilde{\varphi}} \right) \tag{1.8}$$

PROOF. We prove each statement.

1. Continuity, convexity and positiveness are obvious.

   To prove that $\inf_{(\varphi,\psi)} \mathcal{K}(\varphi,\psi) = 0$, we have to consider two cases. If the pair (g_N, g_D) is compatible, this is direct since, choosing $\varphi^* := \partial_{\mathbf{n}} u_{ex}|_{\Gamma_i}$ and $\psi^* := u_{ex}|_{\Gamma_i}$, we obtain immediately $\mathcal{K}(\varphi^*,\psi^*) = 0$. Let us now focus on the non-compatible case. Thanks to the density lemma 1.2, we can approximate g_D by a sequence $(g_D^n)_n$ in a way that the pairs $(g_N, g_D^n)_n$ are compatibles for all $n \in \mathbb{N}$. For each n, consider (φ_n^*, ψ_n^*) the minimizer of the Kohn-Vogelius function for the data (g_N, g_D^n) which implies that $\nabla u_{\varphi_n^*}^{g_D^n} = \nabla u_{\psi_n^*}^{g_N}$. Then we have:

$$\begin{aligned} \mathcal{K}(\varphi_n^*,\psi_n^*) &= \tfrac{1}{2}\left| u_{\varphi_n^*}^{g_D} - u_{\psi_n^*}^{g_N} \right|^2_{\mathrm{H}^1(\Omega)} = \tfrac{1}{2}\left| u_{\varphi_n^*}^{g_D} - u_{\varphi_n^*}^{g_D^n} \right|^2_{\mathrm{H}^1(\Omega)} = \tfrac{1}{2}\left| u_0^{g_D - g_D^n} \right|^2_{\mathrm{H}^1(\Omega)} \\ &\leq C\|g_D - g_D^n\|^2_{\mathrm{H}^{1/2}(\Gamma_i)} \underset{n\to\infty}{\longrightarrow} 0, \end{aligned}$$

   which concludes the proof.

2. The first and second assertions are obvious from the definition of the functional $\mathcal{K}$. To see that u_{φ^*} solves the Cauchy problem, first notice that u_{φ^*} satisfies (as this is equal to u_{ψ^*} up to a constant) the system:

$$\begin{cases} -\Delta u_{\varphi^*} = 0 & \text{in } \Omega \\ u_{\varphi^*} = g_D & \text{on } \Gamma_{obs} \\ \partial_{\mathbf{n}} u_{\varphi^*} = g_N & \text{on } \Gamma_{obs} \\ \partial_{\mathbf{n}} u_{\varphi^*} = \varphi^* & \text{on } \Gamma_i. \end{cases}$$

   Therefore u_{φ^*} solves the Cauchy problem (1.1).

3. This comes from the definition of quotient space.

4. A standard computation gives the directly the left hand side, the right hand side becomes

$$\int_\Omega \nabla(u_0^{g_N} - u_0^{g_D}) \cdot \nabla(v_\varphi - v_\psi),$$

   and we get the result noticing that

$$\int_\Omega \nabla u_0^{g_D} \cdot \nabla v_{\widetilde{\varphi}} = 0 \quad \text{and} \quad \int_\Omega \nabla u_0^{g_N} \cdot \nabla v_{\widetilde{\psi}} = 0.$$

□

For a given Cauchy pair (g_N, g_D), we introduce the bilinear form $a : \left(\mathrm{H}^{-1/2}(\Gamma_i) \times \mathrm{H}^{1/2}(\Gamma_i)\right)^2 \to \mathbb{R}$ and the linear form $\ell : \mathrm{H}^{-1/2}(\Gamma_i) \times \mathrm{H}^{1/2}(\Gamma_i) \to \mathbb{R}$ respectively defined, for all (φ,ψ), $(\widetilde{\varphi},\widetilde{\psi}) \in \mathrm{H}^{-1/2}(\Gamma_i) \times \mathrm{H}^{1/2}(\Gamma_i)$, by

$$\begin{aligned} a\left((\varphi,\psi),(\widetilde{\varphi},\widetilde{\psi})\right) &= \int_\Omega \nabla(v_\varphi - v_\psi) \cdot \nabla(v_{\widetilde{\varphi}} - v_{\widetilde{\psi}}) \\ \ell(\varphi,\psi) &= \int_\Omega (\nabla u_0^{g_D} \cdot \nabla v_\psi + \nabla u_0^{g_N} \cdot \nabla v_\varphi) \\ &= \int_\Omega \nabla(u_0^{g_N} - u_0^{g_D}) \cdot \nabla(v_\varphi - v_\psi). \end{aligned} \tag{1.9}$$

Then, note that the optimality condition (1.8) can be rewritten as

$$a((\varphi^*,\psi^*),(\widetilde{\varphi},\widetilde{\psi})) = \ell(\widetilde{\varphi},\widetilde{\psi}), \qquad \forall(\widetilde{\varphi},\widetilde{\psi}) \in \mathrm{H}^{-1/2}(\Gamma_\mathrm{i}) \times \mathrm{H}^{1/2}(\Gamma_\mathrm{i}). \tag{1.10}$$

By the fact that $\mathcal{K}$ is not coercive, we cannot assume that $\mathcal{K}$ reaches its minimum in general. Anyway, we can consider the following definition which generalizes the concept of first order optimality condition:

Definition 1.5 *We say that a sequence* $(\varphi_n,\psi_n) \subset \mathrm{H}^{-1/2}(\Gamma_\mathrm{i})\times\mathrm{H}^{1/2}(\Gamma_\mathrm{i})$ *is a* ***pseudo-solution*** *of* (1.2) *if*

$$\lim_{n\to\infty} \sup_{(\widetilde{\varphi},\widetilde{\psi})\in \mathrm{H}^{-1/2}(\Gamma_\mathrm{i})\times\mathrm{H}^{1/2}(\Gamma_\mathrm{i})} \frac{|a((\varphi_n,\psi_n),(\widetilde{\varphi},\widetilde{\psi})) - \ell(\widetilde{\varphi},\widetilde{\psi})|}{\|(\widetilde{\varphi},\widetilde{\psi})\|_{\mathrm{H}^{-1/2}(\Gamma_\mathrm{i})\times\mathrm{H}^{1/2}(\Gamma_\mathrm{i})}} = 0. \tag{1.11}$$

Using the density Lemma 1.2, we can prove that there always exists a pseudo-solution of (1.2). Moreover, we can assert an alternative in which, given a condition over a pseudo-solution we can obtain the existence and (weakly-)convergence to the solution of the Cauchy problem. In order to assert and prove the result, we need a preliminary lemma.

Lemma 1.6 *Let* $\eta \in \mathrm{H}^{-1/2}(\Gamma_{obs})$ *such that* $\forall\psi \in \mathrm{H}^{1/2}(\Gamma_\mathrm{i})$ *we have:*

$$\langle \eta, v_\psi\rangle_{\Gamma_{obs}} = 0,$$

then $\eta = 0$.

Proof. Let us consider the following well-posed problem:

$$\begin{cases} -\Delta w_\eta &= 0 & \text{in } \Omega \\ \partial_{\mathbf{n}} w_\eta &= \eta & \text{on } \Gamma_{obs} \\ w_\eta &= 0 & \text{on } \Gamma_\mathrm{i}. \end{cases}$$

By hypothesis we have $\forall\psi \in \mathrm{H}^{1/2}(\Gamma_\mathrm{i})$

$$0 = \langle \eta, v_\psi\rangle_{\Gamma_{obs}} = -\langle \partial_{\mathbf{n}} w_\eta, \psi\rangle_{\Gamma_\mathrm{i}} + \int_\Omega \nabla v_\psi \cdot \nabla w_\eta,$$

however, we also have due to the boundary conditions satisfied by w_η and v_ψ

$$\int_\Omega \nabla v_\psi \cdot \nabla w_\eta = \langle \partial_{\mathbf{n}} v_\psi, w_\eta\rangle_{\partial\Omega} = \langle \partial_{\mathbf{n}} v_\psi, w_\eta\rangle_{\Gamma_\mathrm{i}} + \langle \partial_{\mathbf{n}} v_\psi, w_\eta\rangle_{\Gamma_{obs}} = 0,$$

therefore, $\forall\psi \in \mathrm{H}^{1/2}(\Gamma_\mathrm{i})$

$$0 = \langle \partial_{\mathbf{n}} w_\eta, \psi\rangle_{\Gamma_\mathrm{i}},$$

then w_η satisfies

$$\begin{cases} -\Delta w_\eta &= 0 & \text{in } \Omega \\ \partial_{\mathbf{n}} w_\eta &= \eta & \text{on } \Gamma_{obs} \\ \partial_{\mathbf{n}} w_\eta &= 0 & \text{on } \Gamma_\mathrm{i} \\ w_\eta &= 0 & \text{on } \Gamma_\mathrm{i}, \end{cases}$$

and by Holmgren theorem we conclude $w_\eta = 0$, which implies in particular $\eta = 0$ □

Proposition 1.7 *For any $(g_N, g_D) \in \mathrm{H}^{-1/2}(\Gamma_{obs}) \times \mathrm{H}^{1/2}(\Gamma_{obs})$, there exists a pseudo-solution $(\varphi_n^*, \psi_n^*) \subset \mathrm{H}^{-1/2}(\Gamma_\mathrm{i}) \times \mathrm{H}^{1/2}(\Gamma_\mathrm{i})$ of (1.2). Moreover, any pseudo-solution satisfies the following alternative:*

1. *$\|(\varphi_n^*, \psi_n^*)\|_{\mathrm{H}^{-1/2}(\Gamma_\mathrm{i}) \times \mathrm{H}^{1/2}(\Gamma_\mathrm{i})}$ is bounded and then weakly converges, up to a subsequence, in $\mathrm{H}^{-1/2}(\Gamma_\mathrm{i}) \times \mathrm{H}^{1/2}(\Gamma_\mathrm{i})$ to $(\varphi^*, \psi^*) \in \mathrm{H}^{-1/2}(\Gamma_\mathrm{i}) \times \mathrm{H}^{1/2}(\Gamma_\mathrm{i})$ which minimizes $\mathcal{K}$. Therefore u_{φ^*} solves the Cauchy problem (1.1) and we have also the weak convergence $u_{\varphi_n^*} \rightharpoonup u_{\varphi^*}$ in $\mathrm{H}^1(\Omega)$;*
2. *$\|(\varphi_n^*, \psi_n^*)\|_{\mathrm{H}^{-1/2}(\Gamma_\mathrm{i}) \times \mathrm{H}^{1/2}(\Gamma_\mathrm{i})}$ diverges.*

Proof. Thanks to the density Lemma 1.2, we approximate g_N by a sequence $(g_N^n)_n$ such that the pairs (g_N^n, g_D) are compatible for all $n \in \mathbb{N}$. Let us call ℓ_n the linear form in $\mathrm{H}^{-1/2}(\Gamma_\mathrm{i}) \times \mathrm{H}^{1/2}(\Gamma_\mathrm{i})$ associated with the pair (g_N^n, g_D), *i.e.*,

$$\ell_n(\varphi, \psi) := \int_\Omega \nabla u_0^{g_D} \cdot \nabla v_\psi + \nabla u_0^{g_N^n} \cdot \nabla v_\varphi = -\int_\Omega \nabla \left(u_0^{g_D} - u_0^{g_N^n} \right) \cdot \nabla \left(v_\varphi - v_\psi \right).$$

As (g_N^n, g_D) is compatible for all n, we call (φ_n^*, ψ_n^*) the minimizing pair for the Kohn-Vogelius considered functional (related to the data (g_N^n, g_D)). Then, for each n, from the first optimality condition (1.10),

$$a((\varphi_n^*, \psi_n^*), (\varphi, \psi)) = \ell_n(\varphi, \psi), \quad \forall (\varphi, \psi) \in \mathrm{H}^{-1/2}(\Gamma_\mathrm{i}) \times \mathrm{H}^{1/2}(\Gamma_\mathrm{i}),$$

or equivalently

$$a((\varphi_n^*, \psi_n^*), (\varphi, \psi)) - \ell(\varphi, \psi) = \ell_n(\varphi, \psi) - \ell(\varphi, \psi), \quad \forall (\varphi, \psi) \in \mathrm{H}^{-1/2}(\Gamma_\mathrm{i}) \times \mathrm{H}^{1/2}(\Gamma_\mathrm{i}).$$

We can estimate the right side of this equality to get

$$\begin{aligned} |\ell_n(\varphi, \psi) - \ell(\varphi, \psi)| &= \left| \int_\Omega \nabla u_0^{g_D} \cdot \nabla v_\psi + \nabla u_0^{g_N} \cdot \nabla v_\varphi - \nabla u_0^{g_D} \cdot \nabla v_\psi - \nabla u_0^{g_N^n} \cdot \nabla v_\varphi \right| \\ &= \left| \int_\Omega \nabla u_0^{g_N - g_N^n} \cdot \nabla v_\varphi \right| \leq C \|(\varphi, \psi)\|_{\mathrm{H}^{-1/2}(\Gamma_\mathrm{i}) \times \mathrm{H}^{1/2}(\Gamma_\mathrm{i})} \cdot \|g_N - g_N^n\|_{\mathrm{H}^{-1/2}(\Gamma_\mathrm{i})}, \end{aligned}$$

which implies, for all n and all no null $(\varphi, \psi) \in \mathrm{H}^{-1/2}(\Gamma_\mathrm{i}) \times \mathrm{H}^{1/2}(\Gamma_\mathrm{i})$,

$$\frac{|a((\varphi_n^*, \psi_n^*), (\varphi, \psi)) - \ell(\varphi, \psi)|}{\|(\varphi, \psi)\|_{\mathrm{H}^{-1/2}(\Gamma_\mathrm{i}) \times \mathrm{H}^{1/2}(\Gamma_\mathrm{i})}} \leq C \|g_N - g_N^n\|_{\mathrm{H}^{-1/2}(\Gamma_\mathrm{i})}.$$

Thus, we conclude that the constructed $(\varphi_n^*, \psi_n^*) \subset \mathrm{H}^{-1/2}(\Gamma_\mathrm{i}) \times \mathrm{H}^{1/2}(\Gamma_\mathrm{i})$ is a pseudo-solution.

Now, let (φ_n^*, ψ_n^*) be a bounded pseudo-solution. Define, for $n \in \mathbb{N}$:

$$S_n := \sup_{(\varphi, \psi) \in \mathrm{H}^{-1/2}(\Gamma_\mathrm{i}) \times \mathrm{H}^{1/2}(\Gamma_\mathrm{i})} \frac{|a((\varphi_n^*, \psi_n^*), (\varphi, \psi)) - \ell(\varphi, \psi)|}{\|(\varphi, \psi)\|_{\mathrm{H}^{-1/2}(\Gamma_\mathrm{i}) \times \mathrm{H}^{1/2}(\Gamma_\mathrm{i})}}.$$

We have, for $(\varphi, \psi) \in \mathrm{H}^{-1/2}(\Gamma_\mathrm{i}) \times \mathrm{H}^{1/2}(\Gamma_\mathrm{i}) \setminus \{(0, 0)\}$:

$$|a((\varphi_n^*, \psi_n^*), (\varphi, \psi)) - \ell(\varphi, \psi)| \leq S_n \|(\varphi, \psi)\| \to 0, \text{ as } n \to 0.$$

so, we have for $(\varphi,\psi)\in \mathrm{H}^{-1/2}(\Gamma_{\mathrm{i}})\times \mathrm{H}^{1/2}(\Gamma_{\mathrm{i}})\setminus\{(0,0)\}$:

$$\lim_n a((\varphi_n^*,\psi_n^*),(\varphi,\psi))=\ell(\varphi,\psi).$$

Now, as the sequence $(\varphi_n^*,\psi_n^*)_n$ is bounded, we have the existence of $(\varphi^*,\psi^*)\in \mathrm{H}^{-1/2}(\Gamma_{\mathrm{i}})\times \mathrm{H}^{1/2}(\Gamma_{\mathrm{i}})$ such that:

$$\varphi_n^*\rightharpoonup\varphi \text{ and } \psi_n^*\rightharpoonup\psi^*, \text{ weakly in } \mathrm{H}^{-1/2}(\Gamma_{\mathrm{i}}) \text{ and } \mathrm{H}^{1/2}(\Gamma_{\mathrm{i}}) \text{ respectively, as } n\to\infty.$$

As $a(\cdot,(\varphi,\psi))$ is a continuous linear functional in $\mathrm{H}^{-1/2}(\Gamma_{\mathrm{i}})\times\mathrm{H}^{1/2}(\Gamma_{\mathrm{i}})$, it is weakly continuous, so we obtain by taking the limit $n\to\infty$, for any $(\varphi,\psi)\in \mathrm{H}^{-1/2}(\Gamma_{\mathrm{i}})\times \mathrm{H}^{1/2}(\Gamma_{\mathrm{i}})\setminus\{(0,0)\}$:

$$a((\varphi^*,\psi^*),(\varphi,\psi))=\ell(\varphi,\psi),$$

which is equivalent to

$$\int_\Omega \nabla(u_{\varphi^*}-u_{\psi^*})\cdot\nabla(v_\varphi-v_\psi)=0,$$

integrating by parts we obtain, $\forall(\varphi,\psi)\in \mathrm{H}^{-1/2}(\Gamma_{\mathrm{i}})\times \mathrm{H}^{1/2}(\Gamma_{\mathrm{i}})\setminus\{(0,0)\}$:

$$\langle\partial_{\mathbf{n}}u_{\varphi^*}-g_N,-v_\psi\rangle_{\Gamma_{obs}}+\langle\varphi^*-\partial_{\mathbf{n}}u_{\psi^*},v_\varphi-\psi\rangle_{\Gamma_{\mathrm{i}}}=0. \tag{1.12}$$

Now, take $\psi=0$ in (1.12), so we obtain, for $\varphi\neq 0$ in $\mathrm{H}^{-1/2}(\Gamma_{\mathrm{i}})$:

$$\langle\varphi^*-\partial_{\mathbf{n}}u_{\psi^*},v_\varphi\rangle_{\Gamma_{\mathrm{i}}}=0,$$

the same applies by definition if $\varphi=0$. with a analogous argument as in Lemma 1.6 we conclude that

$$\partial_{\mathbf{n}}u_{\psi^*}=\varphi^* \text{ in } \mathrm{H}^{-1/2}(\Gamma_{\mathrm{i}}),$$

then (1.12) is reduced to, for $\psi\in \mathrm{H}^{1/2}(\Gamma_{\mathrm{i}})$

$$\langle\partial_{\mathbf{n}}u_{\varphi^*}-g_N,-v_\psi\rangle_{\Gamma_{obs}}=0,$$

using Lemma 1.6 we obtain that

$$\partial_{\mathbf{n}}u_{\varphi^*}=g_N \text{ in } \mathrm{H}^{-1/2}(\Gamma_{obs}),$$

and then u_{φ^*} solves:

$$\begin{cases} -\Delta u_{\varphi^*} &= 0 & \text{in } \Omega\\ u_{\varphi^*} &= g_D & \text{on } \Gamma_{obs}\\ \partial_{\mathbf{n}}u_{\varphi^*} &= g_N & \text{on } \Gamma_{obs}\\ \partial_{\mathbf{n}}u_{\varphi^*} &= \varphi^* & \text{on } \Gamma_{\mathrm{i}}, \end{cases}$$

this is, u_{φ^*} is the unique solution of the Cauchy problem (1.1).

On the other hand, we have proved that $\partial_{\mathbf{n}} u_{\psi^*} = \varphi^* = \partial_{\mathbf{n}} u_{\varphi^*}$ in $\mathrm{H}^{-1/2}(\Gamma_{\mathrm{i}})$, so, u_{ψ^*} solves:

$$\left\{\begin{array}{rcll} -\Delta u_{\psi^*} & = & 0 & \text{in } \Omega \\ \partial_{\mathbf{n}} u_{\psi^*} & = & g_N & \text{on } \Gamma_{obs} \\ \partial_{\mathbf{n}} u_{\psi^*} & = & \varphi^* & \text{on } \Gamma_{\mathrm{i}} \\ u_{\psi^*} & = & \psi^* & \text{on } \Gamma_{\mathrm{i}}. \end{array}\right.$$

Taking $w := u_{\psi^*} - u_{\varphi^*} \in \mathrm{H}^1(\Omega)$, we have

$$\left\{\begin{array}{rcll} -\Delta w & = & 0 & \text{in } \Omega \\ \partial_{\mathbf{n}} w & = & 0 & \text{on } \partial\Omega, \end{array}\right.$$

this implies $u_{\psi^*} = u_{\varphi^*} + C$ with $C \in \mathbb{R}$ and therefore the pair (φ^*, ψ^*) is a minimizer of the Kohn-Vogelius functional: $\mathcal{K}(\varphi^*, \psi^*) = 0$.

In order to obtain the weak convergence $u_{\varphi_n^*} \rightharpoonup u_{\varphi^*}$, we first notice that, as (φ_n^*, ψ_n^*) is bounded in $\mathrm{H}^{-1/2}(\Gamma_{\mathrm{i}}) \times \mathrm{H}^{1/2}(\Gamma_{\mathrm{i}})$, then the sequences $(u_{\varphi_n^*}, u_{\psi_n^*})$ are bounded in $\mathrm{H}^1(\Omega)$, therefore there exists $(u_1, u_2) \in \mathrm{H}^1(\Omega) \times \mathrm{H}^1(\Omega)$ such that

$$u_{\varphi_n^*} \rightharpoonup u_1 \text{ and } u_{\psi_n^*} \rightharpoonup u_2,$$

weakly in $\mathrm{H}^1(\Omega)$. By weak-continuity of trace and normal derivative operators and the uniqueness of the weak limit, we conclude that $u_1 = u_{\varphi^*} = u_{ex}$ and $u_2 = u_{\psi^*}$ □

Finally, we have the following result about the minimizing sequences of $\mathcal{K}$:

Proposition 1.8 *For any $(g_N, g_D) \in \mathrm{H}^{-1/2}(\Gamma_{obs}) \times \mathrm{H}^{1/2}(\Gamma_{obs})$, let $(\varphi_n, \psi_n) \subset \mathrm{H}^{-1/2}(\Gamma_{\mathrm{i}}) \times \mathrm{H}^{1/2}(\Gamma_{\mathrm{i}})$ a minimizing sequence of $\mathcal{K}$. Then (φ_n, ψ_n) is a pseudo-solution of* (1.8).

Proof. Let us take a minimizing sequence for $\mathcal{K}$.For $t \in \mathbb{R}$ and $(\varphi, \psi) \in \mathrm{H}^{-1/2}(\Gamma_{\mathrm{i}}) \times \mathrm{H}^{1/2}(\Gamma_{\mathrm{i}})$, we have

$$\begin{aligned} \mathcal{K}((\varphi_n, \psi_n) + t(\varphi, \psi)) &= \frac{1}{2}|u_{\varphi_n + t\varphi} - u_{\psi_n + t\psi}|^2_{\mathrm{H}^1(\Omega)} = \frac{1}{2}|u_{\varphi_n} - u_{\psi_n} + t(v_\varphi - v_\psi)|^2_{\mathrm{H}^1(\Omega)} \\ &= \frac{1}{2}|u_{\varphi_n} - u_{\psi_n}|^2_{\mathrm{H}^1(\Omega)} + \frac{t^2}{2}|v_\varphi - v_\psi|^2_{\mathrm{H}^1(\Omega)} \\ &\qquad + t\int_\Omega \nabla(u_{\varphi_n} - u_{\psi_n}) \cdot \nabla(v_\varphi - v_\psi)\,\mathrm{d}x \\ &= \frac{1}{2}|u_{\varphi_n} - u_{\psi_n}|^2_{\mathrm{H}^1(\Omega)} + \frac{t^2}{2}|v_\varphi - v_\psi|^2_{\mathrm{H}^1(\Omega)} \\ &\qquad + t\, a((\varphi_n, \psi_n), (\varphi, \psi)) - \ell(\varphi, \psi). \end{aligned}$$

Notice that this expression can be seen as the polynomial $at^2 + bt + c$ and should be greater than 0 by the positiveness of the $\mathcal{K}$ functional. Thus, we must have $b^2 - 4ac \leq 0$ or equivalently

$$(a((\varphi_n, \psi_n), (\varphi, \psi)) - \ell(\varphi, \psi))^2 - 4\,\frac{1}{2}|v_\varphi - v_\psi|^2_{\mathrm{H}^1(\Omega)}\,\frac{1}{2}|u_{\varphi_n} - u_{\psi_n}|^2_{\mathrm{H}^1(\Omega)} \leq 0,$$

for all $(\varphi,\psi)\in \mathrm{H}^{-1/2}(\Gamma_{\mathrm{i}})\times \mathrm{H}^{1/2}(\Gamma_{\mathrm{i}})$. This leads

$$\left(a((\varphi_n,\psi_n),(\varphi,\psi))-\ell(\varphi,\psi)\right)^2 \leq C\,\|(\varphi,\psi)\|^2_{\mathrm{H}^{-1/2}(\Gamma_{\mathrm{i}})\times \mathrm{H}^{1/2}(\Gamma_{\mathrm{i}})}\,|u_{\varphi_n}-u_{\psi_n}|^2_{\mathrm{H}^1(\Omega)}$$

and finally

$$\forall(\varphi,\psi)\in \mathrm{H}^{-1/2}(\Gamma_{\mathrm{i}})\times \mathrm{H}^{1/2}(\Gamma_{\mathrm{i}}),\quad \frac{\left(a((\varphi_n,\psi_n),(\varphi,\psi))-\ell(\varphi,\psi)\right)^2}{\|(\varphi,\psi)\|^2_{\mathrm{H}^{-1/2}(\Gamma_{\mathrm{i}})\times \mathrm{H}^{1/2}(\Gamma_{\mathrm{i}})}}\leq C\,\mathcal{K}(\varphi_n,\psi_n).$$

We conclude taking supremum over $(\varphi,\psi)\in \mathrm{H}^{-1/2}(\Gamma_{\mathrm{i}})\times \mathrm{H}^{1/2}(\Gamma_{\mathrm{i}})$ and passing to the limit when $n\to\infty$. □

Remark Using this result with Proposition 1.7 we conclude that, if we have a bounded minimizing sequence $(\varphi_n,\psi_n)_n$ of the functional $\mathcal{K}$, then, the Cauchy problem (1.1) has a solution and we have the weak convergence $u_{\varphi_n}\rightharpoonup u_{\mathrm{ex}}$ as $n\to\infty$.

1.2.2 The Regularized Functional $\mathcal{K}_\varepsilon$ and its properties.

As mentioned above, it may be possible that our minimization problem does not have solution due to the lack of coercivity of the Kohn-Vogelius functional. Additionally, as recalled in Section 1.1, the data completion problem is ill-posed in the sense that, in case of the existence of solution, there is not a continuous dependence on the given data. Thus, any little error in the measurement of the data (which is natural in any application) could lead to a big error in the obtained solution in relation with the real one (see [18, 55] for details).

In order to overcome these difficulties, we can consider a regularization of the considered functional. In our case, we will consider a *Tikhonov regularization*, which, roughly speaking, allows us to get coerciveness to the new functional and a better behavior with respect to noisy data. There is an extensive literature related to this type of regularization: we recommend (as we followed this approach) the book of Engl *et al.* [48] which describes in detail and in full generality the considered regularization.

Hence, let us consider now the regularized Kohn-Vogelius functional $\mathcal{K}_\varepsilon : \mathrm{H}^{-1/2}(\Gamma_{\mathrm{i}})\times \mathrm{H}^{1/2}(\Gamma_{\mathrm{i}})\to\mathbb{R}$ given by

$$\mathcal{K}_\varepsilon(\varphi,\psi):=\mathcal{K}(\varphi,\psi)+\frac{\varepsilon}{2}\left(\|v_\varphi\|^2_{\mathrm{H}^1(\Omega)}+\|v_\psi\|^2_{\mathrm{H}^1(\Omega)}\right)=:\mathcal{K}(\varphi,\psi)+\frac{\varepsilon}{2}\|(v_\varphi,v_\psi)\|^2_{(\mathrm{H}^1(\Omega))^2},\tag{1.13}$$

where $\mathcal{K}$ is the previous Kohn-Vogelius functional given by (1.6). The regularizing term adds coerciveness to the functional which leads to important advantages. For example, we can always obtain a pair $(\varphi^*_\varepsilon,\psi^*_\varepsilon)$ which minimizes $\mathcal{K}_\varepsilon$. The immediate question is how can we relate this optimal pair to the possible optimal pair (φ^*,ψ^*) of $\mathcal{K}$. We will explore in this section several properties of the regularized functional $\mathcal{K}_\varepsilon$ and we start with a list of basic ones.

Proposition 1.9 *Given $\varepsilon > 0$, the functional $\mathcal{K}_\varepsilon$ satisfies the following properties.*

1. *$\mathcal{K}_\varepsilon(\varphi, \psi)$ is continuous, strictly convex and coercive in $\mathrm{H}^{-1/2}(\Gamma_\mathrm{i}) \times \mathrm{H}^{1/2}(\Gamma_\mathrm{i})$. Therefore, there exists*

$$(\varphi_\varepsilon^*, \psi_\varepsilon^*) = \operatorname*{argmin}_{(\varphi,\psi)} \mathcal{K}_\varepsilon(\varphi, \psi).$$

2. *The optimality condition for $(\varphi_\varepsilon^*, \psi_\varepsilon^*)$ to be a minimizer of $\mathcal{K}_\varepsilon$ is: for all $(\widetilde{\varphi}, \widetilde{\psi}) \in \mathrm{H}^{-1/2}(\Gamma_\mathrm{i}) \times \mathrm{H}^{1/2}(\Gamma_\mathrm{i})$,*

$$a((\varphi_\varepsilon^*, \psi_\varepsilon^*), (\widetilde{\varphi}, \widetilde{\psi})) + \varepsilon \cdot b((\varphi_\varepsilon^*, \psi_\varepsilon^*), (\widetilde{\varphi}, \widetilde{\psi})) = \ell(\widetilde{\varphi}, \widetilde{\psi}) \tag{1.14}$$

   where $a(\cdot,\cdot)$ and $\ell(\cdot)$ are previously defined by (1.9) and $b(\cdot,\cdot)$ is defined by:

$$b((\varphi_1, \psi_1), (\varphi_2, \psi_2)) = ((v_{\varphi_1}, v_{\psi_1}), (v_{\varphi_2}, v_{\psi_2}))_{\mathrm{H}^1(\Omega)\times\mathrm{H}^1(\Omega)}. \tag{1.15}$$

3. *The bilinear form b defines an inner product in $\mathrm{H}^{-1/2}(\Gamma_\mathrm{i}) \times \mathrm{H}^{1/2}(\Gamma_\mathrm{i})$ which associated norm is equivalent to the standard one in that space.*

Proof. We prove each statement:

1. The continuity and convexity are obvious. In order to see that $\mathcal{K}_\varepsilon$ is coercive, let us suppose it is not. Then, there exists a sequence $(\varphi_n, \psi_n)_n$ and a constant $C > 0$ such that:

$$\lim_{n\to\infty} \|(\varphi_n, \psi_n)\|_{\mathrm{H}^{-1/2}(\Gamma_\mathrm{i})\times\mathrm{H}^{1/2}(\Gamma_\mathrm{i})} = +\infty \quad \text{and} \quad \mathcal{K}_\varepsilon(\varphi_n, \psi_n) < C.$$

   This implies $\|v_{\varphi_n}\|_{\mathrm{H}^1(\Omega)} < C$ and $\|v_{\psi_n}\|_{\mathrm{H}^1(\Omega)} < C$ for all n which, by the continuity of trace and normal derivative operators, implies $\|(\varphi_n, \psi_n)\|_{\mathrm{H}^{-1/2}(\Gamma_\mathrm{i})\times\mathrm{H}^{1/2}(\Gamma_\mathrm{i})} < C$ which is in contradiction with the original assumption.

   The existence of minimizers comes from the continuity, convexity and coerciveness of $\mathcal{K}_\varepsilon$ (see, e.g., [28, Chapter 3]).
2. As in the proof of Proposition 1.4, the result comes from a standard computation.
3. The fact that b defines an inner product is immediate from its bilinearity and the well-posedness of the problems solved by v_φ and v_ψ. The equivalence of norms comes from the continuity of the trace and normal derivative operator and the well-posedness of the problems solved by v_φ and v_ψ.

□

In the case when (g_D, g_N) is compatible, we have the following convergence result:

Theorem 1.10 *Let us suppose that (g_D, g_N) is compatible data related to u_{ex} and let us denote by $u_{\varphi_\varepsilon^*}$ the function associated with φ_ε^* minimizer of $\mathcal{K}_\varepsilon$. Then*

$$\lim_{\varepsilon\to 0} \|u_{\varphi_\varepsilon^*} - u_{\mathrm{ex}}\|_{\mathrm{H}^1(\Omega)} = 0. \tag{1.16}$$

PROOF. Let us recall that

$$\mathcal{K}_\varepsilon(\varphi,\psi)=\mathcal{K}(\varphi,\psi)+\frac{\varepsilon}{2}\|(v_\varphi,v_\psi)\|^2_{(\mathrm{H}^1(\Omega))^2}\quad\text{and}\quad(\varphi^*_\varepsilon,\psi^*_\varepsilon):=\operatorname*{argmin}_{(\varphi,\psi)}\mathcal{K}_\varepsilon(\varphi,\psi)$$

and let us define $\varphi_{ex}:=\partial_{\mathbf{n}}u_{\mathrm{ex}}|_{\Gamma_{\mathrm{i}}}$ and $\psi_{ex}:=u_{\mathrm{ex}}|_{\Gamma_{\mathrm{i}}}$. Notice that we have $\mathcal{K}(\varphi_{\mathrm{ex}},\psi_{\mathrm{ex}})=0$ and $\mathcal{K}(\varphi^*_\varepsilon,\psi^*_\varepsilon)\le\mathcal{K}_\varepsilon(\varphi^*_\varepsilon,\psi^*_\varepsilon)\le\mathcal{K}_\varepsilon(\varphi_{\mathrm{ex}},\psi_{\mathrm{ex}})=\frac{\varepsilon}{2}\|(v_{\varphi_{\mathrm{ex}}},v_{\psi_{\mathrm{ex}}})\|^2_{(\mathrm{H}^1(\Omega))^2}$. This implies:

$$|u_{\varphi^*_\varepsilon}-u_{\psi^*_\varepsilon}|^2_{\mathrm{H}^1(\Omega)}\le\varepsilon\left(\|v_{\varphi_{\mathrm{ex}}}\|^2_{\mathrm{H}^1(\Omega)}+\|v_{\psi_{\mathrm{ex}}}\|^2_{\mathrm{H}^1(\Omega)}\right),\tag{1.17}$$

$$\|v_{\varphi^*_\varepsilon}\|^2_{\mathrm{H}^1(\Omega)}+\|v_{\psi^*_\varepsilon}\|^2_{\mathrm{H}^1(\Omega)}\le\|v_{\varphi_{\mathrm{ex}}}\|^2_{\mathrm{H}^1(\Omega)}+\|v_{\psi_{\mathrm{ex}}}\|^2_{\mathrm{H}^1(\Omega)}.\tag{1.18}$$

Now, let us consider an arbitrary sequence of positive numbers $(\varepsilon_n)_n$ such that $\lim_{n\to\infty}\varepsilon_n=0$. From (1.18) we have that the sequences $(v_{\varphi^*_{\varepsilon_n}})_{\varepsilon_n}$ and $(v_{\psi^*_{\varepsilon_n}})_{\varepsilon_n}$ are bounded in $\mathrm{H}^1(\Omega)$. Then there exist subsequences, which will be denoted as the original sequences, such that $v_{\varphi^*_{\varepsilon_n}}\rightharpoonup v_{\varphi^*}$ and $v_{\psi^*_{\varepsilon_n}}\rightharpoonup v_{\psi^*}$ in $\mathrm{H}^1(\Omega)$. This implies

$$u_{\varphi^*_{\varepsilon_n}}=u_0^{g_D}+v_{\varphi^*_{\varepsilon_n}}\rightharpoonup u_0^{g_D}+v_{\varphi^*}=u_{\varphi^*}\quad\text{and}\quad u_{\psi^*_{\varepsilon_n}}=u_0^{g_N}+v_{\psi^*_{\varepsilon_n}}\rightharpoonup u_0^{g_N}+v_{\psi^*}=u_{\psi^*}.$$

Moreover, by (1.17), letting $n\to\infty$, we have, for $C\in\mathbb{R}$: $u_{\varphi^*}=u_{\psi^*}+C=u_{\psi^*+C}$. By continuity of trace and normal derivative trace operator, we have: $v_{\varphi^*}|_{\Gamma_{obs}}=0$ and $\partial_{\mathbf{n}}v_{\psi^*}|_{\Gamma_{obs}}=0$. Then $u_{\varphi^*}|_{\Gamma_{obs}}=g_D$ and $\partial_{\mathbf{n}}u_{\psi^*}|_{\Gamma_{obs}}=g_N$ and, since $\partial_{\mathbf{n}}u_{\varphi^*}|_{\Gamma_{obs}}=\partial_{\mathbf{n}}u_{\psi^*}|_{\Gamma_{obs}}=g_N$, the function $u_{\varphi^*}\in\mathrm{H}^1(\Omega)$ satisfies

$$\left\{\begin{array}{rcll}-\Delta u_{\varphi^*}&=&0&\text{in }\Omega\\ u_{\varphi^*}&=&g_D&\text{on }\Gamma_{obs}\\ \partial_{\mathbf{n}}u_{\varphi^*}&=&g_N&\text{on }\Gamma_{obs}.\end{array}\right.$$

therefore, by uniqueness of the Cauchy problem, we have $u_{\varphi^*}=u_{\mathrm{ex}}$ and, in particular, $u_{\psi^*}=u_{\mathrm{ex}}+C$ for some $C\in\mathbb{R}$.

So, we have now:

$$u_{\varphi^*_{\varepsilon_n}}\rightharpoonup u_{\mathrm{ex}}\quad\text{and}\quad u_{\psi^*_{\varepsilon_n}}\rightharpoonup u_{\mathrm{ex}}+C.\tag{1.19}$$

In order to obtain the strong convergence let us prove first the strong convergence of $v_{\varphi^*_{\varepsilon_n}}$ to $v_{\varphi_{\mathrm{ex}}}=v_{\varphi^*}=u_{\varphi^*}-u^{g_D}=u_{\mathrm{ex}}-u^{g_D}$. To this notice that

$$\mathcal{K}_{\varepsilon_n}(\varphi^*_{\varepsilon_n},\psi^*_{\varepsilon_n})\le\mathcal{K}_{\varepsilon_n}(\varphi_{\mathrm{ex}},\psi_{\mathrm{ex}}+C)=\frac{\varepsilon_n}{2}\|(v_{\varphi_{\mathrm{ex}}},v_{\psi_{\mathrm{ex}}+C})\|^2_{(\mathrm{H}^1(\Omega))^2}.$$

Hence,

$$\limsup_n\|(v_{\varphi^*_{\varepsilon_n}},v_{\psi^*_{\varepsilon_n}})\|_{(\mathrm{H}^1(\Omega))^2}\le\|(v_{\varphi_{\mathrm{ex}}},v_{\psi_{\mathrm{ex}}}+C)\|_{(\mathrm{H}^1(\Omega))^2}.$$

This result with the weak convergences (1.19) gives the desired strong convergence, which implies the desired result up to a subsequence. A standard argument by contradiction gives the result for the full sequence. □

Remark We can note that we also have, for some $C\in\mathbb{R}$,

$$u_{\psi^*_\varepsilon}\to u_{\mathrm{ex}}+C\ \text{ in }\mathrm{H}^1(\Omega).$$

We now prove a series of properties to our considered functionals when they are considered as functions of the regularizing parameter ε. This properties will be useful for next sections in which our aim will be to define a regularizing parameter ε such that we can obtain convergence properties when the data (g_N, g_D) is polluted with noise. In order to obtain uniqueness of such a choice, we need to have for example, monotony of the functionals involved when they are considered as a functions of ε.

Proposition 1.11 *Let $(\varphi_\varepsilon^*, \psi_\varepsilon^*) \in \mathrm{H}^{-1/2}(\Gamma_\mathrm{i}) \times \mathrm{H}^{1/2}(\Gamma_\mathrm{i})$ the minimizer of $\mathcal{K}_\varepsilon$. We have the following statements.*

1. *The application $F : \varepsilon \to \left(u_{\varphi_\varepsilon^*}, u_{\psi_\varepsilon^*}\right) \in \mathrm{H}^1(\Omega) \times \mathrm{H}^1(\Omega)$ is continuous for $\varepsilon > 0$ and, if the data (g_N, g_D) is compatible, it could be continuously extended to 0 with $F(0) = (u_{\varphi_\mathrm{ex}}, u_{\psi_\mathrm{ex}})$.*
2. *The application F is (at least) in $\mathcal{C}^2((0,\infty), \mathrm{H}^1(\Omega) \times \mathrm{H}^1(\Omega))$. Its derivative is given by $F'(\varepsilon) = (v_{\varphi'_\varepsilon}, v_{\psi'_\varepsilon})$ where the pair $(\varphi'_\varepsilon, \psi'_\varepsilon) \in \mathrm{H}^{-1/2}(\Gamma_\mathrm{i}) \times \mathrm{H}^{1/2}(\Gamma_\mathrm{i})$ is the unique solution of*

$$a((\varphi'_\varepsilon, \psi'_\varepsilon), (\varphi, \psi)) + \varepsilon b((\varphi'_\varepsilon, \psi'_\varepsilon), (\varphi, \psi)) = -b((\varphi_\varepsilon, \psi_\varepsilon), (\varphi, \psi)), \quad \forall (\varphi, \psi) \in \mathrm{H}^{-1/2}(\Gamma_\mathrm{i}) \times \mathrm{H}^{1/2}(\Gamma_\mathrm{i}). \quad (1.20)$$

   Their second derivative is given by $F''(\varepsilon) = (v_{\varphi''_\varepsilon}, v_{\psi''_\varepsilon})$ where the pair $(\varphi''_\varepsilon, \psi''_\varepsilon) \in \mathrm{H}^{-1/2}(\Gamma_\mathrm{i}) \times \mathrm{H}^{1/2}(\Gamma_\mathrm{i})$ is the unique solution of

$$a((\varphi''_\varepsilon, \psi''_\varepsilon), (\varphi, \psi)) + \varepsilon b((\varphi''_\varepsilon, \psi''_\varepsilon), (\varphi, \psi)) = -2 \cdot b((\varphi'_\varepsilon, \psi'_\varepsilon), (\varphi, \psi)), \quad \forall (\varphi, \psi) \in \mathrm{H}^{-1/2}(\Gamma_\mathrm{i}) \times \mathrm{H}^{1/2}(\Gamma_\mathrm{i}). \quad (1.21)$$

3. *The map $\varepsilon \mapsto \frac{1}{2}|u_{\varphi_\varepsilon^*} - u_{\psi_\varepsilon^*}|^2_{\mathrm{H}^1(\Omega)}$ is strictly increasing for $\varepsilon > 0$.*
4. *The map $\varepsilon \mapsto \frac{1}{2}\| \left(v_{\varphi_\varepsilon^*}, v_{\psi_\varepsilon^*}\right) \|^2_{\mathrm{H}^1(\Omega)\times\mathrm{H}^1(\Omega)}$ is decreasing for $\varepsilon > 0$.*
5. *The map $\varepsilon \mapsto \frac{1}{2}|u_{\varphi_\varepsilon^*} - u_{\psi_\varepsilon^*}|^2_{\mathrm{H}^1(\Omega)} + \frac{\varepsilon}{2}\| \left(v_{\varphi_\varepsilon^*}, v_{\psi_\varepsilon^*}\right) \|^2_{\mathrm{H}^1(\Omega)\times\mathrm{H}^1(\Omega)}$ is increasing for $\varepsilon > 0$.*
6. *If the data (g_N, g_D) is compatible, the map $\varepsilon \mapsto \frac{1}{2}\| \left(u_{\varphi_\varepsilon^*} - u_\mathrm{ex}, u_{\psi_\varepsilon^*} - u_\mathrm{ex}\right) \|^2_{\mathrm{H}^1(\Omega)\times\mathrm{H}^1(\Omega)}$ is increasing for $\varepsilon > 0$.*

Proof. Let us prove each statement.[1]

1. To prove the continuity, let $h \in \mathbb{R}$ such that $\varepsilon + h > 0$, we have to prove that

$$\|u_{\varphi^*_{\varepsilon+h}} - u_{\varphi^*_\varepsilon}, u_{\psi^*_{\varepsilon+h}} - u_{\psi^*_\varepsilon}\|_{(\mathrm{H}^1(\Omega))^2} \underset{h\to 0}{\longrightarrow} 0.$$

   Then, let us consider the optimal pairs $(\varphi^*_{\varepsilon+h}, \psi^*_{\varepsilon+h})$ and $(\varphi^*_\varepsilon, \psi^*_\varepsilon)$. Subtracting the optimality conditions of both pairs, we obtain, for all $(\varphi, \psi) \in \mathrm{H}^{-1/2}(\Gamma_\mathrm{i}) \times \mathrm{H}^{1/2}(\Gamma_\mathrm{i})$,

$$a((\varphi^*_{\varepsilon+h} - \varphi^*_\varepsilon, \psi^*_{\varepsilon+h} - \psi^*_\varepsilon), (\varphi, \psi)) + \varepsilon \cdot b((\varphi^*_{\varepsilon+h} - \varphi^*_\varepsilon, \psi^*_{\varepsilon+h} - \psi^*_\varepsilon), (\varphi, \psi)) = -h \cdot b((\varphi^*_{\varepsilon+h} - \varphi^*_\varepsilon, \psi^*_{\varepsilon+h} - \psi^*_\varepsilon), (\varphi, \psi)).$$

[1] In this proof we use the notation $(\mathrm{H}^1(\Omega))^2 := \mathrm{H}^1(\Omega) \times \mathrm{H}^1(\Omega)$ for readers convenience.

Choosing $\varphi := \varphi^*_{\varepsilon+h} - \varphi^*_\varepsilon$ and $\psi := \psi^*_{\varepsilon+h} - \psi^*_\varepsilon$, we get:

$$|v_{\varphi^*_{\varepsilon+h}} - v_{\varphi^*_\varepsilon} - (v_{\psi^*_{\varepsilon+h}} - v_{\psi^*_\varepsilon})|^2_{\mathrm{H}^1(\Omega)} + \varepsilon\|(v_{\varphi^*_{\varepsilon+h}} - v_{\varphi^*_\varepsilon}, v_{\psi^*_{\varepsilon+h}} - v_{\psi^*_\varepsilon}\|^2_{(\mathrm{H}^1(\Omega))^2} = -h \cdot ((v_{\varphi^*_{\varepsilon+h}}, v_{\psi^*_{\varepsilon+h}}), (v_{\varphi^*_{\varepsilon+h}-\varphi^*_\varepsilon}, v_{\psi^*_{\varepsilon+h}-\psi^*_\varepsilon}))_{(\mathrm{H}^1(\Omega))^2}.$$

Now, notice we have

$$|((v_{\varphi^*_{\varepsilon+h}}, v_{\psi^*_{\varepsilon+h}}), (v_{\varphi^*_{\varepsilon+h}-\varphi^*_\varepsilon}, v_{\psi^*_{\varepsilon+h}-\psi^*_\varepsilon}))|_{(\mathrm{H}^1(\Omega))^2} \leq \|(v_{\varphi^*_{\varepsilon+h}}, v_{\psi^*_{\varepsilon+h}})\|_{(\mathrm{H}^1(\Omega))^2} \|(v_{\varphi^*_{\varepsilon+h}-\varphi^*_\varepsilon}, v_{\psi^*_{\varepsilon+h}-\psi^*_\varepsilon})\|_{(\mathrm{H}^1(\Omega))^2}$$

which gives

$$\|(v_{\varphi^*_{\varepsilon+h}} - v_{\varphi^*_\varepsilon}, v_{\psi^*_{\varepsilon+h}} - v_{\psi^*_\varepsilon})\|^2_{(\mathrm{H}^1(\Omega))^2} \leq \frac{|h|}{\varepsilon}\|(v_{\varphi^*_{\varepsilon+h}}, v_{\psi^*_{\varepsilon+h}})\|_{(\mathrm{H}^1(\Omega))^2} \|(v_{\varphi^*_{\varepsilon+h}} - v_{\varphi^*_\varepsilon}, v_{\psi^*_{\varepsilon+h}} - v_{\psi^*_\varepsilon})\|_{(\mathrm{H}^1(\Omega))^2}$$

and then

$$\|(v_{\varphi^*_{\varepsilon+h}} - v_{\varphi^*_\varepsilon}, v_{\psi^*_{\varepsilon+h}} - v_{\psi^*_\varepsilon})\|_{(\mathrm{H}^1(\Omega))^2} \leq \frac{|h|}{\varepsilon}\|(v_{\varphi^*_{\varepsilon+h}}, v_{\psi^*_{\varepsilon+h}})\|_{(\mathrm{H}^1(\Omega))^2}.$$

Moreover, by definition of $\mathcal{K}_{\varepsilon+h}$,

$$(\varepsilon+h)\|(v_{\varphi^*_{\varepsilon+h}}, v_{\psi^*_{\varepsilon+h}})\|^2_{\mathrm{H}^1(\Omega)} \leq \mathcal{K}_{\varepsilon+h}(\varphi^*_{\varepsilon+h}, \psi^*_{\varepsilon+h}) \leq \mathcal{K}_{\varepsilon+h}(0,0).$$

Noticing that

$$\mathcal{K}_{\varepsilon+h}(0,0) = \frac{1}{2}|u_0^{g_D} - u_0^{g_N}|^2_{\mathrm{H}^1(\Omega)} \leq C\left(\|g_D\|^2_{\mathrm{H}^{1/2}(\Gamma_{obs})} + \|g_N\|^2_{\mathrm{H}^{-1/2}(\Gamma_{obs})}\right),$$

we obtain

$$\|(v_{\varphi^*_{\varepsilon+h}} - v_{\varphi^*_\varepsilon}, v_{\psi^*_{\varepsilon+h}} - v_{\psi^*_\varepsilon})\|_{(\mathrm{H}^1(\Omega))^2} \leq \frac{|h|}{\varepsilon}\|(v_{\varphi^*_{\varepsilon+h}}, v_{\psi^*_{\varepsilon+h}})\|_{(\mathrm{H}^1(\Omega))^2} \leq \left(\|g_D\|^2_{\mathrm{H}^{1/2}(\Gamma_{obs})} + \|g_N\|^2_{\mathrm{H}^{-1/2}(\Gamma_{obs})}\right)\frac{|h|}{\varepsilon\sqrt{\varepsilon+h}} \underset{h\to 0}{\longrightarrow} 0, \quad (1.22)$$

which concludes the proof.

2. First, the existence and uniqueness of the solution $(\varphi'_\varepsilon, \psi'_\varepsilon) \in \mathrm{H}^{-1/2}(\Gamma_\mathrm{i}) \times \mathrm{H}^{1/2}(\Gamma_\mathrm{i})$ of Problem (1.20) is due to Lax-Milgram theorem. Indeed, the continuity of the bilinear form $a(\cdot,\cdot)+\varepsilon b(\cdot,\cdot)$ and of the linear form $-b\left((\varphi^*_\varepsilon, \psi^*_\varepsilon), (\cdot,\cdot)\right)$ are due to the well-posedness of the problems solved by v_φ and v_ψ and the continuity of $a(\cdot,\cdot) + \varepsilon b(\cdot,\cdot)$ is due to the continuity of trace operator and normal derivative operator.

   Now, let us prove that the derivative of the function F is $F'(\varepsilon) = (v_{\varphi'_\varepsilon}, v_{\psi'_\varepsilon})$. For this, let $h \in \mathbb{R}$ such that $\varepsilon + h > 0$. From the optimality conditions for $(\varphi^*_\varepsilon, \psi^*_\varepsilon)$ and $(\varphi^*_{\varepsilon+h}, \psi^*_{\varepsilon+h})$ and the condition satisfied from $(\varphi'_\varepsilon, \psi'_\varepsilon)$, we obtain

$$a((\varphi^*_{\varepsilon+h} - \varphi^*_\varepsilon - h\varphi'_\varepsilon, \psi^*_{\varepsilon+h} - \psi^*_\varepsilon - h\psi'_\varepsilon), (\varphi,\psi)) + \varepsilon \cdot b((\varphi^*_{\varepsilon+h} - \varphi^*_\varepsilon - h\varphi'_\varepsilon, \psi^*_{\varepsilon+h} - \psi^*_\varepsilon - h\psi'_\varepsilon), (\varphi,\psi)) = h \cdot b((\varphi^*_\varepsilon - \varphi^*_{\varepsilon+h}, \psi^*_\varepsilon - \psi^*_{\varepsilon+h}), (\varphi,\psi)).$$

Taking $\varphi := \varphi^*_{\varepsilon+h} - \varphi^*_\varepsilon - h\varphi'_\varepsilon$ and $\psi := \psi^*_{\varepsilon+h} - \psi^*_\varepsilon - h\psi'_\varepsilon$, we use Holder inequality on the right side to get

$$\begin{aligned}|u_{\varphi^*_{\varepsilon+h}-\varphi^*_\varepsilon-h\varphi'_\varepsilon} - u_{\psi^*_{\varepsilon+h}-\psi^*_\varepsilon-h\psi'_\varepsilon}|^2_{\mathrm{H}^1(\Omega)} + \varepsilon\cdot\|(v_{\varphi^*_{\varepsilon+h}-\varphi^*_\varepsilon-h\varphi'_\varepsilon}, v_{\psi^*_{\varepsilon+h}-\psi^*_\varepsilon-h\psi'_\varepsilon})\|^2_{(\mathrm{H}^1(\Omega))^2}\\ \leq |h|\|(v_{\varphi^*_\varepsilon-\varphi^*_{\varepsilon+h}}, v_{\psi^*_\varepsilon-\psi^*_{\varepsilon+h}})\|_{(\mathrm{H}^1(\Omega))^2}\,\|(v_{\varphi^*_{\varepsilon+h}-\varphi^*_\varepsilon-h\varphi'_\varepsilon}, v_{\psi^*_{\varepsilon+h}-\psi^*_\varepsilon-h\psi'_\varepsilon})\|_{(\mathrm{H}^1(\Omega))^2}\end{aligned}$$

and then,

$$\|v_{\varphi^*_{\varepsilon+h}-\varphi^*_\varepsilon-h\varphi'_\varepsilon}, v_{\psi^*_{\varepsilon+h}-\psi^*_\varepsilon-h\psi'_\varepsilon}\|_{(\mathrm{H}^1(\Omega))^2} \leq \frac{|h|}{\varepsilon}\|v_{\varphi^*_\varepsilon-\varphi^*_{\varepsilon+h}}, v_{\psi^*_\varepsilon-\psi^*_{\varepsilon+h}}\|_{(\mathrm{H}^1(\Omega))^2}.$$

Hence, using the previous bound (1.22), we obtain

$$\begin{aligned}\|u_{\varphi^*_{\varepsilon+h}} - u_{\varphi^*_\varepsilon} - h\,v_{\varphi'_\varepsilon}, u_{\psi^*_{\varepsilon+h}} - u_{\psi^*_\varepsilon} - h\,v_{\psi'_\varepsilon}\|_{(\mathrm{H}^1(\Omega))^2}&\\ \leq \frac{|h|}{\varepsilon}\,C\frac{|h|}{\varepsilon\sqrt{\varepsilon+h}} = C\frac{h^2}{\varepsilon^2\sqrt{\varepsilon+h}} \underset{h\to 0}{\longrightarrow} 0.&\end{aligned}$$

To conclude, the continuity of the application F' follows an identical proof of the continuity of F and the proof for $F''(\varphi,\psi) = (v_{\varphi''_\varepsilon}, v_{\psi''_\varepsilon})$ is analog to the first derivative case.

3. Let us call $g(\varepsilon) := \frac{1}{2}|u_{\varphi^*_\varepsilon} - u_{\psi^*_\varepsilon}|^2_{\mathrm{H}^1(\Omega)} = \frac{1}{2}\|\nabla(u_{\varphi^*_\varepsilon} - u_{\psi^*_\varepsilon})\|^2_{(\mathrm{L}^2(\Omega))^{\mathrm{d}}}$. We have, thanks to the optimality condition for $(\varphi^*_\varepsilon, \psi^*_\varepsilon)$ and the system solved by $(\varphi'_\varepsilon, \psi'_\varepsilon)$,

$$\begin{aligned}g'(\varepsilon) &= (\nabla(u_{\varphi^*_\varepsilon} - u_{\psi^*_\varepsilon}), \nabla(v_{\varphi'_\varepsilon} - v_{\psi'_\varepsilon}))_{(\mathrm{L}^2(\Omega))^{\mathrm{d}}}\\ &= a((\varphi^*_\varepsilon,\psi^*_\varepsilon),(\varphi'_\varepsilon,\psi'_\varepsilon)) - \ell(\varphi'_\varepsilon,\psi'_\varepsilon)\\ &= -\varepsilon\cdot b((\varphi^*_\varepsilon,\psi^*_\varepsilon),(\varphi'_\varepsilon,\psi'_\varepsilon))\\ &= \varepsilon\cdot a((\varphi'_\varepsilon,\psi'_\varepsilon),(\varphi'_\varepsilon,\psi'_\varepsilon)) + \varepsilon^2\cdot b((\varphi'_\varepsilon,\psi'_\varepsilon),(\varphi'_\varepsilon,\psi'_\varepsilon))\\ &= \varepsilon\int_\Omega |\nabla v_{\varphi'_\varepsilon} - \nabla v_{\psi'_\varepsilon}|^2 + \varepsilon^2\|(v_{\varphi'_\varepsilon}, v_{\psi'_\varepsilon})\|^2_{(\mathrm{H}^1(\Omega))^2}.\end{aligned}$$

So, $g'(\varepsilon) > 0$ if $\varepsilon > 0$ and we conclude.

4. Let us call $G(\varepsilon) := \frac{1}{2}\|(v_{\varphi^*_\varepsilon}, v_{\psi^*_\varepsilon})\|^2_{(\mathrm{H}^1(\Omega))^2}$. We have:

$$\begin{aligned}G'(\varepsilon) = ((v_{\varphi^*_\varepsilon}, v_{\psi^*_\varepsilon}),(v_{\varphi'_\varepsilon}, v_{\psi'_\varepsilon}))_{(\mathrm{H}^1(\Omega))^2} &= b((\varphi^*_\varepsilon,\psi^*_\varepsilon),(\varphi'_\varepsilon,\psi'_\varepsilon))\\ &= -a((\varphi'_\varepsilon,\psi'_\varepsilon),(\varphi'_\varepsilon,\psi'_\varepsilon)) - \varepsilon\cdot b((\varphi'_\varepsilon,\psi'_\varepsilon),(\varphi'_\varepsilon,\psi'_\varepsilon)) \leq 0.\end{aligned}$$

So, $G'(\varepsilon) \leq 0$ and we conclude.

5. Let us call $h(\varepsilon) := \mathcal{K}_\varepsilon(\varphi^*_\varepsilon, \varphi^*_\varepsilon)$. From the previous computations, we have

$$h'(\varepsilon) = \underbrace{a((\varphi^*_\varepsilon,\psi^*_\varepsilon),(\varphi'_\varepsilon,\psi'_\varepsilon)) - \ell(\varphi'_\varepsilon,\psi'_\varepsilon) + \varepsilon\cdot b((\varphi^*_\varepsilon,\psi^*_\varepsilon),(\varphi'_\varepsilon,\psi'_\varepsilon))}_{=0} + \frac{1}{2}\|v_{\varphi^*_\varepsilon}, v_{\psi^*_\varepsilon}\|^2 \geq 0.$$

So, $h'(\varepsilon) \geq 0$ and we conclude.

6. Let us call $H(\varepsilon) := \frac{1}{2}\|u_{\varphi^*_\varepsilon} - u_{\mathrm{ex}}, u_{\psi^*_\varepsilon} - u_{\mathrm{ex}}\|^2_{(\mathrm{H}^1(\Omega))^2}$. We have

$$\begin{aligned}H'(\varepsilon) &= ((u_{\varphi^*_\varepsilon} - u_{\mathrm{ex}}, u_{\psi^*_\varepsilon} - u_{\mathrm{ex}}),(v_{\varphi'_\varepsilon}, v_{\psi'_\varepsilon}))_{(\mathrm{H}^1(\Omega))^2},\\ H''(\varepsilon) &= \|v_{\varphi'_\varepsilon}, v_{\psi'_\varepsilon}\|^2_{(\mathrm{H}^1(\Omega))^2} + ((u_{\varphi^*_\varepsilon} - u_{\mathrm{ex}}, u_{\psi^*_\varepsilon} - u_{\mathrm{ex}}),(v_{\varphi''_\varepsilon}, v_{\psi''_\varepsilon}))_{(\mathrm{H}^1(\Omega))^2}.\end{aligned}$$

Then, we have:

$$\begin{aligned}
\varepsilon H''(\varepsilon) &= \varepsilon\|(v_{\varphi'_\varepsilon}, v_{\psi'_\varepsilon})\|^2_{(\mathrm{H}^1(\Omega))^2} - a((\varphi^*_\varepsilon, \psi^*_\varepsilon), (\varphi''_\varepsilon, \psi''_\varepsilon)) \\
&\quad -2b((\varphi^*_\varepsilon - \varphi_{\mathrm{ex}}, \psi^*_\varepsilon - \psi_{\mathrm{ex}}), (\varphi'_\varepsilon, \psi'_\varepsilon)) \\
&= \varepsilon\|(v_{\varphi'_\varepsilon}, v_{\psi'_\varepsilon})\|^2_{(\mathrm{H}^1(\Omega))^2} - 2H'(\varepsilon) - a((\varphi^*_\varepsilon, \psi^*_\varepsilon), (\varphi''_\varepsilon, \psi''_\varepsilon)) \\
&= \varepsilon\|(v_{\varphi'_\varepsilon}, v_{\psi'_\varepsilon})\|^2_{(\mathrm{H}^1(\Omega))^2} - 2H'(\varepsilon) + b((\varphi^*_\varepsilon, \psi^*_\varepsilon), (\varphi''_\varepsilon, \psi''_\varepsilon)) \\
&= \varepsilon\|(v_{\varphi'_\varepsilon}, v_{\psi'_\varepsilon})\|^2_{(\mathrm{H}^1(\Omega))^2} - 2H'(\varepsilon) + -\varepsilon a((\varphi'_\varepsilon, \psi'_\varepsilon), (\varphi''_\varepsilon, \psi''_\varepsilon)) \\
&\quad -\varepsilon^2 b((\varphi'_\varepsilon, \psi'_\varepsilon), (\varphi''_\varepsilon, \psi''_\varepsilon)) \\
&= -2H'(\varepsilon) + \varepsilon\|(v_{\varphi'_\varepsilon}, v_{\psi'_\varepsilon})\|^2_{(\mathrm{H}^1(\Omega))^2} + \varepsilon \cdot 2b((\varphi'_\varepsilon, \psi'_\varepsilon), (\varphi'_\varepsilon, \psi'_\varepsilon)) \\
&= -2H'(\varepsilon) + 3 \cdot \varepsilon\|(v_{\varphi'_\varepsilon}, v_{\psi'_\varepsilon})\|^2_{(\mathrm{H}^1(\Omega))^2}.
\end{aligned}$$

So, we obtain $(\varepsilon^2 H(\varepsilon))' = \varepsilon(\varepsilon H''(\varepsilon + 2H'(\varepsilon))) = 3 \cdot \varepsilon\|(v_{\varphi'_\varepsilon}, v_{\psi'_\varepsilon})\|^2_{(\mathrm{H}^1(\Omega))^2} \geq 0$ which implies that the function $\varepsilon \mapsto \varepsilon^2 H'(\varepsilon)$ is increasing. Moreover,

$$|\varepsilon^2 H'(\varepsilon)| = \varepsilon^2 |((u_{\varphi^*_\varepsilon} - u_{\mathrm{ex}}, u_{\psi^*_\varepsilon} - u_{\mathrm{ex}}), (v_{\varphi'_\varepsilon}, v_{\psi'_\varepsilon}))_{(\mathrm{H}^1(\Omega))^2}| \leq C\varepsilon \, \|u_{\mathrm{ex}}\|_{\mathrm{H}^1(\Omega)} \underset{\varepsilon\to 0}{\longrightarrow} 0.$$

Therefore $H'(\varepsilon) \geq 0$ and we conclude.

□

The following theorem relates the sequence of optimal values $(\varphi^*_\varepsilon, \psi^*_\varepsilon)$ of $\mathcal{K}_\varepsilon$ with the functional $\mathcal{K}$.

Theorem 1.12 *For each $\varepsilon > 0$, let $(\varphi^*_\varepsilon, \psi^*_\varepsilon) \in \mathrm{H}^{-1/2}(\Gamma_{\mathrm{i}}) \times \mathrm{H}^{1/2}(\Gamma_{\mathrm{i}})$ the minimizer of $\mathcal{K}_\varepsilon$. The sequence $(\varphi^*_\varepsilon, \psi^*_\varepsilon)_\varepsilon$ ($\varepsilon \to 0$) defines a minimizing sequence of $\mathcal{K}$ and therefore a defines a pseudo-solution of (1.2). If $(\varphi^*_\varepsilon, \psi^*_\varepsilon)_\varepsilon$ is bounded, then this sequence converges in $\mathrm{H}^{-1/2}(\Gamma_{\mathrm{i}}) \times \mathrm{H}^{1/2}(\Gamma_{\mathrm{i}})$ to (φ^*, ψ^*) minimizer of $\mathcal{K}$.*

Proof. For all $\varepsilon > 0$, by definition of $(\varphi^*_\varepsilon, \psi^*_\varepsilon) = \operatorname{argmin} \mathcal{K}_\varepsilon(\varphi, \psi)$,

$$0 \leq \mathcal{K}(\varphi^*_\varepsilon, \psi^*_\varepsilon) \leq \mathcal{K}_\varepsilon(\varphi^*_\varepsilon, \psi^*_\varepsilon) \leq \mathcal{K}_\varepsilon(\varphi, \psi), \quad \forall (\varphi, \psi) \in \mathrm{H}^{-1/2}(\Gamma_{\mathrm{i}}) \times \mathrm{H}^{1/2}(\Gamma_{\mathrm{i}}).$$

Moreover, by definition of an infimum, for $\eta > 0$, there exists $(\varphi_\eta, \psi_\eta) \in \mathrm{H}^{-1/2}(\Gamma_{\mathrm{i}}) \times \mathrm{H}^{1/2}(\Gamma_{\mathrm{i}})$ such that $\mathcal{K}(\varphi_\eta, \psi_\eta) \leq \frac{\eta}{2}$. Inserting this pair in the first inequality, we have

$$0 \leq \mathcal{K}(\varphi^*_\varepsilon, \psi^*_\varepsilon) \leq \mathcal{K}_\varepsilon(\varphi^*_\varepsilon, \psi^*_\varepsilon) \leq \mathcal{K}_\varepsilon(\varphi_\eta, \psi_\eta) \leq \frac{\varepsilon}{2}\|(v_{\varphi_\eta}, v_{\psi_\eta})\|^2_{\mathrm{H}^1(\Omega)} + \frac{\eta}{2}.$$

Taking $\varepsilon^* > 0$ sufficiently small such that $\frac{\varepsilon}{2}\|(v_{\varphi_\eta}, v_{\psi_\eta})\|^2_{\mathrm{H}^1(\Omega)} \leq \frac{\eta}{2}$ for all $\varepsilon \in (0, \varepsilon^*)$, we have:

$$0 \leq \mathcal{K}(\varphi^*_\varepsilon, \psi^*_\varepsilon) \leq \mathcal{K}_\varepsilon(\varphi^*_\varepsilon, \psi^*_\varepsilon) \leq \eta, \quad \forall \varepsilon \in (0, \varepsilon^*).$$

Hence,

$$\mathcal{K}(\varphi^*_\varepsilon, \psi^*_\varepsilon) \underset{\varepsilon\to 0}{\longrightarrow} 0 \qquad (\text{and } \mathcal{K}_\varepsilon(\varphi^*_\varepsilon, \psi^*_\varepsilon) \underset{\varepsilon\to 0}{\longrightarrow} 0).$$

Let us now assume that the sequence $(\varphi^*_\varepsilon, \psi^*_\varepsilon)_\varepsilon$ is bounded. Then, given any sequence $(\varepsilon_n)_n$ such that $\varepsilon_n \to 0$, we have from Proposition 1.7 that $(\varphi^*_{\varepsilon_n}, \psi^*_{\varepsilon_n}) \rightharpoonup$

(φ^*, ψ^*) weakly in $\mathrm{H}^{-1/2}(\Gamma_\mathrm{i}) \times \mathrm{H}^{1/2}(\Gamma_\mathrm{i})$, where (φ^*, ψ^*) is the minimizer of $\mathcal{K}$. In order to obtain the strong convergence, notice that

$$0 \leq \frac{\varepsilon_n}{2}\|(\varphi^*_{\varepsilon_n}, \psi^*_{\varepsilon_n})\|_b^2 \leq \mathcal{K}_{\varepsilon_n}(\varphi^*_{\varepsilon_n}, \psi^*_{\varepsilon_n}) \leq \mathcal{K}_{\varepsilon_n}(\varphi^*, \psi^*) = \frac{\varepsilon_n}{2}\|(\varphi^*, \psi^*)\|_b^2,$$

and then, passing to the lim sup,

$$\limsup_n \|(\varphi^*_{\varepsilon_n}, \psi^*_{\varepsilon_n})\|_b \leq \|(\varphi^*, \psi^*)\|_b.$$

□

Remark As we obtain the existence of a minimizer (φ^*, ψ^*) of $\mathcal{K}$, we have the existence of a solution $u_{ex} \in \mathrm{H}^1(\Omega)$ of the Cauchy problem. Therefore we also have, from Theorem 1.10 the strong convergence $u_{\varphi^*_\varepsilon} \to u_{ex}$ in $\mathrm{H}^1(\Omega)$ as $\varepsilon \to 0$. Moreover, thanks to Proposition 1.11 part 6, this convergence is monotone.

1.3 Theoretical results concerning the data completion problem with noise

Let us consider again a given Cauchy pair $(g_N, g_D) \in \mathrm{H}^{-1/2}(\Gamma_{obs}) \times \mathrm{H}^{1/2}(\Gamma_{obs})$ that may be compatible or not. As one can expect, in real situations, the data (g_N, g_D) cannot be measured with complete precision: noise is intrinsically attached with any measurement method. So we just can expect to obtain (g_N^δ, g_D^δ) as a measured data which we will assume that satisfy the following condition:

$$\|g_D - g_D^\delta\|_{\mathrm{H}^{1/2}(\Gamma_{obs})} + \|g_N - g_N^\delta\|_{\mathrm{H}^{-1/2}(\Gamma_{obs})} \leq \delta, \tag{1.23}$$

where δ is the amplitude of noise on the data. Moreover, notice that we do not know if the associated noisy data (g_N^δ, g_D^δ) is compatible or not.

In the following, we explore the convergence of some minimizers of the Kohn-Vogelius functional $\mathcal{K}_\varepsilon$ associated to noisy data to the minimum of the same functional without noise and also, when it is possible, to the solution of our Cauchy problem. For this we will need to consider the following notation: when we have noisy data (g_N^δ, g_D^δ), we consider the Kohn-Vogelius functional associated with the noisy data

$$\mathcal{K}^\delta(\varphi, \psi) = \frac{1}{2}\int_\Omega |\nabla u_\varphi^{g_D^\delta} - \nabla u_\psi^{g_N^\delta}|^2,$$

their regularization (noticing that the regularization term remains unchanged),

$$\mathcal{K}_\varepsilon^\delta(\varphi, \psi) = \mathcal{K}^\delta(\varphi, \psi) + \frac{\varepsilon}{2}\|(v_\varphi, v_\psi)\|^2_{\mathrm{H}^1(\Omega)\times\mathrm{H}^1(\Omega)},$$

and the associated minimizers $(\varphi^*_{\varepsilon,\delta}, \psi^*_{\varepsilon,\delta})$. Also, we consider the linear form ℓ^δ associated with the optimality condition for $(\varphi^*_{\varepsilon,\delta}, \psi^*_{\varepsilon,\delta})$ and we will introduce $\mathrm{d}\ell^\delta := \ell^\delta - \ell$ which is the linear form associated with $(\mathrm{d}g_N, \mathrm{d}g_D) := (g_N^\delta - g_N, g_D^\delta - g_D)$. We finally recall that $(\varphi^*_\varepsilon, \psi^*_\varepsilon) := \operatorname{argmin} \mathcal{K}_\varepsilon(\varphi, \psi)$. Moreover, if (g_N, g_D) is compatible, we note $(\varphi^*, \psi^*) := \operatorname{argmin} \mathcal{K}(\varphi, \psi)$.

1.3.1 A convergence result

The most important result, in order to obtain the desired convergence from noisy data to the solution of our problem, is the following:

Proposition 1.13 *We have*

$$\|(\varphi_\varepsilon^*, \psi_\varepsilon^*) - (\varphi_{\varepsilon,\delta}^*, \psi_{\varepsilon,\delta}^*)\|_{\mathrm{H}^{-1/2}(\Gamma_\mathrm{i})\times\mathrm{H}^{1/2}(\Gamma_\mathrm{i})} \leq C\frac{\delta}{\sqrt{\varepsilon}}. \tag{1.24}$$

Proof. First, notice that

$$\begin{aligned}\mathrm{d}\ell^\delta(\varphi,\psi) = (\ell^\delta - \ell)(\varphi,\psi) &= \left(\int_\Omega \nabla\left(u^{g_D-g_D^\delta} - u^{g_N-g_N^\delta}\right)\cdot\nabla\left(v_\varphi - v_\psi\right)\right)\\ &\leq |u^{g_D-g_D^\delta} - u^{g_N-g_N^\delta}|_{\mathrm{H}^1(\Omega)}\,|v_\varphi - v_\psi|_{\mathrm{H}^1(\Omega)} \leq C\,\delta\,|v_\varphi - v_\psi|_{\mathrm{H}^1(\Omega)},\end{aligned}$$

Let us take $\widetilde{\varphi} := \varphi_{\varepsilon,\delta}^* - \varphi_\varepsilon^*$ and $\widetilde{\psi} := \psi_{\varepsilon,\delta}^* - \psi_\varepsilon^*$ in the optimality conditions associated with (g_N, g_D) and (g_N^δ, g_D^δ) and subtract the obtained equations, to get

$$a((\widetilde{\varphi},\widetilde{\psi}),(\widetilde{\varphi},\widetilde{\psi})) + \varepsilon\cdot b((\widetilde{\varphi},\widetilde{\psi}),(\widetilde{\varphi},\widetilde{\psi})) = \mathrm{d}\ell(\widetilde{\varphi},\widetilde{\psi}).$$

Hence,

$$|v_{\widetilde{\varphi}} - v_{\widetilde{\psi}}|^2_{\mathrm{H}^1(\Omega)} + \varepsilon\|\widetilde{\varphi},\widetilde{\psi}\|_b^2 \leq C\cdot\delta\cdot|v_{\widetilde{\varphi}} - v_{\widetilde{\psi}}|_{\mathrm{H}^1(\Omega)}$$

and, since $a^2 + b^2 \geq 2ab$,

$$|v_{\widetilde{\varphi}} - v_{\widetilde{\psi}}|^2_{\mathrm{H}^1(\Omega)} + \varepsilon\|\widetilde{\varphi},\widetilde{\psi}\|_b^2 \geq 2\sqrt{\varepsilon}\,|v_{\widetilde{\varphi}} - v_{\widetilde{\psi}}|_{\mathrm{H}^1(\Omega)}\,\|\widetilde{\varphi},\widetilde{\psi}\|_b.$$

Joining the previous results, we obtain:

$$\|\widetilde{\varphi},\widetilde{\psi}\|_b = \|\varphi_{\varepsilon,\delta}^* - \varphi_\varepsilon^*, \psi_{\varepsilon,\delta}^* - \psi_\varepsilon^*\|_b \leq C\cdot\frac{\delta}{\sqrt{\varepsilon}},$$

which gives the result by the equivalence of norms $\|\cdot\|_b$ and $\|\cdot\|_{\mathrm{H}^{-1/2}(\Gamma_\mathrm{i})\times\mathrm{H}^{1/2}(\Gamma_\mathrm{i})}$. □

In the case of the compatibility of the data (g_N, g_D), we can deduce the following result, which states in a very general way the conditions that the regularization parameter ε must meet in order to have convergence in the noisy case.

Corollary 1.14 *Given (g_N, g_D) compatible data associated with exact solution (φ^*, ψ^*). Let us consider $\varepsilon = \varepsilon(\delta)$ such that*

$$\lim_{\delta\to 0}\varepsilon(\delta) = 0 \qquad \textit{and} \qquad \lim_{\delta\to 0}\frac{\delta}{\sqrt{\varepsilon}} = 0. \tag{1.25}$$

Then, we have:

$$\lim_{\delta\to 0}\|(\varphi_{\varepsilon,\delta}^*, \psi_{\varepsilon,\delta}^*) - (\varphi^*, \psi^*)\|_{\mathrm{H}^{-1/2}(\Gamma_\mathrm{i})\times\mathrm{H}^{1/2}(\Gamma_\mathrm{i})} = 0.$$

Proof. This result is direct from the triangle inequality, theorem 1.12 and proposition 1.13. □

1.3.2 Strategy for choosing ε

The last result gives us a guide on *how our regularization parameter ε should be chosen* in order to have convergence to the real solution (when it exists) in the noisy case. However, these conditions are general and do not respond to any precise objective. In this section we explore a well-known criterion for choosing the regularization parameter ε based on the definition of a *discrepancy measure*: the so-called *Morozov discrepancy principle* (see [48] for more details in the general regularization of inverse problems context). We follow the same strategy as Ben Belgacem *et al.* in [20] which is in fact natural with our strategy of considering the Kohn-Vogelius functional as the core of our work. Notice that we will consider the choice of our parameter depending on the noise level δ and into the noisy data (g_N^δ, g_D^δ), this is $\varepsilon = \varepsilon(\delta, (g_N^\delta, g_D^\delta))$. This is called a *a-posteriori choice parameter rule*. One may consider a *a-priori choice parameter rule* which is only based on the noise, this is $\varepsilon = \varepsilon(\delta)$. However, in order to obtain optimal order of convergence, one must have some *abstract smoothness conditions* on the real solution which is, in our opinion, unrealistic in our setting. The interested reader can see [48] for more details on those strategies.

First, let us assume that our problem has a solution, *i.e.* the Kohn-Vogelius functional $\mathcal{K}$ associated with the compatible data (g_N, g_D) has a minimizer (φ^*, ψ^*). Let us define the *discrepancy measure* as the error in the Kohn-Vogelius functional with noisy data when we evaluate it on the solution of our problem, this is:

$$\mathcal{K}^\delta(\varphi^*, \psi^*) = \frac{1}{2}\int_\Omega |\nabla u_{\varphi^*}^{g_D^\delta} - \nabla u_{\psi^*}^{g_N^\delta}|^2 = \frac{1}{2}\int_\Omega |\nabla u_0^{\mathrm{d}g_D} - \nabla u_0^{\mathrm{d}g_N}|^2,$$

where the second equality is obtained by rewriting $u_{\varphi^*}^{g_D^\delta} = u_{\varphi^*}^{g_D^\delta - g_D + g_D} = u_0^{\mathrm{d}g_D} + u_{\varphi^*}^{g_D}$, with an analogous expression for $u_{\psi^*}^{g_N^\delta}$ and expanding and imposing the optimality condition for each term. Now, from the well-posedness of the problems associated with $u_0^{\mathrm{d}g_D}$ and $u_0^{\mathrm{d}g_N}$ and using (1.23) we obtain:

$$\mathcal{K}^\delta(\varphi^*, \psi^*) = \frac{1}{2}\int_\Omega |\nabla u_0^{\mathrm{d}g_D} - \nabla u_0^{\mathrm{d}g_N}|^2 \leq C\,\delta^2. \tag{1.26}$$

Keeping this in mind, we redefine the noise amount to $\mathcal{K}^\delta(\varphi^*, \psi^*) = \delta^2$ and we will consider the discrepancy principle based on this notion of noise. Notice that this consideration basically says we will consider, for the discrepancy principle, that the noise level will be taken in a sort of $\mathrm{H}^1 \times \mathrm{H}^1$ seminorm in Ω instead of an $\mathrm{H}^{1/2} \times \mathrm{H}^{-1/2}$ norm in the unaccessible boundary Γ_{i}.

In Proposition 1.11 part 3, we have proved that the application $\varepsilon \mapsto \mathcal{K}^\delta(\varphi_{\varepsilon,\delta}^*, \psi_{\varepsilon,\delta}^*)$ is strictly increasing and therefore injective. Moreover, it is easy to see that if $\varepsilon \in [0, \infty)$ then $\mathcal{K}^\delta(\varphi_{\varepsilon,\delta}^*, \psi_{\varepsilon,\delta}^*) \in [0, \mathcal{K}^\delta(0,0))$. Now, let us assume that there exists $\tau > 1$ such that $\tau\delta^2 \in [0, \mathcal{K}^\delta(0,0))$. This demand is natural as we expect that the data we have is not of the same order as the noise. Indeed, if this is the case, we can simply take $(\varphi^*, \psi^*) = (0,0)$ as the exact solution. So, the discrepancy principle

consists, in our case on choosing ε such that

$$\varepsilon = \sup\left\{\varepsilon:\ \mathcal{K}^{\delta}(\varphi^*_{\varepsilon,\delta}, \psi^*_{\varepsilon,\delta}) \leq \tau\delta^2\right\}. \tag{1.27}$$

The idea of choosing the sup is based on the fact that a small regularization parameter involves less stability, so the *natural* strategy is to choose the biggest regularization parameter such that the discrepancy is in the order of the noise. The injectivity and increasing monotonicity of the application $\mathcal{K}^{\delta}$ implies that ε is simply the parameter such that

$$\mathcal{K}^{\delta}(\varphi^*_{\varepsilon,\delta}, \psi^*_{\varepsilon,\delta}) = \tau\delta^2. \tag{1.28}$$

Remark It is important to notice that the 'redefinition' of the noise estimate does not involve, for real computations, the knowledge of the real solution (φ^*, ψ^*). In fact, we only use the real solution in order when we evaluate it into the Kohn-Vogelius functional with noisy data $(g_N^{\delta}, g_D^{\delta})$ obtaining the estimate (1.26). We can observe that this quantity only depends on constants and the error estimate δ, so, by assuming that $C \leq 1$ (which is itself a strong assumption, as C depends on Poincaré inequality constant and trace theorem constant, this should be analyzed in detail and is beyond the scope of this work) we can consider $\mathcal{K}^{\delta}(\varphi^*, \psi^*) = \delta^2$ as the error measure between the real and measured data which leads to the discrepancy principle formulation given by (1.27).

Now let us see that this *a posteriori* choice parameter rule has (the expected) convergence properties.

Proposition 1.15 *Given (g_N, g_D) compatible data associated with exact solution (φ^*, ψ^*). If we consider the regularization parameter choice $\varepsilon = \varepsilon(\delta, (g_N^{\delta}, g_D^{\delta}))$ given by the Morozov discrepancy principle* (1.28)*, then we have*

$$\lim_{\delta\to 0} \|(\varphi^*_{\varepsilon,\delta}, \psi^*_{\varepsilon,\delta}) - (\varphi^*, \psi^*)\|_{\mathrm{H}^{-1/2}(\Gamma_{\mathrm{i}})\times\mathrm{H}^{1/2}(\Gamma_{\mathrm{i}})} = 0.$$

Proof. Given ε computed by the discrepancy principle, this is, given by (1.28). We have by definition

$$\begin{array}{rcl} \mathcal{K}^{\delta}_{\varepsilon}(\varphi^*_{\varepsilon,\delta}, \psi^*_{\varepsilon,\delta}) & \leq & \mathcal{K}^{\delta}_{\varepsilon}(\varphi^*, \psi^*) \\ \Leftrightarrow \frac{\varepsilon}{2}\|(\varphi^*_{\varepsilon,\delta}, \psi^*_{\varepsilon,\delta})\|_b^2 + \mathcal{K}^{\delta}(\varphi^*_{\varepsilon,\delta}, \psi^*_{\varepsilon,\delta}) & \leq & \frac{\varepsilon}{2}\|(\varphi^*, \psi^*)\|_b^2 + \mathcal{K}^{\delta}(\varphi^*, \psi^*) \end{array}$$

and then using (1.26),

$$\begin{array}{rcl} \frac{\varepsilon}{2}\|(\varphi^*_{\varepsilon,\delta}, \psi^*_{\varepsilon,\delta})\|_b^2 + \tau\delta^2 & \leq & \frac{\varepsilon}{2}\|(\varphi^*, \psi^*)\|_b^2 + \delta^2 \\ \Leftrightarrow \frac{\varepsilon}{2}\|(\varphi^*_{\varepsilon,\delta}, \psi^*_{\varepsilon,\delta})\|_b^2 - \frac{\varepsilon}{2}\|(\varphi^*, \psi^*)\|_b^2 & \leq & (1-\tau)\delta^2 < 0. \end{array}$$

So, we have:

$$\|(\varphi^*_{\varepsilon,\delta}, \psi^*_{\varepsilon,\delta})\|_b^2 \leq \|(\varphi^*, \psi^*)\|_b^2, \quad \forall\delta > 0.$$

This implies that the sequence $(\varphi^*_{\varepsilon,\delta}, \psi^*_{\varepsilon,\delta})_{\delta}$ is bounded in $(\mathrm{H}^{-1/2}(\Gamma_{\mathrm{i}}) \times \mathrm{H}^{1/2}(\Gamma_{\mathrm{i}}), \|\cdot\|_b)$ (and in $(\mathrm{H}^{-1/2}(\Gamma_{\mathrm{i}}) \times \mathrm{H}^{1/2}(\Gamma_{\mathrm{i}}), \|\cdot\|_{\mathrm{H}^{-1/2}(\Gamma_{\mathrm{i}})\times\mathrm{H}^{1/2}(\Gamma_{\mathrm{i}})})$ due to the equivalence of norms). Therefore there exists $(\widetilde{\varphi}, \widetilde{\psi}) \in \mathrm{H}^{-1/2}(\Gamma_{\mathrm{i}}) \times \mathrm{H}^{1/2}(\Gamma_{\mathrm{i}})$ such that $(\varphi^*_{\varepsilon,\delta}, \psi^*_{\varepsilon,\delta})_{\delta}$ converges,

up to a subsequence, weakly in $\mathrm{H}^{-1/2}(\Gamma_\mathrm{i}) \times \mathrm{H}^{1/2}(\Gamma_\mathrm{i})$ to $(\widetilde{\varphi}, \widetilde{\psi})$. On the other side, taking lim sup in the last inequality we obtain:

$$\limsup_{\delta \to 0} \|(\varphi^*_{\varepsilon,\delta}, \psi^*_{\varepsilon,\delta})\|_b \leq \|(\varphi^*, \psi^*)\|_b.$$

Now, taking the limit in the optimality condition (which is possible due to the continuity of the restricted continuous bilinear forms) we obtain that $(\widetilde{\varphi}, \widetilde{\psi}) = (\varphi^*, \psi^*)$ and we conclude. □

The following corollary claims that the regularization parameter choice given by the Morozov discrepancy principle satisfies the conditions of Corollary 1.14.

Corollary 1.16 *The regularization parameter choice given by the Morozov discrepancy principle satisfies*

$$\lim_{\delta \to 0} \varepsilon(\delta) = 0 \qquad \textit{and} \qquad \lim_{\delta \to 0} \frac{\delta}{\sqrt{\varepsilon}} = 0.$$

Proof. The first condition is obvious from the definition of ε. Let us see the second limit. From the previous proof, we have:

$$0 < 2(\tau - 1)\frac{\delta^2}{\varepsilon} \leq \|(\varphi^*, \psi^*)\|_b^2 - \|(\varphi^*_{\varepsilon,\delta}, \psi^*_{\varepsilon,\delta})\|_b^2 = \|(v_{\varphi^*}, v_{\psi^*})\|^2_{\mathrm{H}^1(\Omega)} - \|(v_{\varphi^*_{\varepsilon,\delta}}, v_{\psi^*_{\varepsilon,\delta}})\|^2_{\mathrm{H}^1(\Omega)}.$$

As $\tau > 1$ we conclude by using Proposition 1.15. □

Chapter 2

Numerical resolution of the data completion problem

In this chapter we perform a numerical reconstruction of the Dirichlet and Neumann boundary data in an unaccessible part of the boundary $\Gamma_{\mathrm{i}} \subset \partial\Omega$ for an harmonic function from the Dirichlet and Neumann boundary data in an accessible part $\Gamma_{obs} \subset \partial\Omega$. As we have seen in the previous chapter, in order to retrieve the unaccessible data, we have to minimize the Kohn-Vogelius functional. However, due to the ill-posedness of the problem, we need to consider a regularization of the functional via a Tikhonov regularization and we have proved that we have convergence of the minimizers of the regularized functional to the actual minimizer of the Kohn-Vogelius functional as the regularization parameter $\varepsilon \to 0$ even when the data is polluted by noise. In order to minimize the regularized functional, we will consider a gradient type algorithm, so, we have to compute the derivatives of the regularized Kohn-Vogelius functional and determine a descent direction.

We test our algorithm using an explicit harmonic function in two main scenarios: when the boundary portions Γ_{i} and Γ_{obs} have points in common and when the boundary portions are completely separated. Such comparisons arises as the regularity theory for the mixed systems asserts that the regularity of the solutions are different on each case, when the boundaries 'touches' between themselves, we have less regularity and as we will see, the numerical errors are higher. We also test the algorithm in the case when data corrupted by noise is available, in which case we observe also an increase of the error between the real solution and the obtained after the minimization.

This chapter is divided in three sections: In the first one we compute the derivatives of the regularized Kohn-Vogelius functional and we compute descent directions in order to implement a gradient algorithm. We introduce some adjoint systems in order to simplify the computation of the descent directions and we conclude an explicit form of them. In the second section we present the framework of the simulations and the algorithm to be utilized. Finally, in the third section, we perform the

simulations as previously described, this is, exploring the non-noisy and noisy cases (explaining what 'noise' means in our context), and the cases when the boundaries have common points or not.

We refer to Chapter 1 for the notations. In particular, we recall that Ω is a bounded connected Lipschitz domain of $\mathbb{R}^{\mathrm{d}}$ (with $\mathrm{d} = 2$ or $\mathrm{d} = 3$) with boundary $\partial\Omega$ which has two components: the nonempty (relatively) open sets Γ_{obs} and Γ_{i} such that $\overline{\Gamma_{obs}} \cup \overline{\Gamma_{\mathrm{i}}} = \partial\Omega$. Then, in order to solve the data completion problem (1.1), we consider, for a given Cauchy pair $(g_N, g_D) \in \mathrm{H}^{-1/2}(\Gamma_{obs}) \times \mathrm{H}^{1/2}(\Gamma_{\mathrm{i}})$ such that $(g_N, g_D) \neq (0,0)$, the following regularized Kohn-Vogelius functional defined on $\mathrm{H}^{-1/2}(\Gamma_{\mathrm{i}}) \times \mathrm{H}^{1/2}(\Gamma_{\mathrm{i}})$

$$\mathcal{K}_\varepsilon(\varphi,\psi) := \frac{1}{2}\int_\Omega |\nabla u_\varphi^{g_D} - \nabla u_\psi^{g_N}|^2 + \frac{\varepsilon}{2}\left(\|v_\varphi\|^2_{\mathrm{H}^1(\Omega)} + \|v_\psi\|^2_{\mathrm{H}^1(\Omega)}\right),$$

where $u_\varphi^{g_D} \in \mathrm{H}^1(\Omega)$ and $u_\psi^{g_N} \in \mathrm{H}^1(\Omega)$ are the respective solutions of

$$\left\{\begin{array}{rcll} -\Delta u_\varphi^{g_D} &=& 0 & \text{in } \Omega \\ u_\varphi^{g_D} &=& g_D & \text{on } \Gamma_{obs} \\ \partial_{\mathbf{n}} u_\varphi^{g_D} &=& \varphi & \text{on } \Gamma_{\mathrm{i}}, \end{array}\right. \quad \text{and} \quad \left\{\begin{array}{rcll} -\Delta u_\psi^{g_N} &=& 0 & \text{in } \Omega \\ \partial_{\mathbf{n}} u_\psi^{g_N} &=& g_N & \text{on } \Gamma_{obs} \\ u_\psi^{g_N} &=& \psi & \text{on } \Gamma_{\mathrm{i}}, \end{array}\right. \tag{2.1}$$

and where $v_\varphi := u_\varphi^0$ and $v_\psi := u_\psi^0$.

2.1 Computation of the derivatives of $\mathcal{K}_\varepsilon$

In order to perform the numerical minimization of the regularized functional $\mathcal{K}_\varepsilon$ via a gradient algorithm we have to compute its derivatives with respect to φ and ψ.

Proposition 2.1 *For all $(\varphi,\psi), (\widetilde{\varphi},\widetilde{\psi}) \in \mathrm{H}^{-1/2}(\Gamma_{\mathrm{i}}) \times \mathrm{H}^{1/2}(\Gamma_{\mathrm{i}})$, the partial derivative of the functional $\mathcal{K}_\varepsilon(\varphi,\psi)$ are given by*

$$\frac{\partial \mathcal{K}_\varepsilon}{\partial \varphi}(\varphi,\psi)\,[\widetilde{\varphi}] = \int_{\Gamma_{\mathrm{i}}} \widetilde{\varphi}\cdot(u_\varphi + \varepsilon v_\varphi + w_D - \psi) \tag{2.2}$$

and

$$\frac{\partial \mathcal{K}_\varepsilon}{\partial \psi}(\varphi,\psi)\left[\widetilde{\psi}\right] = \langle(\partial_\nu u_\psi + \varepsilon\partial_\nu v_\psi + \partial_\nu w_N - \varphi), \widetilde{\psi}\rangle_{\Gamma_{\mathrm{i}}} \tag{2.3}$$

where, $w_N, w_D \in \mathrm{H}^1(\Omega)$ are the respective solutions of the following adjoint problems:

$$\left\{\begin{array}{rcll} -\Delta w_N &=& -\varepsilon v_\psi & \text{in } \Omega \\ \partial_\nu w_N &=& \partial_\nu u_\varphi - g_N & \text{on } \Gamma_{obs} \\ w_N &=& 0 & \text{on } \Gamma_{\mathrm{i}} \end{array}\right. \tag{2.4}$$

and

$$\left\{\begin{array}{rcll} -\Delta w_D &=& \varepsilon v_\varphi & \text{in } \Omega \\ w_D &=& u_\psi - g_D & \text{on } \Gamma_{obs} \\ \partial_\nu w_D &=& 0 & \text{on } \Gamma_{\mathrm{i}}. \end{array}\right. \tag{2.5}$$

In particular, the directions $\left(\widetilde{\varphi},\widetilde{\psi}\right) \in \mathrm{H}^{-1/2}(\Gamma_\mathrm{i}) \times \mathrm{H}^{1/2}(\Gamma_\mathrm{i})$ *given by:*

$$\widetilde{\varphi} = \psi - u_\varphi|_{\Gamma_\mathrm{i}} - \varepsilon v_\varphi|_{\Gamma_\mathrm{i}} - w_D|_{\Gamma_\mathrm{i}}, \tag{2.6}$$

and

$$\widetilde{\psi} = -v_W|_{\Gamma_\mathrm{i}}, \tag{2.7}$$

with $W = \varphi - \partial_\nu u_\psi|_{\Gamma_\mathrm{i}} - \varepsilon\partial_\nu v_\psi|_{\Gamma_\mathrm{i}} - \partial_\nu w_N|_{\Gamma_\mathrm{i}} \in \mathrm{H}^{-1/2}(\Gamma_\mathrm{i})$*, are descent directions.*

For reader's convenience, we recall that $v_\varphi, v_\psi \in \mathrm{H}^1(\Omega)$ are the respective solutions of the following problems:

$$\left\{\begin{array}{rcll} -\Delta v_\varphi &=& 0 & \text{in } \Omega \\ v_\varphi &=& 0 & \text{on } \Gamma_{obs} \\ \partial_{\mathbf{n}} v_\varphi &=& \varphi & \text{on } \Gamma_\mathrm{i} \end{array}\right. \quad \text{and} \quad \left\{\begin{array}{rcll} -\Delta v_\psi &=& 0 & \text{in } \Omega \\ \partial_{\mathbf{n}} v_\psi &=& 0 & \text{on } \Gamma_{obs} \\ v_\psi &=& \psi & \text{on } \Gamma_\mathrm{i}. \end{array}\right. \tag{2.8}$$

Proof. Let $(\varphi,\psi),(\widetilde{\varphi},\widetilde{\psi}) \in \mathrm{H}^{-1/2}(\Gamma_\mathrm{i}) \times \mathrm{H}^{1/2}(\Gamma_\mathrm{i})$. Easy computations gives

$$\frac{\partial \mathcal{K}_\varepsilon}{\partial \varphi}(\varphi,\psi)\,[\widetilde{\varphi}] = \int_\Omega \nabla v_{\widetilde{\varphi}} \cdot (\nabla u_\varphi + \varepsilon \nabla v_\varphi - \nabla u_\psi) + \varepsilon \int_\Omega v_{\widetilde{\varphi}}\, v_\varphi \tag{2.9}$$

and

$$\frac{\partial \mathcal{K}_\varepsilon}{\partial \psi}(\varphi,\psi)\left[\widetilde{\psi}\right] = \int_\Omega \nabla v_{\widetilde{\psi}} \cdot (\nabla u_\psi + \varepsilon \nabla v_\psi - \nabla u_\varphi) + \varepsilon \int_\Omega v_{\widetilde{\psi}}\, v_\psi, \tag{2.10}$$

where $v_{\widetilde{\varphi}}, v_{\widetilde{\psi}} \in \mathrm{H}^1(\Omega)$ are the respective solutions of

$$\left\{\begin{array}{rcll} -\Delta v_{\widetilde{\psi}} &=& 0 & \text{in } \Omega \\ \partial_\nu v_{\widetilde{\psi}} &=& 0 & \text{on } \Gamma_{obs} \\ v_{\widetilde{\psi}} &=& \widetilde{\psi} & \text{on } \Gamma_\mathrm{i} \end{array}\right. \tag{2.11}$$

and

$$\left\{\begin{array}{rcll} -\Delta v_{\widetilde{\varphi}} &=& 0 & \text{in } \Omega \\ v_{\widetilde{\varphi}} &=& 0 & \text{on } \Gamma_{obs} \\ \partial_\nu v_{\widetilde{\varphi}} &=& \widetilde{\varphi} & \text{on } \Gamma_\mathrm{i}. \end{array}\right. \tag{2.12}$$

Then, using Green formula in the adjoints problem (2.4) and in problem (2.11) and in the adjoints problem (2.5) and in problem (2.12), we get

$$\int_{\Gamma_\mathrm{i}} \widetilde{\psi}\, \partial_\nu w_N = \varepsilon \int_\Omega v_\psi v_{\widetilde{\psi}} + \int_{\Gamma_{obs}} v_{\widetilde{\psi}}\,(g_N - \partial_\nu u_\varphi)$$

and

$$\int_{\Gamma_\mathrm{i}} \widetilde{\varphi}\, w_D = \varepsilon \int_\Omega v_\varphi v_{\widetilde{\varphi}} + \int_{\Gamma_{obs}} \partial_\nu v_{\widetilde{\varphi}}\,(g_D - u_\psi).$$

Thus, from the expression (2.9), we get

$$\frac{\partial \mathcal{K}_\varepsilon}{\partial \varphi}(\varphi,\psi)\,[\widetilde{\varphi}] = \int_{\partial\Omega} \partial_\nu v_{\widetilde{\varphi}}\,(u_\varphi + \varepsilon v_\varphi - u_\psi) + \varepsilon \int_\Omega v_{\widetilde{\varphi}}\, v_\varphi = \int_{\Gamma_\mathrm{i}} \widetilde{\varphi}\,(u_\varphi + \varepsilon v_\varphi - u_\psi + w_D).$$

With an analogous procedure for (2.10) we obtain (2.3).

Is important to remark that the formula for $\widetilde{\varphi}$ should be understood as the representative of the natural linear functional associated to the given expression (which is in $\mathrm{H}^{1/2}(\Gamma_{\mathrm{i}})$) in order to be understood in the proper space. For the descent direction $\widetilde{\psi}$ we should notice the following, using the W notation:

$$\frac{\partial \mathcal{K}_\varepsilon}{\partial \psi}[\widetilde{\psi}] = \langle W, \widetilde{\psi} \rangle,$$

however, from the variational formulation of v_W, we have $\forall u \in \mathrm{H}^1(\Omega), u|_{\Gamma_{obs}} = 0$:

$$\int_\Omega \nabla v_W \cdot \nabla u = \langle W, u \rangle,$$

so, taking $u = -v_W$, we obtain

$$-\int_\Omega |\nabla v_W|^2 = \langle W, -v_W \rangle < 0,$$

and we conclude. □

2.2 Framework of the numerical simulations

To make the numerical simulations presented here, we use $P1$ finite elements discretization to solve the Laplace's equations (1.7) and (2.8), and Poisson's equations (2.4) and (2.5) related to the adjoint states.

The framework is the following: the exterior boundary is assumed to be the boundary of the square $\Omega = [-0.5, 0.5] \times [-0.5, 0.5]$. Except when mentioned, we consider here $\Gamma_{obs} = ([-0.5, 0.5] \times \{-0.5\}) \cup (\{-0.5\} \times [-0.5, 0.5]) \cup (\{0.5\} \times [-0.5, 0.5])$ and $\Gamma_{\mathrm{i}} = [-0.5, 0.5] \times \{0.5\}$. The Cauchy data (g_N, g_D) will be chosen from explicit harmonic functions. The inclusion of noise will depend on the test itself and is described below.

In order to chose a suitable initial guess for the data (φ, ψ) into Γ_{i} we perform a sort-of interpolation of the data based on the points p_1, p_2, where $\overline{\Gamma_{\mathrm{i}}} \cap \overline{\Gamma_{obs}} = \{p_1, p_2\}$. For example, in our case when Γ_{i} is an horizontal line, we define ψ as follows:

1. If $u(p_1) \cdot u(p_2) \neq 0$, then ψ is the piecewise-polynomial of degree 2 such that: $\psi(p_1) = u(p_1)$, $\psi(p_2) = u(p_2)$ and $\psi((p_1 + p_2)/2) = 0$.
2. If $u(p_1) \cdot u(p_2) = 0$, then take ψ as the linear interpolation between the values of $u(p_1)$ and $u(p_2)$.

In the case when there are no common points between Γ_{obs} and Γ_{i} we just simply put homogeneous boundary conditions as the initial guess, this is $(\varphi_0, \psi_0) = (0, 0)$.

In order to update the construction of (φ, ψ) to approach $(\varphi_\varepsilon^*, \psi_\varepsilon^*)$, we follow a gradient algorithm, for which the descent directions are given in detail in Proposition 2.1.

Algorithm

1. Let $k = 0$. Fix k_{max} (max. number of iterations) and tol (tolerance), build (φ_0, ψ_0) as the initial guess of the missing data following the previously mentioned strategy.
2. Solve Problems (1.7) with (φ_k, ψ_k), extract the solutions $u_{\varphi_k}, u_{\psi_k}$ and compute $\mathcal{K}(\varphi_k, \psi_k)$.
   - If $\mathcal{K}(\varphi_k, \psi_k) < tol$: STOP.
   - Else: continue to next step.
3. Solve Problems (2.4), (2.5) and (2.8) with (φ_k, ψ_k), extract the solutions v_{φ_k}, v_{ψ_k}, $w_N(\varphi_k, \psi_k)$ and $w_D(\varphi_k, \psi_k)$.
4. Compute the descent directions $\widetilde{\varphi}$, $\widetilde{\psi}$ using formulas (2.6), (2.7) with (φ_k, ψ_k) and the solutions given in steps 2 and 3.
5. Update $\varphi_k \leftarrow (\varphi_k - \alpha_1 \widetilde{\varphi})$, $\psi_k \leftarrow \left(\psi_k - \alpha_2 \widetilde{\psi}\right)$.
6. While $k \leq k_{max}$ and $\mathcal{K}_\varepsilon(\varphi_k, \psi_k) - \mathcal{K}_\varepsilon(\varphi_{k-1}, \psi_{k-1}) < tol$, get back to the step 2, $k \leftarrow k + 1$.

The step lengths α_1, α_2 can be set with a line search algorithm (e.g. via Wolfe conditions or a golden ratio search) or set as fixed parameters. To conclude, we remark that we have used the finite elements library FreeFEM++ (see [60]) to make the simulations. We present several simulations, with or without noise, in the following sections and comment these results in Section 2.3.3

2.3 Simulations

2.3.1 Simulations without noise

We will explore the behavior of our algorithm for the data completion problem in two basic situations, when the unaccessible boundary Γ_{i} is completely separated from the accessible boundary Γ_{obs}, *i.e.* when $\overline{\Gamma_{obs}} \cap \overline{\Gamma_{\mathrm{i}}} = \emptyset$ and the opposite case, *i.e.* when $\overline{\Gamma_{obs}} \cap \overline{\Gamma_{\mathrm{i}}} \neq \emptyset$. In all the involved cases we intend to approximate the harmonic function

$$u(x, y) = y^3 - 3x^2 y.$$

We remark that, in order to be able to perform the case $\overline{\Gamma_{obs}} \cap \overline{\Gamma_{\mathrm{i}}} = \emptyset$, our framework slightly changes: in this case, Ω is the square $[-0.5, 0.5]^2$ from where we remove a disk centered in the origin with radius $r = 0.25$, *i.e.* $\Omega = [-0.5, 0.5]^2 \setminus D((0,0), 0.25)$, and then we consider $\Gamma_{obs} = \partial\left([-0.5, 0.5]^2\right)$ and $\Gamma_{\mathrm{i}} = \partial D((0,0), 0.25)$. We intend

to explore these two different situations as the regularity of the solutions could be different, while for the "non touching boundaries" case the regularity results just follow from classic elliptic regularity results, for the "touching boundaries" case the regularity becomes a more delicate problem from theoretical and numerical point of view (see the work of Savaré [75]). However, as explained by Savaré, when the boundaries in the two-dimensional case have a non-empty intersection with an 'internal intersection angle' less than π (in this case, the angle will be $\frac{\pi}{2}$), we have regularity estimates for the solution, which in any case are lower in comparison from the 'non touching' case.

We summarize the obtained results in Figure 2.1 and Table 2.1 for the case $\overline{\Gamma_{obs}} \cap \overline{\Gamma_{\mathrm{i}}} \neq \emptyset$ and in Figure 2.2 and Table 2.2 for the case $\overline{\Gamma_{obs}} \cap \overline{\Gamma_{\mathrm{i}}} = \emptyset$.

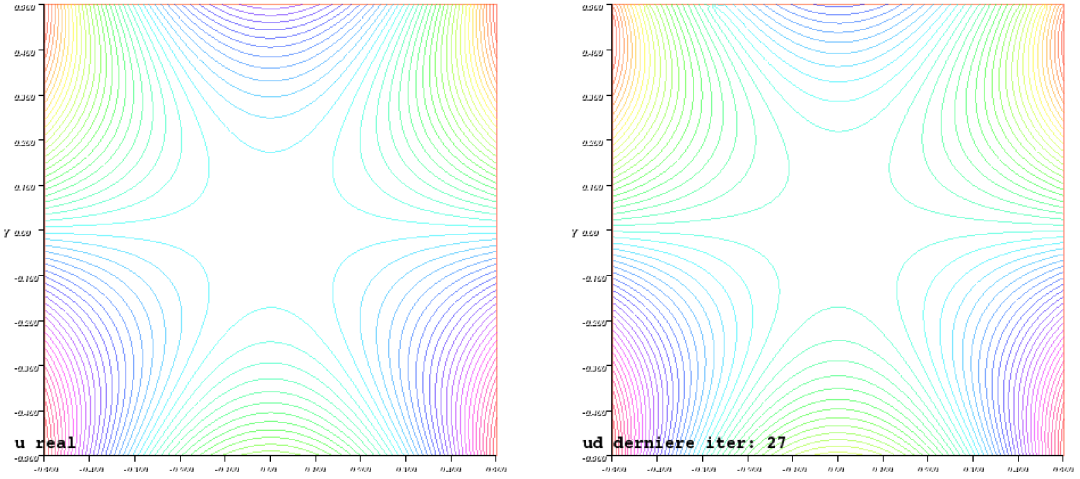

Figure 2.1: Case $\overline{\Gamma_{obs}} \cap \overline{\Gamma_{\mathrm{i}}} \neq \emptyset$

Table 2.1: Touching boundaries, non noisy case.

Case $\overline{\Gamma_{obs}} \cap \overline{\Gamma_{\mathrm{i}}} \neq \emptyset$		initial error ($k=0$)	$\varepsilon = 0.1$	$\varepsilon = 0.01$	$\varepsilon = 0.001$
$\mathrm{L}^2(\Omega)$ rel. error	u_D	0.0450	0.0343	0.0272	0.0255
	u_N	0.1244	0.0857	0.0860	0.0860
$\mathrm{L}^2(\Gamma_{\mathrm{i}})$ rel. error	u_D	0.0401	0.0411	0.0390	0.0381
	u_N	0.1679	0.0975	0.0985	0.0984

Table 2.2: Non touching boundaries, non noisy case.

Case $\overline{\Gamma_{obs}} \cap \overline{\Gamma_{\mathrm{i}}} = \emptyset$		initial error ($k=0$)	$\varepsilon = 0.1$	$\varepsilon = 0.01$	$\varepsilon = 0.001$
$\mathrm{L}^2(\Omega)$ rel. error	u_D	0.0080	0.0051	0.0039	0.0052
	u_N	0.0103	0.0037	0.0037	0.0037
$\mathrm{L}^2(\Gamma_{\mathrm{i}})$ rel. error	u_D	0.0261	0.0128	0.0103	0.0129
	u_N	0.0155	0.0138	0.0137	0.0137

In each case, we obtain a small error between the exact solution and the approximated solution, which means that the reconstruction of the data (and of the

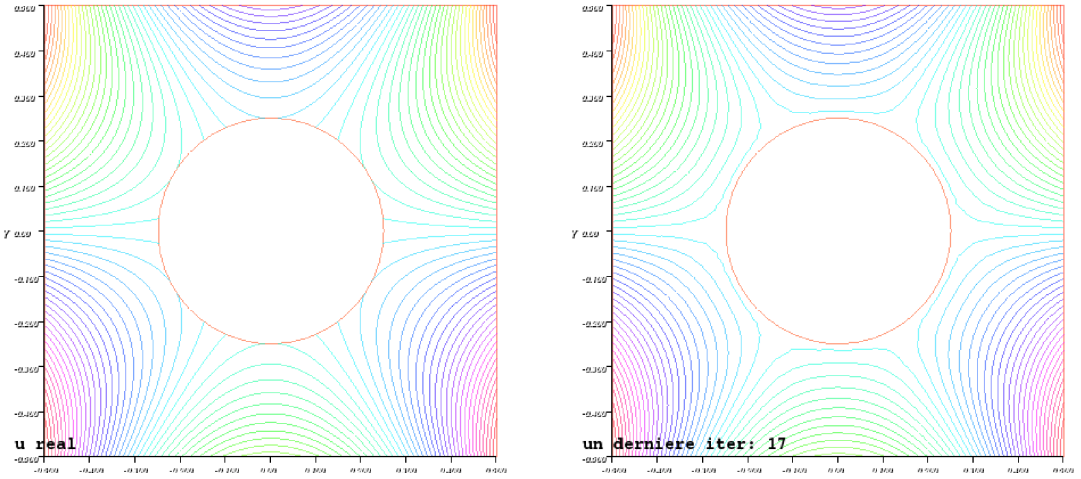

Figure 2.2: Case $\overline{\Gamma_{obs}} \cap \overline{\Gamma_{\mathrm{i}}} = \emptyset$

solution) is effective.

2.3.2 Simulations with noise

The framework here is the same as in the previous section: we explore the same two different settings with the same harmonic function as the real one. However we introduce noise into the measurements in the following way for each one: given a measure g in a region $O \subset \partial\Omega$, we introduce the noisy version of g, denoted g^σ, as:

$$g^\sigma := g + \sigma \frac{\|g\|_{\mathrm{L}^2(O)}}{\|u\|_{\mathrm{L}^2(O)}} u,$$

where u is a random variable given by an uniform distribution in $[-0.5, 0.5)$ and $\sigma > 0$ is a scaling parameter. Notice that this definition implies that the data g is contaminated by some relative error of amplitude σ in $\mathrm{L}^2(O)$. So, the noisy data into Γ_{obs} will be (g_N^σ, g_D^σ). In the following simulations we will consider $\sigma = 0.05$, which corresponds to a noise of 5% with respect to the original measurements.

The results are given in Figure 2.3 and Table 2.3 for the case $\overline{\Gamma_{obs}} \cap \overline{\Gamma_{\mathrm{i}}} \neq \emptyset$ and in Figure 2.4 and Table 2.4 for the case $\overline{\Gamma_{obs}} \cap \overline{\Gamma_{\mathrm{i}}} = \emptyset$. Here again, the reconstruction

Table 2.3: Touching boundaries, noisy case.

Case $\overline{\Gamma_{obs}} \cap \overline{\Gamma_{\mathrm{i}}} \neq \emptyset$		initial error ($k = 0$)	$\varepsilon = 0.1$	$\varepsilon = 0.01$	$\varepsilon = 0.001$
$\mathrm{L}^2(\Omega)$ rel. error	u_D	0.0793	0.0220	0.0317	0.0302
	u_N	0.1532	0.0874	0.0857	0.0879
$\mathrm{L}^2(\Gamma_{\mathrm{i}})$ rel. error	u_D	0.0544	0.0360	0.0450	0.0476
	u_N	0.1688	0.1034	0.0961	0.1049

of the data (and of the solution) is effective.

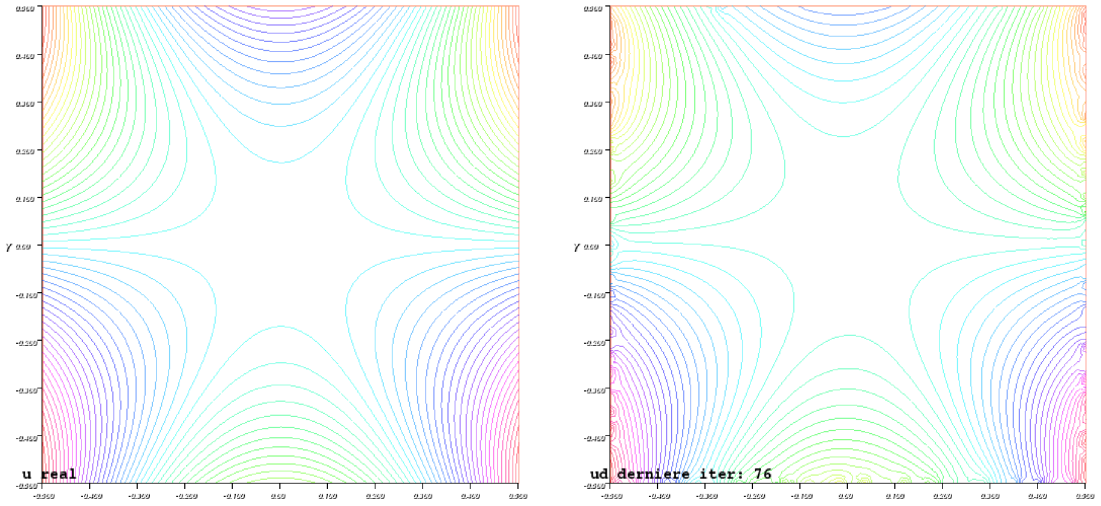

Figure 2.3: Case $\overline{\Gamma_{obs}} \cap \overline{\Gamma_{\mathrm{i}}} \neq \emptyset$

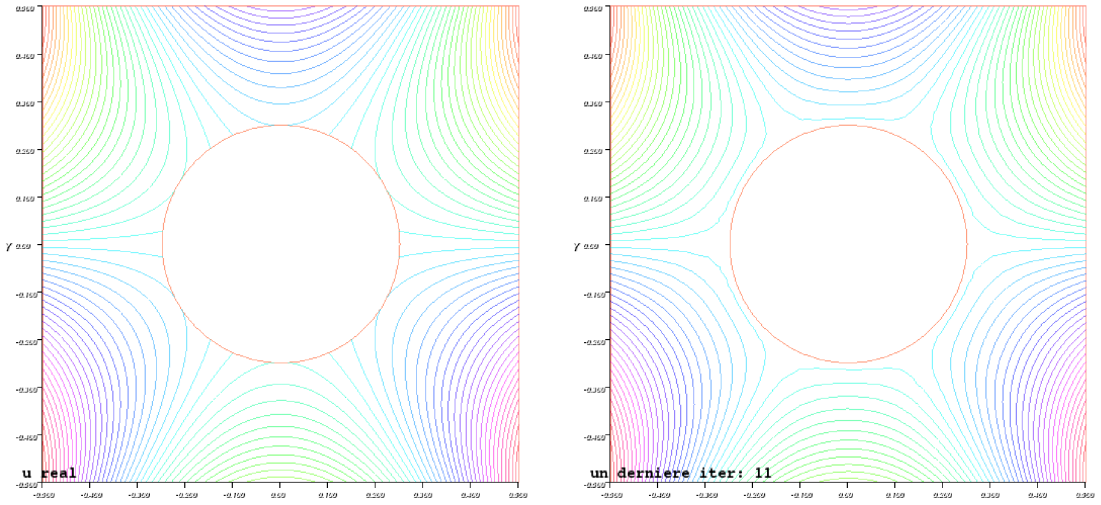

Figure 2.4: Case $\overline{\Gamma_{obs}} \cap \overline{\Gamma_{\mathrm{i}}} = \emptyset$

Table 2.4: Non touching boundaries, noisy case.

Case $\overline{\Gamma_{obs}} \cap \overline{\Gamma_{\mathrm{i}}} = \emptyset$		initial error ($k = 0$)	$\varepsilon = 0.1$	$\varepsilon = 0.01$	$\varepsilon = 0.001$
$\mathrm{L}^2(\Omega)$ rel. error	u_D	0.0399	0.0168	0.0374	0.0095
	u_N	0.0245	0.0050	0.0375	0.0037
$\mathrm{L}^2(\Gamma_{\mathrm{i}})$ rel. error	u_D	0.0465	0.0255	0.0530	0.0167
	u_N	0.0156	0.0138	0.0138	0.0137

2.3.3 Comments on the simulations

From these simulations we can observe that our algorithm is able to approximate the desired harmonic function into Γ_{i} in the considered cases. Is interesting to notice that the error order is almost one time higher into the case of touching boundaries in contrast with non-touching boundaries, which is expected as we mentioned before.

For the noisy setting, we observe that our algorithm is robust for a reasonable (5%) amount of noise, as the obtained approximations are with the same order of error in both cases. We can also observe that the regularization parameter ε reveals more consistent results for the values 10^{-2} and 10^{-3}, which is in concordance with the results obtained in [13].

Chapter 3

Obstacle detection with incomplete data via geometrical shape optimization

In this chapter we perform a numerical reconstruction of an obstacle inside a domain governed by the Laplace equation only from partial boundary measurements, this is, from boundary measurements obtained from an accessible part of the boundary. In order to perform this reconstruction we use a tool from geometrical optimization: the shape gradient. The shape gradient of a functional allows to estimate how the functional varies when a normal regular deformation is applied to the boundary of the obstacle, therefore using this tool we can estimate the directions of perturbations for which we can deform the obstacle in order to minimize the cost functional.

This chapter is divided in four sections: In the first one we recall the inverse problem of obstacle detection and we describe this problem when we only have boundary measurements from the accessible part of the boundary $\Gamma_{obs} \subset \partial\Omega$ as the minimization of an ad-hoc regularized Kohn-Vogelius functional. In the second section we present the shape derivative definition and we compute the first order shape derivative of the Kohn-Vogelius functional, with the corresponding adjoint states which will simplify the numerical implementation of the algorithm. In the third section we present the framework for the simulations and the algorithm for the obstacle reconstruction. Finally, in fourth section we perform several simulations in order to explore the algorithm capacities under some initial configurations and under the presence of noisy data.

3.1 The inverse obstacle problem with partial Cauchy data

Let Ω be a bounded connected (at least) Lipschitz open set of $\mathbb{R}^{\mathrm{d}}$ (with $\mathrm{d} = 2$ or $\mathrm{d} = 3$) with a boundary $\partial\Omega$ which has two components: the nonempty (relatively) open sets Γ_{obs} and Γ_{i}, such that $\overline{\Gamma_{obs}} \cup \overline{\Gamma_{\mathrm{i}}} = \partial\Omega$. We will say that Γ_{obs} is the observable part of $\partial\Omega$ where we will be able to obtain measurements on our system, that is the Cauchy data $(g_N, g_D) \in \mathrm{H}^{-1/2}(\Gamma_{obs}) \times \mathrm{H}^{1/2}(\Gamma_{obs})$, and Γ_{i} will be considered as the inaccessible part of the boundary $\partial\Omega$ where we cannot obtain any information of our system.

Our aim is to detect an unknown object ω^*, referred as the obstacle, strictly included in Ω from the measurements (g_N, g_D) on the observable part Γ_{obs} (see Figure 3.1 for an illustration of the notations). This object ω^* will be assumed as a

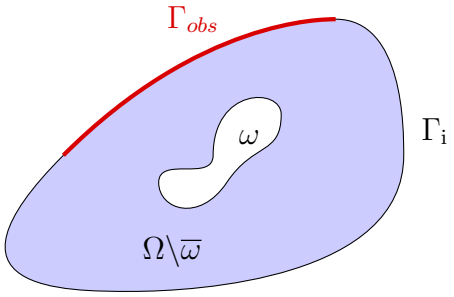

Figure 3.1: An example domain for the obstacle problem.

bounded regular domain, specifically such that it belongs to the following family of subsets of Ω:

$$\mathcal{D} := \big\{\omega \subset\subset \Omega : \ \omega \text{ is a simply connected open set, } \partial\omega \text{ is of class } \mathrm{W}^{2,\infty}, \\ \mathrm{d}(x, \partial\Omega) > \mathrm{d}_0 \text{ for all } x \in \omega,\ \Omega\backslash\overline{\omega} \text{ is connected}\big\}, \quad (3.1)$$

where d_0 is a fixed (small) parameter. Then, for a given nontrivial Cauchy pair $(g_N, g_D) \in \mathrm{H}^{-1/2}(\Gamma_{obs}) \times \mathrm{H}^{1/2}(\Gamma_{obs})$, we introduce the following inverse problem:

$$\begin{gathered} \textit{find a set } \omega^* \in \mathcal{D} \textit{ and a solution } u \in \mathrm{H}^1\left(\Omega\backslash\overline{\omega^*}\right) \cap C^0\left(\overline{\Omega\backslash\overline{\omega^*}}\right) \\ \textit{of the following overdetermined boundary value problem:} \\ \left\{\begin{array}{rcll} -\Delta u &=& 0 & \text{in } \Omega\backslash\overline{\omega^*} \\ u &=& g_D & \text{on } \Gamma_{obs} \\ \partial_{\mathbf{n}} u &=& g_N & \text{on } \Gamma_{obs} \\ u &=& 0 & \text{on } \omega^*. \end{array}\right. \end{gathered} \quad (3.2)$$

In the literature there exists several references to similar problems for many differential operators. Here, we focus on the case of the Laplacian as an example of our proposed method for a numerical reconstruction. The main novelty of our approach

is that we do not assume any knowledge on the inaccessible part $\Gamma_{\rm i}$. This means that we cannot use directly a shape optimization approach by minimizing a shape cost functional (see for example [3] for the EIT case or [37] for the Stokes case). Indeed, the definition of a shape functional in order to solve this kind of inverse problems uses the solution of a well-posed partial differential equation, in particular uses the data on the whole boundary $\partial\Omega$. However, the *identifiability result*, which claims that the solution of this inverse problem is unique, does not need any information on $\Gamma_{\rm i}$. Hence, our aim is to provide a reconstruction method of the object which *respects* this identifiability result that we recall below for reader's convenience[1] (see for example [25, Theorem 1.1] or [44, Proposition 4.4, page 87]):

Theorem 3.1 *The domain ω and the function u that satisfy* (3.2) *are uniquely defined by the Cauchy data $(g_N, g_D) \neq (0,0)$.*

Thus, in order to solve the inverse obstacle problem, that is reconstruct the shape ω^*, as a shape optimization problem, our idea is to use the previously explored inverse problem: the *data completion problem*, that is reconstruct the function u. The idea is to *complete* the data on the inaccessible part $\Gamma_{\rm i}$ which will permit to define a shape functional through some boundary value problems. In this chapter we propose a strategy which integrates the completion of the data and the detection of the unknown object in order to solve the inverse problem (3.2).

We will now focus on the numerical reconstruction of an unknown object ω^* (*i.e.* the obstacle), included into our domain of study Ω, which is characterized by an homogeneous Dirichlet boundary condition, only from the knowledge of the Cauchy data (g_N, g_D) measured into the observable part Γ_{obs} of $\partial\Omega$. In order to study this initial inverse problem (3.2), we extend the optimization problem (1.2) studied in Chapter 1 by considering a new unknown: the obstacle ω^*, this is, by considering the following optimization problem with an 'extended' Kohn-Vogelius functional:

$$(\omega^*, \varphi^*, \psi^*) \in \underset{(\omega,\varphi,\psi)\in\mathcal{D}\times \mathrm{H}^{-1/2}(\Gamma_{\rm i})\times \mathrm{H}^{1/2}(\Gamma_{\rm i})}{\operatorname{argmin}} \mathcal{K}(\omega,\varphi,\psi) \tag{3.3}$$

where $\mathcal{K}$ is the nonnegative Kohn-Vogelius cost functional defined now by:

$$\mathcal{K}(\omega,\varphi,\psi) = \frac{1}{2}\int_{\Omega\setminus\overline{\omega}} |\nabla u_\varphi(\omega) - \nabla u_\psi(\omega)|^2 \tag{3.4}$$

where $u_\varphi(\omega) := u_\varphi^{g_D}(\omega) \in \mathrm{H}^1(\Omega\setminus\overline{\omega})$ and $u_\psi(\omega) := u_\psi^{g_N}(\omega) \in \mathrm{H}^1(\Omega\setminus\overline{\omega})$ are redefined as being the solutions of the following problems

$$\left\{\begin{array}{rcll} -\Delta u_\varphi(\omega) &=& 0 & \text{in } \Omega\setminus\overline{\omega} \\ u_\varphi(\omega) &=& g_D & \text{on } \Gamma_{obs} \\ \partial_{\mathbf{n}} u_\varphi(\omega) &=& \varphi & \text{on } \Gamma_{\rm i} \\ u_\varphi(\omega) &=& 0 & \text{on } \partial\omega \end{array}\right. \quad \text{and} \quad \left\{\begin{array}{rcll} -\Delta u_\psi(\omega) &=& 0 & \text{in } \Omega\setminus\overline{\omega} \\ \partial_{\mathbf{n}} u_\psi(\omega) &=& g_N & \text{on } \Gamma_{obs} \\ u_\psi(\omega) &=& \psi & \text{on } \Gamma_{\rm i} \\ u_\psi(\omega) &=& 0 & \text{on } \partial\omega. \end{array}\right. \tag{3.5}$$

[1] Note that Theorem 3.1 is true only assuming that ω has a continuous boundary (see [25, Theorem 1.1]).

It is important to recall that, if the inverse problem (3.2) has a solution, then the identifiability result 3.1 ensures that $\mathcal{K}(\omega,\varphi,\psi)=0$ if and only if $(\omega,\varphi,\psi)=(\omega^*,\varphi^*,\psi^*)$ (and we can notice that, in this case, $u_{\varphi^*}^{g_D}=u_{\psi^*}^{g_N}=u$ where u is the solution of the Cauchy problem in $\Omega\backslash\overline{\omega^*}$). Thus, from now, we focus on the optimization problem (3.3).

We also redefine the functions $v_\varphi:=u_\varphi^0$ and $v_\psi:=u_\psi^0$ (which also depend on ω). We precise that they satisfy now, respectively

$$\left\{\begin{array}{rcll} -\Delta v_\varphi &=& 0 & \text{in } \Omega\backslash\overline{\omega}\\ v_\varphi &=& 0 & \text{on } \Gamma_{obs}\\ \partial_{\mathbf{n}} v_\varphi &=& \varphi & \text{on } \Gamma_{\mathrm{i}}\\ v_\varphi &=& 0 & \text{on } \partial\omega \end{array}\right. \quad \text{and} \quad \left\{\begin{array}{rcll} -\Delta v_\psi &=& 0 & \text{in } \Omega\backslash\overline{\omega}\\ \partial_{\mathbf{n}} v_\psi &=& 0 & \text{on } \Gamma_{obs}\\ v_\psi &=& \psi & \text{on } \Gamma_{\mathrm{i}}\\ v_\psi &=& 0 & \text{on } \partial\omega. \end{array}\right. \tag{3.6}$$

However, taking into account our previous theoretical study of the data completion problem in Chapter 1, we have to regularize the Kohn-Vogelius functional $\mathcal{K}$. Hence, in the following, we will consider, instead of (3.3), the following optimization problem

$$(\omega^*,\varphi^*,\psi^*)\in \underset{(\omega,\varphi,\psi)\in\mathcal{D}\times \mathrm{H}^{-1/2}(\Gamma_{\mathrm{i}})\times \mathrm{H}^{1/2}(\Gamma_{\mathrm{i}})}{\operatorname{argmin}} \mathcal{K}_\varepsilon(\omega,\varphi,\psi)$$

where $\mathcal{K}_\varepsilon$ is the nonnegative Kohn-Vogelius cost functional defined by

$$\begin{array}{rcl} \mathcal{K}_\varepsilon(\omega,\varphi,\psi) &:=& \mathcal{K}(\omega,\varphi,\psi)+\dfrac{\varepsilon}{2}\|(v_\varphi,v_\psi)\|^2_{\mathrm{H}^1(\Omega\backslash\overline{\omega})}\\ &=& \dfrac{1}{2}\displaystyle\int_{\Omega\backslash\overline{\omega}}|\nabla u_\varphi-\nabla u_\psi|^2+\dfrac{\varepsilon}{2}\|(v_\varphi,v_\psi)\|^2_{\mathrm{H}^1(\Omega\backslash\overline{\omega})} \end{array}$$

where $u_\varphi\in \mathrm{H}^1(\Omega\backslash\overline{\omega})$ and $u_\psi\in \mathrm{H}^1(\Omega\backslash\overline{\omega})$ are the respective solutions of Problems (3.5) and where $v_\varphi\in \mathrm{H}^1(\Omega\backslash\overline{\omega})$ and $v_\psi\in \mathrm{H}^1(\Omega\backslash\overline{\omega})$ are the respective solutions of Problems (3.6).

Since we want to minimize the functional $\mathcal{K}_\varepsilon$, we have to compute this gradient in order to make a descent method to reconstruct numerically the solution. The partial derivatives of with respect to φ and ψ are given by Proposition 2.1 and we will compute the shape gradient in the following subsection.

Remark We have to mention that all the results obtained into the study of the data completion problem in Chapter 1 are extended in this case without any difficulty, indeed, the convergence theorem 1.10 assures that:

$$\lim_{\varepsilon\to 0}\|u_{\varphi_\varepsilon^*}-u_{\mathrm{ex}}\|_{\mathrm{H}^1(\Omega)}=0,$$

but the supplementary Dirichlet boundary condition over $\partial\omega$ also ensures the convergence:

$$\lim_{\varepsilon\to 0}\|u_{\psi_\varepsilon^*}-u_{\mathrm{ex}}\|_{\mathrm{H}^1(\Omega)}=0.$$

3.2 Shape derivative of the Kohn-Vogelius functional

We recall that the set of admissible geometries $\mathcal{D}$ is given by (3.1). We also define Ω_{d_0} an open set with a C^∞ boundary such that

$$\{x \in \Omega\,;\ \mathrm{d}(x, \partial\Omega) > \mathrm{d}_0/2\} \subset \Omega_{\mathrm{d}_0} \subset \{x \in \Omega\,;\ \mathrm{d}(x, \partial\Omega) > \mathrm{d}_0/3\}\,.$$

In order to define the shape derivatives, we will use the *velocity method* introduced by Murat and Simon in [69]. To this end, we need to introduce the following space of admissible deformations

$$\boldsymbol{U} := \left\{\boldsymbol{V} \in \mathbf{W}^{2,\infty}(\mathbb{R}^{\mathrm{d}});\ \mathrm{Supp}\ \boldsymbol{V} \subset \overline{\Omega_{\mathrm{d}_0}}\right\}.$$

In particular we are interested in the shape gradient of $\mathcal{K}_\varepsilon$ defined by

$$\mathrm{D}\mathcal{K}_\varepsilon(\omega)\cdot\boldsymbol{V} := \lim_{t\to 0}\frac{\mathcal{K}_\varepsilon\left((\mathbf{I}+t\boldsymbol{V})(\omega)\right) - \mathcal{K}_\varepsilon(\omega)}{t}.$$

We remark that in this section we will omit the dependence with respect to φ and ψ of the functional $\mathcal{K}_\varepsilon$. We will write $\mathcal{K}_\varepsilon(\omega)$ instead of $\mathcal{K}_\varepsilon(\omega,\varphi,\psi)$. For details concerning the differentiation with respect to the domain, we refer to the papers of Simon [78, 79] and the books of Henrot and Pierre [61] and of Sokołowski and Zolésio [81].

We consider a domain $\omega \in \mathcal{D}$. Then, we have the following proposition.

Proposition 3.2 (First order shape derivative of the functional) *For $\boldsymbol{V} \in \boldsymbol{U}$, the regularized Kohn-Vogelius cost functional $\mathcal{K}_\varepsilon$ is differentiable at ω in the direction $\boldsymbol{V}$ with*

$$\begin{aligned}\mathrm{D}\mathcal{K}_\varepsilon(\Omega\backslash\overline{\omega})\cdot\boldsymbol{V} = &-\int_{\partial\omega}(\partial_{\mathbf{n}}\rho_N^u\cdot\partial_{\mathbf{n}}u_\varphi + \partial_{\mathbf{n}}\rho_N^v\cdot\partial_{\mathbf{n}}v_\varphi)(\boldsymbol{V}\cdot\mathbf{n}) + \frac{1}{2}\int_{\partial\omega}|\nabla w|^2\,(\boldsymbol{V}\cdot\mathbf{n})\\ &-\int_{\partial\omega}(\partial_{\mathbf{n}}\rho_D^u\cdot\partial_{\mathbf{n}}u_\psi + \partial_{\mathbf{n}}\rho_D^v\cdot\partial_{\mathbf{n}}v_\psi)(\boldsymbol{V}\cdot\mathbf{n})\\ &+\frac{\varepsilon}{2}\int_{\partial\omega}(|\nabla v_\varphi|^2 + |\nabla v_\psi|^2 + |v_\varphi|^2 + |v_\psi|^2)(\boldsymbol{V}\cdot\mathbf{n}),\end{aligned} \tag{3.7}$$

where $w := u_\varphi - u_\psi$ and where $\rho_D^u, \rho_N^u, \rho_D^v, \rho_N^v \in \mathrm{H}^1(\Omega\backslash\overline{\omega})$ are the respective solutions of the following adjoint states

$$\left\{\begin{array}{rcll} -\Delta\rho_N^u &=& 0 & \text{in } \Omega\backslash\overline{\omega}\\ \rho_N^u &=& g_D - u_\psi & \text{on } \Gamma_{obs}\\ \partial_{\mathbf{n}}\rho_N^u &=& 0 & \text{on } \Gamma_{\mathrm{i}}\\ \rho_N^u &=& 0 & \text{on } \partial\omega, \end{array}\right. \qquad \left\{\begin{array}{rcll} -\Delta\rho_N^v &=& -\varepsilon v_\varphi & \text{in } \Omega\backslash\overline{\omega}\\ \rho_N^v &=& 0 & \text{on } \Gamma_{obs}\\ \partial_{\mathbf{n}}\rho_N^v &=& 0 & \text{on } \Gamma_{\mathrm{i}}\\ \rho_N^v &=& 0 & \text{on } \partial\omega \end{array}\right. \tag{3.8}$$

and

$$\left\{\begin{array}{rcll} -\Delta\rho_D^u &=& 0 & \text{in } \Omega\backslash\overline{\omega}\\ \partial_{\mathbf{n}}\rho_D^u &=& 0 & \text{on } \Gamma_{obs}\\ \rho_D^u &=& \psi - u_\varphi & \text{on } \Gamma_{\mathrm{i}}\\ \rho_D^u &=& 0 & \text{on } \partial\omega, \end{array}\right. \qquad \left\{\begin{array}{rcll} -\Delta\rho_D^v &=& -\varepsilon v_\psi & \text{in } \Omega\backslash\overline{\omega}\\ \partial_{\mathbf{n}}\rho_D^v &=& 0 & \text{on } \Gamma_{obs}\\ \rho_D^v &=& \varepsilon\psi & \text{on } \Gamma_{\mathrm{i}}\\ \rho_D^v &=& 0 & \text{on } \partial\omega. \end{array}\right. \tag{3.9}$$

PROOF. First, notice that the existence of the shape derivatives $u'_\varphi, v'_\varphi, u'_\psi,\ v'_\psi \in \mathrm{H}^1(\Omega\backslash\overline{\omega})$ is standard and is based on Implicit function theorem. We refer to [61, Chapter 5] for details (see also [14] for example). Moreover, these shape derivatives are respectively characterized as the solution of the following problems (see again [61, Chapter 5]):

$$\left\{\begin{array}{rcll} -\Delta u'_\varphi &=& 0 & \text{in } \Omega\backslash\overline{\omega} \\ u'_\varphi &=& 0 & \text{on } \Gamma_{obs} \\ \partial_{\mathbf{n}} u'_\varphi &=& 0 & \text{on } \Gamma_{\mathrm{i}} \\ u'_\varphi &=& -\partial_{\mathbf{n}} u_\varphi(\boldsymbol{V}\cdot\mathbf{n}) & \text{on } \partial\omega, \end{array}\right. \qquad \left\{\begin{array}{rcll} -\Delta v'_\varphi &=& 0 & \text{in } \Omega\backslash\overline{\omega} \\ v'_\varphi &=& 0 & \text{on } \Gamma_{obs} \\ \partial_{\mathbf{n}} v'_\varphi &=& 0 & \text{on } \Gamma_{\mathrm{i}} \\ v'_\varphi &=& -\partial_{\mathbf{n}} v_\varphi(\boldsymbol{V}\cdot\mathbf{n}) & \text{on } \partial\omega \end{array}\right. \tag{3.10}$$

and

$$\left\{\begin{array}{rcll} -\Delta u'_\psi &=& 0 & \text{in } \Omega\backslash\overline{\omega} \\ \partial_{\mathbf{n}} u'_\psi &=& 0 & \text{on } \Gamma_{obs} \\ u'_\psi &=& 0 & \text{on } \Gamma_{\mathrm{i}} \\ u'_\psi &=& -\partial_{\mathbf{n}} u_\psi(\boldsymbol{V}\cdot\mathbf{n}) & \text{on } \partial\omega, \end{array}\right. \qquad \left\{\begin{array}{rcll} -\Delta v'_\psi &=& 0 & \text{in } \Omega\backslash\overline{\omega} \\ \partial_{\mathbf{n}} v'_\psi &=& 0 & \text{on } \Gamma_{obs} \\ v'_\psi &=& 0 & \text{on } \Gamma_{\mathrm{i}} \\ v'_\psi &=& -\partial_{\mathbf{n}} v_\psi(\boldsymbol{V}\cdot\mathbf{n}) & \text{on } \partial\omega. \end{array}\right. \tag{3.11}$$

Introducing $w := u_\varphi - u_\psi$ and $w' := u'_\varphi - u'_\psi$, we use Hadamard formula (see [61, Theorem 5.2.2]) to get

$$\begin{aligned} \mathrm{D}\mathcal{K}_\varepsilon(\Omega\backslash\overline{\omega})\cdot\boldsymbol{V} = \int_{\Omega\backslash\overline{\omega}} \nabla w'\cdot\nabla w + \frac{1}{2}\int_{\partial\omega} |\nabla w|^2\,(\boldsymbol{V}\cdot\mathbf{n}) \\ + \varepsilon\int_{\Omega\backslash\overline{\omega}} \left(\nabla v'_\varphi\cdot\nabla v_\varphi + \nabla v'_\psi\cdot\nabla v_\psi + v'_\varphi\, v_\varphi + v'_\psi\, v_\psi\right) \\ + \frac{\varepsilon}{2}\int_{\partial\omega} \left(|\nabla v_\varphi|^2 + |\nabla v_\psi|^2 + |v_\varphi|^2 + |v_\psi|^2\right)(\boldsymbol{V}\cdot\mathbf{n}). \end{aligned}$$

Using Green formula into the variational formulation of (3.8) and (3.10) and of (3.9) and (3.11) respectively, we obtain:

$$\begin{aligned} \int_{\Omega\backslash\overline{\omega}} \nabla w\cdot\nabla u'_\varphi + \varepsilon\int_{\Omega\backslash\overline{\omega}} \left(\nabla v'_\varphi\cdot\nabla v_\varphi + v'_\varphi\cdot v_\varphi\right) = -\int_{\partial\omega} \partial_{\mathbf{n}}\rho_N^u\cdot\partial_{\mathbf{n}} u_\varphi(\boldsymbol{V}\cdot\mathbf{n}) \\ - \int_{\partial\omega} \partial_{\mathbf{n}}\rho_N^v\cdot\partial_{\mathbf{n}} v_\varphi(\boldsymbol{V}\cdot\mathbf{n}) \end{aligned}$$

and

$$\begin{aligned} -\int_{\Omega\backslash\overline{\omega}} \nabla w\cdot\nabla u'_\psi + \varepsilon\int_{\Omega\backslash\overline{\omega}} \left(\nabla v'_\psi\cdot\nabla v_\psi + v'_\psi\cdot v_\psi\right) = -\int_{\partial\omega} \partial_{\mathbf{n}}\rho_D^u\cdot\partial_{\mathbf{n}} u_\psi(\boldsymbol{V}\cdot\mathbf{n}) \\ - \int_{\partial\omega} \partial_{\mathbf{n}}\rho_D^v\cdot\partial_{\mathbf{n}} v_\psi(\boldsymbol{V}\cdot\mathbf{n}), \end{aligned}$$

which concludes the proof. □

3.3 Framework for the numerical simulations

Theorem 2 in [3] explains the difficulties encountered to solve numerically the reconstruction of ω. Indeed, the shape gradient has not an uniform sensitivity with respect to the deformation direction. Hence, since the problem is severely ill-posed, we need some regularization methods to solve it numerically, for example by adding to the functional a penalization in terms of the perimeter (see [29] or [43]). Here, we choose to make a regularization by parametrization using a parametric model of shape variations.

As before, all the involved systems will be discretized using $P1$ finite elements. The framework will be the same as in Section 2.2 for the domain Ω and the boundaries Γ_{obs} and Γ_{i}. The real object ω^* will be detailed on each simulation, as well as their initial guess ω_0. In order to have a suitable pair of Cauchy data and real domain ω^*, we will use synthetic data: we fix a shape ω^*, we solve the Laplace's equation in $\Omega\backslash\overline{\omega^*}$ with an explicit g_D (we will use $g_D(x,y) = y^3 - 3x^2y$) over $\partial\Omega$ and homogeneous Dirichlet boundary condition over $\partial\omega$ using another finite elements method (here a $P2$ finite elements discretization) and we extract the Cauchy data g_N by computing the value $\partial_{\mathbf{n}}u$ on Γ_{obs}.

For the obstacle numerical reconstruction, we follow the same strategy than in [3] or in [37] that we recall for readers convenience. We restrict ourselves to star-shaped domains and use polar coordinates for parametrization: the boundary $\partial\omega$ of the object can be then parametrized by

$$\partial\omega = \left\{ \begin{pmatrix} x_0 \\ y_0 \end{pmatrix} + r(\theta) \begin{pmatrix} \cos\theta \\ \sin\theta \end{pmatrix},\ \theta \in [0, 2\pi) \right\},$$

where $x_0, y_0 \in \mathbb{R}$ and where r is a $C^{1,1}$ function, 2π-periodic and without double point. Taking into account of the ill-posedness of the problem, we approximate the polar radius r by its truncated Fourier series

$$r_N(\theta) := a_0^N + \sum_{k=1}^{N} a_k^N \cos(k\theta) + b_k^N \sin(k\theta),$$

for the numerical simulations. Indeed this regularization by projection permits to remove *high frequencies* generated by $\cos(k\theta)$ and $\sin(k\theta)$ for $k >> 1$, for which the functional is degenerated. Then, the unknown shape is entirely defined by the coefficients $(a_{\mathrm{i}}, b_{\mathrm{i}})$. Hence, for $k = 1, \ldots, N$, the corresponding deformation directions are respectively,

$$\boldsymbol{V}_1 := \boldsymbol{V}_{x_0} := \begin{pmatrix} 1 \\ 0 \end{pmatrix},\quad \boldsymbol{V}_2 := \boldsymbol{V}_{y_0} := \begin{pmatrix} 0 \\ 1 \end{pmatrix},\quad \boldsymbol{V}_3(\theta) := \boldsymbol{V}_{a_0}(\theta) := \begin{pmatrix} \cos\theta \\ \sin\theta \end{pmatrix},$$

$$\boldsymbol{V}_{2k+2}(\theta) := \boldsymbol{V}_{a_k}(\theta) := \cos(k\theta) \begin{pmatrix} \cos\theta \\ \sin\theta \end{pmatrix},\ \boldsymbol{V}_{2k+3}(\theta) := \boldsymbol{V}_{b_k}(\theta) := \sin(k\theta) \begin{pmatrix} \cos\theta \\ \sin\theta \end{pmatrix},$$

$\theta \in [0, 2\pi)$. The gradient is then computed component by component using its characterization (see Proposition 5.1, formula (5.2)):

$$\Big(\nabla \mathcal{K}_\varepsilon(\Omega \backslash \overline{\omega})\Big)_k = \mathrm{D}\mathcal{K}_\varepsilon(\Omega \backslash \overline{\omega}) \cdot \boldsymbol{V}_k, \qquad k = 1, \dots, 2N+3.$$

3.3.1 Algorithm

The algorithm in this part is basically the same as the one for the data completion problem: we follow again a scheme of gradient algorithm but now we include also the modification of the shape of ω, so, it should be updated on each iteration by the value of the shape derivative of our functional on each direction considered in the parametrization of ω.

Algorithm

1. Let $k = 0$. Fix k_{max} (max. number of iterations) and tol (tolerance), build (φ_0, ψ_0) as the initial guess of the missing data following the strategy mentioned in Section 2.2 and fix ω_0.
2. Solve problems (3.5) and (3.6) with $(\omega_k, \varphi_k, \psi_k)$, extract the solutions $u_D^k(\omega_k, \varphi_k, \psi_k) := u_{\varphi_k}, u_N^k(\omega_k, \varphi_k, \psi_k) := u_{\psi_k}, v_D^k(\omega_k, \varphi_k, \psi_k) := v_{\varphi_k}$, $v_N^k(\omega_k, \varphi_k, \psi_k) := v_{\psi_k}$ and compute $\mathcal{K}(\omega_k, \varphi_k, \psi_k)$.
   - If $\mathcal{K}(\omega_k, \varphi_k, \psi_k) < tol$: STOP.
   - Else: continue to next step.
3. Solve problems (2.4), (2.5) (defined into $\Omega \setminus \overline{\omega_k}$ with homogeneous Dirichlet condition over $\partial\omega$), (3.8) and (3.9) with $(\omega_k, \varphi_k, \psi_k)$, extract the solutions $w_N(\omega_k, \varphi_k, \psi_k)$, $w_D(\omega_k, \varphi_k, \psi_k)$, $\rho_D^u(\omega_k, \varphi_k, \psi_k)$, $\rho_N^u(\omega_k, \varphi_k, \psi_k)$, $\rho_D^v(\omega_k, \varphi_k, \psi_k)$ and $\rho_N^v(\omega_k, \varphi_k, \psi_k)$.
4. Compute the descent directions $\widetilde{\varphi}$, $\widetilde{\psi}$ using formulas (2.6), (2.7) with (φ_k, ψ_k) and the solutions given in steps 2 and 3.
5. Compute $\nabla \mathcal{K}_\varepsilon(\Omega \setminus \overline{\omega_k})$ using formula (5.2),
6. Update $\varphi_k \leftarrow (\varphi_k - \alpha_1 \widetilde{\varphi})$, $\psi_k \leftarrow \Big(\psi_k - \alpha_2 \widetilde{\psi}\Big)$, $\omega_k \leftarrow \omega_k - \alpha_3 \nabla \mathcal{K}_\varepsilon(\Omega \setminus \overline{\omega_k})$.
7. While $k \leq k_{max}$ and $\mathcal{K}_\varepsilon(\varphi_k, \psi_k) - \mathcal{K}_\varepsilon(\varphi_{k-1}, \psi_{k-1}) < tol$, get back to the step 2, $k \leftarrow k + 1$.

As before, the step lengths $\alpha_1, \alpha_2, \alpha_3$ can be set with a line search algorithm (e.g. via Wolfe conditions, or a golden ratio search) or set as fixed parameters. We precise that we here use the *adaptive method* described in [37, Section 4.3]. It consists in increasing gradually the number of parameters during the algorithm to a fixed final number of parameters. For example, if we want to work with nineteen parameters, we begin by working with two parameters during five iterations, then with three parameters (we add the radius) during five more iterations, and then we add two search parameters every fifteen iterations. The algorithm is then the same than the

one described above only replacing step 6. by

$$\omega_k(1:m) \leftarrow \omega_k(1:m) - \alpha_{\mathrm{i}} \nabla \mathcal{K}_\varepsilon(\Omega \setminus \overline{\omega_k})(1:m),$$

where $\omega_k(1:m)$ represents the m first coefficients parameterizing the shape ω_k (the same notation holds for $\nabla \mathcal{K}_\varepsilon(\Omega \setminus \overline{\omega_k})(1:m)$). The number m grows to the fixed final number of parameters following the procedure described previously.

To conclude, we remark that we have used, as before, the finite element library FreeFEM++ (see [60]) to make the simulations into this part and the noisy case has the same considerations, in particular the construction of noise, as the ones of the data completion part.

3.4 Simulations

For all the simulations in this part we consider Ω, Γ_{obs} and Γ_{i} as the ones described in the framework (see section 3.3). In our first series of simulations (with and without noise) we try to detect a disk centered in the origin with radius $r = 0.25$, this is, $\omega^* = D((0,0), 0.25)$. We consider the initial object ω_0 as the disk centered in $(-0.1, 0.1)$ with radius $r = 0.20$, this is: $\omega_0 = D((-0.1, 0.1), 0.20)$. The number of parameters is set to the maximum of 15, but the algorithm stops due to an increment of the attained value of the Kohn-Vogelius when we introduce the fourth parameter into the parametrization of $\partial\omega$, this may be considered a valuable property of the adaptive method: if we introduce the maximum number of parameters from the beginning, the algorithm may stop immediately due to the excessive number of parameters to detect the disk, which is described by a fewer quantity of parameters.

Table 3.1: Data completion for the object detection problem, non noisy case.

		$\varepsilon = 0.1$	$\varepsilon = 0.01$	$\varepsilon = 0.001$
Approximated Center		(-0.019,-0.006)	(-0.022,-0.003)	(-0.023,-0.002)
$L^2(\Gamma_{\mathrm{i}})$ relative error	u_D	0.0958	0.0902	0.0899
	u_N	0.0919	0.0927	0.0928

Table 3.2: Data completion for the object detection problem, noisy case.

		$\varepsilon = 0.1$	$\varepsilon = 0.01$	$\varepsilon = 0.001$
Approximated Center		(-0.021,-0.017)	(-0.021,-0.003)	(-0.024,-0.001)
$L^2(\Gamma_{\mathrm{i}})$ relative error	u_D	0.0998	0.0930	0.1033
	u_N	0.0946	0.0935	0.0953

In a second series of simulations, we consider now a much more complicated obstacle to test the method: we try to detect a square with relative center $C = (0.0, -0.1)$ and side d = 0.4. The idea is to study the behavior of the method in the case where a non regular obstacle is introduced. The initial object ω_0 is set to be the disk centered in $(0.0, 0.0)$ with radius $r = 0.2$, this is: $\omega_0 = D((0.0, 0.0), 0.2)$.

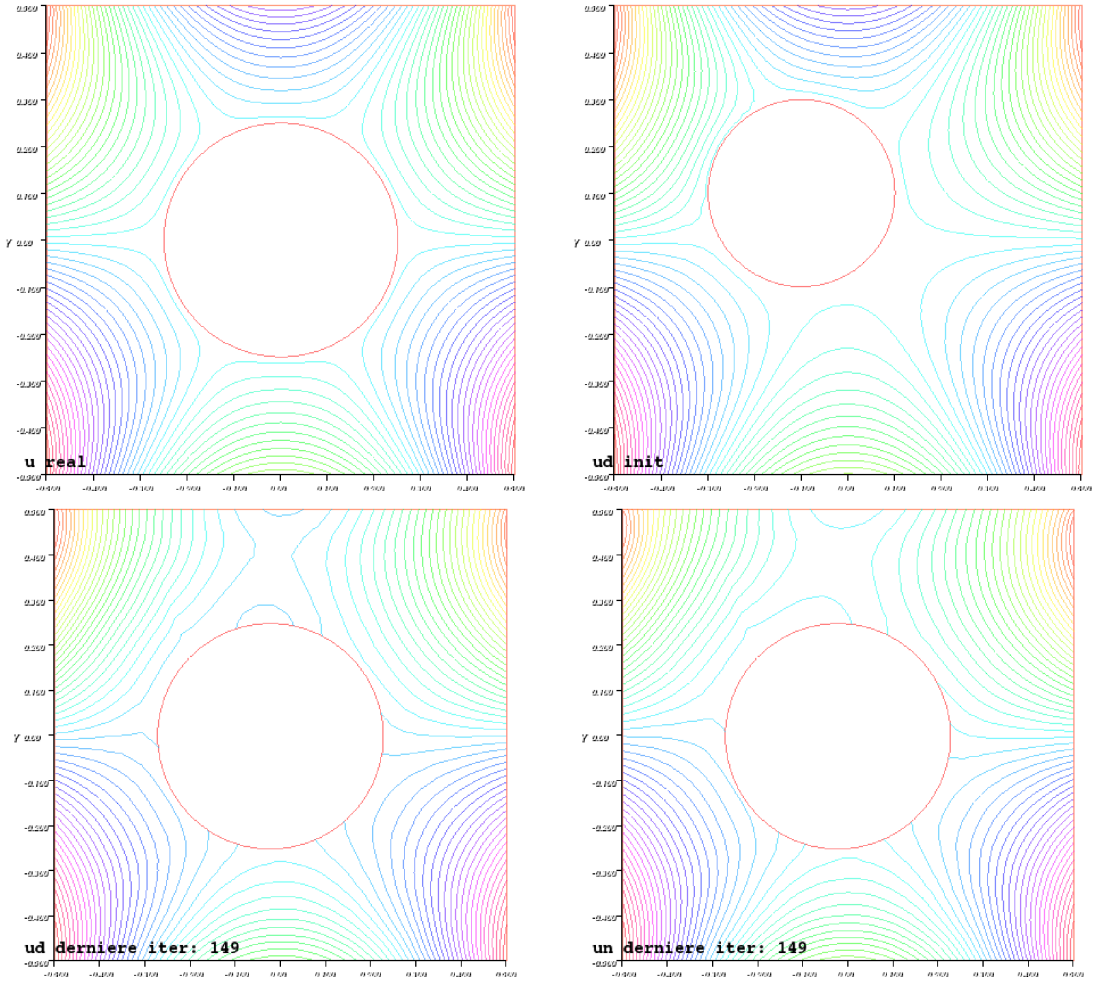

Figure 3.2: Object detection without noise: Real solution and initial guess (up) and obtained solutions u_D, u_N respectively (down).

As before, the number of parameters is set to the maximum of 15. This time the algorithm reaches the number of 9 parameters until it stops as the functional begin to increase, which is an expected property, as the increment on the number of active parameters is linked with the deformation of the circle, in order to approximate the corners of the square.

Table 3.3: Data completion for the object detection problem, non-noisy case.

		$\varepsilon = 0.1$	$\varepsilon = 0.01$	$\varepsilon = 0.001$
Relative Center		(-0.000,-0.071)	(-0.000,-0.082)	(-0.000,-0.086)
$L^2(\Gamma_i)$ relative error	u_D	0.0758	0.0688	0.0666
	u_N	0.0901	0.0878	0.0869

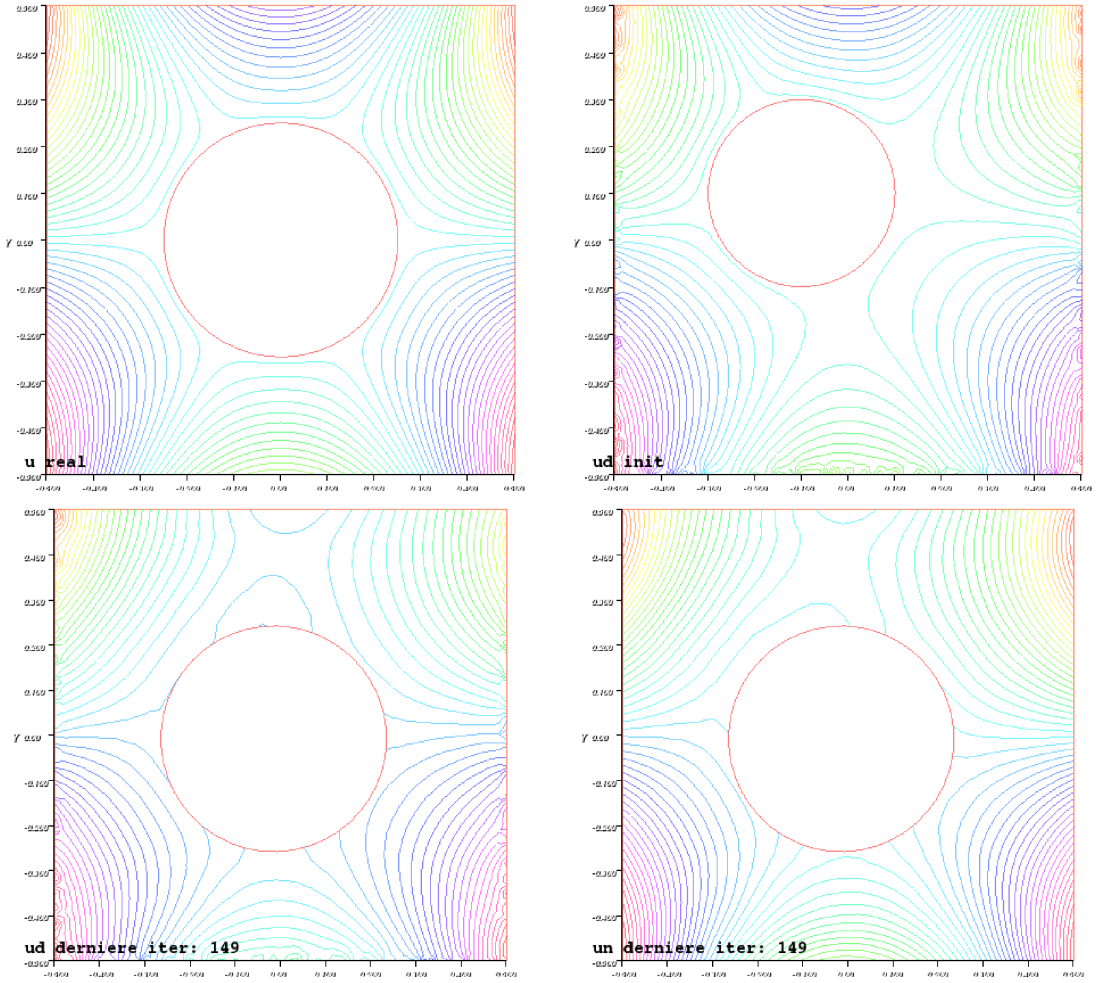

Figure 3.3: Object detection with noise: Real solution and initial guess (up) and obtained solutions u_D, u_N respectively (down).

Table 3.4: Data completion for the object detection problem, noisy case.

		$\varepsilon = 0.1$	$\varepsilon = 0.01$	$\varepsilon = 0.001$
Relative Center		(0.012,-0.068)	(-0.001,-0.087)	(-0.000,-0.084)
$L^2(\Gamma_i)$ relative error	u_D	0.0868	0.0727	0.0667
	u_N	0.0917	0.0905	0.0871

3.4.1 Comments on the simulations

We observe from these simulations that our algorithm is capable to correct the guess localization of the introduced disk in order to obtain a very proximal location, the data completion on Γ_i has the same order of error for the $L^2(\Gamma_i)$ norm, but we can observe an error of the approximation of the real solution around the unaccessible boundary. We remark that we do not compute the $L^2(\Omega \backslash \overline{\omega^*})$-error as the solutions are not defined in the same region, then this quantity is not well defined. The robustness for a reasonable (5%) amount of noise is also observed as the approxi-

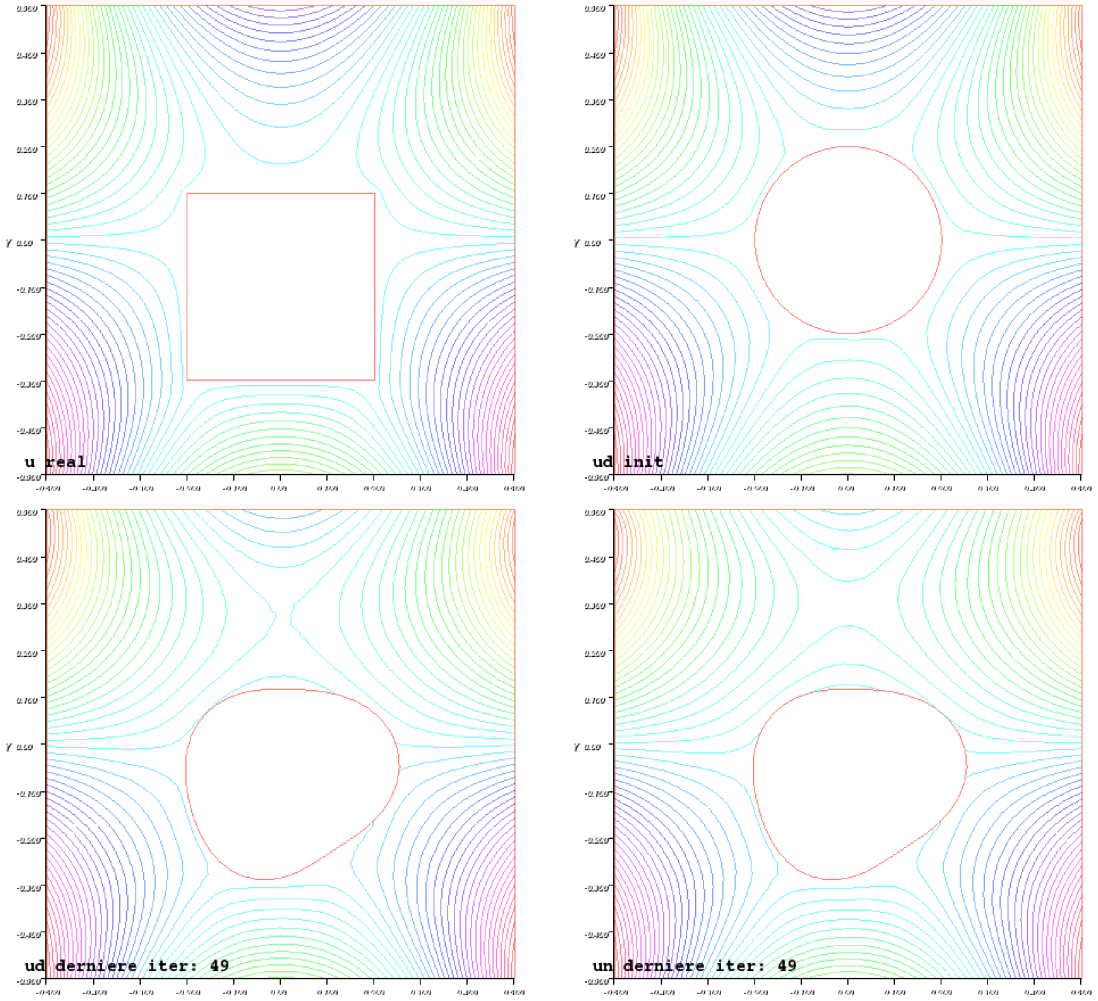

Figure 3.4: Object detection without noise: Real solution and initial guess (up) and obtained solutions u_D, u_N respectively (down).

mation into both cases, for the object detection, is very similar to the one into the unpolluted case.

It is interesting to remark that, as described before, the algorithm is capable to notice that the number of active parameters could be wrong, as in the first series of simulations the algorithm stops when trying to include more parameters than the real ones (only 3, as we are approximating a circle). In the second series of examples the algorithm continues until the inclusion of 9 parameters, which approximates better the corners and the relative area covered by the square.

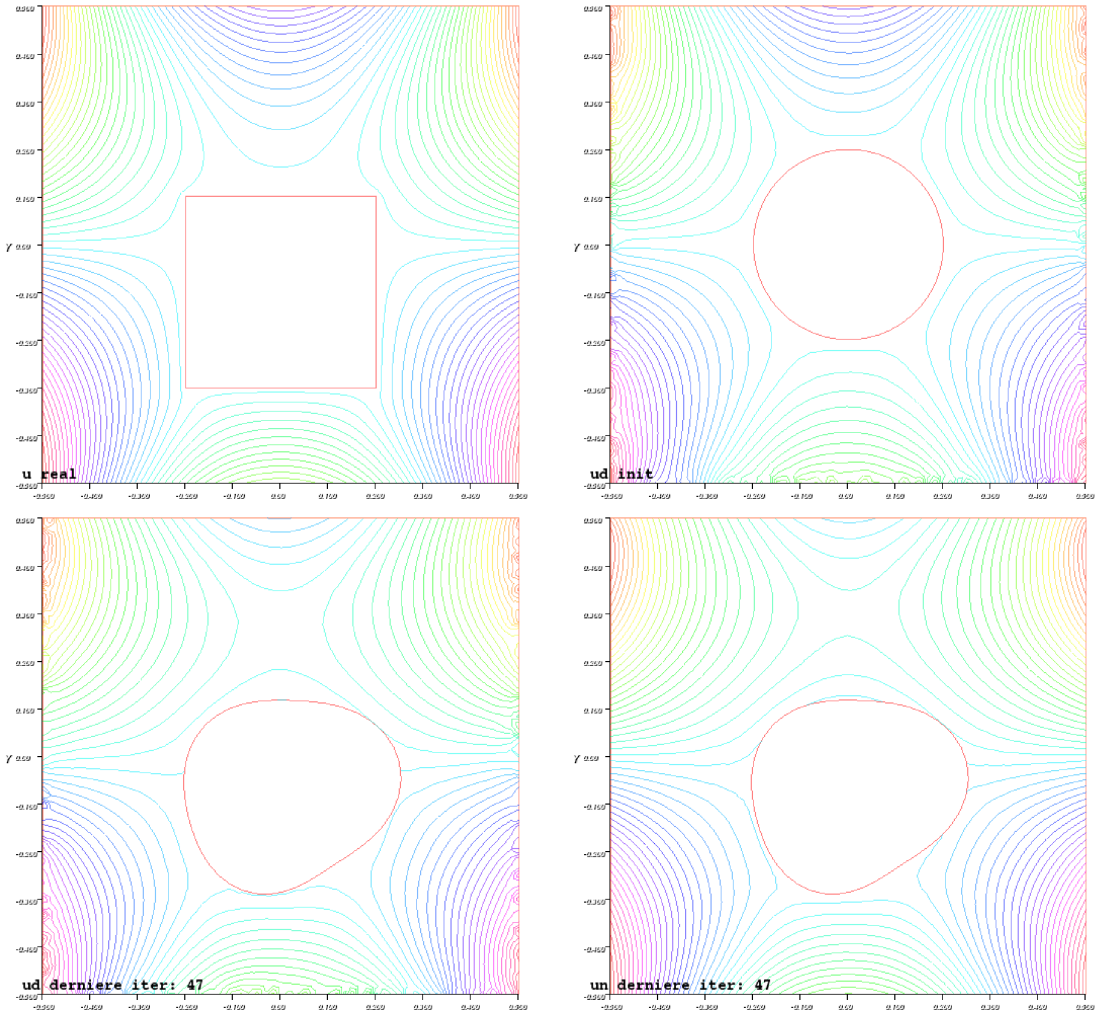

Figure 3.5: Object detection with noise: Real solution and initial guess (up) and obtained solutions u_D, u_N respectively (down).

Part II

The inverse obstacle problem using topological shape optimization in a bidimensional Stokes flow

Chapter 4

Small object detection using topological optimization for bidimensional Stokes equations

In this chapter we change our point of view: We consider the problem of detecting small obstacles immersed in a stationary two-dimensional fluid which is governed by the incompressible Stokes equations. Here again we will formulate the inverse problem as a shape optimization problem, by minimizing a shape cost-functional: the Kohn-Vogelius functional. The smallness hypothesis leads us to consider a different tool than the shape gradient used before: the topological gradient. Using the hypothesis of small obstacles, we can perform an asymptotic expansion, with respect to the inclusion of a small obstacle into the domain of study, of the solution of the involved systems and then of the considered cost functional. Into this asymptotic expansion the topological gradient plays a key role which will allow us to determine the number and relative location of the unknown obstacles.

This chapter is divided in four sections. In the first one we present the problem, the corresponding notations and we characterize the resolution of the inverse problem as the minimization of the Kohn-Vogelius functional adapted to this vector setting. In the second section we present the main tool of our analysis: the topological gradient and we present our main result: the topological asymptotic expansion for the Kohn-Vogelius functional. In the third section we obtain an asymptotic expansion, with respect to a topological variation, of the solution of the Stokes systems involved in our problem. We discuss the heuristics which leads to the proposed expansions and then we prove that, in fact, the *ansatz* satisfy the expected residual sizes. Finally, in the fourth section, we finish the main proof, using the previous asymptotic expansions of the involved Stokes systems solutions into a *decoupled expression* of the variation of the Kohn-Vogelius functional.

Our main references to this work are [9, 17, 22, 36]. We remark that the fact of being in a two-dimensional setting changes strongly the way that the asymptotic

expansion of the solution for the Stokes system should be proposed and performed, in this case the approximation by an exterior problem is no longer valid and we rely to a similar procedure to the one presented by Bonnaillie-Noël and Dambrine [22] to obtain the desired expansion in this case. Then the final part of the proof of the main result is similar to the one exposed in [36], however as the approximation performed is different, some arguments should be modified. Finally we remark the fact that, unlike the three-dimensional case, the expression of the topological gradient that we will obtain is independent of the shape of the obstacle(s), which has been seen in several other cases (see for example [9, 10, 11, 17, 54]).

4.1 Framework

Let Ω be a bounded Lipschitz open set of $\mathbb{R}^2$ containing a Newtonian and incompressible fluid with coefficient of kinematic viscosity $\nu > 0$. Let $\omega \subset \mathbb{R}^2$ a fixed bounded Lipschitz domain containing the origin, such that $\overline{\omega} \subset B(0,1)$. For $z \in \Omega$ and $0 < \varepsilon << 1$, we denote

$$\omega_{z,\varepsilon} := z + \varepsilon\omega.$$

The aim of this work is to detect some unknown objects included in Ω. We assume that a finite number m^* of obstacles $\omega_{z_j^*,\varepsilon_j^*} \subset \Omega,\ j \in \{1,\dots,m^*\}$ have to be detected. Moreover, we assume that they are well separated (that is: $\overline{\omega}_{z_{\mathrm{i}}^*,\varepsilon_{\mathrm{i}}^*} \cap \overline{\omega}_{z_j^*,\varepsilon_j^*} = \emptyset$ for all $1 \leq \mathrm{i}, j \leq m^*$ with $\mathrm{i} \neq j$) and have the geometry form

$$\omega_{z_k^*,\varepsilon_k^*} = z_k^* + \varepsilon_k^*\omega, \qquad 1 \leq k \leq m^*,$$

where ε_k^* is the diameter and the points $z_k^* \in \Omega$, $1 \leq k \leq m^*$, determine the location of the objects. Finally, we assume that, for all $1 \leq k \leq m^*$, $\omega_{z_k,\varepsilon_k}^*$ is far from the boundary $\partial\Omega$.

Let $\boldsymbol{f} \in \mathbf{H}^{1/2}(\partial\Omega)$ such that $\boldsymbol{f} \neq \mathbf{0}$ satisfying the compatibility condition

$$\int_{\partial\Omega} \boldsymbol{f} \cdot \mathbf{n} = 0. \tag{4.1}$$

In order to determine the location of the objects, we make a measurement $\boldsymbol{g} \in \mathbf{H}^{-1/2}(O)$ on a part O of the exterior boundary $\partial\Omega$ with $O \subset \partial\Omega,\ O \neq \partial\Omega$. Then, we denote

$$\omega_\varepsilon^* := \bigcup_{k=1}^{m^*} \omega_{z_k^*,\varepsilon_k^*},$$

and consider the following overdetermined Stokes problem

$$\left\{\begin{array}{rcll} -\nu\Delta\boldsymbol{u} + \nabla p &=& \mathbf{0} & \text{in } \Omega\backslash\overline{\omega_\varepsilon^*} \\ \operatorname{div}\boldsymbol{u} &=& 0 & \text{in } \Omega\backslash\overline{\omega_\varepsilon^*} \\ \boldsymbol{u} &=& \boldsymbol{f} & \text{on } \partial\Omega \\ \boldsymbol{u} &=& \mathbf{0} & \text{on } \partial\omega_\varepsilon^* \\ \sigma(\boldsymbol{u},p)\mathbf{n} &=& \boldsymbol{g} & \text{on } O \subset \partial\Omega. \end{array}\right. \tag{4.2}$$

Here $\boldsymbol{u}$ represents the velocity of the fluid and p the pressure and $\sigma(\boldsymbol{u}, p)$ represents the stress tensor defined by

$$\sigma(\boldsymbol{u}, p) := \nu \left(\nabla \boldsymbol{u} + {}^t \nabla \boldsymbol{u} \right) - p\mathrm{I}.$$

We assume here that there is no body force and consider the homogeneous Dirichlet boundary conditions on the obstacles, which is the so-called *no-slip boundary condition*. Notice that, if $\operatorname{div} \boldsymbol{u} = 0$ in Ω, we have

$$-\nu \Delta \boldsymbol{u} + \nabla p = -\operatorname{div} \left(\nu \mathcal{D}(\boldsymbol{u}) \right) + \nabla p = -\operatorname{div} \left(\sigma(\boldsymbol{u}, p) \right) \quad \text{in } \Omega,$$

with $\mathcal{D}(\boldsymbol{u}) := \left(\nabla \boldsymbol{u} + {}^t \nabla \boldsymbol{u} \right)$. Thus we consider the following geometric inverse problem:

Find $\omega_\varepsilon^* \subset\subset \Omega$ *and a pair* $(\boldsymbol{u}, p)$ *which satisfy the overdetermined problem* (4.2). (4.3)

To study this inverse problem, we consider two forward problems:

$$\left\{ \begin{array}{l} \text{Find } (\boldsymbol{u}_D^\varepsilon, p_D^\varepsilon) \in \mathbf{H}^1(\Omega \backslash \overline{\omega_\varepsilon}) \times \mathrm{L}_0^2(\Omega \backslash \overline{\omega_\varepsilon}) \text{ such that} \\ \qquad \begin{array}{rcll} -\nu \Delta \boldsymbol{u}_D^\varepsilon + \nabla p_D^\varepsilon &=& \mathbf{0} & \text{in } \Omega \backslash \overline{\omega_\varepsilon} \\ \operatorname{div} \boldsymbol{u}_D^\varepsilon &=& 0 & \text{in } \Omega \backslash \overline{\omega_\varepsilon} \\ \boldsymbol{u}_D^\varepsilon &=& \boldsymbol{f} & \text{on } \partial\Omega \\ \boldsymbol{u}_D^\varepsilon &=& \mathbf{0} & \text{on } \partial\omega_\varepsilon \end{array} \end{array} \right. \tag{4.4}$$

and

$$\left\{ \begin{array}{l} \text{Find } (\boldsymbol{u}_M^\varepsilon, p_M^\varepsilon) \in \mathbf{H}^1(\Omega \backslash \overline{\omega_\varepsilon}) \times \mathrm{L}^2(\Omega \backslash \overline{\omega_\varepsilon}) \text{ such that} \\ \qquad \begin{array}{rcll} -\nu \Delta \boldsymbol{u}_M^\varepsilon + \nabla p_M^\varepsilon &=& \mathbf{0} & \text{in } \Omega \backslash \overline{\omega_\varepsilon} \\ \operatorname{div} \boldsymbol{u}_M^\varepsilon &=& 0 & \text{in } \Omega \backslash \overline{\omega_\varepsilon} \\ \sigma(\boldsymbol{u}_M^\varepsilon, p_M^\varepsilon)\mathbf{n} &=& \boldsymbol{g} & \text{on } O \\ \boldsymbol{u}_M^\varepsilon &=& \boldsymbol{f} & \text{on } \partial\Omega \backslash \overline{O} \\ \boldsymbol{u}_M^\varepsilon &=& \mathbf{0} & \text{on } \partial\omega_\varepsilon, \end{array} \end{array} \right. \tag{4.5}$$

where $\omega_\varepsilon := \bigcup_{k=1}^m \omega_{z_k, \varepsilon_k}$ for a finite number m of objects located in $z_1, \ldots, z_m$. These two forward problems are classically well-defined. We refer to [27, 52] for the results of existence and uniqueness of $(\boldsymbol{u}_D^\varepsilon, p_D^\varepsilon)$. Notice that the compatibility condition (4.1) associated with Problem (4.4) is satisfied. The existence and the uniqueness of $(\boldsymbol{u}_M^\varepsilon, p_M^\varepsilon)$ is detailed in Appendix B, Section B.1. We underline the fact that p_M^ε does not need to be normalized to be unique due to the Neumann boundary conditions imposed on O.

One can remark that, assuming that $\boldsymbol{f}, \boldsymbol{g}$ are the real data (this is, obtained without error), if ω_ε coincides with the actual domain ω_ε^*, then $\boldsymbol{u}_D^\varepsilon = \boldsymbol{u}_M^\varepsilon$ in $\Omega \backslash \overline{\omega_\varepsilon}$. According to this observation, we propose a resolution of the inverse problem (4.3) of reconstructing ω_ε^* based on the minimization of the following Kohn-Vogelius functional

$$\mathcal{F}_\varepsilon^{KV}(\boldsymbol{u}_D^\varepsilon, \boldsymbol{u}_M^\varepsilon) := \frac{1}{2} \int_{\Omega \backslash \overline{\omega_\varepsilon}} \nu |\mathcal{D}(\boldsymbol{u}_D^\varepsilon) - \mathcal{D}(\boldsymbol{u}_M^\varepsilon)|^2.$$

We then define

$$\mathcal{J}_{KV}(\Omega \backslash \overline{\omega_\varepsilon}) := \mathcal{F}_\varepsilon^{KV}(\boldsymbol{u}_D^\varepsilon, \boldsymbol{u}_M^\varepsilon).$$

We can notice that, integrating by parts the expression of $\mathcal{F}_\varepsilon^{KV}(\boldsymbol{u}_D^\varepsilon, \boldsymbol{u}_M^\varepsilon)$, we get that $\mathcal{F}_\varepsilon^{KV}(\boldsymbol{u}_D^\varepsilon, \boldsymbol{u}_M^\varepsilon) = \nu \displaystyle\int_O (\boldsymbol{f} - \boldsymbol{u}_M^\varepsilon) \cdot (\sigma(\boldsymbol{u}_D^\varepsilon, p_D^\varepsilon)\mathbf{n} - \boldsymbol{g})$. This expression shows that the error can be expressed by an integral involving only the part of the boundary where we make the measurement and reveals the coupling of the solutions *via* this functional. Finally, we can notice that the Dirichlet error is weighted by the Neumann error, and *vice versa*.

Remark In order to guarantee that the inverse problem of finding ω_ε^* and a pair $(\boldsymbol{u}, p)$ satisfying (4.2) has a solution, we have to assume the existence of such a ω_ε^*. This means that the measurement $\boldsymbol{g}$ is perfect, that is to say without error. Then, according to the identifiability result [6, Theorem 1.2] proved by Alvarez *et al.*, the domain ω_ε^* is unique. Notice that in [6], ω_ε^* is assumed to have a $C^{1,1}$ boundary but we can only assume that it has a Lipschitz boundary in the Stokes case (see [14, Theorem 2.1]). Hence, if we find ω_ε^* such that $\mathcal{J}_{KV}(\Omega \setminus \omega_\varepsilon^*) = 0$, then $\boldsymbol{u}_D^\varepsilon = \boldsymbol{u}_M^\varepsilon$ in $\Omega \setminus \omega_\varepsilon^*$, i.e. $\boldsymbol{u}_D^\varepsilon$ satisfies (4.2) and thus $\omega_\varepsilon = \omega_\varepsilon^*$ is the real domain.

In the following, for $\varepsilon = 0$, we will consider as a convention that $\omega_0 = \emptyset$ (instead of $\omega_0 = \bigcup_{k=1}^m \{z_k\}$, which comes from the definition of ω_ε), and therefore: $\Omega_0 = \Omega$. Then, we will denote $(\boldsymbol{u}_D^0, p_D^0) \in \mathbf{H}^1(\Omega) \times \mathrm{L}_0^2(\Omega)$ and $(\boldsymbol{u}_M^0, p_M^0) \in \mathbf{H}^1(\Omega) \times \mathrm{L}^2(\Omega)$ the respective solutions of the following systems:

$$\left\{\begin{array}{l} \text{Find } (\boldsymbol{u}_D^0, p_D^0) \in \mathbf{H}^1(\Omega) \times \mathrm{L}_0^2(\Omega) \text{ such that} \\ \qquad \begin{array}{rcll} -\nu\Delta \boldsymbol{u}_D^0 + \nabla p_D^0 & = & \mathbf{0} & \text{in } \Omega \\ \operatorname{div} \boldsymbol{u}_D^0 & = & 0 & \text{in } \Omega \\ \boldsymbol{u}_D^0 & = & \boldsymbol{f} & \text{on } \partial\Omega \end{array} \end{array}\right.$$

and

$$\left\{\begin{array}{l} \text{Find } (\boldsymbol{u}_M^0, p_M^0) \in \mathbf{H}^1(\Omega) \times \mathrm{L}^2(\Omega) \text{ such that} \\ \qquad \begin{array}{rcll} -\nu\Delta \boldsymbol{u}_M^0 + \nabla p_M^0 & = & \mathbf{0} & \text{in } \Omega \\ \operatorname{div} \boldsymbol{u}_M^0 & = & 0 & \text{in } \Omega \\ \sigma(\boldsymbol{u}_M^0, p_M^0)\mathbf{n} & = & \boldsymbol{g} & \text{on } O \\ \boldsymbol{u}_M^0 & = & \boldsymbol{f} & \text{on } \partial\Omega \backslash \overline{O}. \end{array} \end{array}\right.$$

4.2 The main result

From now on, we consider the problem of seeking a single obstacle $\omega_{z,\varepsilon} := z + \varepsilon\omega$, located at a point $z \in \Omega$. Notice that in the case of several inclusions, we proceed by detecting the objects one by one. Thus, after detecting a first obstacle $\omega_{z_1,\varepsilon_1}$, we work replacing the whole domain Ω by $\Omega \backslash \overline{\omega_{z_1,\omega_1}}$ (and then we have $\partial\omega_{z_1,\varepsilon_1} \subset \partial\left(\Omega \backslash \overline{\omega_{z_1,\omega_1}}\right) \backslash \overline{O}$) and the results presented below (in particular the topological derivative) are still valid for a new inclusion $\omega_{z,\varepsilon}$. Note that, the asymptotic expansion of the solution of elliptic boundary value problem in multiply perforated domains is studied in [23, 66].

4.2.1 Introduction of the needed functional tools

We recall that the topological sensitivity analysis consists in the study of the variations of a design functional $\mathcal{J}$ with respect to the insertion of a small obstacle $\omega_{z,\varepsilon}$ at the point $z \in \Omega$ (with no-slip boundary conditions). The aim is to obtain an asymptotic expansion of $\mathcal{J}$ of the form

$$\mathcal{J}(\Omega_{z,\varepsilon}) = \mathcal{J}(\Omega) + \xi(\varepsilon)\delta\mathcal{J}(z) + o(\xi(\varepsilon)) \qquad \forall z \in \Omega, \tag{4.6}$$

where $\varepsilon > 0$, ξ is a positive scalar function intended to tend to zero with ε and where

$$\Omega_{z,\varepsilon} := \Omega \backslash \overline{\omega_{z,\varepsilon}},$$

with $\omega_{z,\varepsilon} := z + \varepsilon\omega$. We summarize the notations concerning the domains in Figure 4.1.

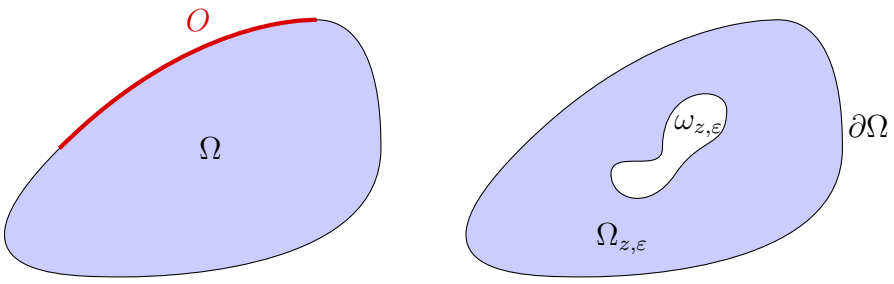

Figure 4.1: The initial domain and the same domain after inclusion of an object

The computation of the topological gradient $\delta\mathcal{J}$ in this work is mainly based on the paper by Caubet and Dambrine [36] which deals with the presented problem in the three-dimensional setting. The work of Bonnaillie-Noël and Dambrine [21], which deals with asymptotic expansions for Laplace equation in a domain with several obstacles, was the basis for the choice of the approximating problem in the two-dimensional setting. We also have been inspired strongly by the works of Sid Idris in [77] and [53, 54] (written with Guillaume), where the authors study topological asymptotic expansions for Laplace and Stokes equations in two and three dimensions, which provides us several techniques specially useful for the technical proofs presented in the appendix. Finally, let us point out the works of Amstutz [9, 10], where the author develops a topological asymptotic expansion for a cost functional in the context of a fluid governed by the stationary Navier-Stokes equations, which contribute to understand better the possibilities for the asymptotic expansion of the solutions for our considered systems. It is important to mention that in all these situations the problem involves only Dirichlet boundary conditions.

We recall the expression of the fundamental solution $(E, \boldsymbol{P})$ to the Stokes system in $\mathbb{R}^2$ given by

$$E(x) = \frac{1}{4\pi\nu}\left(-\log\|x\|\mathrm{I} + \mathrm{e}_r{}^t\mathrm{e}_r\right), \qquad \boldsymbol{P}(x) = \frac{x}{2\pi\|x\|^2}, \tag{4.7}$$

with $\mathrm{e}_r = \dfrac{x}{\|x\|}$; that is $-\nu\Delta E_j + \nabla \boldsymbol{P}_j = \delta \mathbf{e}_j$, where E_j denotes the j^{th} column of E, $(\mathbf{e}_j)_{j=1}^2$ is the canonical basis of $\mathbb{R}^2$ and δ is the Dirac distribution.

4.2.2 The result

The following theorem gives us the expression of the topological gradient of the Kohn-Vogelius functional $\mathcal{J}_{KV}$:

Theorem 4.1 *For $z \in \Omega$, the functional $\mathcal{J}_{KV}$ admits the following topological asymptotic expansion*

$$\mathcal{J}_{KV}(\Omega_{z,\varepsilon}) - \mathcal{J}_{KV}(\Omega) = \frac{4\pi\nu}{-\log\varepsilon}(|\boldsymbol{u}_D^0(z)|^2 - |\boldsymbol{u}_M^0(z)|^2) + o\left(\frac{1}{-\log\varepsilon}\right),$$

where $\boldsymbol{u}_D^0 \in \mathbf{H}^1(\Omega)$ and $\boldsymbol{u}_M^0 \in \mathbf{H}^1(\Omega)$ solve respectively Problems (4.4) and (4.5) with $\omega_\varepsilon = \emptyset$ and $o(f(\varepsilon))$ is the set of functions $g(\varepsilon)$ such that $\lim_{\varepsilon\to 0} \frac{g(\varepsilon)}{f(\varepsilon)} = 0$. Therefore, we have

$$\xi(\varepsilon) = \frac{1}{-\log\varepsilon} \quad \text{and} \quad \delta\mathcal{J}_{KV}(z) = 4\pi\nu(|\boldsymbol{u}_D^0(z)|^2 - |\boldsymbol{u}_M^0(z)|^2)$$

in the general asymptotic expansion (4.6).

Remark Notice that, contrary to the 3 dimensional case [36, Theorem 3.1] the topological gradient doesn't depend on the geometry of ω. The formula applies for all shapes in 2D. This phenomena is described by Finn and Smith in [50] and is known as the *Finn-Smith paradox*, which is also consistent with the results obtained by several authors in similar problems, see for example [9, 11, 17, 53, 54].

Remark For simplicity in what follows we will work with an origin-centered inclusion, that means: $\omega_{z,\varepsilon} = \omega_{0,\varepsilon} =: \omega_\varepsilon$ also consider $\Omega_\varepsilon := \Omega_{0,\varepsilon}$. The procedure for all $z \in \Omega$ is exactly the same just by taking into account the change of variable $y = z + \varepsilon x$, instead of $y = \varepsilon x$ that we will use.

4.3 Asymptotic expansion of the solution of the Stokes problem

In order to provide an asymptotic expansion of the Kohn-Vogelius functional $\mathcal{J}_{KV}$, we need first an asymptotic expansion of the solution of the Stokes problems (4.4) and (4.5).

Unlike the three-dimensional case, the two-dimensional problem cannot be approximated by an 'exterior problem', which in general in this case doesn't have

a solution which vanishes at infinity. This kind of problem has been treated by Bonnaillie-Noël and Dambrine in [21] for the Laplace equation in the plane: we will follow this procedure in order to find a suitable approximation for the Stokes problem.

We recall that we here focus on the detection of a single obstacle (see the beginning of Section 4.2). This section is devoted to the proof of the following proposition:

Proposition 4.2 *The respective solutions* $\boldsymbol{u}_D^\varepsilon \in \mathbf{H}^1(\Omega_{z,\varepsilon})$ *and* $\boldsymbol{u}_M^\varepsilon \in \mathbf{H}^1(\Omega_{z,\varepsilon})$ *of Problems* (4.4) *and* (4.5) *admit the following asymptotic expansion (with the subscript* $\natural = D$ *and* $\natural = M$ *respectively):*

$$\boldsymbol{u}_\natural^\varepsilon(x) = \boldsymbol{u}_\natural^0(x) + h_\varepsilon(\boldsymbol{C}_\natural(x) - \boldsymbol{U}_\natural(x)) + O_{\mathbf{H}^1(\Omega_{z,\varepsilon})}\left(\frac{1}{-\log\varepsilon}\right),$$

where $(\boldsymbol{U}_\natural, P_\natural) \in \mathbf{H}^1(\Omega) \times \mathrm{L}^2_0(\Omega)$ *solves the following Stokes problem defined in the whole domain* Ω

$$\left\{\begin{array}{rcll} -\nu\Delta\boldsymbol{U}_\natural + \nabla P_\natural &=& \boldsymbol{0} & \text{in } \Omega \\ \operatorname{div}\boldsymbol{U}_\natural &=& 0 & \text{in } \Omega \\ \boldsymbol{U}_\natural &=& \boldsymbol{C}_\natural & \text{on } \partial\Omega, \end{array}\right. \tag{4.8}$$

with $h_\varepsilon := \frac{1}{-\log\varepsilon}$ *and*

$$\boldsymbol{C}_\natural(x) := -4\pi\nu E(x-z)\boldsymbol{u}_\natural^0(z), \tag{4.1 bis}$$

where E *is the fundamental solution of the Stokes equations in* $\mathbb{R}^2$ *given by* (4.7). *The notation* $O_{\mathbf{H}^1(\Omega_{z,\varepsilon})}\left(\frac{1}{-\log\varepsilon}\right)$ *means that there exist a constant* $c > 0$ *(independent of* ε*) and* $\varepsilon_1 > 0$ *such that for all* $0 < \varepsilon < \varepsilon_1$

$$\left\|\boldsymbol{u}_\natural^\varepsilon(x) - \boldsymbol{u}_\natural^0(x) - h_\varepsilon(\boldsymbol{C}_\natural(x) - \boldsymbol{U}_\natural(x))\right\|_{1,\Omega_{z,\varepsilon}} \leq \frac{c}{-\log\varepsilon}.$$

4.3.1 Defining the approximation

As we mentioned above, the approximation should be done in a different setting compared to the three-dimensional case, following the same strategy as in [21]. This basically consists in building 'a correction term' to the solution given by $E(x-z)\boldsymbol{u}_\natural^0$ which has a logarithmic term and then tends to infinity at infinity and is not of finite energy in $\mathbb{R}^2 \setminus \overline{\omega}$. Therefore it has to be considered only in Ω. To this, we consider the pair $(\boldsymbol{U}_\natural, \boldsymbol{P}_\natural) \in \mathbf{H}^1(\Omega) \times \mathrm{L}^2_0(\Omega)$ solution of Problem (4.8) and we combine these solutions with unknown scale parameters $a(\varepsilon)$ and $b(\varepsilon)$. Imposing the desired scales to the error function, we will be able to determine the scale factors $a(\varepsilon)$ and $b(\varepsilon)$ which define completely the approximation for $\boldsymbol{u}_\natural^\varepsilon$. Here, we will detail the Dirichlet case, the treatment of Neumann case is analogous.

Consider the solution $(\boldsymbol{U}_D, \boldsymbol{P}_D) \in \mathbf{H}^1(\Omega) \times \mathrm{L}^2_0(\Omega)$ of Problem (4.8) with $\natural = D$. The idea is to combine this solution and the function $\boldsymbol{C}_D$ to build a proper corrector. To build this, we search coefficients $a(\varepsilon)$ and $b(\varepsilon)$, such that the error $\boldsymbol{r}_D^\varepsilon$ defined by:

$$\boldsymbol{u}_D^\varepsilon(x) = \boldsymbol{u}_D^0(x) + a(\varepsilon)\,\boldsymbol{C}_D(x) + b(\varepsilon)\,\boldsymbol{U}_D(x) + \boldsymbol{r}_D^\varepsilon(x)$$

is reduced with respect to $\boldsymbol{R}_D^\varepsilon := \boldsymbol{u}_D^\varepsilon - \boldsymbol{u}_D^0$. Notice that the remainder $\boldsymbol{r}_D^\varepsilon$ satisfies:

$$\left\{\begin{array}{rcll} -\nu\Delta \boldsymbol{r}_D^\varepsilon + \nabla p_{r_D^\varepsilon} &=& \boldsymbol{0} & \text{in } \Omega_\varepsilon \\ \operatorname{div} \boldsymbol{r}_D^\varepsilon &=& 0 & \text{in } \Omega_\varepsilon \\ \boldsymbol{r}_D^\varepsilon &=& -(a(\varepsilon)+b(\varepsilon))\,\boldsymbol{C}_D(x) & \text{on } \partial\Omega \\ \boldsymbol{r}_D^\varepsilon &=& -\boldsymbol{u}_D^0(x) - a(\varepsilon)\,\boldsymbol{C}_D(x) - b(\varepsilon)\,\boldsymbol{U}_D(x) & \text{on } \partial\omega_\varepsilon, \end{array}\right. \tag{4.9}$$

where $p_{r_D^\varepsilon}$ is defined in analogous way with pressure terms, that is

$$p_{r_D^\varepsilon}(x) := p_D^\varepsilon(x) - p_D^0(x) - a(\varepsilon)\Pi_D(x) - b(\varepsilon)P_D(x)$$

with $\Pi_D(x) := -4\pi\nu \boldsymbol{P}(x)\cdot \boldsymbol{u}_D^0(0)$.

For $x \in \partial\Omega$, we have:

$$\boldsymbol{r}_D^\varepsilon(x) = o(\boldsymbol{1}) \Leftrightarrow a(\varepsilon) + b(\varepsilon) = o(1),$$

Let us assume for a while that ω is a disk. Then, for $x \in \partial\omega_\varepsilon$, there exists $X \in \partial B(0,1)$ such that $x = \varepsilon X$ and we have

$$\boldsymbol{r}_D^\varepsilon(x) = o(\boldsymbol{1}) \Leftrightarrow -\boldsymbol{u}_D^0(\varepsilon X) - a(\varepsilon)\,\boldsymbol{C}_D(\varepsilon X) - b(\varepsilon)\,\boldsymbol{U}_D(\varepsilon X) = o(\boldsymbol{1}),$$

We can expand the terms $\boldsymbol{U}_D(\varepsilon X)$ and $\boldsymbol{u}_D^0(\varepsilon X)$ via Taylor expansions:

$$\boldsymbol{u}_D^0(\varepsilon X) = \boldsymbol{u}_D^0(0) + O(\varepsilon) \text{ and } \boldsymbol{U}_D(\varepsilon X) = \boldsymbol{U}_D(0) + O(\varepsilon),$$

and thus, we get (noticing that $O(\varepsilon)$ is contained in $o(1)$):

$$\boldsymbol{r}_D^\varepsilon(x) = o(\boldsymbol{1}) \Leftrightarrow -\boldsymbol{u}_D^0(0) - a(\varepsilon)\,\boldsymbol{C}_D(\varepsilon X) - b(\varepsilon)\,\boldsymbol{U}_D(0) = o(\boldsymbol{1}),$$

where $\mathrm{i} = 1, 2$. Therefore, we have the linear system in unknowns $(a(\varepsilon), b(\varepsilon))$:

$$\left\{\begin{array}{rcl} a(\varepsilon) + b(\varepsilon) &=& 0 \\ a(\varepsilon)\,\boldsymbol{C}_D(\varepsilon X) + b(\varepsilon)\,\boldsymbol{U}_D(0) &=& -\boldsymbol{u}_D^0(0). \end{array}\right.$$

We easily get that $b(\varepsilon) = -a(\varepsilon)$ which implies:

$$a(\varepsilon)\,(\boldsymbol{C}_D(\varepsilon X) - \boldsymbol{U}_D(0)) = -\boldsymbol{u}_D^0(0).$$

This vectorial equality implies two possible choices for $a(\varepsilon)$, recalling that $\boldsymbol{C}_D(\varepsilon X) = -4\pi\nu E(\varepsilon X)\boldsymbol{u}_D^0(0)$, we get (for $\mathrm{i}, j \in \{1,2\}, \mathrm{i} \neq j$)

$$a(\varepsilon) = \frac{(\boldsymbol{u}_D^0(0))_\mathrm{i}}{c_1\,(\boldsymbol{u}_D^0(0))_\mathrm{i} - \log\varepsilon\cdot(\boldsymbol{u}_D^0(0))_\mathrm{i} + c_2\,(\boldsymbol{u}_D^0(0))_j + (\boldsymbol{U}_D(0))_\mathrm{i}},$$

where c_1 and c_2 are two positive constants. This leads that $a(\varepsilon)$ can be expressed as $a(\varepsilon) = \frac{1}{C - \log\varepsilon}$ for another positive constant denoted by C in the two possible cases, and then, we get the following scale:

$$\frac{1}{-\log\varepsilon} + O\left(\frac{1}{\log^2\varepsilon}\right) =: h_\varepsilon + O\left(\frac{1}{\log^2\varepsilon}\right) \quad as\ \varepsilon \to 0.$$

It is important to notice, as has been pointed out in [21, Remark 2.2], that this construction is performed in the case of a disk, where $|x| = \varepsilon$ for $x \in \partial\omega_\varepsilon$. In the general case, ω is not a ball and then $\log|x| \neq \log\varepsilon$ for all $x \in \partial\omega_\varepsilon$ and one has to add correctors as performed by Maz'ya *et al.* in [67, Section 2.4, p. 60–64]. This correction of $\log\varepsilon$ is of order zero, is then negligible with respect to the logarithmic term. The linear system in $(a(\varepsilon), b(\varepsilon))$ remains unchanged and so h_ε is still the same rational fraction.

Hence, we approximate $\boldsymbol{u}_D^\varepsilon$ by:

$$\boldsymbol{u}_D^\varepsilon(x) = \boldsymbol{u}_D^0(x) + h_\varepsilon(\boldsymbol{C}_D - \boldsymbol{U}_D) + \boldsymbol{r}_D^\varepsilon(x).$$

Analogously, we approximate $\boldsymbol{u}_M^\varepsilon$ by:

$$\boldsymbol{u}_M^\varepsilon(x) = \boldsymbol{u}_M^0(x) + h_\varepsilon(\boldsymbol{C}_M - \boldsymbol{U}_M) + \boldsymbol{r}_M^\varepsilon(x).$$

4.3.2 An explicit bound of $\mathbf{r}_D^\varepsilon$ and $\mathbf{r}_M^\varepsilon$ with respect to ε

The Dirichlet case

Notice that, in this case, the remainder $\boldsymbol{r}_D^\varepsilon$ satisfies:

$$\left\{\begin{array}{rcll} -\nu\Delta\boldsymbol{r}_D^\varepsilon + \nabla p_{r_D^\varepsilon} &=& \mathbf{0} & \text{in } \Omega_\varepsilon \\ \operatorname{div}\boldsymbol{r}_D^\varepsilon &=& 0 & \text{in } \Omega_\varepsilon \\ \boldsymbol{r}_D^\varepsilon &=& \mathbf{0} & \text{on } \partial\Omega \\ \boldsymbol{r}_D^\varepsilon &=& -\boldsymbol{u}_D^0 - h_\varepsilon(\boldsymbol{C}_D - \boldsymbol{U}_D) & \text{on } \partial\omega_\varepsilon. \end{array}\right. \tag{4.10}$$

The key point to obtain a bound of $\boldsymbol{r}_D^\varepsilon$ is the following lemma.

Lemma 4.3 *Let $\varepsilon > 0$. For $\boldsymbol{\varphi} \in \mathbf{H}^{1/2}(\partial\omega_{z,\varepsilon})$, $\boldsymbol{\Phi} \in \mathbf{H}^{1/2}(\partial\Omega)$, let $(\boldsymbol{v}_\varepsilon, q_\varepsilon) \in \mathbf{H}^1(\Omega_{z,\varepsilon}) \times \mathrm{L}_0^2(\Omega_{z,\varepsilon})$ be the solution of the problem*

$$\left\{\begin{array}{rcll} -\nu\Delta\boldsymbol{v}_\varepsilon + \nabla q_\varepsilon &=& \mathbf{0} & \text{in } \Omega_{z,\varepsilon} \\ \operatorname{div}\boldsymbol{v}_\varepsilon &=& 0 & \text{in } \Omega_{z,\varepsilon} \\ \boldsymbol{v}_\varepsilon &=& \boldsymbol{\Phi} & \text{on } \partial\Omega \\ \boldsymbol{v}_\varepsilon &=& \boldsymbol{\varphi} & \text{on } \partial\omega_{z,\varepsilon}. \end{array}\right. \tag{4.11}$$

There exists a constant $c > 0$ (independent of ε) such that:

$$\|\boldsymbol{v}_\varepsilon\|_{1,\Omega_{z,\varepsilon}} \leq c\left(\|\boldsymbol{\Phi}\|_{1/2,\partial\Omega} + \|\boldsymbol{\varphi}(\varepsilon X)\|_{1/2,\partial\omega}\right). \tag{4.12}$$

The proof of Lemma 4.3 is decomposed in the following three lemmas which are based in the ones presented in [77, Chapter 3]. We will use the notations introduced in section B.3.2.

Lemma 4.4 *Let $\varepsilon > 0$. For $\mathbf{\Phi} \in \mathbf{H}^{1/2}(\partial\Omega)$, let $(\boldsymbol{v}_\varepsilon, q_\varepsilon) \in \mathbf{H}^1(\Omega_{z,\varepsilon}) \times \mathrm{L}^2_0(\Omega_{z,\varepsilon})$ be the solution of the Stokes problem*

$$\left\{\begin{array}{rcll} -\nu\Delta\boldsymbol{v}_\varepsilon + \nabla q_\varepsilon &=& \mathbf{0} & \text{in } \Omega_{z,\varepsilon} \\ \operatorname{div}\boldsymbol{v}_\varepsilon &=& 0 & \text{in } \Omega_{z,\varepsilon} \\ \boldsymbol{v}_\varepsilon &=& \mathbf{\Phi} & \text{on } \partial\Omega \\ \boldsymbol{v}_\varepsilon &=& \mathbf{0} & \text{on } \partial\omega_{z,\varepsilon}. \end{array}\right. \tag{4.13}$$

Then there exists a constant $c > 0$ (independent of ε and $\mathbf{\Phi}$) and $\varepsilon_1 > 0$ such that for all $0 < \varepsilon < \varepsilon_1$

$$\|\boldsymbol{v}_\varepsilon\|_{1,\Omega_{z,\varepsilon}} \leq c\,\|\mathbf{\Phi}\|_{1/2,\partial\Omega}\,. \tag{4.14}$$

Proof. Let $\varepsilon_0 > 0$. Consider $\boldsymbol{v}_{\varepsilon_0}$ solution of (4.13) for $\varepsilon = \varepsilon_0$. It satisfies:

$$|\boldsymbol{v}_{\varepsilon_0}|_{1,\Omega_{\varepsilon_0}} = \int_{\Omega_{\varepsilon_0}} |\nabla\boldsymbol{v}_{\varepsilon_0}|^2 \mathrm{d}x \leq c(\varepsilon_0)\|\mathbf{\Phi}\|_{1/2,\partial\Omega}.$$

Now consider $\widetilde{\boldsymbol{v}_{\varepsilon_0}}$ the extension by $\mathbf{0}$ of $\boldsymbol{v}_{\varepsilon_0}$ to all Ω, and consider $\boldsymbol{v}$ the solution of the system

$$\left\{\begin{array}{rcll} -\nu\Delta\boldsymbol{v} + \nabla q &=& \mathbf{0} & \text{in } \Omega \\ \operatorname{div}\boldsymbol{v} &=& 0 & \text{in } \Omega \\ \boldsymbol{v} &=& \mathbf{\Phi} & \text{on } \partial\Omega, \end{array}\right.$$

i.e. when we consider $\varepsilon = 0$ in (4.13). Notice that, by minimization of energy, we have:

$$|\boldsymbol{v}|_{1,\Omega} \leq |\widetilde{\boldsymbol{v}_{\varepsilon_0}}|_{1,\Omega} = |\boldsymbol{v}_{\varepsilon_0}|_{1,\Omega_{\varepsilon_0}}.$$

Also, the well-posedness of the problem gives the existence of $c > 0$ ($c = c(\Omega)$) such that:

$$|\boldsymbol{v}|_{0,\Omega} \leq c\|\mathbf{\Phi}\|_{1/2,\partial\Omega}.$$

Now, notice that if $\varepsilon_1 < \varepsilon_0$ we have $\varepsilon_1\omega \subset \varepsilon_0\omega$ and then $\Omega_{\varepsilon_0} \subset \Omega_{\varepsilon_1}$, so, for all $\varepsilon \in (0, \varepsilon_1)$, we have:

$$|\boldsymbol{v}_\varepsilon|_{1,\Omega_\varepsilon} \leq |\widetilde{\boldsymbol{v}_{\varepsilon_0}}|_{1,\Omega_\varepsilon} = |\boldsymbol{v}_{\varepsilon_0}|_{1,\Omega_{\varepsilon_0}} \leq c(\varepsilon_0)\|\mathbf{\Phi}\|_{1/2,\partial\Omega}.$$

Noticing that $\widetilde{\boldsymbol{v}_\varepsilon} - \boldsymbol{v} \in \mathbf{H}^1_0(\Omega)$ and thanks to Poincaré inequality, we have:

$$\begin{array}{rcl} |\widetilde{\boldsymbol{v}_\varepsilon}|_{0,\Omega} = |\boldsymbol{v}_\varepsilon|_{0,\Omega_\varepsilon} &\leq& |\widetilde{\boldsymbol{v}_\varepsilon} - \boldsymbol{v}|_{0,\Omega} + |\boldsymbol{v}|_{0,\Omega} \leq c|\widetilde{\boldsymbol{v}_\varepsilon} - \boldsymbol{v}|_{1,\Omega} + c\|\mathbf{\Phi}\|_{1/2,\partial\Omega} \\ &\leq& c|\boldsymbol{v}_\varepsilon|_{1,\Omega_\varepsilon} + c|\boldsymbol{v}|_{1,\Omega} + c\|\mathbf{\Phi}\|_{1/2,\partial\Omega} \leq c(\varepsilon_0,\Omega)\|\mathbf{\Phi}\|_{1/2,\partial\Omega}. \end{array}$$

Also, denoting by $\widetilde{\boldsymbol{v}_{\varepsilon_0}}$ the extension by zero of $\boldsymbol{v}_{\varepsilon_0}$ to Ω_ε, we get, by minimization of energy that:

$$|\boldsymbol{v}_\varepsilon|_{1,\Omega_\varepsilon} \leq |\widetilde{\boldsymbol{v}_{\varepsilon_0}}|_{1,\Omega_\varepsilon} = |\boldsymbol{v}_{\varepsilon_0}|_{1,\Omega_{\varepsilon_0}} \leq c(\varepsilon_0)\|\mathbf{\Phi}\|_{1/2,\partial\Omega}.$$

Combining the last two inequalities we get the desired result. □

From the previous Lemma, we get the following one:

Lemma 4.5 *Let $\varepsilon > 0$. For $\boldsymbol{\varphi} \in \mathbf{H}^1(\Omega)$ such that $\operatorname{div} \boldsymbol{\varphi} = 0$ in Ω, let $(\boldsymbol{v}_\varepsilon, q_\varepsilon) \in \mathbf{H}^1(\Omega_{z,\varepsilon}) \times \mathrm{L}^2_0(\Omega_{z,\varepsilon})$ be the solution of the Stokes problem*

$$\left\{\begin{array}{rcll} -\nu\Delta \boldsymbol{v}_\varepsilon + \nabla q_\varepsilon &=& \mathbf{0} & \text{in } \Omega_{z,\varepsilon} \\ \operatorname{div} \boldsymbol{v}_\varepsilon &=& 0 & \text{in } \Omega_{z,\varepsilon} \\ \boldsymbol{v}_\varepsilon &=& \mathbf{0} & \text{on } \partial\Omega \\ \boldsymbol{v}_\varepsilon &=& \boldsymbol{\varphi} & \text{on } \partial\omega_{z,\varepsilon}. \end{array}\right. \tag{4.15}$$

If there exists $q \in \mathrm{L}^2_0(\Omega)$ such that $-\nu\Delta\boldsymbol{\varphi} + \nabla q = 0$ in Ω, then there exists a constant $c > 0$ (independent of ε and $\boldsymbol{\varphi}$) and $\varepsilon_1 > 0$ such that for all $0 < \varepsilon < \varepsilon_1$

$$\|\boldsymbol{v}_\varepsilon\|_{1,\Omega_{z,\varepsilon}} \leq c\,\|\boldsymbol{\varphi}\|_{1/2,\partial\Omega}\,. \tag{4.16}$$

Proof. We consider the pair $(\boldsymbol{w}_\varepsilon := \boldsymbol{v}_\varepsilon - \boldsymbol{\varphi},\ l_\varepsilon := q_\varepsilon - q)$. This satisfies:

$$\left\{\begin{array}{rcll} -\nu\Delta \boldsymbol{w}_\varepsilon + \nabla l_\varepsilon &=& \mathbf{0} & \text{in } \Omega_{z,\varepsilon} \\ \operatorname{div} \boldsymbol{w}_\varepsilon &=& 0 & \text{in } \Omega_{z,\varepsilon} \\ \boldsymbol{w}_\varepsilon &=& -\boldsymbol{\varphi} & \text{on } \partial\Omega \\ \boldsymbol{w}_\varepsilon &=& \mathbf{0} & \text{on } \partial\omega_{z,\varepsilon}. \end{array}\right.$$

By the previous lemma, we have for all $\varepsilon < \varepsilon_1$:

$$\|\boldsymbol{w}_\varepsilon\|_{1,\Omega_{z,\varepsilon}} \leq c\|\boldsymbol{\varphi}\|_{1/2,\partial\Omega}.$$

Noticing that $\boldsymbol{\varphi}$ is defined in the whole domain and is the solution of the Stokes system, we have:

$$\|\boldsymbol{\varphi}\|_{1,\Omega_{z,\varepsilon}} \leq \|\boldsymbol{\varphi}\|_{1,\Omega} \leq c\|\boldsymbol{\varphi}\|_{1/2,\partial\Omega}.$$

Therefore, we finally get:

$$\|\boldsymbol{v}_\varepsilon\|_{1,\Omega_{z,\varepsilon}} \leq \|\boldsymbol{w}_\varepsilon\|_{1,\Omega_{z,\varepsilon}} + \|\boldsymbol{\varphi}\|_{1,\Omega_{z,\varepsilon}} \leq c\|\boldsymbol{\varphi}\|_{1/2,\partial\Omega}.$$

□

Lemma 4.6 *Let $\varepsilon > 0$. For $\boldsymbol{\lambda} \in \mathbb{R}^2$, let $(\boldsymbol{v}_\varepsilon, q_\varepsilon) \in \mathbf{H}^1(\Omega_{z,\varepsilon}) \times \mathrm{L}^2_0(\Omega_{z,\varepsilon})$ be the solution of the Stokes problem*

$$\left\{\begin{array}{rcll} -\nu\Delta \boldsymbol{v}_\varepsilon + \nabla q_\varepsilon &=& \mathbf{0} & \text{in } \Omega_{z,\varepsilon} \\ \operatorname{div} \boldsymbol{v}_\varepsilon &=& 0 & \text{in } \Omega_{z,\varepsilon} \\ \boldsymbol{v}_\varepsilon &=& \mathbf{0} & \text{on } \partial\Omega \\ \boldsymbol{v}_\varepsilon &=& \boldsymbol{\lambda} & \text{on } \partial\omega_{z,\varepsilon}. \end{array}\right. \tag{4.17}$$

There exists a constant $c > 0$ (independent of ε) such that:

$$\|\boldsymbol{v}_\varepsilon\|_{1,\Omega_{z,\varepsilon}} \leq c\frac{|\boldsymbol{\lambda}|}{\sqrt{-\log\varepsilon}}. \tag{4.18}$$

PROOF. Consider the following sets:

$$\Gamma_r := \left\{x \in \mathbb{R}^2 : \ \|x\| = r\right\} \text{ and } C(r_1, r_2) := \left\{x \in \mathbb{R}^2 : r_1 < \|x\| < r_2\right\}.$$

Also, consider the following quantity:

$$r^* := \sup\left\{r > 0 : \ B(0,r) \subset \Omega\right\}.$$

Let us now consider the pair $(\boldsymbol{w}_\varepsilon, l_\varepsilon)$, the unique solution of the system:

$$\left\{\begin{array}{rcll} -\nu\Delta\boldsymbol{w}_\varepsilon + \nabla l_\varepsilon &=& \mathbf{0} & \text{in } C(1, r^*/\varepsilon) \\ \operatorname{div}\boldsymbol{w}_\varepsilon &=& 0 & \text{in } C(1, r^*/\varepsilon) \\ \boldsymbol{w}_\varepsilon &=& \mathbf{0} & \text{on } \Gamma_{r^*/\varepsilon} \\ \boldsymbol{w}_\varepsilon &=& \boldsymbol{\lambda} & \text{on } \Gamma_1. \end{array}\right.$$

Also, consider the functions $\hat{\boldsymbol{v}}_\varepsilon(y) = \boldsymbol{v}_\varepsilon(x)$ and $\hat{q}_\varepsilon(y) = \frac{1}{\varepsilon}q_\varepsilon(x)$ with $y = \frac{x}{\varepsilon}$. The pair $(\hat{\boldsymbol{v}}_\varepsilon, \hat{q}_\varepsilon)$ satisfies:

$$\left\{\begin{array}{rcll} -\nu\Delta\hat{\boldsymbol{v}}_\varepsilon + \nabla\hat{q}_\varepsilon &=& \mathbf{0} & \text{in } \dfrac{\Omega}{\varepsilon} \\ \operatorname{div}\hat{\boldsymbol{v}}_\varepsilon &=& 0 & \text{in } \dfrac{\Omega}{\varepsilon} \\ \hat{\boldsymbol{v}}_\varepsilon &=& \mathbf{0} & \text{on } \partial\left(\dfrac{\Omega}{\varepsilon}\right) \\ \hat{\boldsymbol{v}}_\varepsilon &=& \boldsymbol{\lambda} & \text{on } \partial\omega. \end{array}\right.$$

Notice that we have: $\overline{\omega} \subset B(0,1) \subset B\left(0, \frac{r^*}{\varepsilon}\right) \subset \frac{\Omega}{\varepsilon}$. Now consider $\widetilde{\boldsymbol{w}_\varepsilon}$ the extension of $\boldsymbol{w}_\varepsilon$ to $\dfrac{\Omega}{\varepsilon} \setminus \overline{\omega}$, by zero in the outer part (respect to the original domain) of the extended domain and by $\boldsymbol{\lambda}$ in the inner part of the extended domain. Therefore, by the principle of minimization of energy we have:

$$|\boldsymbol{v}_\varepsilon|_{1,\Omega_\varepsilon} = |\hat{\boldsymbol{v}}_\varepsilon|_{1,\frac{\Omega}{\varepsilon}\setminus\overline{\omega}} \leq |\widetilde{\boldsymbol{w}_\varepsilon}|_{1,\frac{\Omega}{\varepsilon}\setminus\overline{\omega}} = |\boldsymbol{w}_\varepsilon|_{1,C(1,\frac{r^*}{\varepsilon})}. \tag{4.19}$$

Let $\boldsymbol{\psi} := \boldsymbol{\lambda} + 4\pi\nu E\frac{\boldsymbol{\lambda}}{\log(r^*/\varepsilon)}$ and $q := 4\pi\nu\boldsymbol{P}\cdot\frac{\boldsymbol{\lambda}}{\log(r^*/\varepsilon)}$ where $(E, \boldsymbol{P})$ is the fundamental solution of Stokes equations in $\mathbb{R}^2$ given by (4.7). We have:

$$\left\{\begin{array}{rcll} -\nu\Delta\boldsymbol{\psi} + \nabla q &=& \mathbf{0} & \text{in } C(1, r^*/\varepsilon) \\ \operatorname{div}\boldsymbol{\psi} &=& 0 & \text{in } C(1, r^*/\varepsilon) \\ \boldsymbol{\psi} &=& \frac{\mathrm{e}_r{}^t\mathrm{e}_r\boldsymbol{\lambda}}{\log(r^*/\varepsilon)} & \text{on } \Gamma_{r^*/\varepsilon} \\ \boldsymbol{\psi} &=& \boldsymbol{\lambda} + \frac{\mathrm{e}_r{}^t\mathrm{e}_r\boldsymbol{\lambda}}{\log(r^*/\varepsilon)} & \text{on } \Gamma_1, \end{array}\right.$$

and a computation provides:

$$|\boldsymbol{\psi}|_{1,C(1,r^*/\varepsilon)} \leq c\frac{|\boldsymbol{\lambda}|}{\sqrt{-\log\varepsilon}}.$$

Now, notice that the pair $(\boldsymbol{w}_\varepsilon - \boldsymbol{\psi}, l_\varepsilon - q)$ is solution of the Stokes equations with boundary condition $-\frac{\mathrm{e}_r{}^t\mathrm{e}_r\boldsymbol{\lambda}}{\log(r^*/\varepsilon)}$ in both boundaries of the domain. Therefore, using the previous lemmas we get that:

$$|\boldsymbol{w}_\varepsilon - \boldsymbol{\psi}|_{1,C(1,r^*/\varepsilon)} = |\hat{\boldsymbol{w}}_\varepsilon - \hat{\boldsymbol{\psi}}|_{1,C(\varepsilon,r^*)} \leq \frac{c}{-\log\varepsilon}\|\mathrm{e}_r{}^t\mathrm{e}_r\boldsymbol{\lambda}\|_{1/2,\Gamma_r^*} \leq \frac{c|\boldsymbol{\lambda}|}{-\log\varepsilon}.$$

So, we get by (4.19):

$$\begin{aligned} |\boldsymbol{v}_\varepsilon|_{1,\Omega_\varepsilon} &\leq |\boldsymbol{w}_\varepsilon|_{1,C(1,\frac{r^*}{\varepsilon})} \leq |\boldsymbol{w}_\varepsilon - \boldsymbol{\psi}|_{1,C(1,\frac{r^*}{\varepsilon})} + |\boldsymbol{\psi}|_{1,C(1,\frac{r^*}{\varepsilon})} \\ &\leq c\frac{|\boldsymbol{\lambda}|}{-\log\varepsilon} + c\frac{|\boldsymbol{\lambda}|}{\sqrt{-\log\varepsilon}} \leq c\frac{|\boldsymbol{\lambda}|}{\sqrt{-\log\varepsilon}}. \end{aligned}$$

Finally, consider $\widetilde{\boldsymbol{v}_\varepsilon}$ the extension of $\boldsymbol{v}_\varepsilon$ to Ω by $\boldsymbol{\lambda}$ (notice that this extension is in $\mathbf{H}_0^1(\Omega)$, therefore we can use Poincaré inequality). We have:

$$\begin{aligned} \|\boldsymbol{v}_\varepsilon\|_{1,\Omega_\varepsilon} &\leq \|\boldsymbol{v}_\varepsilon\|_{0,\Omega_\varepsilon} + |\boldsymbol{v}_\varepsilon|_{1,\Omega_\varepsilon} \leq c\|\widetilde{\boldsymbol{v}_\varepsilon}\|_{0,\Omega} + |\boldsymbol{v}_\varepsilon|_{1,\Omega_\varepsilon} \\ &\leq c|\widetilde{\boldsymbol{v}_\varepsilon}|_{1,\Omega} + |\boldsymbol{v}_\varepsilon|_{1,\Omega_\varepsilon} = (c+1)|\boldsymbol{v}_\varepsilon|_{1,\Omega_\varepsilon} \leq c\frac{|\boldsymbol{\lambda}|}{\sqrt{-\log\varepsilon}}. \end{aligned}$$

□

Proof of Lemma 4.3. If $\boldsymbol{\varphi}$ is constant on $\partial\omega_\varepsilon$ and $\boldsymbol{\Phi} = \mathbf{0}$, the previous lemma gives the desired result. If $\boldsymbol{\Phi} \neq \mathbf{0}$ another previous lemma gives the desired estimate. So, let's focus on the case where $\boldsymbol{\varphi}$ is not constant. Let $\boldsymbol{V}$ the bounded solution of

$$\begin{cases} -\nu\Delta\boldsymbol{V} + \nabla P_V &= \mathbf{0} & \text{in } \mathbb{R}^2 \setminus \overline{\omega} \\ \operatorname{div}\boldsymbol{V} &= 0 & \text{in } \mathbb{R}^2 \setminus \overline{\omega} \\ \boldsymbol{V} &= \boldsymbol{\varphi}(\varepsilon x) & \text{on } \partial\omega. \end{cases}$$

We have by (B.9) $\boldsymbol{V} = \boldsymbol{\lambda} + \boldsymbol{W}$ with $\boldsymbol{\lambda} \in \mathbb{R}^2$ and $\boldsymbol{W} = O(1/r)$. Notice that this implies $\boldsymbol{W}(\frac{x}{\varepsilon}) = O(\varepsilon)$. We define $\boldsymbol{z}_\varepsilon := \boldsymbol{v}_\varepsilon - \boldsymbol{W}\left(\frac{x}{\varepsilon}\right)$ and $p_{\boldsymbol{z}_\varepsilon} := q_\varepsilon - \frac{1}{\varepsilon}P_W\left(\frac{x}{\varepsilon}\right)$, where P_W is defined by (B.10) with $y = x/\varepsilon$. Notice that $\boldsymbol{z}_\varepsilon$ satisfies:

$$\begin{cases} -\nu\Delta\boldsymbol{z}_\varepsilon + \nabla p_{\boldsymbol{z}_\varepsilon} &= \mathbf{0} & \text{in } \Omega_\varepsilon \\ \operatorname{div}\boldsymbol{z}_\varepsilon &= 0 & \text{in } \Omega_\varepsilon \\ \boldsymbol{z}_\varepsilon &= \boldsymbol{\Phi} - \boldsymbol{W}\left(\frac{x}{\varepsilon}\right) & \text{on } \partial\Omega \\ \boldsymbol{z}_\varepsilon &= \boldsymbol{\lambda} & \text{on } \partial\omega_\varepsilon. \end{cases}$$

Using the previous lemmas we can bound the terms of this function, and $\boldsymbol{\lambda}$ can be bounded thanks to (B.11). Finally we have that $\boldsymbol{W}\left(\frac{x}{\varepsilon}\right)$ satisfies the desired estimate by Lemma B.5 and we conclude by triangle inequality. □

Using the lemmas we are now ready to prove the main proposition into the Dirichlet case

Proof of Proposition 4.2, Dirichlet case. From lemma 4.3, we get:

$$\|\boldsymbol{r}_D^\varepsilon\|_{1,\Omega_\varepsilon} \leq c\left\|\boldsymbol{u}_D^0(\varepsilon X) + h_\varepsilon(\boldsymbol{C}_D(\varepsilon X) - \boldsymbol{U}_D(\varepsilon X))\right\|_{1/2,\partial\omega}.$$

Notice that:

$$\begin{aligned} &\boldsymbol{u}_D^0(\varepsilon X) + h_\varepsilon(\boldsymbol{C}_D(\varepsilon X) - \boldsymbol{U}_D(\varepsilon X)) \\ &\quad= \boldsymbol{u}_D^0(\varepsilon x) + \frac{1}{-\log\varepsilon}[(\log(\varepsilon\|X\|) - \mathrm{e}_r{}^t\mathrm{e}_r)\cdot\boldsymbol{u}_D^0(0) - \boldsymbol{U}_D(\varepsilon X)] \\ &\quad= \boldsymbol{u}_D^0(\varepsilon X) - \boldsymbol{u}_D^0(0) + \frac{1}{-\log\varepsilon}[(\log(\|X\|) - \mathrm{e}_r{}^t\mathrm{e}_r)\cdot\boldsymbol{u}_D^0(0) - \boldsymbol{U}_D(\varepsilon X)] \\ &\quad= \varepsilon\nabla\boldsymbol{u}_D^0(\zeta_x) + \frac{1}{-\log\varepsilon}[(\log(\|X\|) - \mathrm{e}_r{}^t\mathrm{e}_r)\cdot\boldsymbol{u}_D^0(0) - \boldsymbol{U}_D(\varepsilon X)]. \end{aligned}$$

We have used a Taylor expansion of $\boldsymbol{u}_D^0$ in the last equality and ζ_x is some point in the line which joins 0 and εX. Now, recalling that $\nabla \boldsymbol{u}_D^0$ is uniformly bounded and using the boundness of $\boldsymbol{U}_D$ and the other terms by their definition, we get that:

$$\|\boldsymbol{u}_D^0(\varepsilon X) + h_\varepsilon(\boldsymbol{C}_D(\varepsilon X) - \boldsymbol{U}_D(\varepsilon X))\|_{1/2,\partial\omega} \leq c\varepsilon + \frac{c}{-\log\varepsilon} \leq \frac{c}{-\log\varepsilon}. \tag{4.20}$$

Therefore:

$$\|\boldsymbol{r}_D^\varepsilon\|_{1,\Omega_\varepsilon} = O\left(\frac{1}{-\log\varepsilon}\right),$$

which concludes the proof of Proposition 4.2 with $\natural = D$. □

The Neumann case

In this case, the reminder $\boldsymbol{r}_M^\varepsilon$ satisfies:

$$\left\{\begin{array}{rcll} -\nu\Delta \boldsymbol{r}_M^\varepsilon + \nabla p_{r_M^\varepsilon} &=& \boldsymbol{0} & \text{in } \Omega_\varepsilon \\ \operatorname{div} \boldsymbol{r}_M^\varepsilon &=& 0 & \text{in } \Omega_\varepsilon \\ \boldsymbol{r}_M^\varepsilon &=& \boldsymbol{0} & \text{on } \partial\Omega \setminus \overline{O} \\ \sigma(\boldsymbol{r}_M^\varepsilon, p_{r_M^\varepsilon})\mathbf{n} &=& \frac{1}{\log\varepsilon}[\sigma(\boldsymbol{C}_M - \boldsymbol{U}_M, \Pi_M - P_M)\mathbf{n}] & \text{on } O \\ \boldsymbol{r}_M^\varepsilon &=& -\boldsymbol{u}_M^0 - h_\varepsilon(\boldsymbol{C}_M - \boldsymbol{U}_M) & \text{on } \partial\omega_\varepsilon, \end{array}\right. \tag{4.21}$$

where the pressure associated to $\boldsymbol{C}_M$ is defined explicitly by the expression

$$\Pi_M(x) := -4\pi\nu \boldsymbol{P}(x) \cdot \boldsymbol{u}_M^0(0). \tag{4.22}$$

In order to be able to bound this rest, we use the following lemma.

Lemma 4.7 *Let $\varepsilon > 0$. For $\boldsymbol{\psi} \in \mathbf{H}^{-1/2}(\mathcal{O})$, $\boldsymbol{\Phi} \in \mathbf{H}^{1/2}(\partial\Omega\backslash\overline{\mathcal{O}})$ and $\boldsymbol{\varphi} \in \mathbf{H}^{1/2}(\partial\omega_{z,\varepsilon})$, let $(\boldsymbol{v}_\varepsilon, q_\varepsilon) \in \mathbf{H}^1(\Omega_{z,\varepsilon}) \times \mathrm{L}^2(\Omega_{z,\varepsilon})$ be the solution of the Stokes problem*

$$\left\{\begin{array}{rcll} -\nu\Delta \boldsymbol{v}_\varepsilon + \nabla q_\varepsilon &=& \boldsymbol{0} & \text{in } \Omega_{z,\varepsilon} \\ \operatorname{div} \boldsymbol{v}_\varepsilon &=& 0 & \text{in } \Omega_{z,\varepsilon} \\ \sigma(\boldsymbol{v}_\varepsilon, q_\varepsilon)\mathbf{n} &=& \boldsymbol{\psi} & \text{on } O \\ \boldsymbol{v}_\varepsilon &=& \boldsymbol{\Phi} & \text{on } \partial\Omega\backslash\overline{O} \\ \boldsymbol{v}_\varepsilon &=& \boldsymbol{\varphi} & \text{on } \partial\omega_{z,\varepsilon}. \end{array}\right. \tag{4.23}$$

There exists a constant $c > 0$ (independent of ε) such that:

$$\|\boldsymbol{v}_\varepsilon\|_{1,\Omega_{z,\varepsilon}} \leq c\left(\|\boldsymbol{\psi}\|_{-1/2,O} + \|\boldsymbol{\Phi}\|_{1/2,\partial\Omega\backslash\overline{O}} + \|\boldsymbol{\varphi}(\varepsilon X)\|_{1/2,\partial\omega}\right). \tag{4.24}$$

As before, in order to prove this 'key' lemma, we need a previous step:

Lemma 4.8 *Let $\varepsilon > 0$. For $\boldsymbol{\psi} \in \mathbf{H}^{-1/2}(\mathcal{O})$, $\boldsymbol{\Phi} \in \mathbf{H}^{1/2}(\partial\Omega\backslash\overline{\mathcal{O}})$ and $\boldsymbol{\lambda} \in \mathbb{R}^2$, let $(\boldsymbol{v}_\varepsilon, q_\varepsilon) \in \mathbf{H}^1(\Omega_{z,\varepsilon}) \times \mathrm{L}^2(\Omega_{z,\varepsilon})$ be the solution of the Stokes problem*

$$\left\{\begin{array}{rcll} -\nu\Delta \boldsymbol{v}_\varepsilon + \nabla q_\varepsilon &=& \boldsymbol{0} & \text{in } \Omega_{z,\varepsilon} \\ \operatorname{div} \boldsymbol{v}_\varepsilon &=& 0 & \text{in } \Omega_{z,\varepsilon} \\ \sigma(\boldsymbol{v}_\varepsilon, q_\varepsilon)\mathbf{n} &=& \boldsymbol{\psi} & \text{on } O \\ \boldsymbol{v}_\varepsilon &=& \boldsymbol{\Phi} & \text{on } \partial\Omega\backslash\overline{O} \\ \boldsymbol{v}_\varepsilon &=& \boldsymbol{\lambda} & \text{on } \partial\omega_{z,\varepsilon}. \end{array}\right. \tag{4.25}$$

Then there exists a constant $c > 0$ (independent of ε) and $\varepsilon_1 > 0$ such that for all $0 < \varepsilon < \varepsilon_1$

$$\|\boldsymbol{v}_\varepsilon\|_{1,\Omega_{z,\varepsilon}} \leq c\left(\|\boldsymbol{\psi}\|_{-1/2,O} + \|\boldsymbol{\Phi}\|_{1/2,\partial\Omega\setminus\overline{O}} + |\boldsymbol{\lambda}|\right).$$

Proof. Let $\varepsilon > 0$ and $(\boldsymbol{v}_\varepsilon, q_\varepsilon) \in \mathbf{H}^1(\Omega_{z,\varepsilon}) \times \mathrm{L}^2(\Omega_{z,\varepsilon})$ be the solution of Problem (4.25). Let $(\boldsymbol{V}_\varepsilon, Q_\varepsilon) \in \mathbf{H}^1(\Omega_{z,\varepsilon}) \times \mathrm{L}^2(\Omega_{z,\varepsilon})$ be the solution of

$$\left\{\begin{array}{rcll} -\nu\Delta\boldsymbol{V}_\varepsilon + \nabla Q_\varepsilon &=& \mathbf{0} & \text{in } \Omega_{z,\varepsilon} \\ \operatorname{div}\boldsymbol{V}_\varepsilon &=& 0 & \text{in } \Omega_{z,\varepsilon} \\ \sigma(\boldsymbol{V}_\varepsilon, Q_\varepsilon)\mathbf{n} &=& \mathbf{0} & \text{on } O \\ \boldsymbol{V}_\varepsilon &=& \boldsymbol{\Phi} & \text{on } \partial\Omega\setminus\overline{O} \\ \boldsymbol{V}_\varepsilon &=& \boldsymbol{\lambda} & \text{on } \partial\omega_{z,\varepsilon}. \end{array}\right. \tag{4.26}$$

Let $\widetilde{\boldsymbol{v}_\varepsilon}$ and $\widetilde{\boldsymbol{V}_\varepsilon}$ denote the respective extensions of $\boldsymbol{v}_\varepsilon$ and $\boldsymbol{V}_\varepsilon$ to Ω by $\boldsymbol{\lambda}$. Then, we have for all $\boldsymbol{\Psi} \in \left\{\boldsymbol{\Psi} \in \mathbf{H}^1(\Omega_{z,\varepsilon}),\ \operatorname{div}\boldsymbol{\Psi} = 0,\ \boldsymbol{\Psi}_{|\partial\omega_{z,\varepsilon}} = \mathbf{0},\ \boldsymbol{\Psi}_{|\partial\Omega\setminus\overline{O}} = \mathbf{0}\right\}$

$$\frac{1}{2}\nu\int_{\Omega_{z,\varepsilon}} \mathcal{D}(\boldsymbol{v}_\varepsilon - \boldsymbol{V}_\varepsilon) : \mathcal{D}(\boldsymbol{\Psi}) = \langle \boldsymbol{\psi}\,,\,\boldsymbol{\Psi}\rangle_O$$

and then taking $\boldsymbol{\Psi} = \boldsymbol{v}_\varepsilon - \boldsymbol{V}_\varepsilon$

$$\frac{1}{2}\nu\left\|\mathcal{D}(\widetilde{\boldsymbol{v}_\varepsilon} - \widetilde{\boldsymbol{V}_\varepsilon})\right\|^2_{0,\Omega} = \langle \boldsymbol{\psi}\,,\,\boldsymbol{v}_\varepsilon - \boldsymbol{V}_\varepsilon\rangle_O.$$

Thus, there exists a constant (independent of ε) such that

$$\left\|\mathcal{D}(\widetilde{\boldsymbol{v}_\varepsilon} - \widetilde{\boldsymbol{V}_\varepsilon})\right\|^2_{0,\Omega} \leq c\,\|\boldsymbol{\psi}\|_{-1/2,O}\left\|\widetilde{\boldsymbol{v}_\varepsilon} - \widetilde{\boldsymbol{V}_\varepsilon}\right\|_{1,\Omega}.$$

Moreover, since $\boldsymbol{v}_\varepsilon - \boldsymbol{V}_\varepsilon = \mathbf{0}$ on $\partial\Omega\setminus\overline{O}$, Korn's inequality (see for example [72, eq. (2.14) page 19]) leads

$$\left\|\widetilde{\boldsymbol{v}_\varepsilon} - \widetilde{\boldsymbol{V}_\varepsilon}\right\|_{1,\Omega} \leq c\left\|\mathcal{D}(\widetilde{\boldsymbol{v}_\varepsilon} - \widetilde{\boldsymbol{V}_\varepsilon})\right\|_{0,\Omega}$$

(with a constant c independent of ε). Hence,

$$\begin{aligned}\|\boldsymbol{v}_\varepsilon - \boldsymbol{V}_\varepsilon\|^2_{1,\Omega_{z,\varepsilon}} = \left\|\widetilde{\boldsymbol{v}_\varepsilon} - \widetilde{\boldsymbol{V}_\varepsilon}\right\|^2_{1,\Omega} &\leq c\,\|\boldsymbol{\psi}\|_{-1/2,O}\left\|\mathcal{D}(\widetilde{\boldsymbol{v}_\varepsilon} - \widetilde{\boldsymbol{V}_\varepsilon})\right\|_{0,\Omega} \\ &\leq c\,\|\boldsymbol{\psi}\|_{-1/2,O}\left\|\widetilde{\boldsymbol{v}_\varepsilon} - \widetilde{\boldsymbol{V}_\varepsilon}\right\|_{1,\Omega} \leq c\,\|\boldsymbol{\psi}\|_{-1/2,O}\,\|\boldsymbol{v}_\varepsilon - \boldsymbol{V}_\varepsilon\|_{1,\Omega_{z,\varepsilon}}.\end{aligned}$$

Thus,

$$\|\boldsymbol{v}_\varepsilon - \boldsymbol{V}_\varepsilon\|_{1,\Omega_{z,\varepsilon}} \leq c\,\|\boldsymbol{\psi}\|_{-1/2,O}.$$

Now, let us prove that $\|\boldsymbol{V}_\varepsilon\|_{1,\Omega_{z,\varepsilon}} \leq c\left(\|\boldsymbol{\Phi}\|_{1/2,\partial\Omega\setminus\overline{O}} + |\boldsymbol{\lambda}|\right)$. For a fixed $\varepsilon_0 > 0$, Problem (4.26) is well-posed and admits a unique solution $(\boldsymbol{V}_{\varepsilon_0}, Q_{\varepsilon_0}) \in \mathbf{H}^1(\Omega_{z,\varepsilon_0}) \times \mathrm{L}^2(\Omega_{z,\varepsilon_0})$ and there exists a constant $c > 0$ such that

$$\|\boldsymbol{V}_{\varepsilon_0}\|_{1,\Omega_{z,\varepsilon_0}} \leq c\left(\|\boldsymbol{\Phi}\|_{1/2,\partial\Omega\setminus\overline{O}} + \|\boldsymbol{\lambda}\|_{1/2,\partial\omega_{z,\varepsilon_0}}\right).$$

Notice that, by (B.2) we get that:

$$\|\boldsymbol{\lambda}\|_{1/2,\partial\omega_{z,\varepsilon_0}} \sim \frac{1}{(\varepsilon_0(-\log\varepsilon_0))^{1/2}} \|\boldsymbol{\lambda}\|_{\mathrm{L}^2(\partial\omega_{z,\varepsilon_0})} + [\boldsymbol{\lambda}]_{p,\partial\omega_{z,\varepsilon_0}}.$$

The later term is zero, because $\boldsymbol{\lambda}$ is constant, so we get, by a change of variables that:

$$\begin{aligned}\|\boldsymbol{\lambda}\|_{1/2,\partial\omega_{z,\varepsilon_0}} \sim \frac{1}{(\varepsilon_0(-\log\varepsilon_0))^{1/2}} \|\boldsymbol{\lambda}\|_{\mathrm{L}^2(\partial\omega_{z,\varepsilon_0})} &= \frac{1}{(-\log\varepsilon_0)^{1/2}} \|\boldsymbol{\lambda}\|_{\mathrm{L}^2(\partial\omega)} \\ &= c(\varepsilon_0,\partial\omega)|\boldsymbol{\lambda}|.\end{aligned}$$

Let $0<\varepsilon_1<\varepsilon_0$ such that $\Omega_{z,\varepsilon_0}\subset\Omega_{z,\varepsilon}$ for all $0<\varepsilon<\varepsilon_1$. Let $\widetilde{\boldsymbol{V}_{\varepsilon_0}}$ the extension of $\boldsymbol{V}_{\varepsilon_0}$ to Ω by $\boldsymbol{\lambda}$. The solution $\boldsymbol{V}_\varepsilon$ of (4.26) can be considered as the solution of the following minimization problem: $\min\limits_{\boldsymbol{V}\in\mathcal{U}}\left\{\nu\,|\boldsymbol{V}|_{1,\Omega_{z,\varepsilon}}\right\}$, where

$$\mathcal{U} := \left\{\boldsymbol{V}\in\mathbf{H}^1(\Omega_{z,\varepsilon}),\ \operatorname{div}\boldsymbol{V}=0 \text{ in } \Omega_{z,\varepsilon},\ \boldsymbol{V}=\boldsymbol{\lambda} \text{ on } \partial\omega_{z,\varepsilon},\ \boldsymbol{V}=\boldsymbol{\Phi} \text{ on } \partial\Omega\backslash\overline{O}\right\}.$$

Hence, for all $0<\varepsilon<\varepsilon_1$, we have

$$|\boldsymbol{V}_\varepsilon|_{1,\Omega_{z,\varepsilon}} \le c\left|\widetilde{\boldsymbol{V}_{\varepsilon_0}}\right|_{1,\Omega_{z,\varepsilon}} = c\,|\boldsymbol{V}_{\varepsilon_0}|_{1,\Omega_{z,\varepsilon_0}} \le c\,\|\boldsymbol{V}_{\varepsilon_0}\|_{1,\Omega_{z,\varepsilon_0}} \le c\left(\|\boldsymbol{\Phi}\|_{1/2,\partial\Omega\backslash\overline{O}} + |\boldsymbol{\lambda}|\right).$$

Notice that $\|\boldsymbol{V}_0\|_{1,\Omega} \le c\,\|\boldsymbol{\Phi}\|_{1/2,\partial\Omega\backslash\overline{O}}$. Hence, using Poincaré inequality,

$$\begin{aligned}\|\boldsymbol{V}_\varepsilon\|_{0,\Omega_{z,\varepsilon}} = \left\|\widetilde{\boldsymbol{V}_\varepsilon}\right\|_{0,\Omega} &\le \left\|\widetilde{\boldsymbol{V}_\varepsilon}-V_0\right\|_{0,\Omega} + \|\boldsymbol{V}_0\|_{0,\Omega} \le c\left|\widetilde{\boldsymbol{V}_\varepsilon}-V_0\right|_{1,\Omega} + \|\boldsymbol{V}_0\|_{0,\Omega} \\ &\le c\left|\widetilde{\boldsymbol{V}_\varepsilon}\right|_{1,\Omega} + c\,\|\boldsymbol{V}_0\|_{1,\Omega} \le c\,|\boldsymbol{V}_\varepsilon|_{1,\Omega_{z,\varepsilon}} + c\,\|\boldsymbol{V}_0\|_{1,\Omega} \le c\left(\|\boldsymbol{\Phi}\|_{1/2,\partial\Omega\backslash\overline{O}} + |\boldsymbol{\lambda}|\right).\end{aligned}$$

Hence, we have the announced result. □

Proof of Lemma 4.7. The proof is similar to the one presented in the previous section for the Dirichlet system. If $\boldsymbol{\varphi}$ is constant on $\partial\omega_\varepsilon$, the previous lemma gives the desired result. So, let's focus on the case where $\boldsymbol{\varphi}$ is not constant. Let $\boldsymbol{V}$ the bounded solution of

$$\left\{\begin{array}{rcll} -\nu\Delta\boldsymbol{V}+\nabla P_V &=& \mathbf{0} & \text{in } \mathbb{R}^2\setminus\overline{\omega} \\ \operatorname{div}\boldsymbol{V} &=& 0 & \text{in } \mathbb{R}^2\setminus\overline{\omega} \\ \boldsymbol{V} &=& \boldsymbol{\varphi}(\varepsilon x) & \text{on } \partial\omega. \end{array}\right.$$

We have by (B.9) $\boldsymbol{V}=\boldsymbol{\lambda}+\boldsymbol{W}$ with $\boldsymbol{\lambda}\in\mathbb{R}^2$ and $\boldsymbol{W}=O(1/r)$, notice that this implies $\boldsymbol{W}(\frac{x}{\varepsilon})=O(\varepsilon)$. We define $\boldsymbol{z}_\varepsilon := \boldsymbol{v}_\varepsilon - \boldsymbol{W}\left(\frac{x}{\varepsilon}\right)$ and $p_{\boldsymbol{z}_\varepsilon} := q_\varepsilon - \frac{1}{\varepsilon}P_W\left(\frac{x}{\varepsilon}\right)$, where P_W is defined by (B.10) with $y=x/\varepsilon$. Notice that the couple $(\boldsymbol{z}_\varepsilon, p_{\boldsymbol{z}_\varepsilon})$ satisfies:

$$\left\{\begin{array}{rcll} -\nu\Delta\boldsymbol{z}_\varepsilon+\nabla p_{\boldsymbol{z}_\varepsilon} &=& \mathbf{0} & \text{in } \Omega_\varepsilon \\ \operatorname{div}\boldsymbol{z}_\varepsilon &=& 0 & \text{in } \Omega_\varepsilon \\ \sigma(\boldsymbol{z}_\varepsilon,p_{\boldsymbol{z}_\varepsilon})\mathbf{n} &=& \boldsymbol{\psi}-\frac{1}{\varepsilon}\sigma\left(\boldsymbol{W}\left(\frac{x}{\varepsilon}\right),P_W\left(\frac{x}{\varepsilon}\right)\right)\mathbf{n} & \text{on } O \\ \boldsymbol{z}_\varepsilon &=& \boldsymbol{\Phi}-\boldsymbol{W}\left(\frac{x}{\varepsilon}\right) & \text{on } \partial\Omega\setminus\overline{O} \\ \boldsymbol{z}_\varepsilon &=& \boldsymbol{\lambda} & \text{on } \partial\omega_\varepsilon. \end{array}\right.$$

The previous lemma gives the existence of $c > 0$ independent of ε such that:

$$\begin{aligned}\|\boldsymbol{z}_\varepsilon\|_{1,\Omega_\varepsilon} &\leq c\Big(\left\|\boldsymbol{\psi} - \tfrac{1}{\varepsilon}\sigma\left(\boldsymbol{W}\left(\tfrac{x}{\varepsilon}\right), P_W\left(\tfrac{x}{\varepsilon}\right)\right)\mathbf{n}\right\|_{-1/2,O} \\ &\qquad + \left\|\boldsymbol{\Phi} - \boldsymbol{W}\left(\tfrac{x}{\varepsilon}\right)\right\|_{1/2,\partial\Omega\setminus\overline{O}} + |\boldsymbol{\lambda}|\Big) \\ &\leq c\Big(\|\boldsymbol{\psi}\|_{-1/2,O} + \tfrac{1}{\varepsilon}\left\|\sigma\left(\boldsymbol{W}\left(\tfrac{x}{\varepsilon}\right), P_W\left(\tfrac{x}{\varepsilon}\right)\right)\mathbf{n}\right\|_{-1/2,O} + \|\boldsymbol{\Phi}\|_{1/2,\partial\Omega\setminus\overline{O}} \\ &\qquad + O(\varepsilon) + \|\boldsymbol{\varphi}(\varepsilon x)\|_{1/2,\partial\omega}\Big).\end{aligned}$$

Notice that we have, using the same argument as in (4.28):

$$\left\|\sigma\left(\boldsymbol{W}\left(\frac{x}{\varepsilon}\right), P_W\left(\frac{x}{\varepsilon}\right)\right)\mathbf{n}\right\|_{-1/2,O} \leq c\left\|(\nabla\boldsymbol{W})\left(\frac{x}{\varepsilon}\right)\right\|_{0,\Omega_R^0}.$$

But:

$$\left\|(\nabla\boldsymbol{W})\left(\frac{x}{\varepsilon}\right)\right\|_{0,\Omega_R^0} = \varepsilon\left\|\left(\nabla\boldsymbol{W}\left(\frac{x}{\varepsilon}\right)\right)\right\|_{0,\Omega_R^0} = \varepsilon^2\|\nabla\boldsymbol{W}\|_{0,\Omega_R^0/\varepsilon} \leq \varepsilon^4\|\boldsymbol{\varphi}(\varepsilon x)\|_{1/2,\partial\omega},$$

where the last inequality comes from Lemma B.5. Notice that $\boldsymbol{\lambda}$ can be bounded thanks to (B.11), so we have:

$$\begin{aligned}\|\boldsymbol{z}_\varepsilon\|_{1,\Omega_\varepsilon} \leq c\Big(&\|\boldsymbol{\psi}\|_{-1/2,O} + \|\boldsymbol{\Phi}\|_{1/2,\partial\Omega\setminus\overline{O}} + O(\varepsilon) + \varepsilon^3\|\boldsymbol{\varphi}(\varepsilon x)\|_{1/2,\partial\omega} \\ &+\|\boldsymbol{\varphi}(\varepsilon x)\|_{1/2,\partial\omega}\Big).\end{aligned}$$

So, finally, for ε small enough, we get:

$$\begin{aligned}\|\boldsymbol{v}_\varepsilon\|_{1,\Omega_\varepsilon} &\leq \|\boldsymbol{z}_\varepsilon\|_{1,\Omega_\varepsilon} + \left\|\boldsymbol{W}\left(\tfrac{x}{\varepsilon}\right)\right\|_{1,\Omega_\varepsilon} \\ &\leq c\Big(\|\boldsymbol{\psi}\|_{-1/2,O} + \|\boldsymbol{\Phi}\|_{1/2,\partial\Omega\setminus\overline{O}} + \|\boldsymbol{\varphi}(\varepsilon x)\|_{1/2,\partial\omega}\Big) + c\|\boldsymbol{\varphi}(\varepsilon x)\|_{1/2,\partial\omega} \\ &\leq c\Big(\|\boldsymbol{\psi}\|_{-1/2,O} + \|\boldsymbol{\Phi}\|_{1/2,\partial\Omega\setminus\overline{O}} + \|\boldsymbol{\varphi}(\varepsilon x)\|_{1/2,\partial\omega}\Big),\end{aligned}$$

and we conclude. □

Now, with the lemma proved, we are ready to finish the proof of our main proposition in the Neumann case:

Proof of Proposition 4.2, Neumann case. Thanks to lemma 4.7, we know that there exists a constant $c > 0$ independent of ε, such that:

$$\begin{aligned}\|\boldsymbol{r}_M^\varepsilon\|_{1,\Omega_\varepsilon} \leq c\Bigg(&\frac{1}{-\log\varepsilon}\Big(\|\sigma(\boldsymbol{C}_M,\Pi_M)\mathbf{n}\|_{-1/2,O} + \|\sigma(\boldsymbol{U}_M,P_M)\mathbf{n}\|_{-1/2,O}\Big) \\ &+\left\|-\boldsymbol{u}_M^0(\varepsilon X) - h_\varepsilon(\boldsymbol{C}_M(\varepsilon X) - \boldsymbol{U}_M(\varepsilon X))\right\|_{1/2,\partial\omega}\Bigg). \quad (4.27)\end{aligned}$$

We have

$$\begin{aligned}&\|\sigma(\boldsymbol{C}_M,\Pi_M)\mathbf{n}\|_{-1/2,O} \leq c|\boldsymbol{C}_M|_{1,\Omega\setminus B(0,1)} \\ &\|\sigma(\boldsymbol{U}_M,P_M)\mathbf{n}\|_{-1/2,O} \leq c|\boldsymbol{U}_M|_{1,\Omega_\varepsilon}.\end{aligned} \quad (4.28)$$

In fact, for all $\boldsymbol{\phi} \in \mathbf{H}^{1/2}(O)$ and all $\boldsymbol{\eta} \in \mathbf{H}^1(\Omega \setminus B(0,1))$, extension of $\boldsymbol{\phi}$ such that $\boldsymbol{\eta}_{|\partial\Omega\setminus\overline{O}} = \mathbf{0}$, we have

$$\begin{aligned}\langle \sigma(\boldsymbol{C}_M, \Pi_M)\mathbf{n}\,,\, \boldsymbol{\phi}\rangle_{-1/2,1/2,O} &= \nu \int_{\Omega\setminus B(0,1)} \mathcal{D}(\boldsymbol{C}_M) : \nabla(\boldsymbol{\eta}) \\ &\leq c\, \|\mathcal{D}(\boldsymbol{C}_M)\|_{0,\Omega\setminus B(0,1)}\, \|\boldsymbol{\eta}\|_{1,\Omega\setminus B(0,1)}\end{aligned}$$

and, choosing $\boldsymbol{\eta}$ such that $\|\boldsymbol{\eta}\|_{1,\Omega\setminus B(0,1)} = \|\boldsymbol{\phi}\|_{1/2,O}$, we obtain that

$$\|\sigma(\boldsymbol{C}_M, \Pi_M)\mathbf{n}\|_{-1/2,O} \leq c\, \|\mathcal{D}(\boldsymbol{C}_M)\|_{0,\Omega\setminus B(0,1)} = c|\boldsymbol{C}_M|_{1,\Omega\setminus B(0,1)}.$$

The same procedure for $\boldsymbol{U}_M$ in Ω_ε instead of $\Omega\setminus\overline{B(0,1)}$ gives the bound for $\sigma(\boldsymbol{U}_M, P_M)$.

Remark Notice that we need to consider the set $\Omega \setminus B(0,1)$ for $\sigma(\boldsymbol{C}_M, \Pi_M)\mathbf{n}$ in order to obtain a bound independent of ε: we need to consider a set sufficiently away from zero, due to the definition of $\boldsymbol{C}_M$. For $\boldsymbol{U}_M$, we don't have this problem because it is defined in the whole Ω.

Now we need estimates for the functions $\boldsymbol{U}_M$ and $\boldsymbol{C}_M$. Notice that, from the well posedness of the problem (4.8) with $\natural = N$, we have:

$$\|\boldsymbol{U}_M\|_{1,\Omega} \leq c\|\boldsymbol{C}_M\|_{1/2,\partial\omega}.$$

But $\boldsymbol{C}_M(x) = -4\pi\nu E(x)\, \boldsymbol{u}^0_\natural(0)$ which is bounded if x is away from zero. The same applies for the derivative of $\boldsymbol{C}_M$ because $\nabla\boldsymbol{C}_M(x) = O(1/r)$. Therefore, on $\partial\omega$, we have $|\boldsymbol{C}_M(x)| \leq c$ and $|\nabla\boldsymbol{C}_M(x)| \leq c$, and then:

$$\|\boldsymbol{U}_M\|_{1,\Omega} \leq c.$$

For $\boldsymbol{C}_M$ we will need a bound for the term $|\boldsymbol{C}_M|_{1,\Omega\setminus B(0,1)}$, for this, first notice that $|\nabla\boldsymbol{C}_M| = O(1/r)$ and let R big enough such that $\Omega \subset B(0,R)$, therefore:

$$\begin{aligned}|\boldsymbol{C}_M|_{1,\Omega\setminus B(0,1)} \leq |\boldsymbol{C}_M|_{1,B(0,R)\setminus B(0,1)} &\leq c\left(\int_{B(0,R)\setminus B(0,1)} \frac{1}{\|x\|^2}\mathrm{d}x\right)^{1/2} \\ &= c\,(2\pi \ln R)^{1/2} = c.\end{aligned}$$

We finally get:

$$\|\boldsymbol{U}_M\|_{1,\Omega} \leq c \text{ and } |\boldsymbol{C}_M|_{1,\Omega\setminus B(0,1)} \leq c.$$

Then, from (4.28),

$$\|\sigma(\boldsymbol{C}_M, \Pi_M)\mathbf{n}\|_{-1/2,O} \leq c \text{ and } \|\sigma(\boldsymbol{U}_M, P_M)\mathbf{n}\|_{-1/2,O} \leq c.$$

The other term of (4.27) is treated identically as in the Dirichlet case (see (4.20)) and therefore, we get:

$$\|\boldsymbol{r}^\varepsilon_M\|_{1,\Omega_\varepsilon} \leq \frac{c}{-\log\varepsilon} + c\varepsilon + \frac{c}{-\log\varepsilon} \leq \frac{c}{-\log\varepsilon},$$

which concludes the proof of Proposition 4.2 with $\natural = N$. □

Remark In order to understand the obtained asymptotic expansion, let us recall some facts inside the proof for the Dirichlet case (similar observations applies to the Neumann case): We have that the Dirichlet traces of $h_\varepsilon(\boldsymbol{C}_D - \boldsymbol{U}_D)$ over $\partial\Omega$ and $\partial\omega_\varepsilon$ are zero and $\boldsymbol{\lambda} + O(\sqrt{-1/\log\varepsilon})$ (with $\boldsymbol{\lambda} \in \mathbb{R}^2$), from which we obtain an $\mathrm{H}^1(\Omega_\varepsilon)$ norm for $h_\varepsilon(\boldsymbol{C}_D - \boldsymbol{U}_D)$ of size $O(-1/\log\varepsilon)$ by Lemma 4.6, additionally we have that the trace of $\boldsymbol{r}_D^\varepsilon$ over $\partial\omega_\varepsilon$ is $o(1)$ (see the end of the proof of Proposition 4.2) which is coherent with the higher order obtained by the $\mathrm{H}^1(\Omega_{z,\varepsilon})$ norm of $\boldsymbol{r}_D^\varepsilon$, this is, $O(-1/\log\varepsilon)$.

4.4 Proof of Theorem 4.1

We recall that we will detail the proof only for the case of an origin-centered inclusion, *i.e.* $z = 0$ (see Remark 4.2.2).

4.4.1 A preliminary lemma

First we need an estimate of the norm $\|\cdot\|_{1/2,\partial\omega_\varepsilon}$ of an uniformly bounded function. Here $\|\cdot\|_{1/2,\partial\omega_\varepsilon}$ has to be seen as the trace norm

$$\|\boldsymbol{f}\|_{1/2,\partial\omega_\varepsilon} := \inf\left\{\|\boldsymbol{u}\|_{\mathbf{H}^1(\Omega\setminus\overline{\omega_{z,\varepsilon}})},\ \boldsymbol{u} \in \mathbf{H}^1(\Omega\setminus\overline{\omega_{z,\varepsilon}}), \boldsymbol{u}_{|\partial\omega_{z,\varepsilon}} = \boldsymbol{f}\right\}.$$

Lemma 4.9 *Let $\varepsilon \in (0, 1/2)$. If $\boldsymbol{u} \in \mathbf{H}^1(\Omega)$ is such that its restriction to $\overline{\omega_1}$ (i.e. ω_ε for $\varepsilon = 1$) is C^1, then there exists a constant $c > 0$ independent of ε such that*

$$\|\boldsymbol{u}\|_{1/2,\partial\omega_\varepsilon} \leq \frac{c}{\sqrt{-\log\varepsilon}}.$$

Proof. From Theorem B.2, there exists a constant $c > 0$ independent of ε such that

$$\|\boldsymbol{u}\|_{1/2,\partial\omega_\varepsilon} \leq c\frac{\varepsilon^{-1/2}}{\sqrt{-\log\varepsilon}}\|\boldsymbol{u}\|_{\mathbf{L}^2(\partial\omega_\varepsilon)} + c\left(\int\!\!\int_{\partial\omega_\varepsilon\times\partial\omega_\varepsilon}\frac{|\boldsymbol{u}(x)-\boldsymbol{u}(y)|^2}{|x-y|^2}\mathrm{ds}(x)\mathrm{ds}(y)\right)$$

Since $\boldsymbol{u}$ is uniformly bounded on $\partial\omega_\varepsilon$, we use the change of variables $y = \varepsilon x$ to prove that there exists a constant $c > 0$ independent of ε such that

$$\|\boldsymbol{u}\|_{\mathbf{L}^2(\partial\omega_\varepsilon)} \leq c\varepsilon^{1/2}.$$

Moreover, using the changes of variables $x = \varepsilon X$ and $y = \varepsilon Y$, the fact that $\boldsymbol{u}(\varepsilon X) = \boldsymbol{u}(0) + \varepsilon\nabla(\boldsymbol{u})(\zeta_X)X$, $\zeta_X \in \omega_\varepsilon$ and $\boldsymbol{u}(z + \varepsilon Y) = \boldsymbol{u}(z) + \varepsilon\nabla(\boldsymbol{u})(\zeta_Y)Y$, $\zeta_Y \in \omega_\varepsilon$ (ζ_X and ζ_Y are some points in the lines which join 0 to εX and εY respectively due to

a Taylor expansion), there exists $c > 0$ independent of ε such that

$$\left(\iint_{\partial\omega_\varepsilon \times \partial\omega_\varepsilon} \frac{|\boldsymbol{u}(x) - \boldsymbol{u}(y)|^2}{|x-y|^2} \mathrm{ds}(x)\mathrm{ds}(y) \right)^{1/2}$$
$$= \left(\iint_{\partial\omega \times \partial\omega} \varepsilon^2 \frac{|\varepsilon\left(\nabla(\boldsymbol{u})(\zeta_X)X - \nabla(\boldsymbol{u})(\zeta_Y)Y\right)|^2}{\varepsilon^2 |X-Y|^2} \mathrm{ds}(x)\mathrm{ds}(y) \right)^{1/2} \leq c\varepsilon.$$

Therefore, we get:

$$\|\boldsymbol{u}\|_{1/2,\partial\omega_\varepsilon} \leq c\varepsilon^{-1/2} \cdot \frac{1}{\sqrt{-\log\varepsilon}} \cdot \varepsilon^{1/2} + c\varepsilon \leq \frac{c}{\sqrt{-\log\varepsilon}}.$$

□

4.4.2 Splitting the variations of the objective

Now, we turn our attention to the Kohn-Vogelius functional given by

$$\mathcal{J}_{KV}(\Omega_\varepsilon) = \frac{1}{2}\nu \int_{\Omega_\varepsilon} |\mathcal{D}(\boldsymbol{u}_D^\varepsilon) - \mathcal{D}(\boldsymbol{u}_M^\varepsilon)|^2.$$

We first recall the following decomposition:

Lemma 4.10 *We have*

$$\mathcal{J}_{KV}(\Omega_\varepsilon) - \mathcal{J}_{KV}(\Omega) = A_D + A_M, \tag{4.29}$$

where

$$A_D := \frac{1}{2}\nu \int_{\Omega_\varepsilon} \mathcal{D}(\boldsymbol{u}_D^\varepsilon - \boldsymbol{u}_D^0) : \mathcal{D}(\boldsymbol{u}_D^\varepsilon - \boldsymbol{u}_D^0)$$
$$+ \nu \int_{\Omega_\varepsilon} \mathcal{D}(\boldsymbol{u}_D^\varepsilon - \boldsymbol{u}_D^0) : \mathcal{D}(\boldsymbol{u}_D^0) - \frac{1}{2}\nu \int_{\omega_\varepsilon} |\mathcal{D}(\boldsymbol{u}_D^0)|^2$$

and

$$A_M := \int_{\partial\omega_\varepsilon} \left[\sigma(\boldsymbol{u}_M^\varepsilon - \boldsymbol{u}_M^0, p_M^\varepsilon - p_M^0)\mathbf{n}\right] \cdot \boldsymbol{u}_M^0 - \frac{1}{2}\nu \int_{\omega_\varepsilon} |\mathcal{D}(\boldsymbol{u}_M^0)|^2.$$

Proof. We integrate by parts and use the conditions satisfied by $(\boldsymbol{u}_D^\varepsilon, p_D^\varepsilon)$, $(\boldsymbol{u}_M^\varepsilon, p_M^\varepsilon)$, $(\boldsymbol{u}_D^0, p_D^0)$ and $(\boldsymbol{u}_M^0, p_M^0)$ to obtain this decomposition. For details see [36, Lemma 5.2]. □

4.4.3 Asymptotic expansion of A_M

We follow here a similar strategy as the one used in the 3D case detailed for example in [36], in contrast to that work we rely on the Stokes fundamental solution properties and the definition of the approximation problem instead of single layer formulas present in the 3D case. We know using elliptic regularity that $\nabla \boldsymbol{u}_M^0$ is uniformly bounded on ω_ε. Thus

$$-\frac{1}{2}\nu \int_{\omega_\varepsilon} |\mathcal{D}(\boldsymbol{u}_M^0)|^2 \leq c \int_\omega \varepsilon^2 = O(\varepsilon^2). \tag{4.30}$$

We recall that:

$$\begin{aligned} \boldsymbol{r}_M^\varepsilon(x) &:= \boldsymbol{u}_M^\varepsilon(x) - \boldsymbol{u}_M^0(x) - h_\varepsilon(\boldsymbol{C}_M(x) - \boldsymbol{U}_M(x)) \\ p_{r_M^\varepsilon}(x) &:= p_M^\varepsilon(x) - p_M^0(x) - h_\varepsilon(\Pi_M(x) - P_M(x)), \end{aligned}$$

where $(\boldsymbol{U}_M, P_M) \in \mathbf{H}^1(\Omega)\times \mathrm{L}^2_0(\Omega)$ solves (4.8), $\boldsymbol{C}_M$ is given by (4.1 bis) (with $\natural = N$) and Π_M is given by (4.22). Then the following equality holds

$$\begin{aligned} \int_{\partial\omega_\varepsilon} \left[\sigma(\boldsymbol{u}_M^\varepsilon - \boldsymbol{u}_M^0, p_M^\varepsilon - p_M^0)\mathbf{n}\right] \cdot \boldsymbol{u}_M^0 = \\ \int_{\partial\omega_\varepsilon} \left[\sigma(\boldsymbol{r}_M^\varepsilon, p_{r_M^\varepsilon})\mathbf{n}\right] \cdot \boldsymbol{u}_M^0 + h_\varepsilon \int_{\partial\omega_\varepsilon} [\sigma(\boldsymbol{C}_M - \boldsymbol{U}_M, \Pi_M - P_M)\mathbf{n}] \cdot \boldsymbol{u}_M^0. \end{aligned} \tag{4.31}$$

Let us first focus on the first term in the right-hand side of (4.31). Using the same argument as the one used in the deduction of (4.28), we get:

$$\left\|\sigma(\boldsymbol{r}_M^\varepsilon, p_{r_M^\varepsilon})\mathbf{n}\right\|_{-1/2,\partial\omega_\varepsilon} \leq c \left\|\mathcal{D}(\boldsymbol{r}_M^\varepsilon)\right\|_{0,\Omega_\varepsilon}. \tag{4.32}$$

Therefore, using the explicit upper bound of $\|\boldsymbol{u}_M^0\|_{1/2,\partial\omega_\varepsilon}$ given by Lemma 4.9, we have

$$\begin{aligned} \left|\int_{\partial\omega_\varepsilon} \left[\sigma(\boldsymbol{r}_M^\varepsilon, p_{r_M^\varepsilon})\mathbf{n}\right] \cdot \boldsymbol{u}_M^0\right| &\leq \left\|\sigma(\boldsymbol{r}_M^\varepsilon, p_{r_M^\varepsilon})\mathbf{n}\right\|_{-1/2,\partial\omega_\varepsilon} \left\|\boldsymbol{u}_M^0\right\|_{1/2,\partial\omega_\varepsilon} \\ &\leq \frac{c}{\sqrt{-\log\varepsilon}} \|\boldsymbol{r}_M^\varepsilon\|_{1,\Omega_\varepsilon}. \end{aligned}$$

Then, using the explicit upper bound of $\|\boldsymbol{r}_M^\varepsilon\|_{1,\Omega_\varepsilon}$ given by Proposition 4.2, we obtain

$$\left|\int_{\partial\omega_\varepsilon} \left[\sigma(\boldsymbol{r}_M^\varepsilon, p_{r_M^\varepsilon})\mathbf{n}\right] \cdot \boldsymbol{u}_M^0\right| \leq \frac{c}{\log^{3/2}\varepsilon} = O\left(\frac{1}{(-\log\varepsilon)^{3/2}}\right). \tag{4.33}$$

For the other term

$$\begin{aligned} \int_{\partial\omega_\varepsilon} [\sigma(\boldsymbol{C}_M - \boldsymbol{U}_M, \Pi_M - P_M)\mathbf{n}] \cdot \boldsymbol{u}_M^0 = \int_{\partial\omega_\varepsilon} [\sigma(\boldsymbol{C}_M, \Pi_M)\mathbf{n}] \cdot \boldsymbol{u}_M^0 \\ - \int_{\partial\omega_\varepsilon} [\sigma(\boldsymbol{U}_M, P_M)\mathbf{n}] \cdot \boldsymbol{u}_M^0, \end{aligned}$$

we study each term separately. For this recall that: $\boldsymbol{u}_M^0(x) = \boldsymbol{u}_M^0(0) + \varepsilon \nabla \boldsymbol{u}_M^0(\zeta_x)$, with $\zeta_x \in \omega_\varepsilon$. Then:

$$\begin{aligned}\int_{\partial\omega_\varepsilon} [\sigma(\boldsymbol{C}_M, \Pi_M)\mathbf{n}] \cdot \boldsymbol{u}_M^0 &= \int_{\partial\omega_\varepsilon} [\sigma(\boldsymbol{C}_M, \Pi_M)\mathbf{n}] \cdot (\boldsymbol{u}_M^0 - \boldsymbol{u}_M^0(0) + \boldsymbol{u}_M^0(0)) \\ &= \varepsilon \int_{\partial\omega_\varepsilon} [\sigma(\boldsymbol{C}_M, \Pi_M)\mathbf{n}] \cdot \nabla \boldsymbol{u}_M^0(\zeta_x) \\ &\qquad + \int_{\partial\omega_\varepsilon} [\sigma(\boldsymbol{C}_M, \Pi_M)\mathbf{n}] \cdot \boldsymbol{u}_M^0(0) \\ &= O(\varepsilon) + \int_{\partial\omega_\varepsilon} [\sigma(\boldsymbol{C}_M, \Pi_M)\mathbf{n}] \cdot \boldsymbol{u}_M^0(0).\end{aligned}$$

We get the last equality because $\nabla \boldsymbol{u}_M^0$ is uniformly bounded and:

$$\int_{\partial\omega_\varepsilon} [\sigma(\boldsymbol{C}_M, \Pi_M)\mathbf{n}] = \int_{\omega_\varepsilon} \operatorname{div}(\sigma(\boldsymbol{C}_M, \Pi_M)) = -\int_{\omega_\varepsilon} (-\nu\Delta \boldsymbol{C}_M + \nabla\Pi_M) = -4\pi\nu \boldsymbol{u}_M^0(0)$$

because of the definition of the pair $(\boldsymbol{C}_M, \Pi_M) = (-4\pi\nu E \boldsymbol{u}_M^0(0), -4\pi\nu \boldsymbol{P} \cdot \boldsymbol{u}_M^0(0))$ in terms of the fundamental solution $(E, \boldsymbol{P})$ of Stokes equation. Analogously:

$$\int_{\partial\omega_\varepsilon} [\sigma(\boldsymbol{U}_M, P_M)\mathbf{n}] \cdot \boldsymbol{u}_M^0 \quad = O(\varepsilon) + \int_{\partial\omega_\varepsilon} [\sigma(\boldsymbol{U}_M, P_M)\mathbf{n}] \cdot \boldsymbol{u}_M^0(0),$$

because of the definition of the pair $(\boldsymbol{U}_M, P_M)$, we get:

$$\int_{\partial\omega_\varepsilon} [\sigma(\boldsymbol{U}_M, P_M)\mathbf{n}] = \int_{\omega_\varepsilon} \operatorname{div} \sigma(\boldsymbol{U}_M, P_M) = \mathbf{0}.$$

Therefore:

$$h_\varepsilon \int_{\partial\omega_\varepsilon} [\sigma(\boldsymbol{C}_M - \boldsymbol{U}_M, \Pi_M - P_M)\mathbf{n}] \cdot \boldsymbol{u}_M^0 = \frac{4\pi\nu}{\log\varepsilon} |\boldsymbol{u}_M^0(0)|^2 + O\left(\frac{\varepsilon}{-\log\varepsilon}\right). \quad (4.34)$$

Gathering (4.30), (4.33) and (4.34), we obtain

$$A_M = \frac{4\pi\nu}{\log\varepsilon} |\boldsymbol{u}_M^0(0)|^2 + o\left(\frac{1}{-\log\varepsilon}\right). \quad (4.35)$$

4.4.4 Asymptotic expansion of A_D

We recall that

$$A_D = \frac{\nu}{2} \int_{\Omega_\varepsilon} \mathcal{D}(\boldsymbol{u}_D^\varepsilon - \boldsymbol{u}_D^0) : \mathcal{D}(\boldsymbol{u}_D^\varepsilon - \boldsymbol{u}_D^0) + \nu \int_{\Omega_\varepsilon} \mathcal{D}(\boldsymbol{u}_D^\varepsilon - \boldsymbol{u}_D^0) : \mathcal{D}(\boldsymbol{u}_D^0) - \frac{1}{2}\nu \int_{\omega_\varepsilon} |\mathcal{D}(\boldsymbol{u}_D^0)|^2$$

and that:

$$\begin{aligned}\boldsymbol{r}_D^\varepsilon(x) &:= \boldsymbol{u}_D^\varepsilon(x) - \boldsymbol{u}_D^0(x) - h_\varepsilon(\boldsymbol{C}_D(x) - \boldsymbol{U}_D(x)) \\ p_{r_D^\varepsilon}(x) &:= p_D^\varepsilon(x) - p_D^0(x) - h_\varepsilon(\Pi_D(x) - P_D(x)),\end{aligned}$$

where $(\boldsymbol{U}_D, P_D) \in \mathbf{H}^1(\Omega) \times \mathrm{L}^2_0(\Omega)$ solves (4.8), $\boldsymbol{C}_D$ is given by (4.1 bis) (with $\natural = D$ and $z = 0$) and the pressure associated to $\boldsymbol{C}_D$ is defined explicitly by the expression

$$\Pi_D(x) := -4\pi\nu \boldsymbol{P}(x) \cdot \boldsymbol{u}^0_D(0).$$

Proceeding as in the previous section 4.4.3, we prove that

$$-\frac{1}{2}\nu \int_{\omega_\varepsilon} |\mathcal{D}(\boldsymbol{u}^0_D)|^2 = O(\varepsilon^2).$$

Moreover, using Green's formula, we have

$$\begin{aligned}\nu \int_{\Omega_\varepsilon} \mathcal{D}(\boldsymbol{u}^\varepsilon_D - \boldsymbol{u}^0_D) : \mathcal{D}(\boldsymbol{u}^0_D) &= 2 \int_{\partial\omega_\varepsilon} \big(\sigma(\boldsymbol{u}^0_D, p^0_D)\mathbf{n}\big) \cdot \big(\boldsymbol{u}^\varepsilon_D - \boldsymbol{u}^0_D\big) \\ &= -2 \int_{\partial\omega_\varepsilon} \big(\sigma(\boldsymbol{u}^0_D, p^0_D)\mathbf{n}\big) \cdot \boldsymbol{u}^0_D = -\nu \int_{\omega_\varepsilon} |\mathcal{D}(\boldsymbol{u}^0_D)|^2 = O(\varepsilon^2).\end{aligned}$$

Now, let us study $\dfrac{1}{2}\nu \displaystyle\int_{\Omega_\varepsilon} \mathcal{D}(\boldsymbol{u}^\varepsilon_D - \boldsymbol{u}^0_D) : \mathcal{D}(\boldsymbol{u}^\varepsilon_D - \boldsymbol{u}^0_D)$. Using Green's formula

$$\begin{aligned}\nu \int_{\Omega_\varepsilon} \big|\mathcal{D}(\boldsymbol{u}^\varepsilon_D - \boldsymbol{u}^0_D)\big|^2 &= 2 \int_{\partial\omega_\varepsilon} \big[\sigma(\boldsymbol{u}^\varepsilon_D - \boldsymbol{u}^0_D, p^\varepsilon_D - p^0_D)\mathbf{n}\big] \cdot \big(\boldsymbol{u}^\varepsilon_D - \boldsymbol{u}^0_D\big) \\ &= -2 \int_{\partial\omega_\varepsilon} \big[\sigma(\boldsymbol{r}^\varepsilon_D, p_{r^\varepsilon_D})\mathbf{n}\big] \cdot \boldsymbol{u}^0_D \\ &\qquad -2h_\varepsilon \int_{\partial\omega_\varepsilon} [\sigma(\boldsymbol{C}_D - \boldsymbol{U}_D, \Pi_D - P_D)\mathbf{n}] \cdot \boldsymbol{u}^0_D.\end{aligned}$$

Proceeding as in the previous section 4.4.3 (see inequality (4.33)), we use an inequality similar to (4.32), the asymptotic expansion of $\boldsymbol{u}^\varepsilon_D$ given by Proposition 4.2 and Lemma 4.9 to obtain

$$\left| \int_{\partial\omega_\varepsilon} \big[\sigma(\boldsymbol{r}^\varepsilon_D, p_{r^\varepsilon_D})\mathbf{n}\big] \cdot \boldsymbol{u}^0_D \right| \leq c \, \|\boldsymbol{u}^0_D\|_{1/2,\partial\omega} \, \|\boldsymbol{r}^\varepsilon_D\|_{1,\Omega_\varepsilon} \leq \frac{c}{(-\log\varepsilon)^{3/2}}.$$

For the other term, we do similar computations as in A_M to prove that

$$\int_{\partial\omega_\varepsilon} [\sigma(\boldsymbol{C}_D - \boldsymbol{U}_D, \Pi_D - P_D)\mathbf{n}] \cdot \boldsymbol{u}^0_D = -4\pi\nu \boldsymbol{u}^0_D(0) + O(\varepsilon).$$

Therefore

$$A_D = \frac{4\pi\nu}{-\log\varepsilon} |\boldsymbol{u}^0_D(0)|^2 + o\left(\frac{1}{-\log\varepsilon}\right). \tag{4.36}$$

4.4.5 Conclusion of the proof: asymptotic expansion of $\mathcal{J}_{KN}$

Gathering (4.29), (4.35) and (4.36), we conclude the proof of Theorem 4.1:

$$\mathcal{J}_{KV}(\Omega_\varepsilon) - \mathcal{J}_{KV}(\Omega) = \frac{4\pi\nu}{-\log\varepsilon}(|\boldsymbol{u}^0_D(0)|^2 - |\boldsymbol{u}^0_M(0)|^2) + o\left(\frac{1}{-\log\varepsilon}\right). \tag{4.37}$$

Chapter 5

Numerical detection of obstacles: Topological and mixed optimization method

In this chapter we perform a numerical reconstruction of small objects immersed in a stationary two-dimensional fluid which is governed by the incompressible Stokes equations. Our main tool in this reconstruction is the topological derivative of the Kohn-Vogelius functional, introduced and computed in the previous chapter (see Theorem 4.1) which allows us to perform the numerical minimization of the functional.

As previously described, the topological derivative helps us to determine numerically the number of inclusions and their relative location. Using a topological gradient type algorithm, we detect small objects immersed in a two-dimensional fluid by means of a boundary measurement. We test our algorithm under several configurations in order to discover the advantages and limitations of our proposed method. From this tests we have concluded that the quality of the reconstruction is severely affected if the object(s) to be detected is(are) far from the boundary where the measurements are made. The size of the objects and the the amount of noise into the measurements could also be a relevant factor into the quality of the numerical results.

Additionally we propose a second algorithm, which combines the topological method with a tool that we have used in Chapter 2: the shape gradient. The idea is to obtain an algorithm which allows to determine the number and relative location of the inclusion(s) and also their approximate shape. We present an example where we can observe a quantitative and qualitative improvement of the results.

This chapter is divided in two big sections: one for each proposed algorithm. After presenting the framework of the simulations we begin by studying the topological gradient algorithm. First series of tests are devoted to explore the effectiveness of

the algorithm, we study if the algorithm is capable to detect several obstacles with simple geometry, circles, and evolving to some more sophisticated geometries, which is the case of squares and a 'donut' object. From this primary simulations we observe that the algorithm is capable to detect several objects when they are not too close between them and the geometry of the objects is not a problem in order to detect their relative size. Then, we try to explore the limitations of the algorithm with a series of test in which we try to push the algorithm to their limits. We test the influence of the distance between the objects and the boundary where measurements are made, we also test the influence of the size of the objects to be detected and we finally test the influence of the contamination of the data by noise. We have obtained each of the studied factors are relevant in order to obtain a better reconstruction, if the obstacles are far from the boundary where the measurements are made the reconstruction may fail, as the relative error of approximately location increases as the distance does and even the number of objects could be wrongly estimated. When the size of the obstacles to be detected becomes of higher, the estimate of the number of objects tends to be incorrect. This last behavior is expected and natural, as the asymptotic expansion is performed by assuming the small size of the obstacles. From the inclusion of noise we have observed that our algorithm behaves in a stable way, the reconstructions are good for a relatively high amount of noise, and becomes incorrect only when the noise level is high.
The second section explores the mixed optimization algorithm, where we introduce the computation of the shape gradient of the Kohn-Vogelius functional. We begin the section by presenting the basic definitions and the theoretical expression of the first order shape derivative of the functional. Then, we present the framework of the simulations where we introduce the parametrization of the boundary by means of truncated Fourier series and then we propose the full algorithm. We finally present an example where we can observe the quantitative and qualitative improvements after the complementary step: the shape of the detected objects is more accurate and the value of the Kohn-Vogelius functional is reduced in a significant order of magnitude.

We refer to Chapter 4 for the notations. In particular, we recall that Ω is a bounded Lipschitz open set of $\mathbb{R}^2$ with an unaccessible obstacle ω_ε^* inside Ω. Let $\boldsymbol{f} \in \mathbf{H}^{1/2}(\partial\Omega)$ such that $\boldsymbol{f} \neq 0$ and $\displaystyle\int_{\partial\Omega} \boldsymbol{f} \cdot \mathbf{n} = 0$, and let $\boldsymbol{g} \in \mathbf{H}^{-1/2}(O)$ be a given measurement on a part O of $\partial\Omega$ with $O \neq \partial\Omega$. Then, in order to solve the geometrical inverse problem (4.3), we consider the following Kohn-Vogelius functional

$$\mathcal{J}_{KV}(\Omega\backslash\overline{\omega_\varepsilon}) := \frac{1}{2}\int_{\Omega\backslash\overline{\omega_\varepsilon}} \nu|\mathcal{D}(\boldsymbol{u}_D^\varepsilon) - \mathcal{D}(\boldsymbol{u}_M^\varepsilon)|^2,$$

where $(\boldsymbol{u}_D^\varepsilon, p_D^\varepsilon) \in \mathbf{H}^1(\Omega\backslash\overline{\omega_\varepsilon}) \times \mathrm{L}_0^2(\Omega\backslash\overline{\omega_\varepsilon})$ and $(\boldsymbol{u}_M^\varepsilon, p_M^\varepsilon) \in \mathbf{H}^1(\Omega\backslash\overline{\omega_\varepsilon}) \times \mathrm{L}^2(\Omega\backslash\overline{\omega_\varepsilon})$ are the respective solutions of the following problems:

$$\left\{\begin{array}{rcll} \text{Find } (\boldsymbol{u}_D^\varepsilon, p_D^\varepsilon) \in \mathbf{H}^1(\Omega\backslash\overline{\omega_\varepsilon}) \times \mathrm{L}^2_0(\Omega\backslash\overline{\omega_\varepsilon}) \text{ such that} & & & \\ -\nu\Delta\boldsymbol{u}_D^\varepsilon + \nabla p_D^\varepsilon & = & \mathbf{0} & \text{in } \Omega\backslash\overline{\omega_\varepsilon} \\ \operatorname{div}\boldsymbol{u}_D^\varepsilon & = & 0 & \text{in } \Omega\backslash\overline{\omega_\varepsilon} \\ \boldsymbol{u}_D^\varepsilon & = & \boldsymbol{f} & \text{on } \partial\Omega \\ \boldsymbol{u}_D^\varepsilon & = & \mathbf{0} & \text{on } \partial\omega_\varepsilon, \end{array}\right.$$

and

$$\left\{\begin{array}{rcll} \text{Find } (\boldsymbol{u}_M^\varepsilon, p_M^\varepsilon) \in \mathbf{H}^1(\Omega\backslash\overline{\omega_\varepsilon}) \times \mathrm{L}^2(\Omega\backslash\overline{\omega_\varepsilon}) \text{ such that} & & & \\ -\nu\Delta\boldsymbol{u}_M^\varepsilon + \nabla p_M^\varepsilon & = & \mathbf{0} & \text{in } \Omega\backslash\overline{\omega_\varepsilon} \\ \operatorname{div}\boldsymbol{u}_M^\varepsilon & = & 0 & \text{in } \Omega\backslash\overline{\omega_\varepsilon} \\ \sigma(\boldsymbol{u}_M^\varepsilon, p_M^\varepsilon)\mathbf{n} & = & \boldsymbol{g} & \text{on } O \\ \boldsymbol{u}_M^\varepsilon & = & \boldsymbol{f} & \text{on } \partial\Omega\backslash\overline{O} \\ \boldsymbol{u}_M^\varepsilon & = & \mathbf{0} & \text{on } \partial\omega_\varepsilon. \end{array}\right.$$

We also recall that the topological gradient for $\mathcal{J}_{KV}$ is given in Theorem 4.1.

5.1 A Topological Gradient Algorithm

5.1.1 Framework of the numerical simulations

The use of the topological derivative aims to give us the number of inclusions and their qualitative location. To make the numerical simulations presented here, we use a $P1$bubble-$P1$ finite element discretization to solve the Stokes equations (4.4) and (4.5). The framework is the following: the exterior boundary is assumed to be the rectangle $[-0.5, 0.5] \times [-0.25, 0.25]$. Except when mentioned, the measurement is assumed to be made on all the faces except on the one given by $y = 0.25$. We consider the exterior Dirichlet boundary condition

$$\boldsymbol{f} := \begin{pmatrix} 1 \\ 1 \end{pmatrix}.$$

In order to have a suitable pair (*measure* $\boldsymbol{g}$, *domain* ω^*), we use a synthetic data: we fix a shape ω^* (more precisely a finite number of obstacles $\omega_1^*, \ldots, \omega_m^*$), solve the Stokes problem (4.4) in $\Omega\backslash\overline{\omega^*}$ using another finite element method (here a $P2$-$P1$ finite element discretization) and extract the measurement $\boldsymbol{g}$ by computing $\sigma(\boldsymbol{u}, p)\mathbf{n}$ on O.

In the practical simulations that we present, we add circular objects. In order to determine the radius of these disks, we use a thresholding method. For an iteration k, it consists in determining the minimum argument P^* of the topological gradient $\delta\mathcal{J}_{KV}$ in $\Omega\backslash\left(\bigcup_{j=1}^k \overline{\omega_j}\right)$ and in defining the set $\mathscr{P}$ of the points $P \in \Omega\backslash\left(\bigcup_{j=1}^k \overline{\omega_j}\right)$ such that

$$\delta\mathcal{J}_{KV}(P) \leq \delta\mathcal{J}_{KV}(P^*) + 0.025 * \left|\delta\mathcal{J}_{KV}(P^*)\right|.$$

Then we fix a minimum radius $r_{\min} := 0.01$ and we define the radius of the k^{th} disk by

$$r_k := \max\left(r_{\min}, \min_{P\in\mathscr{P}\setminus\{P^*\}}(|x_P - x_{P^*}|, |y_P - y_{P^*}|)\right). \tag{5.1}$$

Notice that this method obviously depends on the mesh.

We use the classical topological gradient algorithm (see for example [38, 54, 58, 9]) that we recall here for reader's convenience:
Algorithm

1. fix an initial shape $\omega_0 = \emptyset$, a maximum number of iterations M and set $\mathrm{i} = 1$ and $k = 0$,
2. solve Problems (4.4) and (4.5) in $\Omega\setminus\left(\bigcup_{j=0}^{k}\overline{\omega_j}\right)$,
3. compute the topological gradient $\delta\mathcal{J}_{KV}$ using Formula (4.37), *i.e.*

$$\delta\mathcal{J}_{KV}(P) = 4\pi\nu\left(\left|\boldsymbol{u}_D^0(z)\right|^2 - \left|\boldsymbol{u}_M^0(z)\right|^2\right) \qquad \forall P\in\Omega\setminus\left(\bigcup_{j=0}^{k}\overline{\omega_j}\right),$$

4. seek $P_{k+1}^* := \operatorname{argmin}\left(\delta\mathcal{J}_{KV}(P),\, P\in\Omega\setminus\left(\bigcup_{j=0}^{k}\overline{\omega_j}\right)\right)$,
5. if $\left\|P_{k+1}^* - C_{j_0}\right\| < r_{k+1} + r_{j_0} + 0.01$ for $j_0\in\{1,\dots,k\}$, where C_{j_0} and r_{j_0} are the center and the radius of ω_{j_0} and r_{k+1} is defined by (5.1), then $r_{j_0} = 1.1 * r_{j_0}$, get back to the step 2. and $\mathrm{i}\leftarrow\mathrm{i}+1$ while $\mathrm{i}\leq M$,
6. set $\omega_{k+1} = B(P_{k+1}^*, r_{k+1})$, where r_{k+1} is defined by (5.1),
7. while $\mathrm{i}\leq M$, get back to the step 2, $\mathrm{i}\leftarrow\mathrm{i}+1$ and $k\leftarrow k+1$.

We add to this algorithm a stop test (in addition of the maximum number of iterations). In every iteration, we compute the functional $\mathcal{J}_{KV}$. This non-negative functional has to decrease at each iteration. Thus, we stop our algorithm when it is not the case, *i.e.* when $\mathcal{J}_{KV}\left(\Omega\setminus\left(\bigcup_{j=0}^{k+1}\overline{\omega_j}\right)\right) > \mathcal{J}_{KV}\left(\Omega\setminus\left(\bigcup_{j=0}^{k}\overline{\omega_j}\right)\right)$.

Notice that with this algorithm, we add only one object at each iteration. This method can be slower than the one proposed by Carpio *et al.* in [34]: they can add several obstacles simultaneously adding points where the topological derivative is large and negative, selecting well calibrated thresholds. The same authors in [31] detailed this approach: they introduce a non-monotone scheme that allows to add and remove points, to create and destroy contours at each stage and even to make holes inside an object. However, in our case, adding only one object at each iteration seems to be more appropriate because otherwise objects can be added wrongly. Moreover, notice that step 5 comes to the assumption that the objects are well separated. Finally, since we assumed that the obstacles are *far from the exterior boundary*, we have to take away the added objects on it. Then, if the minimum of the topological gradient is on the exterior boundary, we push the added inclusion inside with a depth 0.005 in the rectangular cases. In origin-centered circular domain

we push the added inclusion inside in a quantity proportional to the point, *i.e.* if the detected point is (x^*, y^*) we force it to be $(\eta \cdot x^*, \eta \cdot y^*)$ where η is usually 0.95 or 0.9.

5.1.2 First simulations

First we want to detect three circles ω_1^*, ω_2^* and ω_3^* centered respectively in $(0.475, -0.235)$, $(-0.475, -0.225)$ and $(0.470, 0.150)$ (*i.e.* near from the exterior boundary) with shared radius $r^* = 0.013$. The detection is quite efficient (see Figure 5.1). Indeed

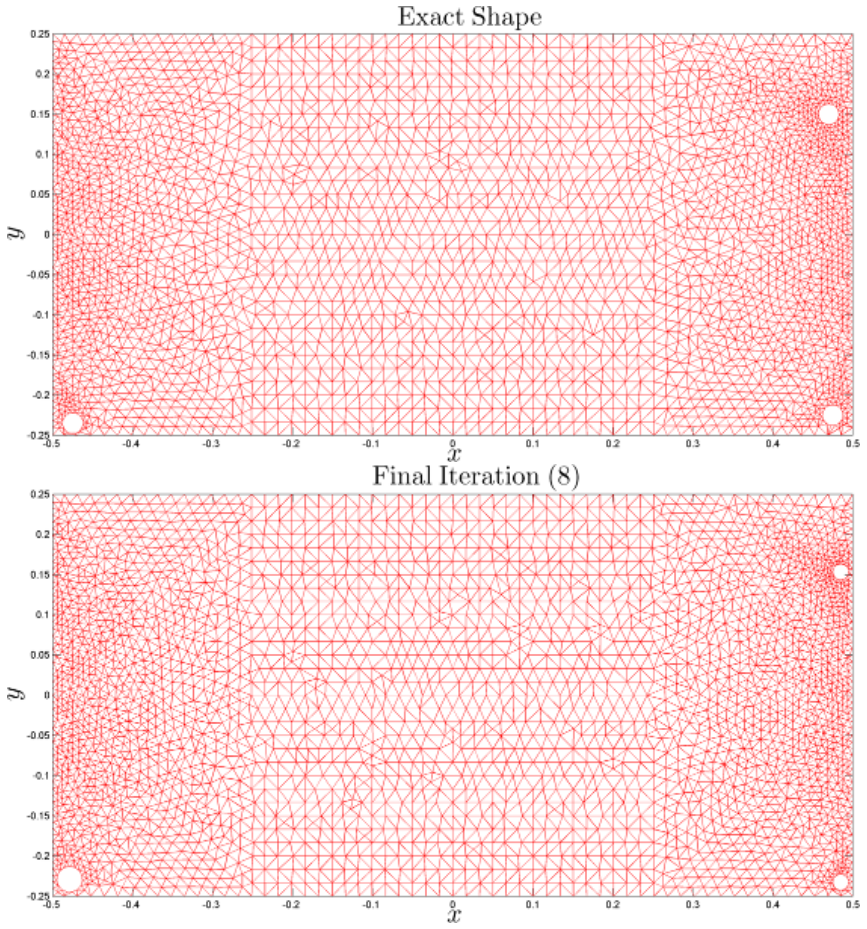

Figure 5.1: Detection of ω_1^*, ω_2^* and ω_3^*

we detect three objects with shared radius $r = 0.01$ for ω_2^* and ω_3^* and $r = 0.015$ for ω_1^*, we summarized the results in Table 5.1. Here, we stop the algorithm because of the functional increases as we can see in Figure 5.2.

Notice that some iterations are being made just to adjust the size of a detected object. We can also remark that the values of the cost functional are still relatively high and this refers to the fact that, up to our knowledge, there does not exist a theoretical result of convergence of this algorithm yet.

Table 5.1: Detection of ω_1^*, ω_2^* and ω_3^*

actual objects	(0.475, -0.235)	(-0.475, -0.225)	(0.470, 0.150)
approximate objects	(0.484, -0.234)	(-0.485, -0.235)	(0.485, 0.166)
relative error $\|c_{real} - c_{app}\|/\mathrm{diam}(\Omega)$	0.0080	0.0126	0.0196

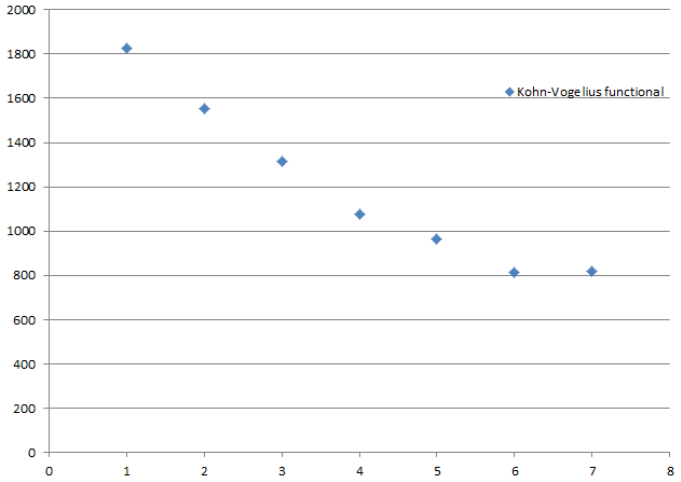

Figure 5.2: Evolution of the functional $\mathcal{J}_{KV}$ during the detection of ω_1^*, ω_2^* and ω_3^*.

In this first simulation, the objects are very far away from each other. But *what happens when the obstacles are close to each other?* Figure 5.3 shows that the detection of close objects is efficient if the distance between the obstacles is big enough. Indeed, we want to detect three circles ω_4^*, ω_5^* and ω_6^* centered respectively in $(-0.475, -0.225)$, $(0.470, 0.100)$ and $(0.470, 0.130)$ with shared radius $r^* = 0.01$. We obtain just two circles with shared radius $r = 0.01$ as summarized in Table 5.2.

Table 5.2: Detection of ω_4^*, ω_5^* and ω_6^*

actual objects	(-0.475, -0.225)	(0.470, 0.100)	(0.470, 0.130)
approximate objects	(-0.482, -0.235)	(0.480, 0.140)	(0.480, 0.140)
relative error $\|c_{real} - c_{app}\|/\mathrm{diam}(\Omega)$	0.0109	0.0368	0.0126

However if we increase the distance of the near circles enough, considering now, for example, the circle ω_{6bis}^* centered at $(0.470, 0.205)$ we get an efficient detection of the three circles, as we summarize in Figure 5.4 and Table 5.3. The distance needed for an efficient 'differentiation' between the objects is relatively high: the required distance in this case is about $2r_{min}$.

Now the question we asked is: *can we detect other shapes than disks?* Thus, we want to detect objects with different shapes: we explore two interesting examples, the first one is the detection of several squares: there are simply defined by their side $a = 0.013$, and their center (the squares have their sides parallel to the axis). So we define the square ω_7^* centered in $(0.475, -0.225)$ the square ω_8^* centered in

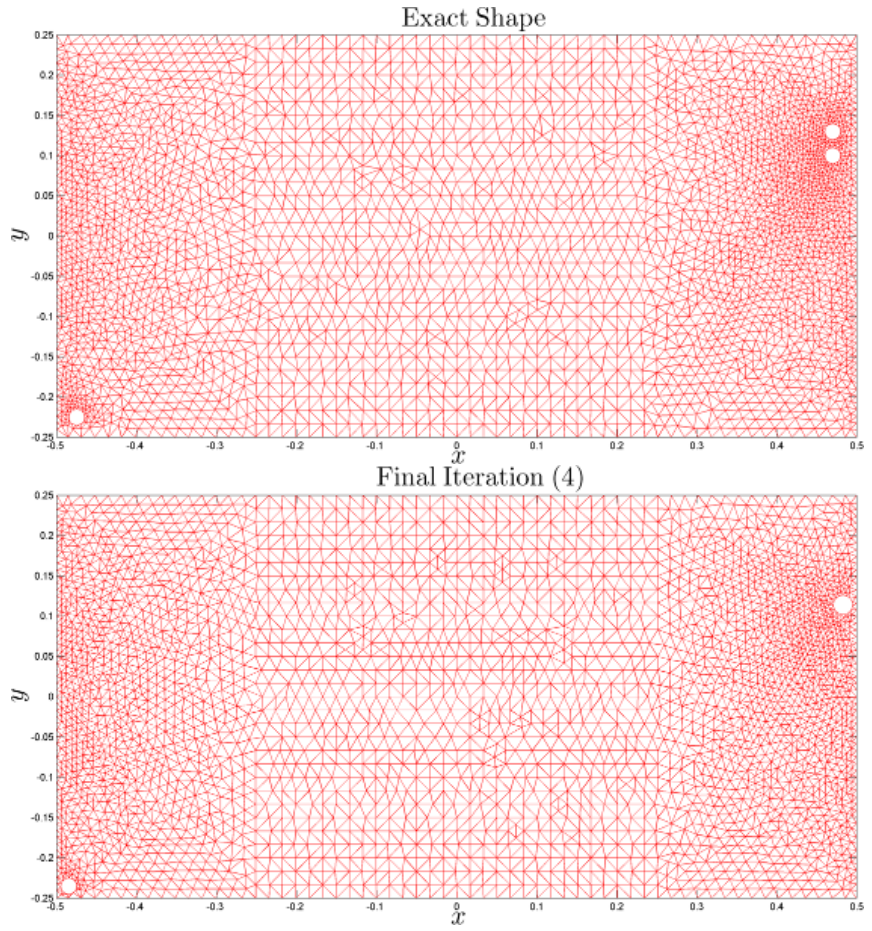

Figure 5.3: Detection of ω_4^*, ω_5^* and ω_6^*

$(-0.475, -0.225)$ and the square ω_9^* centered in $(0.470, 0.150)$. We obtain Figure 5.5: a circle centered in $(0.485, -0.235)$ one centered in $(-0.482, -0.235)$ and one centered in $(0.485, 0.155)$ with shared radius $r = 0.01$.

The next example deals with a more complex geometry, we have to detect a circle ω_{10}^* and a non convex object ω_{11}^* composed by several circle arcs as a boundary. The algorithm is capable to detect both objects and increase the radio of the approximating ball for the non convex object in order to cover it properly. The results are adjoint in Figure 5.6.

In conclusion of these first simulations, this method permits to give us the number of objects we have to determine and their qualitative location if they are separated enough. Moreover, it is efficient to detect different types of shapes, including objects with corners, or even non convex obstacles, in the sense that this topological algorithm is able not only to find the number and relative location of this objects, it is also able to determine their 'relative size' (with respect to its topological set diameter, for example).

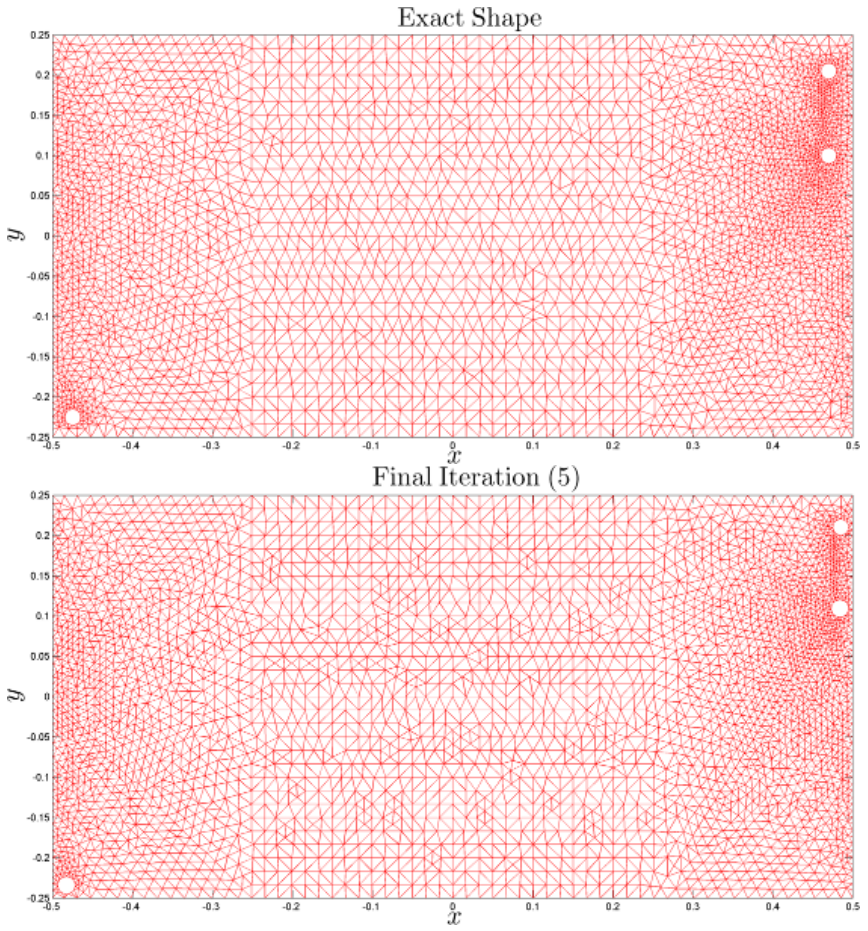

Figure 5.4: Detection of ω_4^*, ω_5^* and ω_{6bis}^*

5.1.3 Influence of the distance to the location of measurements

As been pointed out in [36] in the 3 dimensional case, the distance to the location of measurements is fundamental in order to get a good detection of the objects. In the following table 5.4, we notice that, when we move the object away from the boundary of measurements, we get a worse estimate of their location, and in a extreme case a completely wrong detection: more objects than the expected ones. This simple example shows that in our case we have the same problem as in 3-dimensional case: when we try to detect an object which is 'far away' from the boundary, the detection tends to locate it near the boundary (one of the coordinates is correctly estimated) but, as the distance increase, we get some problematic behavior, as we see in our example when the algorithm declares more objects than the real ones. This phenomenon of bad detection can be explained by the regularizing behavior of the Stokes equations (which is related to the behavior of the fundamental solution (4.7)). We emphasize this difficulty of detection pointing out that the functional $\mathcal{J}_{KV}$ and its topological gradient are less sensitive to the addition of obstacles when they are far away from the exterior boundary.

Table 5.3: Detection of ω_4^*, ω_5^* and ω_{6bis}^*

actual objects	(-0.475, -0.225)	(0.470, 0.100)	(0.470, 0.205)
approximate objects	(-0.480, -0.235)	(0.482, 0.105)	(0.485, 0.210)
relative error $\|c_{real} - c_{app}\|/\mathrm{di}am(\Omega)$	0.0100	0.0116	0.0141

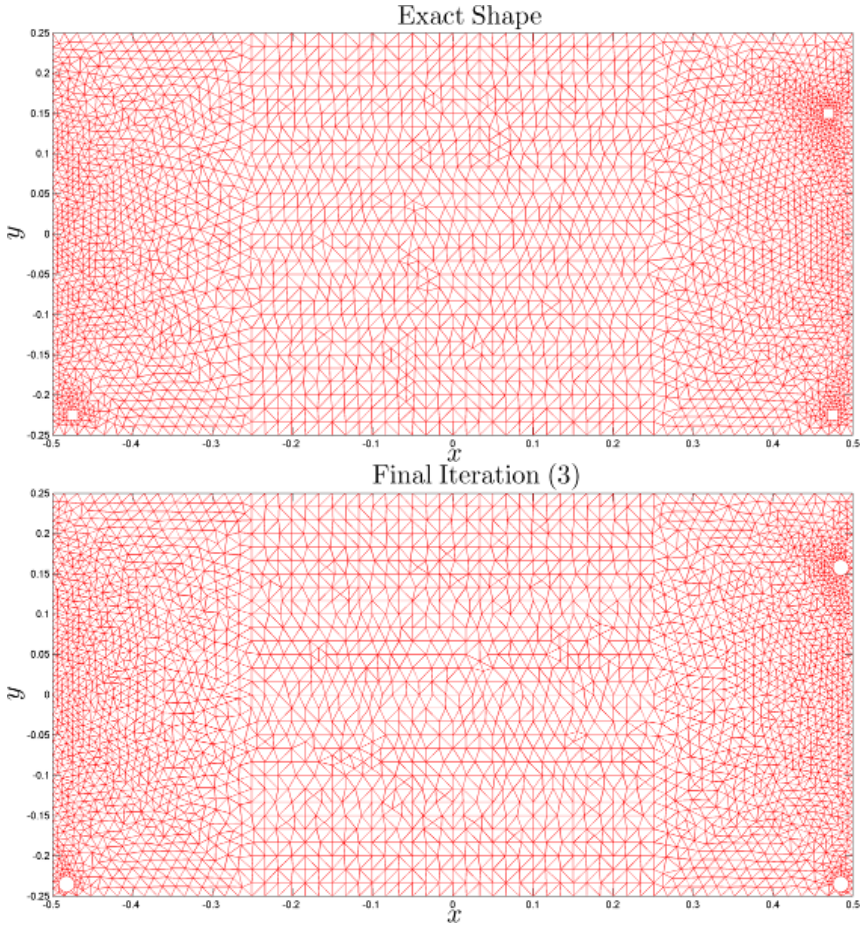

Figure 5.5: Detection of ω_7^*, ω_8^* and ω_9^*

5.1.4 Influence of the size of the objects

We now want to study how the size of an object (or several objects) modifies the quality of the detection given by our algorithm. In order to do that, we start by testing how is the detection of a single circle while we increase the radius. Notice that we consider the circle near to the boundary in order to get the best possible approximation as we have seen in the previous section. The following table 5.5 resumes this first test.

From this we can notice that, when the object is relatively small, the detection is quite efficient, but the quality is decreasing when the object becomes 'too big'. Notice that the main error is linked with the size of the approximation object, and

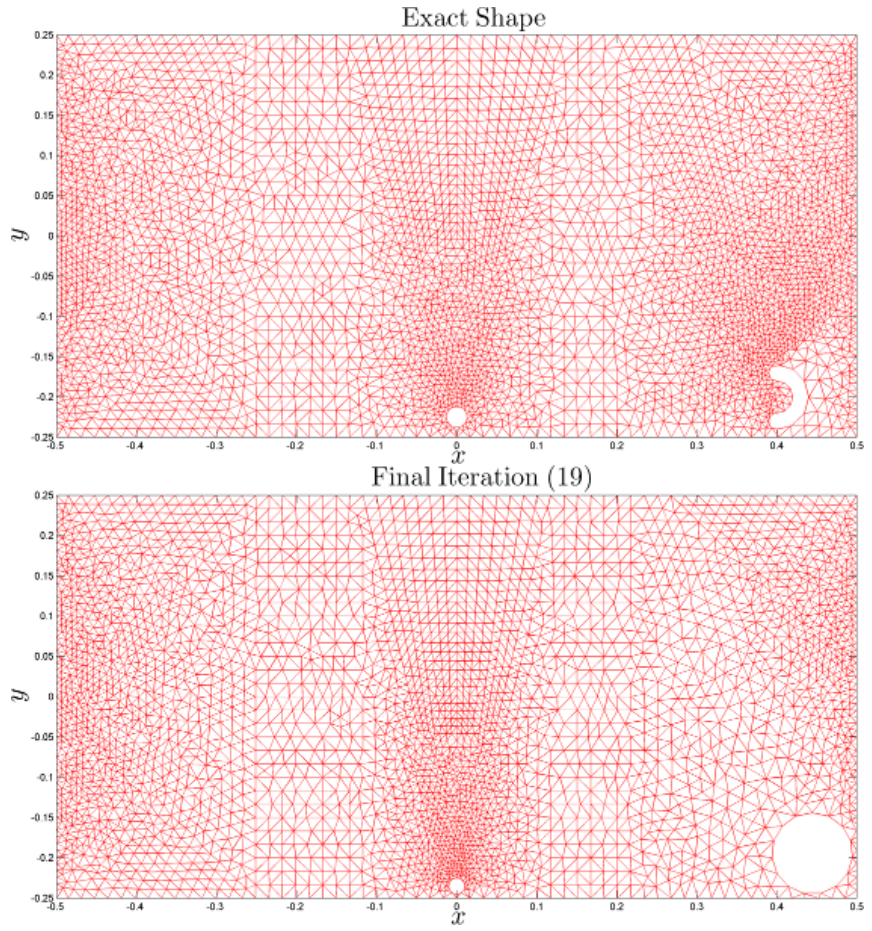

Figure 5.6: Detection of ω_{10}^* and ω_{11}^*

not with their relative position.

A more extreme example is putting a 'very big sized' object. In that case, which can be seen in Figure 5.7, we notice that the detection is completely wrong: we get an incorrect estimate of the number of objects.

Interesting results we get when we introduce several objects with higher size, as we can see in Figure 5.8: the coordinate location is relatively good, but the size approximation tends to stuck in one of the objects. The algorithm choses one of the objects in order to adjust its size on each iteration.

We can conclude that the detection of the objects depends strongly on their number and size. If we are trying to detect a single object we get a reasonable tolerance on the size of the object in order to get a good estimates of their position and size, and only 'big objects' are badly detected. In the case of several objects, the algorithm tends to predict their relative location but only the size of one object is improved between iterations.

Table 5.4: Detection when we move away from boundary

real object	approximation	relative error $\|c_{real} - c_{app}\|/\mathrm{diam}(\Omega)$
(0.475, 0.220)	(0.485, 0.223)	0.0093
(0.435, 0.180)	(0.480, 0.184)	0.0404
(0.395, 0.140)	(0.480, 0.144)	0.0761
(0.355, 0.100)	(0.470, 0.100)	0.1028
(0.300, 0.050)	2 objects	no value

Table 5.5: Detection when we increase the size of the object, with center rel. error $= \|c_{real} - c_{app}\|/\mathrm{diam}(\Omega)$ and radio rel. error $= |r_{real} - r_{app}|/r_{real}$

real object	approximation	center rel. error	radio rel. error
(0.475, 0.225), r=0.013	(0.485, 0.220), r=0.010	0.0100	0.2308
(0.470, 0.220), r=0.030	(0.469, 0.219), r=0.025	0.0012	0.1667
(0.450, 0.200), r=0.050	(0.449, 0.199), r=0.045	0.0012	0.1000
(0.420, 0.160), r=0.080	(0.439, 0.189), r=0.055	0.0310	0.3125

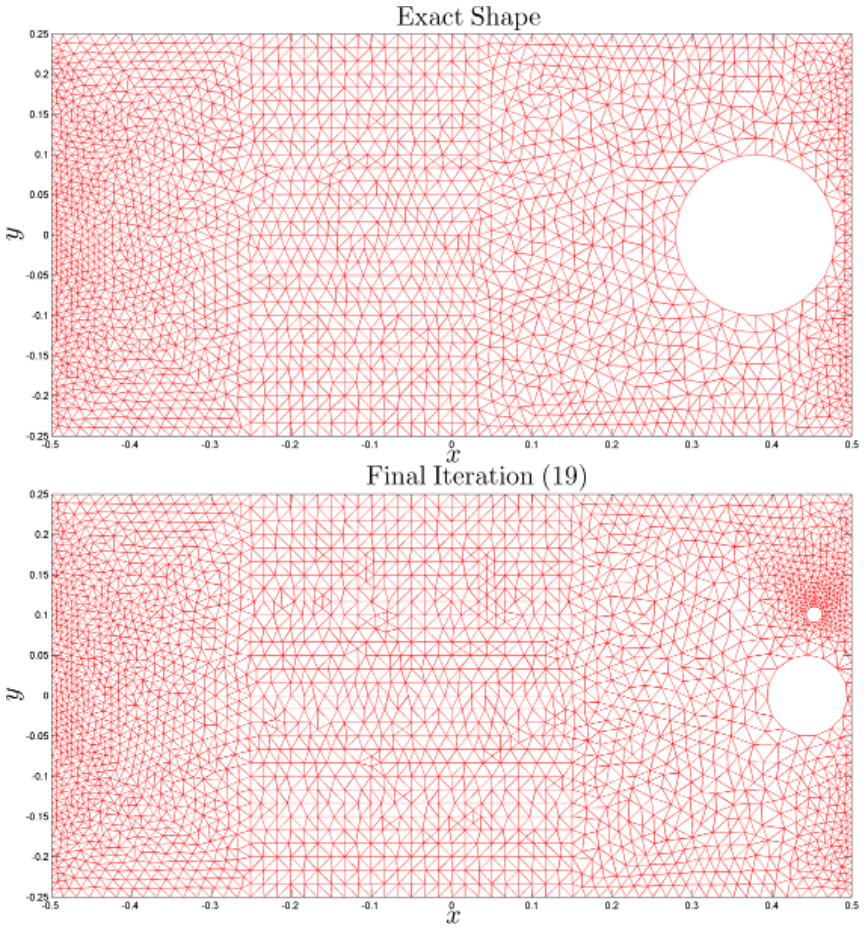

Figure 5.7: Bad Detection for a 'very big sized' object

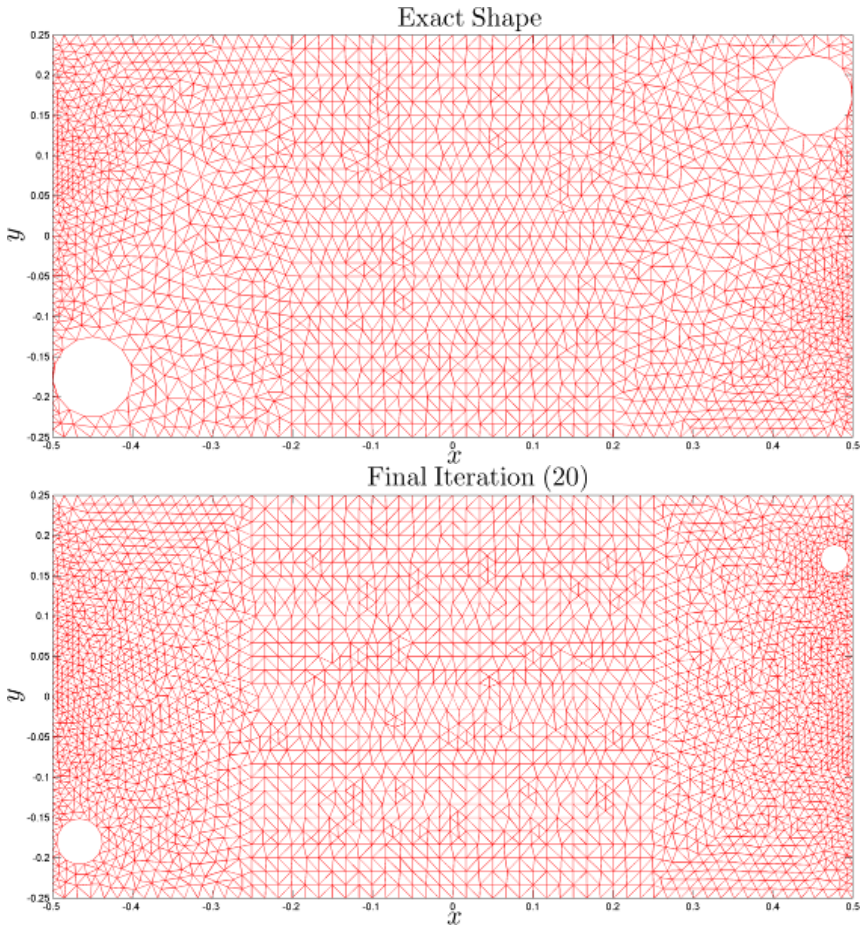

Figure 5.8: Detection of several 'big sized' objects

5.1.5 Simulations with noisy data

We now want to study how robust is our algorithm in presence of noisy data. For this, we decompose the measurement $\boldsymbol{g} = g_1\mathbf{e_1} + g_2\mathbf{e_2}$ (where $(\mathbf{e_1}, \mathbf{e_2})$ is the canonical basis of $\mathbb{R}^2$) and we consider the following noisy versions of g_1 and g_2:

$$g_1^\sigma := g_1 + \sigma\frac{\|g_1\|_{\mathrm{L}^2(O)}}{\|u_1\|_{\mathrm{L}^2(O)}}u_1 \quad \text{and} \quad g_2^\sigma := g_2 + \sigma\frac{\|g_2\|_{\mathrm{L}^2(O)}}{\|u_2\|_{\mathrm{L}^2(O)}}u_2,$$

where u_1, u_2 are random variables given by an uniform distribution in $[-0.5, 0.5)$ and $\sigma > 0$ is a scaling parameter. Notice that this definition implies that the data g_1 and g_2 are contaminated by some relative error of amplitude σ in $\mathrm{L}^2(O)$. Then, the noisy data will be:

$$\boldsymbol{g}^\sigma = g_1^\sigma\mathbf{e_1} + g_2^\sigma\mathbf{e_2}.$$

For this test, we consider the same domain Ω and and the same measure region O as in the previous ones and the objects are the circles or radius $r = 0.015$ centered in $(0, -0.230)$, $(-0.350, -0.230)$ and $(0.470, 0.150)$. The results are presented in tables 5.6 and 5.7.

Table 5.6: Detection when we introduce noisy data: results.

Noise Level	real objects	approximations
$\sigma = 0\%$	(0.350, -0.230), r=0.013 (-0.350, -0.230), r=0.013 (0.470, 0.150), r=0.013	(0.350, -0.232), r=0.011 (-0.355, -0.231), r=0.013 (0.480, 0.152), r=0.011
$\sigma = 5\%$	(0.350, -0.230), r=0.013 (-0.350, -0.230), r=0.013 (0.470, 0.150), r=0.013	(0.350, -0.235), r=0.012 (-0.358, -0.234), r=0.011 (0.482, 0.149), r=0.010
$\sigma = 15\%$	(0.350, -0.230), r=0.013 (-0.350, -0.230), r=0.013 (0.470, 0.150), r=0.013	(0.350, -0.235), r=0.010 (-0.358, -0.234), r=0.011 (0.485, 0.157), r=0.010
$\sigma = 25\%$	(0.350, -0.230), r=0.013 (-0.350, -0.230), r=0.013 (0.470, 0.150), r=0.013	(0.350, -0.235), r=0.010 (-0.358, -0.235), r=0.010 (-0.111, -0.235), r=0.010
$\sigma = 30\%$	(0.350, -0.230), r=0.013 (-0.350, -0.230), r=0.013 (0.470, 0.150), r=0.013	4 objects found

From this tables we can observe that our algorithm is able to detect with precision the number and relative position of several small obstacles near the boundary O where the measurements are taken, when the boundary data $\boldsymbol{g}$ is contaminated with a moderated amount of noise. When the boundary data contains a higher level of noise, the relative position becomes for one object is wrong and finally the algorithm detects an incorrect number of obstacles and therefore the detection becomes completely wrong.

5.2 A blending method which combines the topological and geometrical shape optimization algorithms

The previous numerical simulations show that, using the topological gradient algorithm, one can detect the number of objects and their qualitative location but we do not have informations about the shapes of the objects. Hence it can provide initial shapes for an optimization method based on the boundary variation method for which we have to know the number of connected objects we have to reconstruct (see [37]). We present here a combination of these two approaches in order to find the number of objects, their locations and their shapes.

As mentioned in the introduction, combinations of several shape optimization methods was recently tested by several authors. The most of them used the level set method (see [4, 59, 30]). We also mention the algorithm proposed by Pantz *et al.* in [73] which uses boundary variations, topological derivatives and homogenization

Table 5.7: Detection when we introduce noisy data: relative errors.

Noise Level	centers rel. errors	radius rel. errors
$\sigma = 0\%$	0.0017	0.1538
	0.0045	0.0000
	0.0091	0.1538
$\sigma = 5\%$	0.0044	0.0769
	0.008	0.1538
	0.0107	0.2308
$\sigma = 15\%$	0.0044	0.2308
	0.008	0.1538
	0.0148	0.2308
$\sigma = 25\%$	0.0044	0.2308
	0.0084	0.2308
	0.6234	0.2308
$\sigma = 30\%$	no value	no value

methods. We here present an algorithm only based on the classical shape gradient and the topological gradient, without using the level set method or some homogenization methods.

We first recall some theoretical results concerning the computation of the shape derivative of the Kohn-Vogelius functional (see [37] for details). We precise that, in this part, in order to simplify the notation, we will not use the index $^\varepsilon$: hence we will use $\omega = \omega_\varepsilon$, $\boldsymbol{u}_D = \boldsymbol{u}_D^\varepsilon$ and $\boldsymbol{u}_M = \boldsymbol{u}_M^\varepsilon$.

5.2.1 Shape derivative of the Kohn-Vogelius functional

Let $\mathrm{d}_0 > 0$ fixed (small). We define $\mathcal{O}_{\mathrm{d}_0}$ the set of all open subsets ω of Ω with a $C^{1,1}$ boundary such that $\mathrm{d}(x, \partial\Omega) > \mathrm{d}_0$ for all $x \in \omega$ and such that $\Omega \backslash \overline{\omega}$ is connected. The set $\mathcal{O}_{\mathrm{d}_0}$ is referred as the set of admissible geometries. We also define Ω_{d_0} an open set with a C^∞ boundary such that

$$\{x \in \Omega\,;\ \mathrm{d}(x, \partial\Omega) > \mathrm{d}_0/2\} \subset \Omega_{\mathrm{d}_0} \subset \{x \in \Omega\,;\ \mathrm{d}(x, \partial\Omega) > \mathrm{d}_0/3\}\,.$$

To define the shape derivatives, we will use the velocity method introduced by Murat and Simon in [69]. To this end, we need to introduce the space of admissible deformations

$$\boldsymbol{U} := \left\{\boldsymbol{\theta} \in \mathbf{W}^{2,\infty}(\mathbb{R}^N);\ \mathrm{Supp}\ \boldsymbol{\theta} \subset \overline{\Omega_{\mathrm{d}_0}}\right\}.$$

For details concerning the differentiation with respect to the domain, we refer to the papers of Simon [78, 79] and the books of Henrot and Pierre [61] and of Sokołowski and Zolésio [81].

We consider a domain $\omega \in \mathcal{O}_{\mathrm{d}_0}$. Then, we have the following proposition (see [37, Proposition 2]):

Proposition 5.1 (First order shape derivative of the functional) *For $\boldsymbol{V} \in \boldsymbol{U}$, the Kohn-Vogelius cost functional $\mathcal{J}_{KV}$ is differentiable at ω in the direction $\boldsymbol{V}$ with*

$$\mathrm{D}\mathcal{J}_{KV}(\Omega\backslash\overline{\omega}) \cdot \boldsymbol{V} = -\int_{\partial\omega} (\sigma(\boldsymbol{w}, q)\,\mathbf{n}) \cdot \partial_{\mathbf{n}} \boldsymbol{u_D} (\boldsymbol{V} \cdot \mathbf{n}) + \frac{1}{2}\nu \int_{\partial\omega} |\mathcal{D}(\boldsymbol{w})|^2 (\boldsymbol{V} \cdot \mathbf{n}), \quad (5.2)$$

where $(\boldsymbol{w}, q)$ is defined by

$$\boldsymbol{w} := \boldsymbol{u}_D - \boldsymbol{u}_M \qquad \text{and} \qquad q := p_D - p_M.$$

Moreover, Proposition 4 in [37] explains the difficulties encountered to solve numerically this problem. Indeed, the gradient has not a uniform sensitivity with respect to the deformation direction. Hence, since the problem is severely ill-posed, we need some regularization methods to solve it numerically, for example by adding to the functional a penalization in terms of the perimeter (see [29] or [43]). Here we choose to make a parametric regularization using a parametric model of shape variations.

5.2.2 Numerical simulations

Framework for the numerical simulations

We follow the same strategy than in [37] that we recall for readers convenience. We restrict ourselves to star-shaped domains and use polar coordinates for parametrization: the boundary $\partial\omega$ of the object can be then parametrized by

$$\partial\omega = \left\{ \begin{pmatrix} x_0 \\ y_0 \end{pmatrix} + r(\theta) \begin{pmatrix} \cos\theta \\ \sin\theta \end{pmatrix},\ \theta \in [0, 2\pi) \right\},$$

where $x_0, y_0 \in \mathbb{R}$ and where r is a $C^{1,1}$ function, 2π-periodic and without double point. Taking into account of the ill-posedness of the problem, we approximate the polar radius r by its truncated Fourier series

$$r_N(\theta) := a_0^N + \sum_{k=1}^{N} a_k^N \cos(k\theta) + b_k^N \sin(k\theta),$$

for the numerical simulations. Indeed this regularization by projection permits to remove *high frequencies* generated by $\cos(k\theta)$ and $\sin(k\theta)$ for $k >> 1$, for which the functional is degenerated.

Then, the unknown shape is entirely defined by the coefficients $(a_{\mathrm{i}}, b_{\mathrm{i}})$. Hence, for $k = 1, \ldots, N$, the corresponding deformation directions are respectively,

$$\boldsymbol{V}_1 := \boldsymbol{V}_{x_0} := \begin{pmatrix} 1 \\ 0 \end{pmatrix}, \quad \boldsymbol{V}_2 := \boldsymbol{V}_{y_0} := \begin{pmatrix} 0 \\ 1 \end{pmatrix}, \quad \boldsymbol{V}_3(\theta) := \boldsymbol{V}_{a_0}(\theta) := \begin{pmatrix} \cos\theta \\ \sin\theta \end{pmatrix},$$

$$\boldsymbol{V}_{2k+2}(\theta) := \boldsymbol{V}_{a_k}(\theta) := \cos(k\theta) \begin{pmatrix} \cos\theta \\ \sin\theta \end{pmatrix}, \boldsymbol{V}_{2k+3}(\theta) := \boldsymbol{V}_{b_k}(\theta) := \sin(k\theta) \begin{pmatrix} \cos\theta \\ \sin\theta \end{pmatrix},$$

$\theta \in [0, 2\pi)$. The gradient is then computed component by component using its characterization (see Proposition 5.1, formula (5.2)):

$$\Big(\nabla \mathcal{J}_{KV}(\Omega \backslash \overline{\omega})\Big)_k = \mathrm{D}\mathcal{J}_{KV}(\Omega \backslash \overline{\omega}) \cdot \boldsymbol{V}_k, \qquad k = 1, \ldots, 2N+3.$$

This equality is simply that

$$\lim_{t \to 0} \frac{\mathcal{J}_{KV}\big((\mathbf{I} + t\boldsymbol{V}_k)(\Omega \backslash \overline{\omega})\big) - \mathcal{J}_{KV}(\Omega \backslash \overline{\omega})}{t} = \mathrm{D}\mathcal{J}_{KV}(\omega) \cdot \boldsymbol{V}_k.$$

Algorithm

The first step is the use of the previous topological gradient algorithm described in Section 5.1.1. It permits to obtain the number of objects and their qualitative location which represents an initial shape ω_0 for a reconstruction using a boundary variation method. Then, the geometrical optimization method used for the numerical simulation is here the classical gradient algorithm with a line search (using the Wolfe conditions: see for example [70, eq. (3.6) page 34]):
Algorithm

1. fix a number of iterations M and take the initial shape ω_0 (which can have several connected components) given by the previous topological algorithm,
2. solve problems (4.4) and (4.5) with $\omega_\varepsilon = \omega_{\mathrm{i}}$,
3. extract $\nabla \boldsymbol{u_D}$, $\nabla \boldsymbol{u_N}$, p_D and p_M on $\partial\omega_{\mathrm{i}}$ and compute $\nabla \mathcal{J}_{KV}(\Omega \setminus \overline{\omega_{\mathrm{i}}})$ using formula (5.2),
4. use the Wolfe conditions to compute a satisfying step length α_{i},
5. move the coefficients associated to the shape: $\omega_{\mathrm{i}+1} = \omega_{\mathrm{i}} - \alpha_{\mathrm{i}} \nabla \mathcal{J}_{KV}(\omega_{\mathrm{i}})$,
6. get back to the step 2. while $\mathrm{i} < M$.

We precise that we here use the *adaptive method* described in [37, Section 4.3]. It consists in increasing gradually the number of parameters during the algorithm to a fixed final number of parameters. For example, if we want to work with nineteen parameters (which will be the case here), we begin by working with two parameters during five iterations, then with three parameters (we add the radius) during five more iterations, and then we add two search parameters every fifteen iterations. The algorithm is then the same than the one described above only replacing step 5. by

$$\omega_{\mathrm{i}+1}(1:m) = \omega_{\mathrm{i}}(1:m) - \alpha_{\mathrm{i}} \nabla \mathcal{J}_{KV}(\omega_{\mathrm{i}})(1:m),$$

where $\omega_{\mathrm{i}}(1:m)$ represents the m first coefficients parametrizing the shape ω_{i} (the same notation holds for $\nabla \mathcal{J}_{KV}(\Omega \setminus \overline{\omega_{\mathrm{i}}})(1:m)$). The number m grows to the fixed final number of parameters following the procedure described previously.

To finish, we precise that we use the finite element library MÉLINA (see [65]) to make this geometrical shape optimization part.

Numerical simulations

The framework is the following: we assume the kinematic viscosity ν is equal to 1, the exterior boundary is assumed to be the unit circle centered at the origin and we consider the exterior Dirichlet boundary condition

$$\boldsymbol{f} := \begin{pmatrix} \mathrm{n}_2 \\ -\mathrm{n}_1 \end{pmatrix} = \left\{ \begin{pmatrix} \sin\theta \\ -\cos\theta \end{pmatrix}, \theta \in [0, 2\pi) \right\},$$

where $\mathbf{n} = (\mathrm{n}_1, \mathrm{n}_2)$ is the exterior unit normal. Notice that $\boldsymbol{f}$ is such that the compatibility condition (4.1) is satisfied. We assume that we make the measurement on the whole disk $\partial\Omega$ except the lower right quadrant. Here, we want to detect two squares ω_{12}^* and ω_{13}^* centered respectively at $(-0.6\,,\,0.3)$ and $(0.6\,,\,0.3)$ with a distance between the center and the vertices equal to 0.2.

The first step, which is the topological approach, leads to two circles of radius 0.15 centered respectively at $(-0.573\,,\,0.328)$ and $(0.533\,,\,0.328)$ (see the 'initial shape' in Figure 5.9). Since the real objects are "big", we impose here $r_{\min} = 0.15$ in the topological algorithm (see (5.1)). This means that, practically, we assume that we know the characteristic size of the objects, *i.e.* if the objects are small or big.

Then, the shape optimization algorithm leads to a good approximation of the shapes, at least for one of the obstacle (see Figure 5.9). We also underline the fact

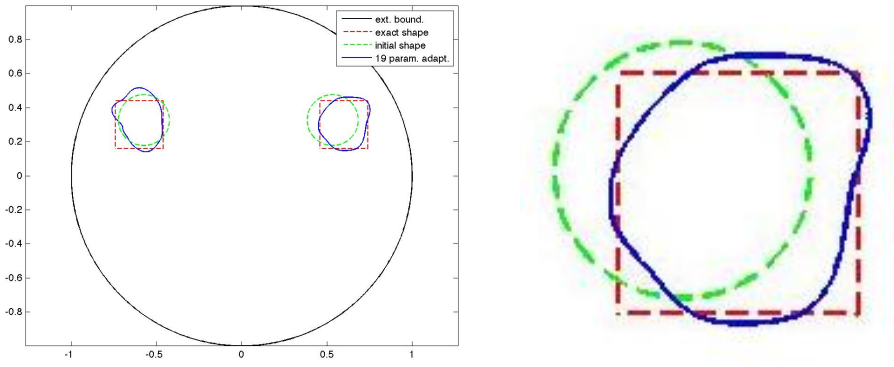

Figure 5.9: Detection of ω_{12}^* and ω_{13}^* with the combined approach (the initial shape is the one obtained after the "topological step") and zoom on the improvement with the geometrical step for ω_{13}^*

that, after the topological step, the cost of the functional is here about 1.26 and that, after the geometrical step, we obtain a cost about $2 \cdot 10^{-2}$ which qualitatively means that we improved the detection.

In conclusion, this blending method which combines the topological and the geometrical shape methods leads to good result in the identification of obstacle immersed in a fluid: we detect both the number of obstacles, their locations and their shapes.

Conclusions and Perspectives

Conclusions

In this thesis work we have addressed the resolution of the inverse problem of obstacle detection via boundary measurements. This problem has been studied by means of optimization methods, using in particular two powerful tools from shape optimization: the geometrical shape optimization and the topological shape optimization.

We have divided this work in two parts, in the first one we have studied a scalar case, in which the boundary measurements are limited only to an accessible region of the boundary. As the data is partial, in order to work with an optimization problem we are forced to develop and perform a method in order to complete the data. For this aim we develop a method to solve the data completion problem, this is, the problem to reconstruct the unaccessible data for a given function which satisfies some PDE (in this case, the Laplace equation). We propose a Kohn-Vogelius approach for the data completion problem and perform the regularization of this functional, in order to lead to a better numerical results. For the regularized functional we have proved convergence properties to the real solution of the original problem and we have proposed a Morozov discrepancy criteria in order to chose the regularization parameter accordingly with the noise level.

With the help of the previous results and in order to solve the inverse problem of obstacle detection, we have extended the Kohn-Vogelius functional in order to consider the unknown obstacle as a variable of this functional. Using two different gradient algorithms: one based on descent directions for the unknown data, and one based on the shape derivative of the functional. With this approach we were able to recover the position and relative shape of several obstacle configurations, even when the available Cauchy data is polluted by noise.

In the second part of this work, using a Kohn-Vogelius approach, we have detected the number of potential objects immersed in a two dimensional fluid and their qualitative location. To do this, we have computed the topological gradient of the considered Kohn-Vogelius functional using an asymptotic expansion of the solution of the Stokes equations in the whole domain when we add small obstacles inside: we adapted the usual 3D techniques to the two dimensional setting case,

in which the classical asymptotic expansion of the solution of the Stokes equations are no longer valid. We obtain a formula valid for any geometry of small obstacles, which is a particular characteristic of the two dimensional setting of the problem. We have made some numerical attempts which have shown that 'not too big' obstacles close to the part of the boundary where we make the measurements can be detected. Once these restrictions are satisfied, the detection is quite efficient, even for objects with corners or non convex shapes. Finally, we have proposed and implemented an algorithm which combines the topological sensitive analysis approach with the classical shape derivative approach. This blending method led us to detect the number of objects using a topological step and, if this first step actually gives the total number of obstacles, a geometrical shape optimization step detects their approximate location and approximate shape from only the boundary measurements. This method gives interesting results in the simulations.

Perspectives

The perspectives from the presented work are numerous, here we present the most straightforward with respect to the results and models presented.

The data completion problem and the inverse obstacle problem with partial boundary data for the (Navier-)Stokes equations

In first place, for the data completion problem, the natural perspective is to consider the vectorial case, in particular for a fluid case. This is, by considering the Stokes and Navier-Stokes data completion problems. The consideration of this problem is natural, some engineering problems can be stated as a data completion problem (for example detect small leaks to control water loss, see [62]).

The problem in this case could be stated as:
Let $\eta \in \{0, 1\}$ (Stokes and Navier-Stokes respectively). Given Cauchy data $(\boldsymbol{g}_N, \boldsymbol{g}_D)$ in $\mathbf{H}^{-1/2}(\Gamma_{obs}) \times \mathbf{H}^{1/2}(\Gamma_{obs})$, *find* $(\boldsymbol{u}, p) \in \mathbf{H}^1(\Omega) \times \mathrm{L}^2(\Omega)$ *such that*

$$\left\{ \begin{array}{rcll} -\nu\Delta\boldsymbol{u} + \eta(\boldsymbol{u}\cdot\nabla)\boldsymbol{u} + \nabla p &=& 0 & \text{in } \Omega \\ \boldsymbol{u} &=& \boldsymbol{g}_D & \text{on } \Gamma_{obs} \\ \sigma(\boldsymbol{u}, p)\mathbf{n} &=& \boldsymbol{g}_N & \text{on } \Gamma_{obs}. \end{array} \right. \tag{5.3}$$

Is interesting to notice that this problem has not got many interest in the past, the number of works is small (see for example the works of Ben Abda *et al.* [16], Aboulaich *et al.* [2] and Bastay *et al.* [15]), and most of them are focused only on numerical methods. From the theoretical point of view, for the Stokes case, a uniqueness result is obtained by the author of this thesis, based on unique continuation theorem (see [49]), as well as an analog density lemma for 'compatible'

data $(\boldsymbol{g}_N, \boldsymbol{g}_D)$ into the space of all possible data, which is fundamental in order to develop a Kohn-Vogelius strategy. Up to our knowledge a Kohn-Vogelius strategy for the Stokes case should be possible, however, for the non-linear case difficulties may be found due to the non-linear term, in order to define optimality conditions and into the study of more fine properties when a regularization term is introduced. Naturally the inverse problem of obstacle detection with partial data may become a natural step after the development of the theory of the data completion problem, following the same strategy as the one adopted in this work.

The data completion problem in an abstract setting

The second perspective is based on a possible generalization of our approach for the data completion problem into an abstract setting, this is, by posing the problem of the minimization of the (regularized) Kohn-Vogelius functional into the resolution of a linear abstract system, by defining an operator A acting between some Hilbert spaces $\mathcal{X}, \mathcal{Y}$ such that:

- A is injective.
- A is not surjective.
- $\overline{Im(A)}^{\mathcal{Y}} = \mathcal{Y}$.

In this setting, y plays the role of the data and x is the solution of the data completion problem. This 'abstract setting' of the data completion problem comes from the abstract theory of inverse problems. For this specific problem Dardé [45] has proposed an abstract setting when the data completion problem is treated by using a quasi-reversibility (QR) approach. The biggest advantage of this formulation is based in the 'easy/natural' extension to other PDEs as been pointed in [45].

Computation of the regularization parameter in the data completion problem

In third place, we address to the development of techniques which allows to compute the regularization parameter ε given by some Morozov discrepancy principle, which takes an important role in the case where only polluted data is available. In the presented work we were able to propose a discrepancy measurement which defines a rule to compute the best regularization parameter $\varepsilon(\delta, y^\delta)$ such that it permits to have convergence of the minimizers from the polluted data to the minimizers of the unpolluted data, however we do not know how to implement it by means of a fast and robust method. We can follow the work of Bourgeois *et al.* in [24] where the authors propose a method in which the computation of the regularization parameter is computed as the solution of an unconstrained optimization problem, by means of using a duality method on the previously proposed abstract setting.

Computation of the topological gradient of the Kohn-Vogelius functional for the 2D Navier-Stokes equations

In fourth place, and now discussing perspectives for the topological approach of the obstacle problem, the natural extension would be to consider the stationary Navier-Stokes equation instead of the Stokes one. This is, by considering now the overdetermined problem

$$\left\{\begin{array}{rcll} -\nu\Delta\boldsymbol{u}+(\boldsymbol{u}\cdot\nabla)\boldsymbol{u}+\nabla p &=& \mathbf{0} & \text{in } \Omega\backslash\overline{\omega_\varepsilon^*} \\ \operatorname{div}\boldsymbol{u} &=& 0 & \text{in } \Omega\backslash\overline{\omega_\varepsilon^*} \\ \boldsymbol{u} &=& \boldsymbol{f} & \text{on } \partial\Omega \\ \boldsymbol{u} &=& \mathbf{0} & \text{on } \partial\omega_\varepsilon^* \\ \sigma(\boldsymbol{u},p)\mathbf{n} &=& \boldsymbol{g} & \text{on } O\subset\partial\Omega, \end{array}\right.$$

instead of (4.2), and therefore considering the auxiliary direct problems

$$\left\{\begin{array}{rcll} \text{Find } (\boldsymbol{u}_D^\varepsilon,p_D^\varepsilon)\in\mathbf{H}^1(\Omega\backslash\overline{\omega_\varepsilon})\times\mathrm{L}^2_0(\Omega\backslash\overline{\omega_\varepsilon}) & & & \text{such that} \\ -\nu\Delta\boldsymbol{u}_D^\varepsilon+(\boldsymbol{u}_D^\varepsilon\cdot\nabla)\boldsymbol{u}_D^\varepsilon+\nabla p_D^\varepsilon &=& \mathbf{0} & \text{in } \Omega\backslash\overline{\omega_\varepsilon} \\ \operatorname{div}\boldsymbol{u}_D^\varepsilon &=& 0 & \text{in } \Omega\backslash\overline{\omega_\varepsilon} \\ \boldsymbol{u}_D^\varepsilon &=& \boldsymbol{f} & \text{on } \partial\Omega \\ \boldsymbol{u}_D^\varepsilon &=& \mathbf{0} & \text{on } \partial\omega_\varepsilon \end{array}\right.$$

and

$$\left\{\begin{array}{rcll} \text{Find } (\boldsymbol{u}_M^\varepsilon,p_M^\varepsilon)\in\mathbf{H}^1(\Omega\backslash\overline{\omega_\varepsilon})\times\mathrm{L}^2(\Omega\backslash\overline{\omega_\varepsilon}) & & & \text{such that} \\ -\nu\Delta\boldsymbol{u}_M^\varepsilon+(\boldsymbol{u}_M^\varepsilon\cdot\nabla)\boldsymbol{u}_M^\varepsilon+\nabla p_M^\varepsilon &=& \mathbf{0} & \text{in } \Omega\backslash\overline{\omega_\varepsilon} \\ \operatorname{div}\boldsymbol{u}_M^\varepsilon &=& 0 & \text{in } \Omega\backslash\overline{\omega_\varepsilon} \\ \sigma(\boldsymbol{u}_M^\varepsilon,p_M^\varepsilon)\mathbf{n} &=& \boldsymbol{g} & \text{on } O \\ \boldsymbol{u}_M^\varepsilon &=& \boldsymbol{f} & \text{on } \partial\Omega\backslash\overline{O} \\ \boldsymbol{u}_M^\varepsilon &=& \mathbf{0} & \text{on } \partial\omega_\varepsilon, \end{array}\right.$$

with the Kohn-Vogelius functional as before:

$$\mathcal{J}_{KV}(\Omega\backslash\overline{\omega_\varepsilon}):=\frac{1}{2}\int_{\Omega\backslash\overline{\omega_\varepsilon}}\nu|\mathcal{D}(\boldsymbol{u}_D^\varepsilon)-\mathcal{D}(\boldsymbol{u}_M^\varepsilon)|^2.$$

Topological shape optimization for non-linear systems is not a big domain of research, the works are very limited, we can mention the thesis work of Chetboun [39] where topological derivatives are computed for cost functionals depending on the solution of the compressible Navier-Stokes system in the context of 'vortex generators' for aerodynamic flows. We can also mention the book of Novotny and Sokołowski [71] where very general cases for several systems are treated. Finally, the works of Amstutz (see [9, 10]) where he computes topological derivatives for stationary Navier-Stokes systems for very general costs functionals are particularly interesting. However, in our case several difficulties may appear, for example:

- The 2-dimensional case, following the methods we have applied in this work, may require some work in order to deal with the non-linearity.

- The decomposition of the difference $\mathcal{J}_{KV}(\Omega_{z,\varepsilon}) - \mathcal{J}_{KV}(\Omega)$ in decoupled terms given by (4.29) is no longer possible, due to the non linear terms on each system.

The obstacle inverse problem for a moving obstacle

Finally, a natural question that arises could be: *what happens if the obstacle is moving inside the domain of reference?*. This problem has been studied before in different settings, Conca *et al.* (see [41]) have studied this problem into the setting where a two-dimensional potential fluid has a rigid solid moving obstacle. In that case, and by means of complex variable techniques the authors were able to prove that the problem in general is ill-posed, but for some shapes with 'good symmetry' properties the detection could be performed and provides conditions for a full detection of the obstacle. In the three dimensional setting Conca, Schwindt and Takahashi [42] have obtained conditions for the identification of a rigid convex body moving in a fluid governed by Stokes equations. Up to our knowledge the problem of the detection of a rigid obstacle moving in a fluid governed by stationary (and then, non-stationary) Navier-Stokes equations is open as well as the development of numerical methods to the reconstruction of moving objects, via shape gradient methods or topological gradient methods. However, the introduction of non-linearities seems to be a gigantic difficulty in all these problems, as the formulation in all of the considered problems uses the linearity consistently and repeatedly.

Bibliography

[1] J. Abouchabaka and C. Tajani. An alternating KMF algorithm to solve the Cauchy problem for Laplace equation. *arXiv preprint arXiv:1405.3235*, 2014.

[2] R. Aboulaich, A. Ben Abda, and M. Kallel. A control type method for solving the Cauchy–Stokes problem. *Applied Mathematical Modelling*, 37(6):4295–4304, 2013.

[3] L. Afraites, M. Dambrine, K. Eppler, and D. Kateb. Detecting perfectly insulated obstacles by shape optimization techniques of order two. *Discrete Contin. Dyn. Syst. Ser. B*, 8(2):389–416 (electronic), 2007.

[4] G. Allaire, F. de Gournay, F. Jouve, and A.-M. Toader. Structural optimization using topological and shape sensitivity via a level set method. *Control Cybernet.*, 34(1):59–80, 2005.

[5] F. Alliot and C. Amrouche. Weak solutions for the exterior Stokes problem in weighted Sobolev spaces. *Math. Methods Appl. Sci.*, 23(6):575–600, 2000.

[6] C. Alvarez, C. Conca, L. Friz, O. Kavian, and J.H. Ortega. Identification of immersed obstacles via boundary measurements. *Inverse Problems*, 21(5):1531–1552, 2005.

[7] C. Amrouche and V. Girault. Problèmes généralisés de Stokes. *Portugal. Math.*, 49(4):463–503, 1992.

[8] C. Amrouche and V. Girault. Decomposition of vector spaces and application to the Stokes problem in arbitrary dimension. *Czechoslovak Math. J.*, 44(119)(1):109–140, 1994.

[9] S. Amstutz. The topological asymptotic for the Navier-Stokes equations. *ESAIM Control Optim. Calc. Var.*, 11(3):401–425 (electronic), 2005.

[10] S. Amstutz. Topological sensitivity analysis for some nonlinear PDE systems. *Journal de mathématiques pures et appliquées*, 85(4):540–557, 2006.

[11] S. Amstutz, M. Masmoudi, and B. Samet. The topological asymptotic for the Helmholtz equation. *SIAM J. Control Optim.*, 42(5):1523–1544 (electronic),

2003.

[12] S. Andrieux, T.N. Baranger, and A. Ben Abda. Solving Cauchy problems by minimizing an energy-like functional. *Inverse Problems*, 22(1):115, 2006.

[13] M. Azaïez, F. Ben Belgacem, and H. El Fekih. On Cauchy's problem: II. Completion, regularization and approximation. *Inverse problems*, 22(4):1307, 2006.

[14] M. Badra, F. Caubet, and M. Dambrine. Detecting an obstacle immersed in a fluid by shape optimization methods. *Math. Models Methods Appl. Sci.*, 21(10):2069–2101, 2011.

[15] G. Bastay, T. Johansson, V.A. Kozlov, and D. Lesnic. An alternating method for the stationary Stokes system. *ZAMM-Journal of Applied Mathematics and Mechanics/Zeitschrift für Angewandte Mathematik und Mechanik*, 86(4):268–280, 2006.

[16] A. Ben Abda, I. Ben Saad, and M. Hassine. Data completion for the Stokes system. *Comptes Rendus Mécanique*, 337(9):703–708, 2009.

[17] A. Ben Abda, M. Hassine, M. Jaoua, and M. Masmoudi. Topological sensitivity analysis for the location of small cavities in Stokes flow. *SIAM J. Control Optim.*, 48(5):2871–2900, 2009/10.

[18] F. Ben Belgacem. Why is the Cauchy problem severely ill-posed? *Inverse Problems*, 23(2):823, 2007.

[19] F. Ben Belgacem and H. El Fekih. On Cauchy's problem: I. A variational Steklov–Poincaré theory. *Inverse Problems*, 21(6):1915, 2005.

[20] F. Ben Belgacem, H. El Fekih, and F. Jelassi. The Lavrentiev regularization of the data completion problem. *Inverse Problems*, 24(4):045009, 2008.

[21] V. Bonnaillie-Noël and M. Dambrine. Interactions between moderately close circular inclusions: the Dirichlet-Laplace equation in the plane. *Asymptot. Anal.*, 84(3-4):197–227, 2013.

[22] V. Bonnaillie-Noël, M. Dambrine, F. Hérau, and G. Vial. On generalized Ventcel's type boundary conditions for Laplace operator in a bounded domain. *SIAM J. Math. Anal.*, 42(2):931–945, 2010.

[23] V. Bonnaillie-Noël, M. Dambrine, S. Tordeux, and G. Vial. Interactions between moderately close inclusions for the Laplace equation. *Math. Models Methods Appl. Sci.*, 19(10):1853–1882, 2009.

[24] L. Bourgeois and J. Dardé. A duality-based method of quasi-reversibility to solve the Cauchy problem in the presence of noisy data. *Inverse Problems*,

26(9):095016, 2010.

[25] L. Bourgeois and J. Dardé. A quasi-reversibility approach to solve the inverse obstacle problem. *Inverse Probl. Imaging*, 4(3):351–377, 2010.

[26] L. Bourgeois and J. Dardé. About stability and regularization of ill-posed elliptic Cauchy problems: the case of Lipschitz domains. *Applicable Analysis*, 89(11):1745–1768, 2010.

[27] F. Boyer and P. Fabrie. *Éléments d'analyse pour l'étude de quelques modèles d'écoulements de fluides visqueux incompressibles*, volume 52 of *Mathématiques & Applications (Berlin)*. Springer-Verlag, Berlin, 2006.

[28] H. Brezis. *Analyse fonctionnelle*. Collection Mathématiques Appliquées pour la Maîtrise. Masson, Paris, 1983. Théorie et applications.

[29] D. Bucur and G. Buttazzo. *Variational methods in shape optimization problems*. Progress in Nonlinear Differential Equations and their Applications, 65. Birkhäuser Boston Inc., Boston, MA, 2005.

[30] M. Burger, B. Hackl, and W. Ring. Incorporating topological derivatives into level set methods. *J. Comput. Phys.*, 194(1):344–362, 2004.

[31] A. Carpio and M.-L. Rapún. Solving inhomogeneous inverse problems by topological derivative methods. *Inverse Problems*, 24(4):045014, 32, 2008.

[32] A. Carpio and M.-L. Rapún. Hybrid topological derivative and gradient-based methods for electrical impedance tomography. *Inverse Problems*, 28(9):095010, 22, 2012.

[33] A. Carpio and M.-L. Rapún. Parameter identification in photothermal imaging. *J. Math. Imaging Vision*, 49(2):273–288, 2014.

[34] A. Carpio and M.L. Rapún. Topological derivatives for shape reconstruction. In *Inverse problems and imaging*, volume 1943 of *Lecture Notes in Math.*, pages 85–133. Springer, Berlin, 2008.

[35] F. Caubet, C. Conca, and M. Godoy. On the detection of several obstacles in 2D Stokes flow: topological sensitivity and combination with shape derivatives. *Inverse problems and Imaging*, 10(2):327–267, 2016.

[36] F. Caubet and M. Dambrine. Localization of small obstacles in Stokes flow. *Inverse Problems*, 28(10):105007, 31, 2012.

[37] F. Caubet, M. Dambrine, D. Kateb, and C.Z. Timimoun. A Kohn-Vogelius formulation to detect an obstacle immersed in a fluid. *Inverse Probl. Imaging*, 7(1):123–157, 2013.

[38] J. Céa, S. Garreau, Ph. Guillaume, and M. Masmoudi. The shape and

topological optimizations connection. *Comput. Methods Appl. Mech. Engrg.*, 188(4):713–726, 2000. IV WCCM, Part II (Buenos Aires, 1998).

[39] J. Chetboun. *Conception de formes aérodynamiques en présence d'écoulements décollés: contrôle et optimisation.* PhD thesis, Ecole Polytechnique, 2010.

[40] A. Cimetiere, F. Delvare, M. Jaoua, and F. Pons. Solution of the Cauchy problem using iterated Tikhonov regularization. *Inverse Problems*, 17(3):553, 2001.

[41] C. Conca, M. Malik, and A. Munnier. Detection of a moving rigid solid in a perfect fluid. *Inverse Problems*, 26(9):095010, 18, 2010.

[42] C. Conca, E.L. Schwindt, and T. Takahashi. On the identifiability of a rigid body moving in a stationary viscous fluid. *Inverse Problems*, 28(1):015005, 2011.

[43] M. Dambrine. On variations of the shape Hessian and sufficient conditions for the stability of critical shapes. *RACSAM Rev. R. Acad. Cienc. Exactas Fís. Nat. Ser. A Mat.*, 96(1):95–121, 2002.

[44] J. Dardé. *Quasi-Reversibility and level set methods applied to elliptic inverse problems.* Theses, Université Paris-Diderot - Paris VII, December 2010.

[45] J. Dardé. Iterated quasi-reversibility method applied to elliptic and parabolic data completion problems. *arXiv preprint arXiv:1503.08641*, 2015.

[46] O. Dorn and D. Lesselier. Level set methods for inverse scattering. *Inverse Problems*, 22(4):R67–R131, 2006.

[47] O. Dorn and D. Lesselier. Level set methods for inverse scattering—some recent developments. *Inverse Problems*, 25(12):125001, 11, 2009.

[48] H.W. Engl, M. Hanke, and A. Neubauer. *Regularization of Inverse Problems*, volume 375. Springer Science & Business Media, 1996.

[49] C. Fabre and G. Lebeau. Prolongement unique des solutions de l'equation de Stokes. *Comm. Partial Differential Equations*, 21(3-4):573–596, 1996.

[50] R. Finn and D. R. Smith. On the linearized hydrodynamical equations in two dimensions. *Archive for Rational Mechanics and Analysis*, 25(1):1–25, 1967.

[51] A.V. Fursikov. *Optimal control of distributed systems. Theory and applications.* American Mathematical Soc., 1999.

[52] G.P. Galdi. *An introduction to the mathematical theory of the Navier-Stokes equations.*, volume 38 of *Springer Tracts in Natural Philosophy*. Springer-Verlag, New York, 1994. Linearized steady problems.

[53] Ph. Guillaume and K. Sid Idris. The topological asymptotic expansion for the Dirichlet problem. *SIAM J. Control Optim.*, 41(4):1042–1072 (electronic), 2002.

[54] Ph. Guillaume and K. Sid Idris. Topological sensitivity and shape optimization for the Stokes equations. *SIAM J. Control Optim.*, 43(1):1–31 (electronic), 2004.

[55] J. Hadamard. *Le probleme de Cauchy et les équations aux dérivées partielles linéaires hyperboliques*, volume 220. Paris, 1932.

[56] H. Han, L. Ling, and T. Takeuchi. An energy regularization for Cauchy problems of Laplace equation in annulus domain. *Communications in Computational Physics*, 9(4):878, 2011.

[57] M. Hassine. Shape optimization for the Stokes equations using topological sensitivity analysis. *ARIMA*, 5:216–229, 2006.

[58] M. Hassine and M. Masmoudi. The topological asymptotic expansion for the quasi-Stokes problem. *ESAIM Control Optim. Calc. Var.*, 10(4):478–504 (electronic), 2004.

[59] L. He, Ch.-Y. Kao, and S. Osher. Incorporating topological derivatives into shape derivatives based level set methods. *J. Comput. Phys.*, 225(1):891–909, 2007.

[60] F. Hecht. Finite Element Library FREEFEM++. `http://www.freefem.org/ff++/`.

[61] A. Henrot and M. Pierre. *Variation et optimisation de formes*, volume 48 of *Mathématiques & Applications (Berlin)*. Springer, Berlin, 2005. Une analyse géométrique.

[62] Y.-J. Kim, K. Miyazaki, and H. Tsukamoto. Leak detection in pipe using transient flow and genetic algorithm. *Journal of mechanical science and technology*, 22(10):1930–1936, 2008.

[63] V.A. Kozlov, V.G. Maz'ya, and A.V. Fomin. An iterative method for solving the Cauchy problem for elliptic equations. *Zhurnal Vychislitel'noi Matematiki i Matematicheskoi Fiziki*, 31(1):64–74, 1991.

[64] A. Litman, D. Lesselier, and F. Santosa. Reconstruction of a two-dimensional binary obstacle by controlled evolution of a level-set. *Inverse Problems*, 14(3):685–706, 1998.

[65] D. Martin. Finite Element Library MÉLINA. `http://homepage.mac.com/danielmartin/melina/`.

[66] V. Maz'ya and A. Movchan. Asymptotic treatment of perforated domains with-

out homogenization. *Math. Nachr.*, 283(1):104–125, 2010.

[67] V. Maz′ya, S. Nazarov, and B. Plamenevskij. *Asymptotic theory of elliptic boundary value problems in singularly perturbed domains. Vol. I*, volume 111 of *Operator Theory: Advances and Applications*. Birkhäuser Verlag, Basel, 2000. Translated from the German by Georg Heinig and Christian Posthoff.

[68] V.G. Maz′ya and S.V. Poborchi. *Differentiable functions on bad domains*. World Scientific Publishing Co. Inc., River Edge, NJ, 1997.

[69] F. Murat and J. Simon. *Sur le contrôle par un domaine géométrique*. Rapport du L.A. 189, 1976. Université de Paris VI, France.

[70] J. Nocedal and S.J. Wright. *Numerical optimization*. Springer Series in Operations Research and Financial Engineering. Springer, New York, second edition, 2006.

[71] A.A. Novotny and J. Sokołowski. *Topological derivatives in shape optimization*. Springer Science & Business Media, 2012.

[72] O. A. Oleĭnik, A. S. Shamaev, and G. A. Yosifian. *Mathematical problems in elasticity and homogenization*, volume 26 of *Studies in Mathematics and its Applications*. North-Holland Publishing Co., Amsterdam, 1992.

[73] O. Pantz and K. Trabelsi. Simultaneous shape, topology, and homogenized properties optimization. *Struct. Multidiscip. Optim.*, 34(4):361–365, 2007.

[74] Osher S. and J.A. Sethian. Fronts propagating with curvature-dependent speed: Algorithms based on Hamilton-Jacobi formulations. *Journal of Computational Physics*, 79(1):12 – 49, 1988.

[75] G. Savaré. Regularity and perturbation results for mixed second order elliptic problems. *Communications in Partial Differential Equations*, 22(5-6):869–899, 1997.

[76] A. Schumacher. Topologieoptimisierung von Bauteilstrukturen unter Verwendung von Lopchpositionierungkrieterien. *Thesis*, 1995. Universität-Gesamthochschule-Siegen.

[77] K. Sid Idris. Sensibilité topologique en optimisation de forme. *Thesis*, 2001. Institut National des Sciences Apliquées.

[78] J. Simon. Differentiation with respect to the domain in boundary value problems. *Numer. Funct. Anal. Optim.*, 2(7-8):649–687 (1981), 1980.

[79] J. Simon. Second variations for domain optimization problems. In *Control and estimation of distributed parameter systems (Vorau, 1988)*, volume 91 of *Internat. Ser. Numer. Math.*, pages 361–378. Birkhäuser, Basel, 1989.

[80] J. Sokołowski and A. Żochowski. On the topological derivative in shape optimization. Technical report, INRIA Lorraine, May 1997.

[81] J. Sokołowski and J.-P. Zolésio. *Introduction to shape optimization*, volume 16 of *Springer Series in Computational Mathematics*. Springer-Verlag, Berlin, 1992. Shape sensitivity analysis.

[82] E. Sonnendrücker. *Three courses on Partial Differential Equations*, volume 4. Walter de Gruyter, 2003.

[83] A.N. Tikhonov and V.I.A. Arsenin. *Solutions of ill-posed problems*. Scripta series in mathematics. Winston, 1977.

Appendices

Appendix A

Useful results for the Data Completion Problem

A.1 Some results about the space $\mathrm{H}^1(\Omega, \Delta)$

As we defined before, we consider into this work the space $\mathrm{H}^1(\Omega, \Delta)$ given by

$$\mathrm{H}^1(\Omega, \Delta) := \left\{ u \in \mathrm{H}^1(\Omega) : \Delta u \in \mathrm{L}^2(\Omega) \right\},$$

in this section we mention some important properties about this space. Proofs can be found in [44, Chapter 1] and [82, Chapter 3].

Proposition A.1 $\mathrm{H}^1(\Omega, \Delta)$ *with the scalar product* $(u, v)_{\mathrm{H}^1(\Omega,\Delta)} = (u, v)_{\mathrm{L}^2(\Omega)} + (\Delta u, \Delta v)_{\mathrm{L}^2(\Omega)}$ *is a Hilbert space.*

In this space we can define the notion of normal derivative in the an open part of the boundary of Ω, as the following result states:

Proposition A.2 *Given* Ω *connected and bounded set in* $\mathbb{R}^{\mathrm{d}}$, Γ *a Lipschitz open part of the boundary* $\partial\Omega$, $\mathbf{n}$ *the exterior normal vector of* Ω *which is defined a.e. on* Γ. *Then, we have* $\forall u \in \mathrm{H}^1(\Omega, \Delta)$*:*

$$\partial_{\mathbf{n}} u := \sum_{j=1}^{\mathrm{d}} \frac{\partial u}{\partial x_j} \mathbf{n}_{\mathrm{i}} \in \mathrm{H}^{-1/2}(\Gamma).$$

Moreover, the map $u \in \mathrm{H}^1(\Omega, \Delta) \mapsto \partial_{\mathbf{n}} u \in \mathrm{H}^{-1/2}(\Gamma)$ *is continuous and surjective.*

With this property, we can define properly, by density, a Green formula:

Proposition A.3 *Given* Ω *connected and bounded set in* $\mathbb{R}^{\mathrm{d}}$ *with Lipschitz bound-*

ary, $\mathbf{n}$ *the exterior normal vector of* Ω*. We have,* $\forall (u, v) \in \mathrm{H}^1(\Omega, \Delta) \times \mathrm{H}^1(\Omega)$*:*

$$\int_\Omega (\Delta u \cdot v + \nabla u \cdot \nabla v)\, \mathrm{d}x = \langle \partial_{\mathbf{n}} u, v \rangle_{\mathrm{H}^{-1/2}, \mathrm{H}^{1/2}}$$

Appendix B

Useful results for Stokes equations

B.1 Some results on the Stokes problem with mixed boundary conditions

We recall classical results about the Stokes problem with mixed boundary conditions: a theorem of existence and uniqueness of the solution and a local regularity result.

We note C a generic positive constant, only depending on the geometry of the domain and on the dimension, which may change from line to line.

First, let us introduce some notations: for Ω an open set of $\mathbb{R}^N$ an open subset $\omega \subset\subset \Omega$ and a part O of the exterior boundary $\partial\Omega$, we define

$$\boldsymbol{V}_O(\Omega\backslash\overline{\omega}) := \left\{\boldsymbol{u} \in \mathbf{H}^1(\Omega\backslash\overline{\omega});\ \operatorname{div}\boldsymbol{u} = 0 \text{ in } \Omega\backslash\overline{\omega},\ \boldsymbol{u} = \mathbf{0} \text{ on } \partial\omega \cup (\partial\Omega\backslash\overline{O})\right\}.$$

Moreover, we denote respectively by $\langle\cdot,\cdot\rangle_{\Omega\backslash\overline{\omega}}$ and $\langle\cdot,\cdot\rangle_{\partial\Omega}$ (or $\langle\cdot,\cdot\rangle_{\partial\omega}$) the duality product between $\left[\mathbf{H}^1(\Omega\backslash\overline{\omega})\right]'$ and $\mathbf{H}^1(\Omega\backslash\overline{\omega})$ and between $\mathbf{H}^{-1/2}(\partial\Omega)$ and $\mathbf{H}^{1/2}(\partial\Omega)$.

Theorem B.1 (Existence and uniqueness of the solution) *Let Ω be a bounded Lipschitz open set of $\mathbb{R}^N$ ($N \in \mathbb{N}^*$) and let $\omega \subset\subset \Omega$ be a Lipschitz open subset of Ω such that $\Omega\backslash\overline{\omega}$ is connected. Let $O \subset \partial\Omega$ be a part of the exterior boundary and $\nu > 0$. Let $\boldsymbol{f} \in \left[\mathbf{H}^1(\Omega\backslash\overline{\omega})\right]'$, $\boldsymbol{h_{ext}} \in \mathbf{H}^{1/2}(\partial\Omega\backslash\overline{O})$, $\boldsymbol{h_O} \in \mathbf{H}^{-1/2}(O)$ and $\boldsymbol{h_{int}} \in \mathbf{H}^{1/2}(\partial\omega)$. Then, the problem*

$$\left\{\begin{array}{rcll} -\nu\Delta\boldsymbol{u} + \nabla p &=& \boldsymbol{f} & \text{in } \Omega\backslash\overline{\omega} \\ \operatorname{div}\boldsymbol{u} &=& 0 & \text{in } \Omega\backslash\overline{\omega} \\ \sigma(\boldsymbol{u},p)\mathbf{n} &=& \boldsymbol{h_O} & \text{on } O \\ \boldsymbol{u} &=& \boldsymbol{h_{ext}} & \text{on } \partial\Omega\backslash\overline{O} \\ \boldsymbol{u} &=& \boldsymbol{h_{int}} & \text{on } \partial\omega \end{array}\right. \tag{B.1}$$

admits a unique solution $(\boldsymbol{u},p) \in \mathbf{H}^1(\Omega\backslash\overline{\omega}) \times \mathrm{L}^2(\Omega\backslash\overline{\omega})$ and the following estimate

holds:

$$\|\boldsymbol{u}\|_{\mathbf{H}^1(\Omega\backslash\overline{\omega})} + \|p\|_{\mathrm{L}^2(\Omega\backslash\overline{\omega})} \leq C\left(\|\boldsymbol{f}\|_{[\mathbf{H}^1(\Omega\backslash\overline{\omega})]'} + \|\boldsymbol{h_{ext}}\|_{\mathbf{H}^{1/2}(\partial\Omega\backslash\overline{O})} + \|\boldsymbol{h}_O\|_{\mathbf{H}^{-1/2}(O)} + \|\boldsymbol{h_{int}}\|_{\mathbf{H}^{1/2}(\partial\omega)}\right).$$

Proof. *Step 1: existence and uniqueness.* According to [8, Lemma 3.3], let us consider $\boldsymbol{H} \in \mathbf{H}^1(\Omega\backslash\overline{\omega})$ such that $\operatorname{div}\boldsymbol{H} = 0$ in $\Omega\backslash\overline{\omega}$, $\boldsymbol{H} = \boldsymbol{h_{int}}$ on $\partial\omega$, $\boldsymbol{H} = \boldsymbol{h_{ext}}$ on $\partial\Omega\backslash\overline{O}$ such that $\displaystyle\int_{\partial\Omega\cup\partial\omega} \boldsymbol{H}\cdot\mathbf{n} = 0$ and satisfying

$$\|\boldsymbol{H}\|_{\mathbf{H}^1(\Omega\backslash\overline{\omega})} \leq C\left(\|\boldsymbol{h_{int}}\|_{\mathbf{H}^{1/2}(\partial\omega)} + \|\boldsymbol{h_{ext}}\|_{\mathbf{H}^{1/2}(\partial\Omega\backslash\overline{O})}\right). \tag{B.2}$$

Then the couple $(\boldsymbol{U} := \boldsymbol{u} - \boldsymbol{H}, p) \in \mathbf{H}^1(\Omega\backslash\overline{\omega}) \times \mathrm{L}^2(\Omega\backslash\overline{\omega})$ satisfies

$$\left\{\begin{array}{rcll} -\nu\Delta\boldsymbol{U} + \nabla p &=& \boldsymbol{f} + \nu\Delta\boldsymbol{H} & \text{in } \Omega\backslash\overline{\omega} \\ \operatorname{div}\boldsymbol{U} &=& 0 & \text{in } \Omega\backslash\overline{\omega} \\ \sigma(\boldsymbol{U}, P)\mathbf{n} &=& \boldsymbol{h_O} + \nu(\nabla\boldsymbol{H} + {}^t\nabla\boldsymbol{H})\mathbf{n} & \text{on } O \\ \boldsymbol{U} &=& \mathbf{0} & \text{on } \partial\Omega\backslash\overline{O} \\ \boldsymbol{U} &=& \mathbf{0} & \text{on } \partial\omega. \end{array}\right.$$

According to Lax-Milgram's theorem, there exists a unique $\boldsymbol{U} \in \boldsymbol{V}_O(\Omega\backslash\overline{\omega})$ such that for all $\boldsymbol{v} \in \boldsymbol{V}_O(\Omega\backslash\overline{\omega})$

$$\nu\int_{\Omega\backslash\overline{\omega}} \nabla\boldsymbol{U} : \nabla\boldsymbol{v} = \langle\boldsymbol{f}, \boldsymbol{v}\rangle_{\Omega\backslash\overline{\omega}} - \nu\int_{\Omega\backslash\overline{\omega}} \nabla\boldsymbol{H} : \nabla\boldsymbol{v} - \left\langle\boldsymbol{h_O} + \nu(\nabla\boldsymbol{H} + {}^t\nabla\boldsymbol{H})\mathbf{n}, \boldsymbol{v}\right\rangle_O \tag{B.3}$$

and we have, using (B.2),

$$\|\boldsymbol{U}\|_{\mathbf{H}^1(\Omega\backslash\overline{\omega})} \leq C\left(\|\boldsymbol{f}\|_{\left[\mathbf{H}^1(\Omega\backslash\overline{\omega})\right]'} + \|\boldsymbol{h_{int}}\|_{\mathbf{H}^{1/2}(\partial\omega)} + \|\boldsymbol{h_{ext}}\|_{\mathbf{H}^{1/2}(\partial\Omega\backslash\overline{O})} + \|\boldsymbol{h_O}\|_{\mathbf{H}^{-1/2}(O)}\right). \tag{B.4}$$

In particular (B.3) is true for all $\boldsymbol{v} \in \boldsymbol{V}_O(\Omega\backslash\overline{\omega}) \cap \mathbf{H}^1_0(\Omega\backslash\overline{\omega})$. Then using De Rham's theorem (see for example [7, Lemma 2.7]), there exists $p \in \mathrm{L}^2(\Omega\backslash\overline{\omega})$, up to an additive constant, such that for all $\boldsymbol{v} \in \mathbf{H}^1_0(\Omega\backslash\overline{\omega})$

$$\nu\int_{\Omega\backslash\overline{\omega}} \nabla\boldsymbol{U} : \nabla\boldsymbol{v} - \int_{\Omega\backslash\overline{\omega}} p\operatorname{div}\boldsymbol{v} = \left\langle\boldsymbol{f}|_{\mathbf{H}^1_0(\Omega\backslash\overline{\omega})}, \boldsymbol{v}\right\rangle_{\mathbf{H}^{-1}(\Omega\backslash\overline{\omega}),\mathbf{H}^1_0(\Omega\backslash\overline{\omega})} - \nu\int_{\Omega\backslash\overline{\omega}} \nabla\boldsymbol{H} : \nabla\boldsymbol{v}. \tag{B.5}$$

According to [8, Lemma 3.3] or [52, Theorem 3.2], we define $\boldsymbol{\varphi}_N \in \mathbf{H}^1(\Omega\backslash\overline{\omega})$ such that $\operatorname{div}\boldsymbol{\varphi}_N = 1$ in $\Omega\backslash\overline{\omega}$, $\boldsymbol{\varphi}_N = \mathbf{0}$ on $\partial\Omega\backslash\overline{O}$ and $\boldsymbol{\varphi}_N = \mathbf{0}$ on $\partial\omega$ with $\displaystyle\int_O \boldsymbol{\varphi}_N\cdot\mathbf{n} \neq 0$. Let $\boldsymbol{v} \in \mathbf{H}^1(\Omega\backslash\overline{\omega})$ such that $\boldsymbol{v} = \mathbf{0}$ on $\partial\Omega\backslash\overline{O}$, $\boldsymbol{v} = \mathbf{0}$ on $\partial\omega$ and define

$$c_b(\boldsymbol{v}) = \frac{1}{\int_{\partial(\Omega\backslash\omega)} \boldsymbol{\varphi}_N\cdot\mathbf{n}} \int_{\partial(\Omega\backslash\overline{\omega})} \boldsymbol{v}\cdot\mathbf{n}.$$

Using again [8, Lemma 3.3] or [52, Theorem 3.2], we define $\boldsymbol{v}_2 \in \boldsymbol{V}_O(\Omega\backslash\overline{\omega})$ in such a way that $\boldsymbol{v} = \boldsymbol{v}_1 + \boldsymbol{v}_2 + c_b(\boldsymbol{v})\boldsymbol{\varphi}_N$, where $\boldsymbol{v}_1 \in \mathbf{H}^1_0(\Omega\backslash\overline{\omega})$ satisfies $\operatorname{div}\boldsymbol{v}_1 = \operatorname{div}(\boldsymbol{v} - c_b(\boldsymbol{v})\boldsymbol{\varphi}_N)$. Using (B.3) and (B.5), we then obtain

$$\begin{aligned}
&\int_{\Omega\backslash\overline{\omega}} \nu\nabla\boldsymbol{U} : \nabla\boldsymbol{v} - \int_{\Omega\backslash\overline{\omega}} p \operatorname{div}\boldsymbol{v} = \langle \boldsymbol{f}, \boldsymbol{v}\rangle_{\Omega\backslash\overline{\omega}} - \nu\int_{\Omega\backslash\overline{\omega}} \nabla\boldsymbol{H} : \nabla\boldsymbol{v} \\
&- \left\langle \boldsymbol{h_O} - \nu(\nabla\boldsymbol{H} + {}^t\nabla\boldsymbol{H})\mathbf{n}, \boldsymbol{v}\right\rangle_O + \int_{\Omega\backslash\overline{\omega}} \nu\nabla\boldsymbol{U} : \nabla(c_b(\boldsymbol{v})\boldsymbol{\varphi}_N) - \int_{\Omega\backslash\overline{\omega}} p\operatorname{div}(c_b(\boldsymbol{v})\boldsymbol{\varphi}_N) \\
&-\langle \boldsymbol{f}, c_b(\boldsymbol{v})\boldsymbol{\varphi}_N\rangle_{\Omega\backslash\overline{\omega}} + \nu\int_{\Omega\backslash\overline{\omega}} \nabla\boldsymbol{H} : \nabla(c_b(\boldsymbol{v})\boldsymbol{\varphi}_N) + \left\langle \boldsymbol{h_O} - \nu(\nabla\boldsymbol{H} + {}^t\nabla\boldsymbol{H})\mathbf{n}, c_b(\boldsymbol{v})\boldsymbol{\varphi}_N\right\rangle_O .
\end{aligned}$$

Therefore, choosing the additive constant for p such that

$$\begin{aligned}
&\int_{\Omega\backslash\overline{\omega}} p = \nu\int_{\Omega\backslash\overline{\omega}} \nabla\boldsymbol{U} : \nabla\boldsymbol{\varphi}_N \\
&-\langle \boldsymbol{f}, c_b(\boldsymbol{v})\boldsymbol{\varphi}_N\rangle_{\Omega\backslash\overline{\omega}} + \nu\int_{\Omega\backslash\overline{\omega}} \nabla\boldsymbol{H} : \nabla(c_b(\boldsymbol{v})\boldsymbol{\varphi}_N) + \left\langle \boldsymbol{h_O} - \nu(\nabla\boldsymbol{H} + {}^t\nabla\boldsymbol{H})\mathbf{n}, c_b(\boldsymbol{v})\boldsymbol{\varphi}_N\right\rangle_O ,
\end{aligned}$$

we prove that there exists a unique pair $(\boldsymbol{U}, p) \in \boldsymbol{V}_O(\Omega\backslash\overline{\omega}) \times \mathrm{L}^2(\Omega\backslash\overline{\omega})$ such that for all $\boldsymbol{v} \in \mathbf{H}^1(\Omega\backslash\overline{\omega})$ with $\boldsymbol{v} = \mathbf{0}$ on $\partial\Omega\backslash\overline{O}$ and $\boldsymbol{v} = \mathbf{0}$ on $\partial\omega$,

$$\int_{\Omega\backslash\overline{\omega}} \nu\nabla\boldsymbol{U} : \nabla\boldsymbol{v} - \int_{\Omega\backslash\overline{\omega}} p\operatorname{div}\boldsymbol{v} = \langle \boldsymbol{f}, \boldsymbol{v}\rangle_{\Omega\backslash\overline{\omega}} - \nu\int_{\Omega\backslash\overline{\omega}} \nabla\boldsymbol{H} : \nabla\boldsymbol{v} - \left\langle \boldsymbol{h_O} - \nu(\nabla\boldsymbol{H} + {}^t\nabla\boldsymbol{H})\mathbf{n}, \boldsymbol{v}\right\rangle_{\partial\Omega} . \tag{B.6}$$

Step 2: estimate. Let $\boldsymbol{v} := \widetilde{\boldsymbol{v}} + c(p)\boldsymbol{\varphi}_N$, where

$$c(p) := \frac{1}{|\Omega\backslash\overline{\omega}|}\int_{\Omega\backslash\overline{\omega}} p$$

and $\widetilde{\boldsymbol{v}} \in \mathbf{H}^1_0(\Omega\backslash\overline{\omega})$ is such that $\operatorname{div}\widetilde{\boldsymbol{v}} = p - c(p)$ and $\|\widetilde{\boldsymbol{v}}\|_{\mathbf{H}^1_0(\Omega\backslash\overline{\omega})} \leq C\,\|p\|_{\mathrm{L}^2(\Omega\backslash\overline{\omega})}$ (see [8, Lemma 3.3]). Using $\boldsymbol{v}$ in (B.6), and according to (B.4), we obtain

$$\begin{aligned}
&\|\boldsymbol{U}\|_{\mathbf{H}^1(\Omega\backslash\overline{\omega})} + \|p\|_{\mathrm{L}^2(\Omega\backslash\overline{\omega})} \\
&\qquad \leq C\left(\|\boldsymbol{f}\|_{\left[\mathbf{H}^1(\Omega\backslash\overline{\omega})\right]'} + \|\boldsymbol{h_{int}}\|_{\mathbf{H}^{1/2}(\partial\omega)} + \|\boldsymbol{h_{ext}}\|_{\mathbf{H}^{1/2}(\partial\Omega\backslash\overline{O})} + \|\boldsymbol{h_O}\|_{\mathbf{H}^{-1/2}(O)}\right)
\end{aligned}$$

and hence

$$\begin{aligned}
&\|\boldsymbol{u}\|_{\mathbf{H}^1(\Omega\backslash\overline{\omega})} + \|p\|_{\mathrm{L}^2(\Omega\backslash\overline{\omega})} \\
&\qquad \leq C\left(\|\boldsymbol{f}\|_{\left[\mathbf{H}^1(\Omega\backslash\overline{\omega})\right]'} + \|\boldsymbol{h_{int}}\|_{\mathbf{H}^{1/2}(\partial\omega)} + \|\boldsymbol{h_{ext}}\|_{\mathbf{H}^{1/2}(\partial\Omega\backslash\overline{O})} + \|\boldsymbol{h_O}\|_{\mathbf{H}^{-1/2}(O)}\right) .
\end{aligned}$$

□

B.2 A result concerning the space of traces

Here we recall a result used in the paper concerning the boundary values of functions, in particular when domains depend on a parameter (see [68, Chapter 4]):

Theorem B.2 ([68] Section 4.1.3. page 214) *Let Ω and ω be two bounded simply connected domains of $\mathbb{R}^N$ ($N \geq 2$) of class $C^{0,1}$. Let $p \in (1, +\infty)$, $\varepsilon \in (0, 1/2)$ and $\omega_\varepsilon := \varepsilon\omega$. Let us assume that $\overline{\omega_\varepsilon} \subset \Omega$ and that there exists a constant $c > 0$ depending only of N, p, ω and Ω such that $\mathrm{d}(\omega_\varepsilon, \partial\Omega) > c\varepsilon$. Then*

$$\langle\cdot\rangle_{p,\partial\omega_\varepsilon} \sim a(\varepsilon)\,\|\cdot\|_{\mathrm{L}^p(\partial\omega_\varepsilon)} + [\cdot]_{p,\partial\omega_\varepsilon}$$

where

$$\begin{aligned}
\langle f\rangle_{p,\partial\omega_\varepsilon} &:= \inf\left\{\|u\|_{\mathrm{W}^{1,p}(\Omega\setminus\overline{\omega_\varepsilon})},\, u \in \mathrm{W}^{1,p}(\Omega\setminus\overline{\omega_\varepsilon}), u_{|\partial\omega_\varepsilon} = f\right\},\\
a(\varepsilon) &:= \begin{cases} \varepsilon^{\frac{1-N}{p}}\min(1, \varepsilon^{\frac{N}{p}-1}), & \text{for } p < N\\ \varepsilon^{\frac{1-N}{p}}\min(1, |\log\varepsilon|^{\frac{1-p}{p}}), & \text{for } p = N\\ \varepsilon^{\frac{1-N}{p}}, & \text{for } p > N, \end{cases}
\end{aligned}$$

and

$$\begin{aligned}
[f]_{1,\partial\omega_\varepsilon} &:= |\partial\omega_\varepsilon|^{-1}\iint_{\partial\omega_\varepsilon\times\partial\omega_\varepsilon} |f(x) - f(y)|\,\mathrm{ds}(x)\mathrm{ds}(y)\\
[f]_{p,\partial\omega_\varepsilon} &:= \left(\iint_{\partial\omega_\varepsilon\times\partial\omega_\varepsilon} \frac{|f(x)-f(y)|^p}{|x-y|^{N+p-2}}\mathrm{ds}(x)\mathrm{ds}(y)\right)^{1/p} \qquad \text{for } p \in (1, +\infty).
\end{aligned}$$

B.3 Some results on the exterior Stokes problem

B.3.1 Definition of the weighted Sobolev spaces

First, we recall the definition of the weighted Sobolev spaces. We introduce the weight function $\rho(x) := (2 + |x|^2)^{1/2}$ and the following Sobolev spaces (for more details, see [5]):

Definition B.3 *Let $1 < p < \infty$. For each real number α and each open set $\mathcal{O} \subset \mathbb{R}^{\mathrm{d}}$, we set*

$$\mathrm{L}^p_\alpha(\mathcal{O}) := \left\{u \in \mathcal{D}'(\mathcal{O}),\, \rho^\alpha u \in \mathrm{L}^p(\mathcal{O})\right\},$$

$$\mathrm{W}^{1,p}_\alpha(\mathcal{O}) := \begin{cases} \left\{u \in \mathcal{D}'(\mathcal{O}),\, u \in \mathrm{L}^p_{\alpha-1}(\mathcal{O}),\, \nabla u \in \mathbf{L}^p_\alpha(\mathcal{O})\right\} & \text{if } \frac{\mathrm{d}}{p} + \alpha \neq 1,\\ \left\{u \in \mathcal{D}'(\mathcal{O}),\, (\ln(\rho))^{-1}u \in \mathrm{L}^p_{\alpha-1}(\mathcal{O}),\, \nabla u \in \mathbf{L}^p_\alpha(\mathcal{O})\right\} & \text{if } \frac{\mathrm{d}}{p} + \alpha = 1. \end{cases}$$

Consider now the space $\overset{\circ}{\mathrm{W}}{}^{1,p}_\alpha(\mathcal{O}) := \overline{\mathcal{D}(\mathcal{O})}^{\|\cdot\|_{\mathrm{W}^{1,p}_\alpha(\mathcal{O})}}$. It is standard to check that

$$\overset{\circ}{\mathrm{W}}{}^{1,p}_\alpha(\mathcal{O}) = \left\{v \in \mathrm{W}^{1,p}_\alpha(\mathcal{O}),\, v_{|\partial\mathcal{O}} = 0\right\}.$$

The dual space of $\overset{\circ}{\mathrm{W}}{}^{1,p}_{\alpha}(\mathcal{O})$ *is denoted by* $\mathrm{W}^{-1,p'}_{-\alpha}(\mathcal{O})$, *where* p' *is such that* $\dfrac{1}{p}+\dfrac{1}{p'}=1$ *(it is a subspace of* $\mathcal{D}'(\mathcal{O})$*).*

Notice that these spaces are reflexive Banach spaces with respect to the norms:

$$\begin{aligned}
\|u\|_{\mathrm{L}^p_\alpha(\mathcal{O})} &:= \|\rho^\alpha u\|_{\mathrm{L}^p(\mathcal{O})}\,,\\
\|u\|_{\mathrm{W}^{1,p}_\alpha(\mathcal{O})} &:= \begin{cases} \left(\|u\|^p_{\mathrm{L}^p_{\alpha-1}(\mathcal{O})}+\|\nabla u\|^p_{\mathbf{L}^p_\alpha(\mathcal{O})}\right)^{1/p} & \text{if } \frac{\mathrm{d}}{p}+\alpha\neq 1,\\ \left(\left\|\frac{u}{\ln(\rho)}\right\|^p_{\mathrm{L}^p_{\alpha-1}(\mathcal{O})}+\|\nabla u\|^p_{\mathbf{L}^p_\alpha(\mathcal{O})}\right)^{1/p} & \text{if } \frac{\mathrm{d}}{p}+\alpha=1. \end{cases}
\end{aligned}$$

B.3.2 The exterior Stokes problem in two dimensions

The following results are presented in [77], we present them here for reader's convenience. We first recall the following lemma concerning the Stokes problem in the whole space $\mathbb{R}^2$:

Lemma B.4 *Let* $(\boldsymbol{u},p)$ *be a solution of*

$$\left\{\begin{array}{rcll} -\nu\Delta\boldsymbol{u}+\nabla p &=& \mathbf{0} & \text{in}\,\mathbb{R}^2\\ \operatorname{div}\boldsymbol{u} &=& 0 & \text{in}\,\mathbb{R}^2. \end{array}\right. \tag{B.7}$$

Then every solution which is a tempered distribution should be a polynomial.

Proof. Applying Fourier transform to (B.7) we immediately notice that the support of $\hat{\boldsymbol{u}}$ and $\hat{p}$ is contained in $\{0\}$. Therefore, those distributions should be a finite sum of Dirac deltas, which implies that $\boldsymbol{u}$ and p are polynomials. □

Decomposition of the solution of the exterior Stokes problem

Let ω be a Lipschitz open set of $\mathbb{R}^2$ and let $\boldsymbol{\mathcal{W}}(\overline{\omega}^c) := \left\{\boldsymbol{v}\in\mathbf{W}^{1,2}_0(\overline{\omega}^c);\operatorname{div}\boldsymbol{v}=0\right\}$ where $\overline{\omega}^c := \mathbb{R}^2\setminus\overline{\omega}$. $\boldsymbol{\mathcal{W}}(\overline{\omega}^c)$ is a closed subspace of $\mathbf{W}^{1,2}_0(\overline{\omega}^c)$ when we consider the induced norm. Notice that the bilinear form $a(\boldsymbol{u},\boldsymbol{v})=\displaystyle\int_{\overline{\omega}^c}\mathcal{D}(\boldsymbol{u}):\mathcal{D}(\boldsymbol{v})$ is coercive in $\boldsymbol{\mathcal{W}}(\overline{\omega}^c)$ (as well as in $\mathbf{W}^{1,2}_0(\omega)$). Therefore, for $\boldsymbol{\varphi}\in\mathbf{H}^{1/2}(\partial\omega)$ such that $\displaystyle\int_{\partial\omega}\boldsymbol{\varphi}\cdot\mathbf{n}=0$, the problem:

$$\left\{\begin{array}{rcll} -\nu\Delta\boldsymbol{u}+\nabla p &=& \mathbf{0} & \text{in } \overline{\omega}^c\\ \operatorname{div}\boldsymbol{u} &=& 0 & \text{in } \overline{\omega}^c\\ \boldsymbol{u} &=& \boldsymbol{\varphi} & \text{on } \partial\omega, \end{array}\right. \tag{B.8}$$

is well-posed and has a unique solution in $\mathbf{W}^{1,2}_0(\overline{\omega}^c)$ (and also in $\mathbf{W}^{1,2}_0(\omega)$). We present here an explicit representation of $\boldsymbol{u}$ and p.

In such case, we have:

$$-\nu\Delta\boldsymbol{u} + \nabla p = [\mathcal{D}(\boldsymbol{u})\mathbf{n}]\delta_{\partial\omega} =: \boldsymbol{T} \text{ in } \boldsymbol{\mathcal{D}}'(\mathbb{R}^2).$$

Now, let us define:

$$\boldsymbol{v} := E * \boldsymbol{T},\ q := \boldsymbol{P} * \boldsymbol{T},$$

where $(E, \boldsymbol{P})$ is the fundamental solution of the Stokes system given by (4.7) and $*$ denotes the convolution product. Then,

$$-\nu\Delta\boldsymbol{v} + \nabla q = \boldsymbol{T} \text{ in } \boldsymbol{\mathcal{D}}'(\mathbb{R}^2).$$

Now notice that the pair $(\boldsymbol{u} - \boldsymbol{v}, p - q)$ solves (B.7), then by the previous lemma this solution should be a polynomial. Then:

$$\boldsymbol{u} = E * \boldsymbol{T} + \boldsymbol{U}_1 = \int_{\partial\omega} \boldsymbol{t}(x)E(y-x)\mathrm{d}s(x) + \boldsymbol{U}_1,$$
$$p = P * \boldsymbol{T} + P_1 = \int_{\partial\omega} \boldsymbol{t}(x)\boldsymbol{P}(y-x)\mathrm{d}s(x) + P_1,$$

where $\boldsymbol{U}_1$ and P_1 are polynomials and $\boldsymbol{t} = \mathcal{D}(\boldsymbol{u})\mathbf{n}$.

Using a Taylor development for $\boldsymbol{u}$ we get a logarithmical term, due to:

$$E(y-x) = E(y) - \nabla E(\theta(y,x))x,$$

where $\theta(y,x) = y - \alpha x$ with $\alpha \in (0,1)$, then:

$$\boldsymbol{u}(y) = E(y)\int_{\partial\omega} \boldsymbol{t}(x)\mathrm{d}s(x) - \int_{\partial\omega} \boldsymbol{t}(x)\nabla E(\theta(y,x))x\mathrm{d}s(x) + \boldsymbol{U}_1.$$

But $\log \notin \mathrm{W}_0^{1,2}(\overline{\omega}^c)$, which implies:

$$\int_{\partial\omega} \boldsymbol{t}(x)\mathrm{d}s(x) = \langle \boldsymbol{t}, 1\rangle = 0.$$

Also, due to $\boldsymbol{U}_1 \in \mathbf{W}_0^{1,2}(\overline{\omega}^c)$, we must have $\boldsymbol{U}_1 = \boldsymbol{\lambda}$, where $\boldsymbol{\lambda}$ is a constant. Therefore, we have:

$$\boldsymbol{u} = O(1) \text{ at infinity.}$$

A similar reasoning gives $p(y) = O(1/r)$, where $r = \|y\|$, and $P_1 = 0$. Therefore we have:

$$\boldsymbol{u}(y) = \boldsymbol{\lambda} - \int_{\partial\omega} \boldsymbol{t}(x)\nabla E(\theta(y,x))x\ \mathrm{d}s(x) = \boldsymbol{\lambda} + \boldsymbol{W}(y), \tag{B.9}$$

$$p(y) = -\int_{\partial\omega} \boldsymbol{t}(x)\nabla \boldsymbol{P}(\theta(y,x))x\ \mathrm{d}s(x), \tag{B.10}$$

and $\boldsymbol{u}, p$ are bounded at infinity. Moreover, we have (see for example [77, Section 2.5.1]) $\boldsymbol{W}(y) = O(1/r)$ which implies, due to the well-posedness of the problem the existence of $c > 0$ such that:

$$|\boldsymbol{\lambda}| \leq c\|\boldsymbol{\varphi}\|_{1/2,\partial\omega}. \tag{B.11}$$

The study of the function $\boldsymbol{W}$ in (B.9) will be useful for important results: we study a priori estimates for this function, in a similar way as Guillaume in [53].

Some notations and preliminaries

For a given function $u \in \mathrm{H}^1(\Omega)$, we define the function $\widetilde{u}$ on $\widetilde{\Omega} := \Omega/\varepsilon$ by $\widetilde{u}(y) = u(x)$, $y = x/\varepsilon$. Using that $\nabla_x u(x) = (\nabla_y \widetilde{u}(y))/\varepsilon$, we obtain

$$|u|^2_{1,\Omega} = \int_\Omega |\nabla_x u(x)|^2 \,\mathrm{dx} = \int_{\widetilde{\Omega}} |\nabla_y \widetilde{u}(y)|^2 \,\mathrm{dy}.$$

Hence,

$$|u|_{1,\Omega} = |\widetilde{u}|_{1,\widetilde{\Omega}}\,. \tag{B.12}$$

Similarly, we obtain

$$\|u\|_{0,\Omega} = \varepsilon\, \|\widetilde{u}\|_{0,\widetilde{\Omega}}\,. \tag{B.13}$$

By changing the origin, the same equalities hold with the change of variables $y = (x - z)/\varepsilon$, for $z \in \Omega$.

Finally, let us introduce some other domains. Let $R > 0$ be such that the closed ball $\overline{B(z,R)}$ is included in Ω and $\omega_{z,\varepsilon} \subset B(z,R)$. We define the domains

$$\Omega^z_R := \Omega \backslash \overline{B(z,R)} \quad \text{and} \quad D^z_\varepsilon := B(z,R) \backslash \overline{\omega_{z,\varepsilon}}$$

(see Figure B.1). Thus, in particular, we denote $\Omega^0_R := \Omega \backslash \overline{B(0,R)}$ and $D^0_\varepsilon :=$

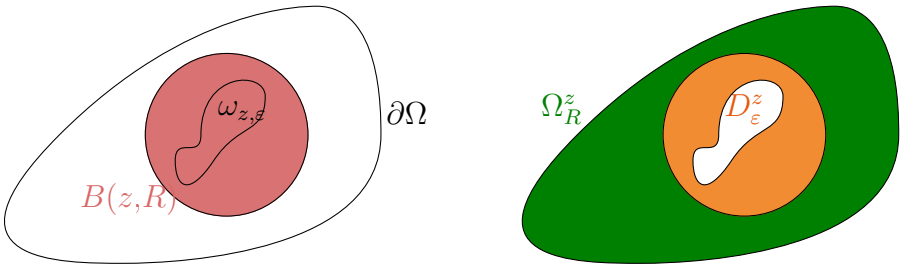

Figure B.1: The truncated domain

$B(0,R) \backslash \overline{\varepsilon\omega}$.

Estimates for $\boldsymbol{W}$

We have the following estimates for $\boldsymbol{W}$:

Lemma B.5 *Let $\boldsymbol{\varphi} \in \mathbf{H}^{1/2}(\partial\omega)$ such that $\displaystyle\int_{\partial\omega} \boldsymbol{\varphi} \cdot \mathbf{n} = 0$ and $z \in \Omega$. We consider $(\boldsymbol{u}, p) \in \mathbf{W}^{1,2}_0(\mathbb{R}^2 \backslash \overline{\omega}) \times \mathrm{L}^2(\mathbb{R}^2 \backslash \overline{\omega})$ the solution of the Stokes exterior problem*

$$\left\{ \begin{array}{rcll} -\nu \Delta \boldsymbol{u} + \nabla p & = & \mathbf{0} & \text{in } \mathbb{R}^2 \backslash \overline{\omega} \\ \operatorname{div} \boldsymbol{u} & = & 0 & \text{in } \mathbb{R}^2 \backslash \overline{\omega} \\ \boldsymbol{u} & = & \boldsymbol{\varphi} & \text{on } \partial\omega. \end{array} \right.$$

Recall that in this case $\boldsymbol{u} = \boldsymbol{\lambda} + \boldsymbol{W}$ *(see* (B.9)*). Then there exists a constant* $c > 0$ *(independent of* ε *and* $\boldsymbol{\varphi}$*) and* $\varepsilon_1 > 0$ *such that for all* $0 < \varepsilon < \varepsilon_1$

$$\begin{array}{rcl} \|\boldsymbol{W}\|_{0,D^z_\varepsilon/\varepsilon} & \leq & c\,(-\log\varepsilon)^{1/2}\,\|\boldsymbol{\varphi}\|_{1/2,\partial\omega}\,, \\ |\boldsymbol{W}|_{1,D^z_\varepsilon/\varepsilon} & \leq & c\,\|\boldsymbol{\varphi}\|_{1/2,\partial\omega} \end{array} \qquad \begin{array}{rcl} \|\boldsymbol{W}\|_{0,\Omega^z_R/\varepsilon} & \leq & c\,\|\boldsymbol{\varphi}\|_{1/2,\partial\omega}\,, \\ |\boldsymbol{W}|_{1,\Omega^z_R/\varepsilon} & \leq & c\,\varepsilon^2\,\|\boldsymbol{\varphi}\|_{1/2,\partial\omega}\,. \end{array} \quad \textit{and}$$

This implies:

$$\left\|\boldsymbol{W}\left(\frac{x-z}{\varepsilon}\right)\right\|_{1,\Omega_{z,\varepsilon}} \leq c\,\|\boldsymbol{\varphi}\|_{1/2,\partial\omega}\,.$$

Proof. For sake of simplicity we will prove this result for $z = 0$, the general case comes from linear change of coordinates.

By the formula given in (B.9) we notice that: $|\boldsymbol{W}(y)| \leq \dfrac{c}{\|y\|}\|\boldsymbol{\varphi}\|_{1/2,\partial\omega}$. Therefore: $|\boldsymbol{W}(x/\varepsilon)| \leq c\dfrac{\varepsilon}{\|x\|}\|\boldsymbol{\varphi}\|_{1/2,\partial\omega}$.

Analogously: $|\nabla\boldsymbol{W}(x/\varepsilon)| \leq c\dfrac{\varepsilon^2}{\|x\|^2}\|\boldsymbol{\varphi}\|_{1/2,\partial\omega}$.

Using these estimates we can bound the following quantities:

$$\begin{array}{rcl} \|\boldsymbol{W}\|_{0,B(0,R/\varepsilon)\setminus\overline{B(0,M)}} & = & \left(\displaystyle\int_{B(0,R)\setminus\overline{B(0,\varepsilon M)}} |\boldsymbol{W}(x/\varepsilon)|^2\frac{1}{\varepsilon^2}\mathrm{d}x\right)^{1/2} \\ & \leq & c\|\boldsymbol{\varphi}\|_{1/2,\partial\omega}\left(\displaystyle\int_{B(0,R)\setminus\overline{B(0,\varepsilon M)}} \frac{1}{\|x\|^2}\mathrm{d}x\right)^{1/2} \\ & = & c\|\boldsymbol{\varphi}\|_{1/2,\partial\omega}(\log R - \log\varepsilon M)^{1/2} \\ & \leq & c\|\boldsymbol{\varphi}\|_{1/2,\partial\omega}(-\log\varepsilon)^{1/2}. \end{array}$$

and

$$\begin{array}{rcl} \|\nabla\boldsymbol{W}\|_{0,B(0,R/\varepsilon)\setminus\overline{B(0,M)}} & \leq & \left(\displaystyle\int_{B(0,R)\setminus\overline{B(0,\varepsilon M)}} c\frac{\varepsilon^4}{\|x\|^4}\|\boldsymbol{\varphi}\|^2_{1/2,\partial\omega}\mathrm{d}x\right)^{1/2} \\ & \leq & c\varepsilon\|\boldsymbol{\varphi}\|_{1/2,\partial\omega}. \end{array}$$

Now, noticing that, in $B(0,M)\setminus\overline{\omega}$, we have classic a priori bounds for $\boldsymbol{W}$:

$$\|\boldsymbol{W}\|_{1,B(0,M)\setminus\overline{\omega}} \leq c\|\boldsymbol{\varphi}\|_{1/2,\partial\omega},$$

we get:

$$\|\boldsymbol{W}\|_{0,B(0,M)\setminus\overline{\omega}} \leq c\|\boldsymbol{\varphi}\|_{1/2,\partial\omega} \text{ and } |\boldsymbol{W}|_{1,B(0,M)\setminus\overline{\omega}} \leq c\|\boldsymbol{\varphi}\|_{1/2,\partial\omega},$$

and then:

$$\|\boldsymbol{W}\|_{0,D^0_\varepsilon/\varepsilon} \leq \|\boldsymbol{W}\|_{0,B(0,R/\varepsilon)\setminus\overline{B(0,M)}} + \|\boldsymbol{W}\|_{0,B(0,M)\setminus\overline{\omega}} \leq c\,(-\log\varepsilon)^{-1/2}\,\|\boldsymbol{\varphi}\|_{1/2,\partial\omega}\,,$$

$$|\boldsymbol{W}|_{1,D^0_\varepsilon/\varepsilon} \leq |\boldsymbol{W}|_{0,B(0,R/\varepsilon)\setminus\overline{B(0,M)}} + |\boldsymbol{W}|_{0,B(0,M)\setminus\overline{\omega}} \leq c\,\|\boldsymbol{\varphi}\|_{1/2,\partial\omega}\,.$$

The other estimates can be computed directly:

$$\begin{aligned}\|\boldsymbol{W}\|_{0,\Omega^0_R/\varepsilon} = \|\boldsymbol{W}\|_{0,\Omega/\varepsilon\setminus\overline{B(0,R/\varepsilon)}} &\leq \left(\int_{\Omega\setminus\overline{B(0,R)}} c\frac{\varepsilon^2}{\|x\|^2}\|\boldsymbol{\varphi}\|^2_{1/2,\partial\omega}\frac{1}{\varepsilon^2}\mathrm{d}x\right)^{1/2}\\ &\leq c\|\boldsymbol{\varphi}\|_{1/2,\partial\omega}\end{aligned}$$

$$\begin{aligned}|\boldsymbol{W}|_{0,\Omega^0_R/\varepsilon} = |\boldsymbol{W}|_{0,\Omega/\varepsilon\setminus\overline{B(0,R/\varepsilon)}} &\leq \left(\int_{\Omega\setminus\overline{B(0,R)}} c\frac{\varepsilon^4}{\|x\|^4}\|\boldsymbol{\varphi}\|^2_{1/2,\partial\omega}\mathrm{d}x\right)^{1/2}\\ &\leq c\varepsilon^2\|\boldsymbol{\varphi}\|_{1/2,\partial\omega}.\end{aligned}$$

From the previous inequalities we can estimate the size of the function $W\left(\frac{x}{\varepsilon}\right)$ in Ω_ε, indeed, by change of variables (recall the equalities given by (B.12), (B.13)), we get that, for small ε:

$$\frac{1}{\varepsilon}\left(\left\|\widetilde{\boldsymbol{W}}\right\|_{0,D^0_\varepsilon} + \left\|\widetilde{\boldsymbol{W}}\right\|_{0,\Omega^0_R}\right) = \|\boldsymbol{W}\|_{0,D^0_\varepsilon/\varepsilon} + \|\boldsymbol{W}\|_{0,\Omega^0_R/\varepsilon} \leq c\,(-\log\varepsilon)^{-1/2}\,\|\boldsymbol{\varphi}\|_{1/2,\partial\omega}\,,$$

then:

$$\left\|\widetilde{\boldsymbol{W}}\right\|_{0,D^0_\varepsilon} + \left\|\widetilde{\boldsymbol{W}}\right\|_{0,\Omega^0_R} \leq c\,\varepsilon\,(-\log\varepsilon)^{-1/2}\,\|\boldsymbol{\varphi}\|_{1/2,\partial\omega}\,.$$

But, by equivalence of norms, we know there exists a constant M which doesn't depend of ε such that:

$$M\left\|\widetilde{\boldsymbol{W}}\right\|_{0,\Omega_\varepsilon} \leq \left\|\widetilde{\boldsymbol{W}}\right\|_{0,D^0_\varepsilon} + \left\|\widetilde{\boldsymbol{W}}\right\|_{0,\Omega^0_R}$$

where we conclude

$$\left\|\widetilde{\boldsymbol{W}}\right\|_{0,\Omega_\varepsilon} \leq c\,\varepsilon\,(-\log\varepsilon)^{-1/2}\,\|\boldsymbol{\varphi}\|_{1/2,\partial\omega}\,.$$

Analogously we get:

$$\left|\widetilde{\boldsymbol{W}}\right|_{1,\Omega_\varepsilon} \leq c\,\|\boldsymbol{\varphi}\|_{1/2,\partial\omega}$$

and therefore:

$$\left\|\widetilde{\boldsymbol{W}}\right\|_{1,\Omega_\varepsilon} = \left\|\boldsymbol{W}\left(\frac{x}{\varepsilon}\right)\right\|_{1,\Omega_\varepsilon} \leq c\,\|\boldsymbol{\varphi}\|_{1/2,\partial\omega}\,.$$

□